The physiological basis of motor cortical oscillations in humans



Magdalena Nowak

The Queen's College

University of Oxford

A thesis submitted for the degree of Doctor of Philosophy

October 2017

The physiological basis of motor cortical oscillations in humans

Magdalena Nowak

Michaelmas Term The Queen's College

A thesis submitted in partial fulfilment of the requirements for the degree of Doctor of Philosophy at the University of Oxford

Abstract

β- and γ-frequency oscillations are the dominant oscillatory activities in the human motor cortex (M1). However, their mechanisms and functional significance remain poorly understood. Controlled modulation of brain oscillations using transcranial alternating current stimulation (tACS) holds promise to advance this knowledge. The primary goal of this thesis was to investigate the neurophysiological mechanisms underlying β and γ oscillations. To this end, tACS was combined with transcranial magnetic stimulation (TMS; Chapters 4 and 5) and ultra-high field (7T) Magnetic Resonance Spectroscopy (MRS; Chapter 6). Additionally, the relationship between MEG-measured oscillations and TMS-assessed physiological measures was examined (Chapter 7).

The findings presented in Chapter 4 demonstrated that γ tACS led to a duration-dependent decrease in resting-state synaptic $GABA_A$ inhibition in M1; this effect was positively correlated with baseline $GABA_A$ decrease during movement preparation, when γ activity in motor circuitry is known to increase, suggesting that tACS may have similar physiological effects to endogenously driven local oscillatory activity. In addition, γ tACS-induced change in $GABA_A$ inhibition was closely related to performance in a motor learning task.

Chapter 5 provided evidence on β tACS-induced modulation of corticospinal excitability (tACS phase-dependent) and extrasynaptic $GABA_A$ inhibition (tACS phase-independent) during movement preparation. Further, β tACS slowed down response time independently of its physiological effects.

In Chapter 6, it was shown that β tACS reduced M1 GABA concentration; this change was dependent on the match between stimulation frequency and endogenous β-frequency, potentially reflecting a complex relationship between local tonic inhibitory activity and β oscillations. In contrast, no effect of β tACS on M1 glutamate levels was observed.

Chapter 7 revealed an inverse relationship between endogenous β oscillatory power and movement-related corticospinal excitability. Moreover, peak frequency of movement-related γ synchronisation was related to performance in a motor learning task; local synaptic $GABA_A$-mediated inhibition played an important role in this association.

In conclusion, the results of the studies contained in this thesis offer a novel insight into the mechanistic basis of human motor cortical rhythms and provide evidence supporting the role of γ oscillations in motor learning, opening an interesting avenue for further research in the motor domain. Nevertheless, further study focused on addressing the limitations of tACS-based approaches is warranted.

This thesis contains approximately 45 000 words.

Contents

1 Introduction 1
1.1 The motor cortex 2
1.2 Neurochemistry 6
1.2.1 Glutamate 6
1.2.2 GABA 8
1.2.2.1 Phasic and tonic inhibition 9
1.3 Motor cortical oscillations 10
1.3.1 Functional significance 14
1.3.1.1 β-frequency oscillations 14
1.3.1.2 γ-frequency oscillations 15
1.3.2 Mechanisms 17
1.3.2.1 γ-frequency oscillations 18
1.3.2.2 β-frequency oscillations 21
1.4 Principles of plasticity 24
1.4.1 Hebbian plasticity 25
1.4.2 Homeostatic plasticity 27
1.5 Aims 29

2 Transcranial stimulation techniques 30
2.1 Transcranial alternating current stimulation (tACS) 31
2.1.1 Background 31
2.1.2 Basic principles 31
2.1.3 Modelling and validating current flow 32
2.1.4 Stimulation parameters 34
2.1.4.1 Frequency 34
2.1.4.2 Power of endogenous oscillations 35
2.1.4.3 Intensity 36
2.1.5 Mechanism of action 37
2.1.5.1 Entrainment by a periodic external drive – general concepts 37
2.1.5.2 Animal and computational modelling studies 38
2.1.5.3 MEG/EEG studies 39
2.1.5.4 TMS studies 40
2.1.5.5 fMRI studies 42
2.1.6 Behavioural effects of tACS 43
2.1.7 Safety of tACS 44

2.2 Transcranial magnetic stimulation (TMS) 46
2.2.1 Underlying principles 46
2.2.2 The physiological basis of TMS 47
2.2.3 Single-pulse TMS 49
2.2.4 Paired-pulse TMS 50
2.2.5 Movement-related TMS 51
2.2.6 Coil types 52
2.2.7 Safety of TMS 52

3 Neuroimaging methods 54
3.1 Electroencephalography (EEG) and magnetoencephalography (MEG) 55
3.1.1 Biophysical events measurable with EEG/MEG 56
3.2 Magnetic resonance spectroscopy (MRS) 59
3.2.1 Basic concepts of MRI 59
3.2.1.1 The magnetic property of a nucleus 60
3.2.1.2 Excitation and relaxation 61
3.2.1.3 Data acquisition: repetition time (TR) and echo time (TE) 63
3.2.2 Basic principles of *in vivo* MRS 64
3.2.3 Analysis and quantification of MR spectra 65
3.2.3.1 Water and outer volume suppression 69
3.2.4 The neurochemical profile detected by MRS 70
3.2.4.1 What does MRS-assessed GABA reflect? 72
3.2.5 Ultra-high field MRS 73

4 The physiological effects of driving β and γ oscillations and their behavioural relevance 74
4.1 Introduction 75
4.2 Methods 78
4.2.1 Participants 78
4.2.2 Experimental design and procedure 78
4.2.3 MEG 81
4.2.3.1 MEG data acquisition 81
4.2.3.2 MEG data analysis 82
4.2.4 Explicit motor learning task 85
4.2.5 Response time task 86
4.2.5.1 Response time data analysis 87
4.2.6 Transcranial alternating current stimulation (tACS) 87
4.2.7 TMS 88

4.2.7.1 TMS data acquisition 88
4.2.7.2 Motor thresholds 89
4.2.7.3 Paired-pulse TMS protocols 89
4.2.7.4 Rest measures 90
4.2.7.5 Pre-movement measures 90
4.2.7.6 MEP data analysis 91
4.2.8 Statistical analysis 92
4.3 Results 93
4.3.1 Quality assessment 93
4.3.2 Effects of tACS on physiological measures at rest 95
4.3.2.1 tACS does not affect corticospinal excitability 95
4.3.2.2 tACS does not affect glutamatergic activity 96
4.3.2.3 Frequency-matched β tACS does not affect motor excitability measures 96
4.3.2.4 γ tACS modulates $GABA_A$ inhibition in a duration-dependent manner 96
4.3.2.5 γ tACS-induced change in $GABA_A$ activity is unrelated to change in corticospinal excitability 99
4.3.2.6 γ tACS-induced change in $GABA_A$ activity is not related to current intensity 99
4.3.2.7 Baseline pre-movement $GABA_A$ activity is related to γ tACS-induced changes in resting $GABA_A$ inhibition 100
4.3.2.8 γ tACS-induced modulation of $GABA_A$ inhibition predicts an individual's ability to learn a motor task 102
4.3.3 tACS has no after-effects on pre-movement physiological measures 104
4.3.4 tACS has no after-effects on response time 106
4.3.4.1 β tACS-induced changes in response time are related to changes in corticospinal excitability 108
4.4 Discussion 110
4.4.1 γ tACS modulates $GABA_A$ inhibition during stimulation 110
4.4.2 β tACS has no effect on motor excitability measures 111
4.4.3 tACS-induced change in resting $GABA_A$ inhibition is related to $GABA_A$ change in a period of γ recruitment 113
4.4.4 γ tACS-induced modulation of $GABA_A$ inhibition predicts motor learning 113
4.4.5 Duration-dependent effects of γ tACS – evidence for homeostatic plasticity? 114
4.4.6 tACS has no after-effects on pre-movement physiological measures 116
4.4.7 tACS has no after-effects on response time 117

4.5 Conclusions 117

5 The physiological effects of driving β oscillations at rest and during movement preparation: a tACS-TMS study 118

5.1 Introduction 119

5.2 Methods 121

5.2.1 Participants 121

5.2.2 Experimental design and procedure 121

5.2.3 EEG 123

5.2.3.1 EEG data analysis 123

5.2.4 Response time task 123

5.2.4.1 Response time data analysis 124

5.2.5 Transcranial alternating current stimulation (tACS) 125

5.2.6 TMS 126

5.2.6.1 TMS data acquisition 126

5.2.6.2 Motor thresholds 127

5.2.6.3 Paired-pulse TMS protocols 127

5.2.6.4 Rest measures 128

5.2.6.5 Pre-movement measures 128

5.2.6.6 MEP data analysis 128

5.2.7 Statistical analysis 129

5.3 Results 131

5.3.1 Quality assessment 131

5.3.2 Comparison between baseline resting-state and pre-movement motor excitability measures 133

5.3.3 Exploring the stability of MEP amplitude during prolonged stimulation 134

5.3.4 β tACS has no phase-independent effects on motor excitability at rest 134

5.3.5 β tACS affects pre-movement $SICI_{1ms}$ in a phase-independent manner 136

5.3.6 β tACS has no phase-dependent effects on motor excitability at rest 137

5.3.7 β tACS affects pre-movement motor excitability in a phase-dependent manner 139

5.3.8 Variable effects of tuning individual spontaneous EEG on motor excitability measures 140

5.3.9 β tACS slows down response time 143

5.4 Discussion 145

5.4.1 Comparison between baseline resting-state and pre-movement motor excitability measures 145

5.4.2 β tACS has no phase-independent effects on resting-state motor excitability measures ... 145
5.4.3 Pre-movement $SICI_{1ms}$ is modulated by β tACS in a phase-independent manner ... 146
5.4.4 β tACS has no phase-dependent effects on resting-state motor excitability measures ... 147
5.4.5 β tACS modulates corticospinal excitability during movement preparation in a phase-dependent manner ... 149
5.4.6 β tACS slows down response time ... 150
5.5 Conclusions ... 150

6 The neurochemical effects of driving β oscillations: a tACS-7T MRS study ... 151
6.1 Introduction ... 152
6.2 Methods ... 154
6.2.1 Participants ... 154
6.2.2 Experimental design and procedure ... 154
6.2.3 EEG ... 155
6.2.3.1 EEG data analysis ... 155
6.2.4 Transcranial alternating current stimulation (tACS) ... 156
6.2.5 Magnetic resonance spectroscopy (MRS) ... 157
6.2.5.1 MRS data acquisition ... 157
6.2.5.2 MRS data analysis ... 158
6.2.6 Statistical analysis ... 158
6.3 Results ... 160
6.3.1 Driving β-band oscillations reduces M1 GABA levels ... 160
6.3.2 The relationship between stimulation frequency and spontaneous β-frequency affects β tACS-induced modulation of M1 GABA ... 161
6.4 Discussion ... 163
6.4.1 Driving β-frequency oscillations reduces MRS-assessed M1 GABA ... 163
6.4.2 β tACS-induced change in M1 GABA levels depends on the match between stimulation frequency and an individual's spontaneous β frequency ... 164
6.5 Conclusions ... 165

7 Relationship between β- and γ-frequency oscillations, motor excitability and motor learning: a multimodal MEG and TMS study ... 167
7.1 Introduction ... 168
7.2 Methods ... 171
7.2.1 Participants ... 171

7.2.2 Experimental design and procedure 171
7.2.3 MEG 173
7.2.3.1 MEG data acquisition 173
7.2.3.1 MEG data analysis 174
7.2.4 Motor learning task 176
7.2.5 Response time task 177
7.2.6 TMS 178
7.2.6.1 TMS data acquisition 178
7.2.6.2 Motor thresholds 178
7.2.6.3 Paired-pulse TMS protocols 179
7.2.6.4 Rest measures 179
7.2.6.5 Pre-movement measures 180
7.2.6.6 MEP data analysis 180
7.2.7 Statistical analysis 181
7.3 Results 182
7.3.1 Spontaneous (resting-state) and movement-related patterns of oscillatory activity 182
7.3.2 β power is inversely correlated with corticospinal excitability 183
7.3.3 MRGS peak frequency is related to motor excitability 186
7.3.4 MRGS peak frequency is related to performance in motor learning task 186
7.4 Discussion 189
7.4.1 β power and corticospinal excitability are inversely related 189
7.4.2 MRGS peak frequency is inversely related to pre-movement corticospinal excitability 190
7.4.3 MRGS peak frequency is related to performance in a motor learning task 191
7.5 Conclusions 191
8 Conclusions, limitations, and future directions 192
8.1 Thesis overview 193
8.2 Limitations and future directions 196
8.2.1 tACS as a tool to study brain oscillations 196
8.2.2 Individual variability of responses to tACS 198
8.2.3 Clinical applications of tACS 199
8.3 General conclusions 200
Appendix 202
Bibliography 204

List of Figures

1.1 The types of cortical GABA interneurons……..3

1.2 Brodmann's map of the human cerebral cortex, cortical layers, motor cortex and the motor homunculus……..5

1.3 Glutamatergic synapse……7

1.4 GABAergic synapse and receptor types……8

1.5 Parameters of brain oscillations……...11

1.6 Grand average time-frequency spectrogram……..13

1.7 Methods used to study β and γ oscillations……18

1.8 The schematic of STDP……....26

1.9 The bidirectional shift of LTP-LTD induction curve predicted by the BCM theory..... 28

2.1 Current flow during tACS……...32

2.2 Electrical field simulation for the classic and the ring montage……..…33

2.3 Power increase by synchronisation……..…38

2.4 Illustration of direction of current flow in a magnetic coil and the induced current in the brain……..47

2.5 Neurophysiological basis of MEP……..….48

3.1 Intra- and extracellular current flow in a pyramidal neuron due to synaptic activation…….56

3.2 Schematic drawing showing the direction of the intracellular electric current and the resulting magnetic fields around the apical dendrites within the crown of a gyrus and a sulcus……..……57

3.3 Nuclear spins in the absence and in the presence of a magnetic field……..61

3.4 The effect of an RF pulse on net magnetization……...62

3.5 T1- and T2-weighting……..…64

3.6 ^{1}H-MR spectrum……..…66

3.7 Quantification of ^{1}H-MR spectra as linear combination of model spectra (LCModel)…….....……..….67

3.8 Water unsuppressed and water suppressed ^{1}H spectra……..…69

3.9 Lipid resonances in the human brain……..70

3.10 Compounds detected in the brain with *in vivo* ^{1}H-MRS……..….71

4.1 Study outline and experimental design……..…80
4.2 Go/NoGo task……....82
4.3 MEG analysis results……..…85
4.4 Average baseline MEP amplitude values……...94
4.5 Effectiveness of paired-pulse TMS protocols at baseline……..…..95
4.6 The effect of tACS on resting-state motor excitability measures……..……98
4.7 Relationship between the magnitude of baseline $SICI_{late}$ and the magnitude of tACS-induced change in $SICI_{T1}$…….....101
4.8 Relationship between motor learning score and tACS-induced change in SICI…….....103
4.9 Distribution of TMS measures during pre-movement period……..…104
4.10 The effect of tACS on pre-movement motor excitability measures……..…...105
4.11 The effect of tACS on dynamic MT_{1mV} and SICI modulation……..…106
4.12 The effect of tACS on response time……108
4.13 Relationship between tACS-induced change in response time and corticospinal excitability…….....109

5.1 Experimental design……122
5.2 Average baseline MEP amplitude values……..…..132
5.3 Inhibition of MEP amplitude values in SICI protocols.....132
5.4 Average baseline rest and pre-movement MEP amplitude values……..133
5.5 Average resting-state MEP amplitude values……135
5.6 Average pre-movement MEP amplitude values……..137
5.7 Phase dependency of β tACS effects on motor excitability at rest……..138
5.8 Phase dependency of β tACS on pre-movement motor excitability……140
5.9 Individual β peak frequencies……141
5.10 The effect of tACS on response time…….……..143

6.1 Experimental design……....155
6.2 Typical placement of the VOI……....…....157
6.3 The effect of β and sham tACS on MRS-assessed M1 GABA and glutamate levels……..…….....……161
6.4 Relationship between tACS-induced change in M1 GABA and the match between stimulation frequency and individual β-frequency…….....162

7.1 Study outline and experimental design……...…172
7.2 The grand average power spectrum of the left motor ROI and topographical map of spontaneous (resting-state) β activity……..…182
7.3 Grand mean time-frequency representation of task data and topographical maps of MRBD and MRGS…….....……..183
7.4 Correlations between β activity and motor excitability measures…….....185
7.5 Correlations between MRGS peak frequency and motor excitability measures ……...186
7.6 Correlation between MRGS peak frequency and motor learning score……..187

List of Tables

Table 2.1 Effects of tACS on TMS-assessed motor excitability measures……..…..41
Table 4.1 Mean motor thresholds (± SD)……..93
Table 4.2 Mean response times (± SD) at baseline and post-tACS for each session……..107
Table 5.1 Mean motor thresholds (± SD)……...131

Acronyms

AC	alternating current
ALS	amyotrophic lateral sclerosis
AMPA	α-amino-3-hydroxy-5-methyl-4-isoxazolepropionic acid
aMT	active motor threshold
ATP	adenosine triphosphate
BA	Brodmann area
BCM	Bienenstock-Cooper-Munro
BOLD	blood oxygenation level-dependent signal
CED	Cambridge Electronic Design
Cho	choline-containing compounds
CNS	central nervous system
Cr	creatine
CRLB	Cramer-Rao lower bounds
CS	conditioning stimulus
CSF	cerebrospinal fluid
CSI	cue-stimulus interval
CSP	cortical silent period
cTBS	continuous theta burst stimulation
DC	direct current
dHb	deoxyhaemoglobin
DNA	deoxyribonucleic acid
E-I	excitatory-inhibitory
EAAT	excitatory amino acid transporter
ECG	electrocardiogram
EDC	extensor digitorum communis
EEG	electroencephalography
EMG	electromyography
EOG	electrooculogram
EPSP	excitatory postsynaptic potential
FDI	first dorsal interosseous
FID	free induction decay
FS	fast-spiking
GABA	γ-aminobutyric acid
GABA-T	GABA transaminase
GAD	glutamic acid decarboxylase

GAT	GABA transporter
Gln	glutamine
Glu	glutamate
GluT	glutamate transporter
Glx	glutamate + glutamine
GRAPPA	generalised autocalibrating partial parallel acquisition
HPI	head-position
I-O	input-output
IBF	individual beta frequency
ICA	independent component analysis
ICF	intracortical facilitation
INB	interneuronal network beta
ING	interneuronal network gamma
IPSP	inhibitory postsynaptic potential
iRT	individual response time
ISI	inter-stimulus interval
iTBS	intermittent theta burst stimulation
LFP	local field potential
LICI	long interval intracortical inhibition
LTD	long-term depression
LTP	long-term potentiation
M1	primary motor cortex
MEG	magnetoencephalography
MEGA-PRESS	Mescher-Garwood point-resolved spectroscopy
MEP	motor evoked potential
mGluR	metabotropic glutamate receptor
MPRAGE	magnetization prepared rapid acquisition gradient echo
MRBD	movement related beta desynchronisation
MRGS	movement related gamma synchronisation
MRI	magnetic resonance imaging
MRS	magnetic resonance spectroscopy
MT	motor threshold
Myo	myoinositol
NAA	N-acetylaspartate
NMDA	N-methyl-D-aspartate
NMR	nuclear magnetic resonance
OSL	OHBA Software Library

OVS	outer volume suppression
PCr	phosphocreatine
PET	positron emission tomography
PINB	pyramidal-interneuronal network beta
PING	pyramidal-interneuronal network gamma
PMBR	post-movement beta rebound
PV	parvalbumin
RC	recruitment curve
RF	radiofrequency
RM ANOVA	repeated measures analysis of variance
RMS	root mean square
rMT	resting motor threshold
RNA	ribonucleic acid
ROI	region of interest
RT	response time
rTMS	repetitive TMS
SD	standard deviation
SEM	standard error of the mean
semi-LASER	semi-localised by adiabatic selective refocusing
SICI	short interval intracortical inhibition
SNR	signal-to-noise ratio
SPSS	statistical package for the social sciences
SQUID	superconducting quantum interference device
SRTT	serial response time task
STDP	spike timing-dependent plasticity
tACS	transcranial alternating current stimulation
tDCS	transcranial direct current stimulation
TE	echo time
TFR	time–frequency
TMS	transcranial magnetic stimulation
TR	repetition time
TS	test stimulus
tSSS	temporal extension of Maxfilter Signal Space Separation
UHF	ultra-high field
VAPOR	variable power RF pulses with optimised relaxation delays
VOI	voxel of interest

Publications

Nowak, M., Hinson, E., van Ede, F., Pogosyan, A., Guerra, A., Quinn, A., Brown, P., Stagg, C.J. (2017). Driving Human Motor Cortical Oscillations Leads to Behaviorally Relevant Changes in Local $GABA_A$ Inhibition: A tACS-TMS Study. *The Journal of Neuroscience*, *37*(17), 4481-4492.

Other publications not directly arising from but related to the work presented in this thesis include:

Guerra, A., Pogosyan, A., **Nowak, M.**, Ferreri, F., Di Lazzaro, V., Brown, P. (2016). Phase Dependency of the Human Primary Motor Cortex and Cholinergic Inhibition Cancelation During Beta tACS. *Cerebral Cortex*, *26*(10), 3977-90.

Weinrich, C.A., Brittain, J.S., **Nowak, M.**, Salimi-Khorshidi, R., Brown, P., Stagg, C.J. (2017). Modulation of Long-Range Connectivity Patterns via Frequency-Specific Stimulation of Human Cortex. *Current Biology*, *pii: S0960-9822*(17), 31115-6.

Acknowledgements

This thesis could not have been completed without the help and support of a number of people. My utmost thanks and gratitude go to the following:

To my truly wonderful and inspiring supervisors, Charlotte J. Stagg and Peter Brown. Thank you for all your support, optimism and for your faith in my sceptical and forever doubting self.

To Charlie, for steering me in the right direction, her enthusiasm, endless ideas, patience, and for instilling a love for GABA in me. Thank you for being the best supervisor I could have asked for.

To Peter, for sharing his insightful knowledge, offering advice and constructive ideas throughout my DPhil journey. Importantly, thank you for having confidence in me (as promised, I will be no shrinking violet).

To Alek Pogosyan, for help in setting up the tACS-TMS experiment presented in Chapter 5 and for magically solving the never-ending technical issues.

To Freek van Ede and Andrew Quinn, for help with the analysis of MEG data.

To Andrea Guerra and the members of the Physiological Neuroimaging Group for assisting with data collection. In particular, thank you to Emily Hinson for spending over 150 hours of her life with me and a TMS machine, and for providing Pret cookies to sweeten those occasionally bitter days.

To the Nuffield Department of Clinical Neurosciences, The Queen's College and, more importantly, to the Wellcome Trust for funding my studies.

To Yousouf, for supporting me every step of the way, helping me see the world from a different perspective, especially in the most difficult moments, and for always being himself.

To Sylwek, for providing a listening ear whenever needed, and for being a male version of myself, who could always understand me like nobody else could.

Last but not least, to my Mum, for being my source of inspiration and the most exceptional parent in the world - without you, I would have never been where I am.

“Thus each organic body of a living being is a kind of divine machine or natural automaton, which infinitely surpasses all artificial automata. Because a machine which is made by man’s art is not a machine in each of its parts; for example, the teeth of a brass wheel have parts or fragments which to us are no longer artificial and have nothing in themselves to show the special use to which the wheel was intended in the machine. But nature’s machines, that is, living bodies, are machines even in the smallest parts, *ad infinitum*. Herein lies the difference between nature and art, that is, between the divine art and ours.”

- No. 64, Gottfried Wilhelm Freiherr von Leibniz,
The Monadology (La Monadologie), 1714

CHAPTER

1

Introduction

This chapter provides an overview of the anatomical and functional organisation of the motor system and the key neurotransmitters, and discusses the mechanisms and functional significance of motor cortical oscillations. Moreover, the basic principles underlying motor cortical plasticity and its relevance to the work performed within this thesis are discussed. Finally, the chapter outlines the overall aims of the thesis.

1.1 The motor cortex

The human cerebral cortex is a highly convoluted laminar structure that controls complex motor and cognitive functions. It consists of two hemispheres (left and right), each of which is divided into four lobes (frontal, temporal, parietal, and occipital). Beyond these gross anatomical divisions, the cortex can be further parcellated based on its microstructure. The "classic" and the most widely used map, known as Brodmann's map, divides human cortex into distinct areas based on differences in cytoarchitecture (Brodmann 1909) (Figure 1.2 A). Subsequent investigations demonstrated that these areas (known as Brodmann's areas), defined purely anatomically, also correspond to functional entities of the cerebral cortex (Foerster 1926; Vogt and Vogt 1926).

The motor areas of the cerebral cortex include the primary motor cortex (M1), the secondary (supplementary) motor cortex, and the premotor cortex, known collectively as the motor cortex. The motor cortex controls pyramidal and extrapyramidal tracts and, together with the basal ganglia and the cerebellum, constitutes a key component of the central motor control.

Most regions of the human cerebral cortex have a six-layered architecture, with the notable exception of the motor cortex, which does not show a clearly recognisable layer IV in adult brains (Brodmann 1909) (Figure 1.2 B). Layer IV is the main target of sensory information from the thalamus, and since the motor cortex is primarily an output region, it receives little sensory information directly from thalamus, which explains the absence of this layer in motor cortical areas. The neurons of the cortex can be broadly defined as principal (projection) neurons and local interneurons. Projections neurons typically have pyramid-shaped cell bodies, are located mainly in layers III, V and VI and use the amino acid glutamate as their primary neurotransmitter at excitatory synapses. The axons of principal neurons convey information to the next

synaptic relay in the system. Local interneurons have axons that remain in the same area where their cell body is located and use the neurotransmitter γ-aminobutyric acid (GABA) at inhibitory synapses. These interneurons constitute 20-25 % of the neurons in the neocortex and are located in all layers. Several types of GABAergic interneurons have been distinguished based on various features such as morphology and neurochemical composition (Figure 1.1) (Owens and Kriegstein 2002; Tremblay et al 2016).

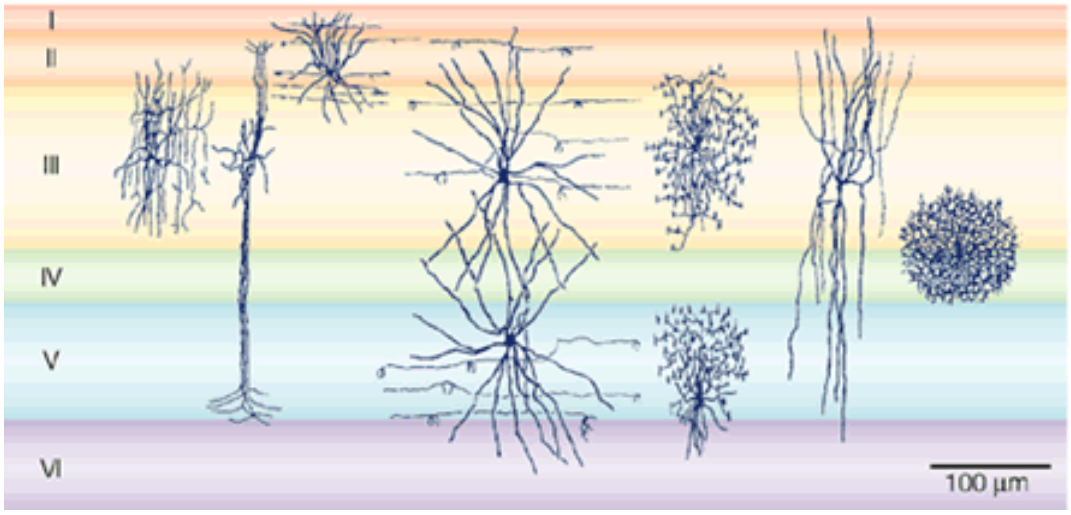


Figure 1.1 The types of cortical GABA interneurons

Cortical GABA interneurons are phenotypically diverse, as illustrated here by classification on the basis of morphological features. This figure illustrates (left to right) an interneuron with axonal arcades, a double bouquet cell, three types of basket cell, two chandelier cells, a cell spanning all cortical layers and a neurogliaform cell. (Adapted from Owens and Kriegstein 2002)

The main focus of this thesis is the M1 (Brodmann's area 4), a major source of descending motor commands for voluntary movement and hence, as has been long known, the area with the lowest threshold for evoking movements by electrical stimulation (Fulton 1935; Penfield and Boldrey 1937). Anatomically, M1 is located in the precentral gyrus, bound by the precentral sulcus anteriorly and the central sulcus posteriorly (Figure 1.2 C). Mapping studies have revealed that M1 contains a somatotopic representation of contralateral body parts, referred to as the motor

homunculus (Figure 1.2 D) (Jackson 1931; Penfield and Boldrey 1937), the findings which have been more recently supported by co-registration of the results of intraoperative cortical mapping with those of transcranial magnetic stimulation (TMS) and magnetic resonance imaging (MRI) (Singh et al 1997; Hlustík et al 2001). In the past few decades, however, it has also become apparent that the organisation of the M1 is not exclusively somatotopic, but that functional aspects of movement are also represented (Georgopoulos et al 1986; Humphrey 1986; Z'Graggen et al 2009). In fact, a large body of experimental data has revealed that M1 has adaptive and dynamic organisation that underlies motor planning, performance, adaptation and learning (Sanes and Donoghue 1997; Sanes and Donoghue 2000). Of particular importance in the context of these processes is the system of widespread horizontal connections (both recurrent pyramidal collaterals and interneurons), which has been shown to functionally associate M1 neurons to form assemblies that construct dynamic motor maps (Jacobs and Donoghue 1991; Sanes and Donoghue 2000).

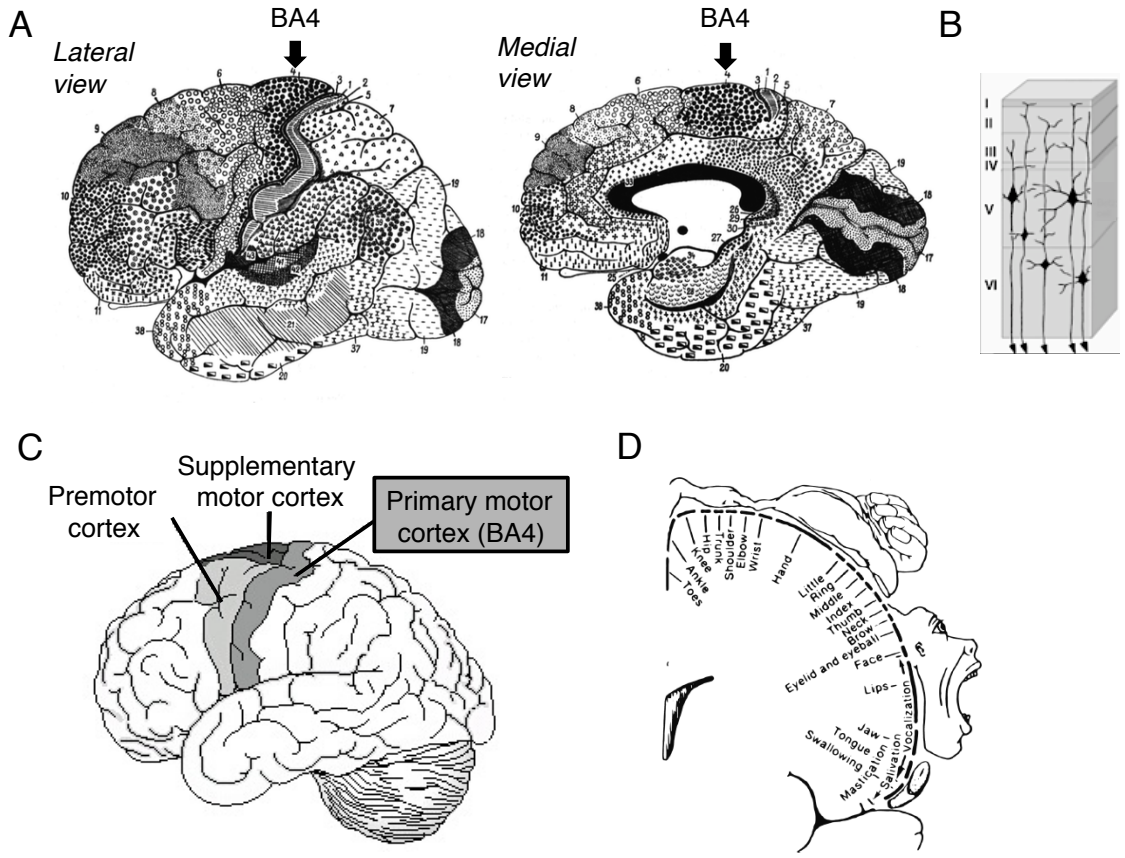


Figure 1.2 Brodmann's map of the human cerebral cortex, cortical layers, motor cortex and the motor homunculus

A. Brodmann's cytoarchitectonic map of the human cerebral cortex. (Adapted from Brodmann 1909). **B.** Schematic of layers of the primary motor cortex. Layer I (molecular layer): occupied by the dendrites of cells located in deeper layers and axons that travel through this layer to make connections in other areas of the cortex. Layer II (external granular layer): contains small spherical neurons. Layer III (external pyramidal layer): contains a variety of cell types, many of which are pyramidally shaped. The axons of pyramidal neurons in layer II and III project locally to other neurons within the same cortical area and other cortical areas, thereby mediating intracortical communication. Layer IV (internal granular layer): M1 essentially does not have this layer and is thus part of the so-called agranular frontal cortex. Layer V (internal pyramidal layer): composed of medium and large pyramidal neurons, including Betz cells distinguished by their large soma and dendrites that emerge from the soma in all directions; axons of pyramidal neurons give rise to the major output pathways of the cortex, projecting to other cortical areas and subcortical structures. Layer VI (multiform layer): neurons here are heterogeneous; this layer blends into the white matter that forms the deep limit of the cortex and carries axons to and from other areas of cortex. **C.** The primary motor cortex together with other adjacent motor cortical areas: supplementary motor area and premotor cortex. **D.** Motor homunculus. (Adapted from Penfield and Rasmussen 1950)

1.2 Neurochemistry

A wide range of molecules in the brain are known to act as neurotransmitters. They can be broadly divided into peptide and small-molecule neurotransmitters. The latter group can be sub-divided into: (i) amino acids (e.g., GABA, glycine, and glutamate), (ii) biogenic amines (e.g., serotonin, dopamine, norepinephrine), and (iii) other (e.g., acetylcholine, adenosine triphosphate). Given the converging evidence on the critical role of GABA and glutamate in cortical oscillations, as well as the possibility of measuring these chemicals *in vivo* in the human brain, they are a primary focus of this section and the thesis in general.

1.2.1 Glutamate

Glutamate is the principal excitatory neurotransmitter in the human cortex. It regulates synaptic transmission by activating ionotropic receptors (N-Methyl-D-aspartate [NMDA], α-amino-3-hydroxy-5-methyl-4-isoxazolepropionic acid [AMPA] and kainate) and metabotropic receptors (mGluR1 to mGluR8). Glutamate is present at very high concentrations within the cells of the central nervous system (CNS), which requires tight regulatory processes to ensure optimal neurotransmission and prevent potential excitotoxicity (Figure 1.3). Importantly, modulations in the sensitivity and density of the NMDA receptor are important for long-term potentiation (LTP) and long-term depression (LTD).

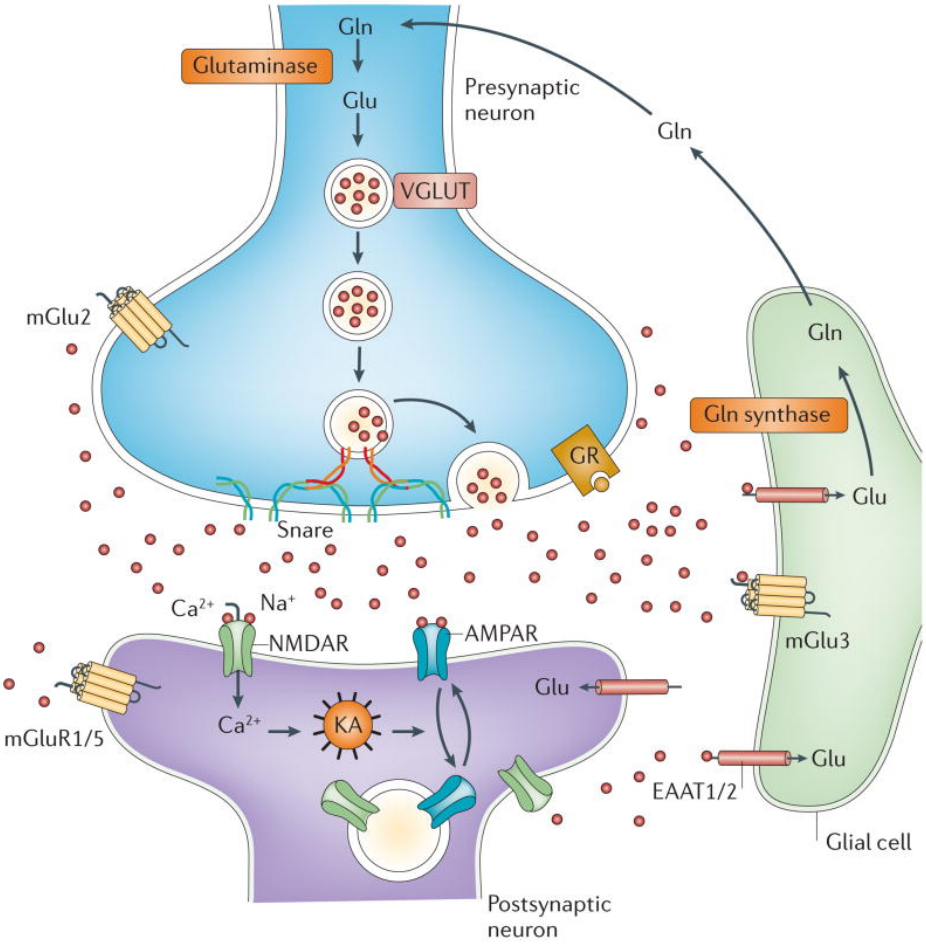


Figure 1.3 Glutamatergic synapse

Glutamate is synthesised *de novo* both from glucose (not shown) and from glutamine (Gln) supplied by glial cells. Glutamate is then packaged into synaptic vesicles by vesicular glutamate transporters (vGluT). SNARE complex proteins mediate the interaction and fusion of vesicles with the presynaptic membrane. After release into the extracellular space, glutamate binds to ionotropic (NMDA, AMPA, kainate [not shown]) and metabotropic (mGluR 1–8) receptors on the membranes of both post-synaptic and pre-synaptic neurons and glial cells. Upon binding, the receptors initiate various responses, including membrane depolarization, activation of intracellular messenger cascades, modulation of local protein synthesis and, eventually, gene expression. Surface expression and function of NMDARs and AMPARs is dynamically regulated by protein synthesis and degradation and receptor trafficking between the postsynaptic membrane and endosomes. The insertion and removal of postsynaptic receptors provide a mechanism for long-term modulation of synaptic strength. Glutamate is cleared from the synapse through excitatory amino acid transporters (EAATs) on neighbouring glial cells (EAAT1 and 2) and, to a lesser extent, on neurons (EAAT 3–5). Within the glial cell, glutamate is converted to glutamine by glutamine synthetase and the glutamine is subsequently released and taken up by neurons via transporters to complete the glutamate–glutamine cycle. (Adapted from Popoli et al 2011)

1.2.2 GABA

GABA is the main inhibitory neurotransmitter in the human cortex. The effects of GABA can be mediated by the activation of either ionotropic or metabotropic receptors, and by both synaptic and non-synaptic mechanisms (Figure 1.4).

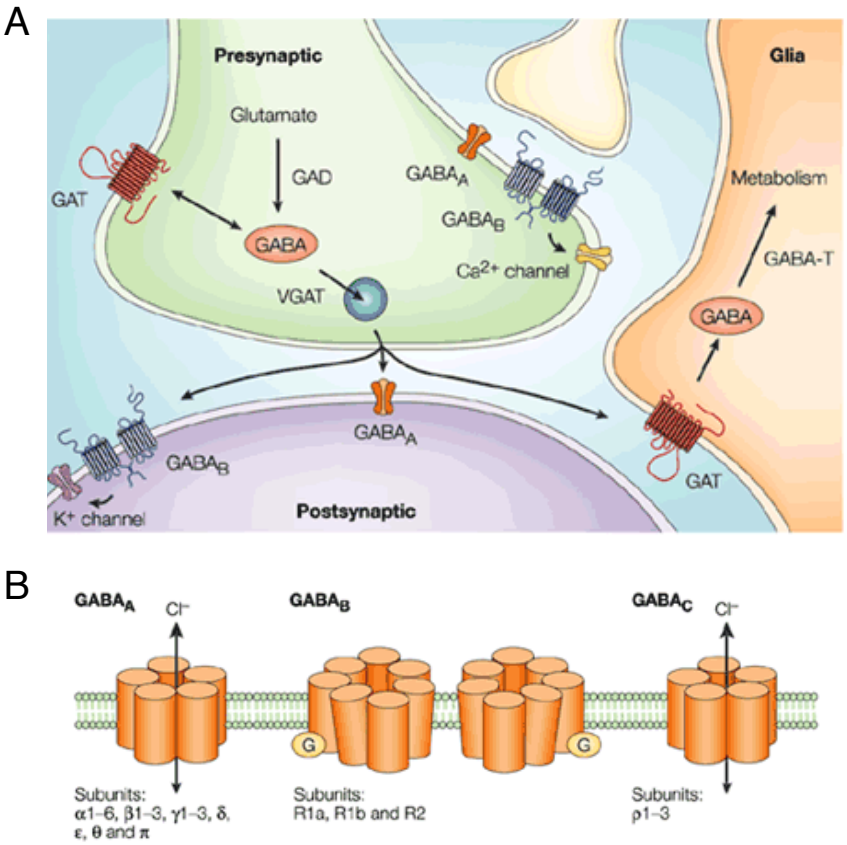


Figure 1.4 GABAergic synapse and receptor types

A. Schematic diagram of the synthesis and transport of GABA at synapses. GABA is synthesised in inhibitory neurons from glutamate by the enzyme glutamic acid decarboxylase (GAD) enzymes (GAD65 and GAD67), and is transported into vesicles by a vesicular neurotransmitter transporter (VGAT) and then released by calcium-dependent exocytosis. GABA receptors are located at pre- and postsynaptic sites. Activation of GABA receptors leads to inhibition: presynaptic activation reduces transmitter release whereas postsynaptic activation hyperpolarizes the cell. Reuptake of GABA by surrounding neurons and glia occurs through the activity of GABA transporters (GAT). Subsequently, GABA is metabolized by a transamination reaction that is catalysed by GABA transaminase (GABA-T). The metabolism of GABA occurs in both neurons (not shown) and glia. **B.** GABA receptors differ in subunit composition and assembly. $GABA_A$ and $GABA_C$ receptors are closely related pentameric receptors that carry chloride; $GABA_A$ receptors are composed of combinations of several subunit types, whereas $GABA_C$ receptors are composed of only single or multiple subunits. $GABA_B$ receptors are metabotropic receptors that exist as R1a, R1b and R2 isoforms. (Adapted from Owens and Kriegstein 2002)

1.2.2.1 Phasic and tonic inhibition

The principal action of GABA, mediated by ubiquitous $GABA_A$ receptors, is to increase membrane permeability to chloride and bicarbonate ions, which leads to a net inward flow of anions and a hyperpolarizing postsynaptic response, known as the inhibitory postsynaptic potential (IPSP). This event occurs when postsynaptic $GABA_A$ receptors are activated following brief exposure to a high concentration of GABA, which is released from presynaptic vesicles. The resultant increase in membrane conductance underlies what is known as 'phasic' inhibition. The transient and specific point-to-point nature of this process has an important role in many aspects of GABA-mediated signalling. For example, one of the important tasks of $GABA_A$-mediated inhibition is preventing over-excitation of neurons, and thereby avoiding the development of pathological states of network activity (Farrant and Nusser 2005). Another important task, particularly relevant in the context of this thesis, is their vital role in generating and maintaining rhythmic activities in neuronal networks (Cobb et al 1995; Mann and Paulsen 2007) (see section 1.3.2 for more details).

In recent years, it has become evident that GABA receptor activation can also take place in a less spatially and temporally restricted manner. GABA escaping from the synaptic cleft can activate receptors on presynaptic terminals or at neighbouring synapses on the same or adjacent neurons (a phenomenon termed 'spillover'). In addition, low GABA concentrations in the extracellular space can result in the persistent or 'tonic' activation of $GABA_A$ receptors, in a manner that is temporally dissociated from phasic synaptic events (Farrant and Nusser 2005). Interestingly, recent evidence from animal studies has demonstrated that tonic inhibition also plays an important role in shaping neuronal network excitability and synchrony (Semyanov et al 2003; Semyanov et al 2004; Mann and Mody 2010; Prokic et al 2015). However,

little work has been done to explore the role of this type of inhibition in synchronous activity in humans.

1.3 Motor cortical oscillations

Brain oscillations are periodic fluctuations in neuronal excitability generated spontaneously or in response to stimuli. Their discovery is generally credited to Hans Berger, a German psychiatrist, who pioneered the first electroencephalogram (EEG) in humans in 1924. Oscillations are characterised by the amplitude (square root of power), frequency and phase (Figure 1.5 A). In terms of frequency, rhythmic activity is classically subdivided into different bands (with the borders between the bands arbitrarily drawn): delta (δ, 1–4 Hz), theta (θ, 5–7 Hz), alpha (α, 8–12 Hz), beta (β, 15–30 Hz), gamma (γ, 30–90 Hz) and high-frequency ("ripple") (> 90 Hz) oscillations. The frequency of an oscillation is inversely related to the size of the underlying network, with high frequencies reflecting activity of small-scale neuronal networks, and lower frequencies reflecting activity of large-scale networks (Buzsáki and Draguhn 2004), a phenomenon that gives rise to the 1/f power characteristics in M/EEG frequency spectra (greater power is observed in low frequency signals) (Singer 1993) (Figure 1.5 B).

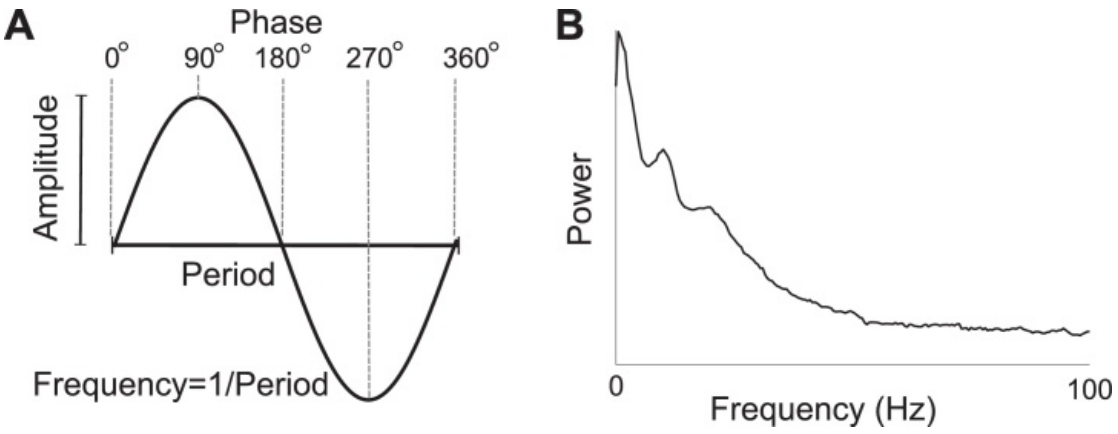


Figure 1.5 Parameters of brain oscillations

A. An oscillation is characterised by its amplitude and frequency. A specific point within an oscillatory cycle is identified by the phase, which reflects the polarity of an oscillation, i.e., it indicates whether the underlying neuronal assembly is in a relatively excitatory or inhibitory state. **B.** Power spectrum showing the typical 1/f pattern. (Adapted from Gross 2014)

The past few decades have witnessed significant advances in unveiling the mechanisms and functional significance of neural oscillations, owing to a confluence of experimental advances. It has been established that oscillatory activity plays a key role in local and long-range neural communication and information processing (Engel et al 2001; Fries 2005; Fries 2015; Maris et al 2016). Importantly, countless studies have demonstrated that specific patterns of oscillations are tightly linked to behavioural processes, such as attention (Hanslmayr et al 2011; Klimesch 2012), conscious awareness (Ward 2003), decision making (Siegel et al 2011), memory (Düzel et al 2010), multisensory integration (Senkowski et al 2008) and motor control (Jenkinson et al 2013; Brittain and Brown 2014). In addition, abnormal neural synchronisation has been linked to a range of neurological and psychiatric disorders, including Parkinson's disease (Brown 2007; Eusebio and Brown 2009), stroke (Hall et al 2010b; Rossiter et al 2014a), amyotrophic lateral sclerosis (ALS) (Proudfoot et al 2017), Alzheimer's disease (Babiloni et al 2016), and schizophrenia (Uhlhaas and Singer 2010).

The work within this thesis focuses on motor cortical β- (15–30 Hz) and γ-frequency oscillations (60–90 Hz). The term "gamma" (γ) is generally used for frequencies

between 30 and 90 Hz (Buzsáki and Wang 2012). Within this band, several independent processes exist, which differ both in terms of the underlying mechanisms and behavioural correlates (Berke 2009; Tort et al 2009; Chen et al 2011; Nicolás et al 2011). In this thesis, the focus is specifically on the higher γ-frequency oscillations (60–90 Hz), which will be referred to as simply γ-frequency oscillations.

β and γ oscillations play a vital role in motor control and represent a fundamental mechanism for sensory-motor processing (MacKay 1997). β-band oscillations are the dominant oscillatory activity in the primary motor cortex (M1) at rest (Murthy and Fetz 1992; Salmelin and Hari 1994a) and are widely associated with static motor control such as tonic or postural contraction (Jenkinson and Brown 2011). Prior to movement onset, there is a strong reduction of β-band power starting ~600-800 ms before movement and continuing for ~400 ms after the movement onset, a feature referred to as movement-related beta desynchronisation (MRBD) (Figure 1.6) (Jasper and Penfield 1949; Baker et al 1997; Pfurtscheller and Lopes da Silva 1999; Cheyne et al 2006). On the other hand, a transient increase in power in the γ-frequency range (60–90 Hz) occurs shortly before movement onset and during movement execution and lasts only ~100-300 ms, a phenomenon referred to as a movement-related γ synchronisation (MRGS) (Figure 1.6) (Pfurtscheller and Lopes da Silva 1999; Cheyne et al 2008; Muthukumaraswamy 2010). This response is more powerful during the first movements of a repetitive sequence than in subsequent movements (Muthukumaraswamy 2010). Upon movement termination, there is a strong increase in β power above the pre-movement baseline levels, which lasts ~1000-2000 ms, and is known as post-movement beta rebound (PMBR) (Figure 1.6) (Pfurtscheller et al 1996; Jurkiewicz et al 2006; Gaetz et al 2010).

In terms of spatial aspect of these movement-related oscillatory activities, MRBD and PMBR are localised bilaterally in sensorimotor cortex, with the strongest source located

in the contralateral sensorimotor cortex (Pfurtscheller and Berghold 1989; Murthy and Fetz 1992; Sanes and Donoghue 1993; Gaetz et al 2011), whereas MRGS is strongly lateralised to the contralateral sensorimotor strip (Crone et al 1998; Cheyne et al 2008; Muthukumaraswamy 2010; Gaetz et al 2011). Finally, although motor cortical β- and γ-frequency oscillations are the main focus of the work presented here, it is worth noting that movement-related changes in these frequency bands are not constrained to the primary motor cortical areas but can be found across the motor network (MacKay and Mendonça 1995; Baker et al 1997; Courtemanche et al 2003; Aumann and Fetz 2004; Alegre et al 2005; Jenkinson et al 2013; Brittain and Brown 2014).

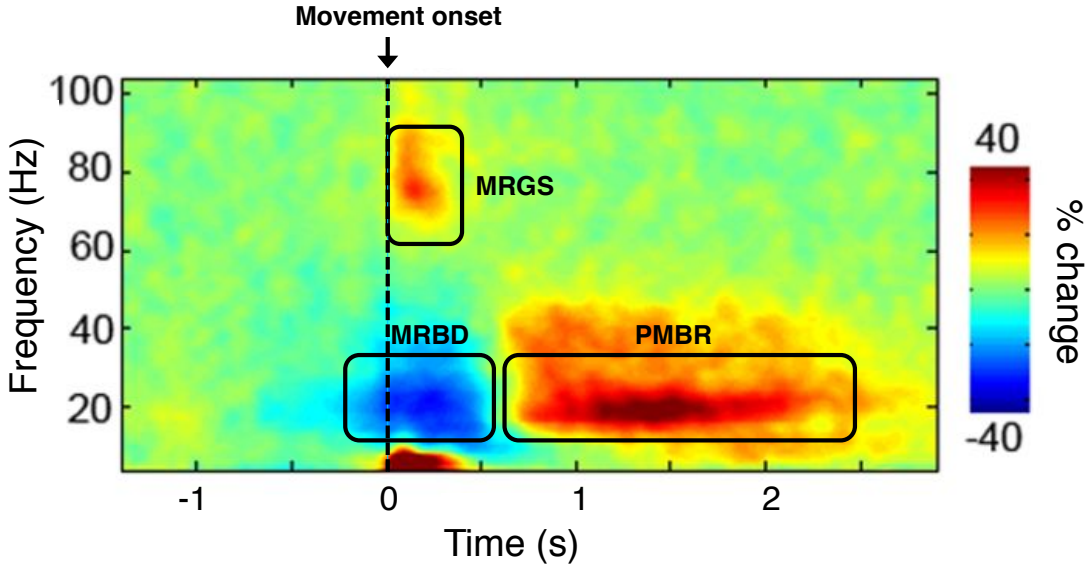


Figure 1.6 Grand average time-frequency spectrogram

Grand average time-frequency plot showing source-level oscillatory amplitude changes following index finger movement. Spectrogram is displayed as the percentage change from the prestimulus baseline. Abbreviations: MRBD, movement-related beta desynchronisation; MRGS, movement-related gamma synchronisation; PMBR, post-movement beta rebound. (Adapted and modified from Muthukumaraswamy et al 2013)

1.3.1 Functional significance

1.3.1.1 β-frequency oscillations

β oscillations have been broadly classified as antikinetic, based on the characteristic desynchronisation in this frequency band prior to and during movement and their association with slower voluntary movements both in healthy populations (Gilbertson et al 2005) and in patients with Parkinson's disease (Brown 2003; Hammond et al 2007). Moreover, direct manipulation of β oscillations via the application of transcranial alternating current stimulation (tACS), an approach with experimentally-supported efficacy in the modulation of brain oscillations (Reato et al 2010; Thut et al 2011; Helfrich and Schneider 2013), slows down movement velocity, suggesting a causal role of β oscillatory activity in motor control (Pogosyan et al 2009; Joundi et al 2012a; Wach et al 2013a). The classification of motor β oscillations as antikinetic seems to be an oversimplification, though, as it does not capture its influence on sensory and cognitive aspects of motor control. For example, MRBD has been shown to be strongly associated with the selection and certainty of the pending movement (Tzagarakis et al 2010; Tzagarakis et al 2015) as well as the complexity of motor plan (Heinrichs-Graham and Wilson 2015), whereas PMBR has been suggested to serve as an index of confidence in feed-forward estimations of sensorimotor control (Tan et al 2016). In general, β activity can be more accurately considered as an immutability rhythm that promotes the current state over novel action selection (Brittain and Brown 2014). This view is consistent with the proposed unified function of β activity, which, irrespective of brain region where it is found, may reflect the *status quo*, i.e., the maintenance of the current sensorimotor or cognitive state (Engel and Fries 2010). Further, a degree of synchrony in the β-frequency band has been suggested to be of key importance in gating computation across neuronal populations (its optimal level within a population is

dynamic, i.e., context- and task-dependent), which in turn may constitute a mechanism of action selection and maintenance (Brittain et al 2014).

Cortical β oscillations have been suggested to have a potential role as a neurophysiological marker of motor system function both in healthy (Takemi et al 2013; Takemi et al 2015; Espenhahn et al 2017) and clinical populations, including Parkinson's disease (Pollok et al 2012; Heinrichs-Graham et al 2014), stroke (Rossiter et al 2014a) and ALS (Proudfoot et al 2017). The utility of β-frequency oscillations as biomarkers has been supported by recent evidence demonstrating that power measures of movement-related β oscillations display high intra-individual reliability over time, thus validating the notion that these measures reflect meaningful and reliable individual differences in the motor system that can be utilised as biomarkers in basic research and clinical studies (Friedrich et al 2013; Espenhahn et al 2017).

1.3.1.2 γ-frequency oscillations

The functional roles of human γ-frequency oscillations have been extensively studied in non-motor cortical areas, particularly in the visual domain (Siegel et al 2007; Adjamian et al 2008; Swettenham et al 2009; Edden et al 2009; Hermes et al 2015). With respect to the motor cortex γ oscillations, our understanding of their precise functional significance is currently very limited. In contrast to motor β-band activity, γ-frequency oscillations are synchronised just prior to and during phasic movements (Crone et al 1998; Pfurtscheller and Lopes da Silva 1999; Cheyne et al 2008; Muthukumaraswamy 2010) and are absent during the sustained phase of isometric movements (Muthukumaraswamy 2010; Muthukumaraswamy 2011). In Parkinson's disease, motor γ-band activity is increased following treatment with levodopa (Brown et al 2001; Alegre et al 2005; Androulidakis et al 2007), which, in turn, is correlated with the degree of improvement in bradykinesia-rigidity (Litvak et al 2012). Moreover, γ activity has been suggested to serve as a compensatory mechanism to counteract

bradykinetic movements sustained by increased β activity in the cortico-striatal loop (Florin et al., 2013). In addition, a recent study has provided evidence of association between motor cortical γ oscillations and a hyperkinetic state (i.e., dyskinesia) in Parkinson's disease (Swann et al 2016). Overall, these findings provide support for the hypothesis that motor γ oscillations serve as a prokinetic rhythm.

Importantly, recent studies employing tACS to manipulate motor cortical γ oscillations have proved particularly valuable in establishing a causal, rather than correlational, relationship between motor cortical γ oscillations and behaviour. Specifically, it was demonstrated that γ-frequency tACS applied to M1 significantly improves motor performance, thus providing the first direct evidence on the causal role of prokinetic γ rhythm in motor control (Joundi et al 2012; Santarnecchi et al 2017).

Overall, the prokinetic role of motor γ oscillations demonstrated both in healthy and clinical populations lays the theoretical ground to employ γ-frequency tACS in order to increase endogenous γ activity, which may prove beneficial in patients with bradykinetic movement disorders.

Nevertheless, similarly to the previously discussed functions of motor cortical β oscillations, referring to motor γ oscillatory activity as prokinetic does not fully reflect its functional complexity. Motor γ oscillations have been suggested to serve as a computational mechanism for sampling peripheral data to properly guide subsequent motor acts (MacKay 1997; Cheyne et al 2008; Santarnecchi et al 2017). This could be achieved by providing a coding scheme of a high temporal resolution that enables fast processing and flexible routing of activity, supporting fast selection and binding of distributed responses, important for online motor control (Fries et al 2007). Another line of research has provided evidence that motor cortical γ-band activity is strongly related to the ongoing motor control and decision-making processes and thus it is likely to be important in response selection and maintenance of an evolving motor plan (Donner et

al 2009; Gaetz et al 2013). In addition, motor γ activity has also been shown to correlate with specific kinematic parameters, such as the speed and scale of voluntary movements (Brucke et al 2012; Joundi et al 2012b), as well as arousal (Kempf et al 2009). Furthermore, it has been recently proposed that rather than being a simple indicator of the global state of arousal or coding for specific kinematic parameters, motor γ oscillations determine response vigour or effort (Jenkinson et al 2013).

Finally, outside the motor network γ oscillations have been shown to predict subsequent learning (Sederberg et al 2006; Headley and Weinberger 2011) and are potentially important regulators of spike timing-dependent plasticity (STDP) (Wespatat et al 2004; Axmacher et al 2006). Based on these findings, as well as a vital role of M1 in the acquisition and consolidation of a motor sequence (Doyon and Benali 2005; Robertson et al 2005; Hardwick et al 2013), it is reasonable to propose that γ-frequency oscillations in M1 play an important role in motor learning in humans. Testing this hypothesis is a secondary objective of the work presented in this thesis (section 1.5).

1.3.2 Mechanisms

Crucial to understanding the precise role of motor β and γ oscillations is an identification of the underlying neural mechanisms. Over the past few decades, various techniques have been used to elucidate the mechanistic basis of these rhythms (Figure 1.7). The current state of knowledge and the questions that remain to be answered, particularly with relation to human motor β and γ oscillations, will be discussed below separately for each frequency band (starting from γ oscillations, which have been studied most extensively).

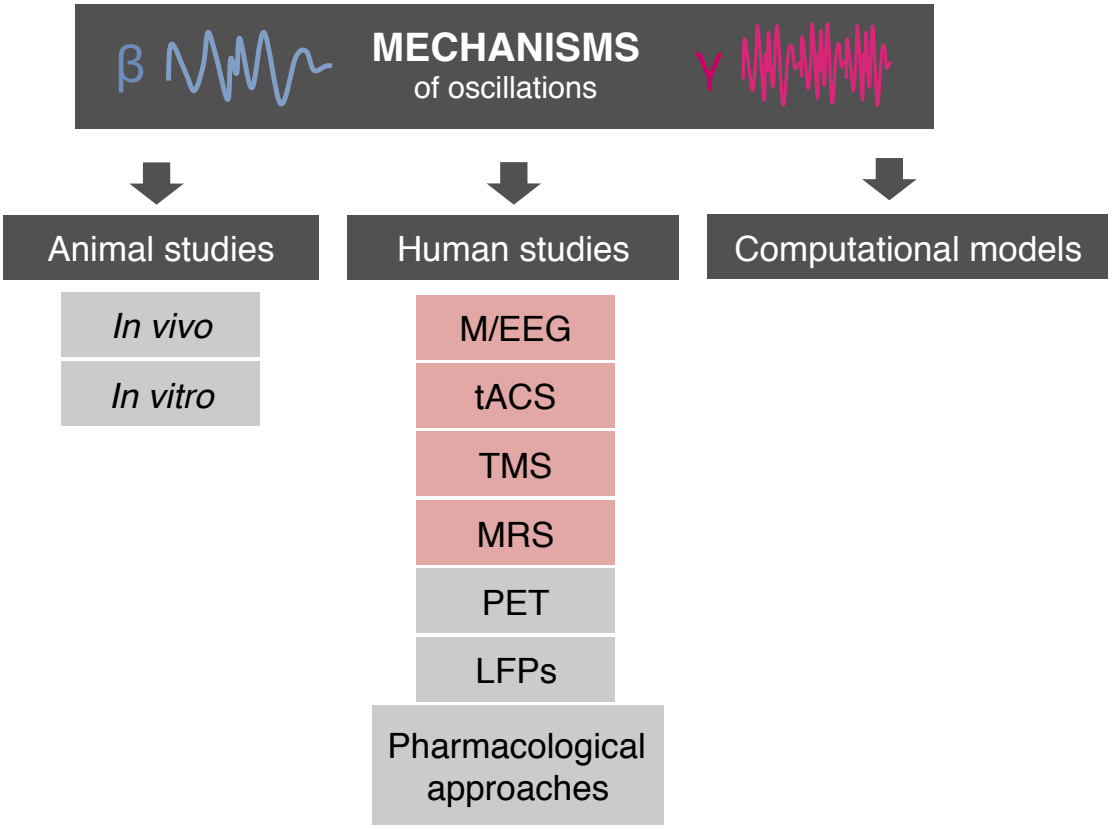


Figure 1.7 Methods used to study β and γ oscillations

A summary of methods used to study mechanisms underlying β and γ oscillations (as well as other frequency bands). The methods highlighted in red represent techniques used in this thesis. Abbreviations: EEG, electroencephalography; LFPs, local field potentials; MEG, magnetoencephalography; MRS, magnetic resonance spectroscopy; PET, positron-emission tomography; tACS, transcranial alternating current stimulation; TMS, transcranial magnetic stimulation.

1.3.2.1 γ-frequency oscillations

From the mechanistic point of view, γ-band activity has been the most extensively studied rhythm. The majority of the work focused on investigating γ oscillations in the rodent hippocampus *in vivo* or in slice preparations (Chrobak and Buzsáki 1996; Traub et al 1996; Wang and Buzsáki 1996). The latter one, in particular, has allowed for both pharmacological and genetic manipulations aimed at identifying the mechanisms underlying neural oscillations. This work then informed computational modelling which identified the dynamical properties determining both frequency and synchronisation

properties (Buzsáki and Wang 2012). As a result of the theoretical work, two key mechanisms that can produce γ-band oscillations have been put forward: (i) the "interneuronal network gamma" (ING) mechanism, also referred to as the I-I, inhibitory-inhibitory, model; and (ii) the "pyramidal–interneuronal network gamma" (PING) mechanism, also known as the E-I, excitatory-inhibitory, model (Whittington et al 2000; Tiesinga and Sejnowski 2009).

The ING-mechanism refers to γ oscillations generated purely as a result of interactions between inhibitory interneurons. ING oscillations arise when a reciprocally connected population of interneurons receives an exogenous excitatory drive (which does not need to be oscillatory). When this drive fires a sufficient number of interneurons simultaneously, they temporarily silence each other and come out of inhibition around the same time, priming them to fire synchronously again. Across several cycles of this, a substantial portion of the network becomes synchronised (Wang and Buzsáki 1996). These oscillations have been observed in hippocampal slice preparations, where the AMPA and NMDA synaptic inputs from pyramidal cells are blocked, and they are abolished if a GABAergic antagonist is applied (Van Vreeswijk et al 1994; Whittington et al 1995). The kinetics of the $GABA_A$ receptor and hence the inhibitory postsynaptic potentials (IPSPs) is a main player in determining the synchronisation properties, including the frequency of oscillations (Traub et al 2003; Traub et al 2004).

γ oscillations can also emerge via the PING mechanism, which employs two different populations of cells: one excitatory and one inhibitory, reciprocally connected to each other (Wilson and Cowan 1972; Ermentrout and Kopell 1998; Whittington et al 2000; Börgers and Kopell 2003). The AMPAergic projections of local pyramidal cells provide the excitatory drive to inhibitory interneurons, which temporarily silence the network by providing feedback inhibition to pyramidal cells and interneurons through GABAergic synapses (Börgers and Kopell 2003). As this inhibition wears off, pyramidal cells regain the ability to fire. The excitatory firing results, a short delay later, in inhibitory firing, thus

bringing the network into an oscillatory state. For this oscillatory state to happen, the strength of inhibition and excitation needs to be properly balanced. The short delay between excitatory and inhibitory firing (composed of both axonal conduction and synaptic delays) is the crucial factor for determining the oscillatory properties in this network (Leung 1982; Börgers and Kopell 2003). Both hippocampal and cortical microcircuits seem ideally suited to produce PING *in vivo* as interneurons are embedded in a network with pyramidal cells and the connection probability between neighboring pyramidal cells and interneurons has been estimated at ~50–60% (Bartos et al 2007; Perrenoud et al 2016).

Given the importance of inhibitory interneurons in generating γ oscillations, multiple efforts have been made to identify different types of inhibition and their involvement in this type of rhythmic activity. As a result, inhibitory interneurons have been broadly classified as fast-spiking (FS) versus non-fast-spiking, and soma-targeting versus dendrite-targeting. Several lines of evidence indicate that FS, soma-targeting basket cell interneurons (specifically, those that express parvalbumin [PV]) are crucial in the generation of γ rhythms (Bartos et al 2007). These cells are abundant (Freund and Buzsaki, 1996), form extensive interconnections amongst one another (Gulyás et al 1999), and a single basket cell can project onto more than one thousand pyramidal cells (Cobb et al 1995). These conditions enable basket cells to impose their γ rhythm onto a pyramidal cell network; the population activity of the pyramidal cells is then reflected in the LFP and MEG signal. Finally, fast-spiking PV basket cells have resonance properties in the γ range and show the greatest entrainment by γ-frequency activity (Pike et al 2000; Cardin et al 2009; Otte et al 2010).

Despite the strong evidence from animal and modelling studies showing a link between $GABA_A$-mediated inhibition and γ oscillations, the results from human studies are currently inconclusive. For example, administration of benzodiazepines, which increase

GABAergic drive, has no effect on spontaneous γ power nor MRGS, as measured using MEG in human M1 (Hall et al 2011). It is worth noting, though, that the resting-state γ activity is very low and inconsistent and therefore difficult to detect with approaches such as MEG. In terms of MRGS, it has been shown to appear stronger in earlier trials in a sequence (Muthukumaraswamy 2010) and this fluctuation may have been influential when changes in MRGS over extended trials were taken into account (Hall et al 2011). MRGS is also unaffected by tiagabine, a selective GABA reuptake inhibitor (Muthukumaraswamy et al 2013b). Similarly, no relationship was found between M1 GABA concentration, as measured using MRS, and MRGS power (Gaetz et al 2011). In contrast, a significant correlation was reported between M1 GABA levels and MRGS frequency (Gaetz et al 2011).

1.3.2.2 β-frequency oscillations

Typically, β oscillations are considered to be generated by similar mechanisms as the γ rhythm. Prior modelling and experiments, primarily from slice recordings, demonstrated that β rhythms can emerge from the interactions of local excitatory and inhibitory populations, the mechanism sometimes referred to as a pyramidal-interneuronal network β mechanism (PINB) (Kopell et al 2000; Roopun et al 2006; Yamawaki et al 2008; Kramer et al 2008). A key factor in β activity generation in these studies was the recruitment of the M-type potassium current (a type of post-hyperpolarization potassium current) in the pyramidal neurons. The suprathreshold activation of the M-current sets the firing time of the pyramidal neurons in mutually coupled excitatory and inhibitory networks (Roopun et al 2006; Yamawaki et al 2008; Kramer et al 2008). Similarly to γ oscillations, the PINB mechanism, however, cannot fully explain how β activity emerges. For example, benzodiazepines increase β oscillation amplitude and decrease the oscillation frequency (Jensen et al 2005; Hall et al 2010b; Hall et al

2011). If β activity was driven purely by a PING mechanism, the net effect on network frequency would be negligible since increasing GABAergic conductances has the effect of decreasing the spiking frequency of the inhibitory cells, thus allowing more of the excitatory cells to fire, which in turn then excites the inhibitory cells more, leading to an equilibrium. In contrast, the mechanism based on the interactions between inhibitory interneurons – the interneuronal network beta (INB) – is able to explain these findings. In this mechanism, the period of the inhibitory cells' firing is determined only by the recurrent inhibitory connections. Therefore, administration of benzodiazepines increases the inhibitory drive of GABAergic interneurons via $GABA_A$ receptors, whereby the IPSP decay-time is lengthened, thereby reducing the frequency of the locally oscillating neuronal network population. Consequently, as the period of the inhibition becomes longer, a larger fraction of pyramidal cells will be released from inhibition during the refractory period. This gives rise to an increase in the amplitude of the oscillatory power, as the participating neuronal pool is increased. This explains the increase in β power in M1 and decrease in frequency with benzodiazepines in sensorimotor areas observed in humans (Jensen et al 2005). In agreement with these findings, the application of picrotoxin, $GABA_A$ receptor antagonist, to motor cortical slices *in vitro* eliminated β-band oscillations (Yamawaki et al 2008). Accordingly, even though the relation between motor cortical oscillatory activity and the spiking activity of single neurons can be complex (Murthy and Fetz 1996), it was found that there is a strong negative correlation between pyramidal neurons spiking rate and β-band power across motor cortical recording sites (Spinks et al 2008). It was also shown that tiagabine (a GABA reuptake inhibitor) increases amplitude of baseline β power (Muthukumaraswamy et al 2013b), suggesting a positive relationship between β power and GABA activity.

The majority of studies on β activity investigated the mechanisms underlying the role of power. In humans, however, it remains unclear whether GABA activity can influence β

peak frequencies in the sensorimotor cortex at rest and without pharmacological modulation. Magnetic resonance spectroscopy (MRS) is a useful approach to address this question as it offers a non-invasive method for *in vivo* quantification of endogenous neurotransmitter concentrations in spatially restricted cortical regions. Recently, a significant positive correlation was found between MRS-assessed GABA concentration and β peak frequency at rest in the sensorimotor cortex (Baumgarten et al 2016).

The main focus of the aforementioned studies was the mechanisms underlying the generation and modulation of ongoing resting-state β activity, primarily in the motor cortex. The mechanisms underlying movement-related β activity have been less explored. A recent study, which utilised pharmaco-MEG approach, showed that diazepam, a type of benzodiazepine, increases MRBD and has no effect on PMBR, suggesting that only MRBD is dependent on GABAergic drive (Hall et al 2011). Since GABAergic drive has been known to enhance oscillatory activity, the mechanism by which it would facilitate desynchronisation is unclear. However, it has been suggested that this phenomenon may not be a reflection of direct GABA-mediated desynchronisation in M1, but rather reflects a facilitation of a remote network resulting in desynchronisation in M1 (Hall et al 2011). In another study, a significant positive relation was observed between M1 GABA concentration and PMBR power (Gaetz et al 2011).

Our understanding of the mechanisms underlying movement-related oscillatory activity in the motor cortex has been significantly improved by transcranial magnetic stimulation (TMS), a valuable tool used to assess the excitability state of the corticospinal and intracortical pathways. It was found that corticospinal excitability is increased shortly prior to and during a self-paced finger movement, i.e., during the sequence of cortical processes that are associated with MRBD recorded from the

same cortical areas (Chen et al 1998). In contrast, PMBR, found after termination of movement, corresponds to a period of decreased corticospinal excitability (Chen et al 1998), suggesting an association between PMBR and selective deactivation of the motor cortex. In addition, tiagabine, the GABA reuptake inhibitor, was shown to enhance MRBD and reduce PMBR (Muthukumaraswamy et al 2013b). Based on these and a range of other studies, it has been proposed that MRBD may be $GABA_A$-mediated process whereas PMBR may be $GABA_B$-receptor mediated (Hall et al 2011; Muthukumaraswamy et al 2013b).

1.4 Principles of plasticity

Neural plasticity can be defined as the ability of the nervous system to reorganise its structure, function and connections in response to experience and use. Plasticity is of relevance in this thesis for the two primary reasons. Firstly, neural oscillations, particularly at γ-frequency range, are potentially important regulators of synaptic plasticity, which in turn plays a vital role in motor learning and functional recovery after a brain injury, such as stroke (Wespatat et al 2004; Axmacher et al 2006; Dayan and Cohen 2011; Takeuchi and Izumi 2013). Secondly, plastic changes are frequently invoked to explain the effects induced by prolonged application of various brain stimulation approaches, including tACS (Zaghi et al 2010a; Moliadze et al 2010; Veniero et al 2015), a tool used here to drive cortical oscillations.

Hebbian and homeostatic plasticity, the two major forms of plasticity in the nervous system, will be briefly discussed below.

1.4.1 Hebbian plasticity

It is widely believed that learning and memory are mediated through strengthening of connections between co-active cells, the process known as Hebbian plasticity: *"*When an axon of cell A is near enough to excite a cell B and repeatedly or persistently takes part in firing it, some growth process or metabolic change takes place in one or both cells such that A's efficiency, as one of the cells firing B, is increased*"* (Hebb 1949). The reverse of Hebb's postulate, i.e., the weakening of a synapse, also occurs and is necessary to optimise information storage in a neural network (Stent 1973; Sejnowski 1977; Bienenstock et al 1982; Malenka 1993). Associative synapse strengthening and weakening are implemented at many synapses by long-term potentiation (LTP) and long-term depression (LTD). LTP occurs when presynaptic spikes (and associated excitatory postsynaptic potentials [EPSPs]) precede postsynaptic spikes by ~0 to 20 ms (defined as positive Δt), and LTD occurs when postsynaptic spikes lead presynaptic spikes and EPSPs by ~0 to 20-100 ms (negative Δt), with a sharp (1-5 ms) transition between LTP and LTD (Levy and Steward 1983; Markram et al 1997; Bi and Poo 1998). This dependence is known as Hebbian spike timing-dependent plasticity (STDP) (Figure 1.8) (Song and Abbott 2001). However, other, non-canonical, forms of STDP also exist (Feldman 2012).

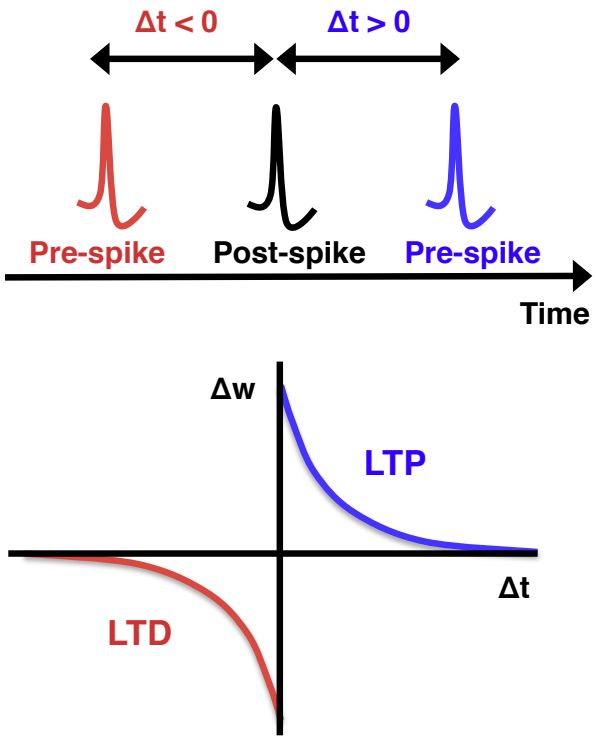


Figure 1.8 The schematic of STDP

The schematic of STDP showing LTP and LTD according to the time-interval between the pre- and post-spikes. Δw, change in synaptic weight; Δt, change in time.

The mechanisms of LTP/LTD vary depending on the brain region. In the neocortex, they are strongly dependent on alterations in glutamatergic and GABAergic transmission (Trepel and Racine 2000), such as changes in receptor configuration and density in the postsynaptic membrane, as well as changes in the pre-synaptic release of neurotransmitters (Citri and Malenka 2008).

Motor learning, recovery after stroke, and neurorehabilitation all depend on the plasticity of neurons and circuits within the motor system and may in fact be mediated by similar neocortical mechanisms of plasticity (Matthews et al 2004). Converging evidence from animal and human studies has demonstrated that the likely substrate for implementing plasticity in M1 is the system of horizontal connections that spans the region, which has been shown to functionally associate M1 neurons to form assemblies

that construct dynamic motor maps (Jacobs and Donoghue 1991; Huntley 1997). The existence of these normally hidden motor maps has been revealed by reducing local and systemic GABAergic transmission, which unmasks horizontal connections most likely blocked by feed-forward inhibition (Jacobs and Donoghue 1991; Ziemann et al 1998b).

1.4.2 Homeostatic plasticity

The positive feedback nature of synaptic plasticity that allows the "rich to get richer" in the case of LTP and the "poor to get poorer" in the case of LTD generates a powerful destabilising force on network function (Turrigiano and Nelson 2000; Abbott and Nelson 2000). Homeostatic plasticity is a form of plasticity that counteracts the destabilising influence of synaptic plasticity by stabilising neural activity within a physiologically reasonable range (Karabanov et al 2015). According to the most influential model of homeostatic plasticity, i.e., Bienenstock-Cooper-Munro (BCM) model, the thresholds for induction of LTP and LTD are dynamically adjusted to the integrated level of previous post-synaptic activity (Bienenstock et al 1982; Karabanov et al 2015). Accordingly, a history of high synaptic activity will shift the synaptic modification threshold favouring the induction of LTD and increase the threshold for LTP. This "sliding threshold" will be adjusted in an opposite manner at a synapse with a history of low post-synaptic activity (Figure 1.9). Since it was first introduced, the BCM model has been supported in a range of animal and human studies and in many brain regions (Wang and Wagner 1999; Hamada et al 2009; Cooper and Bear 2012).

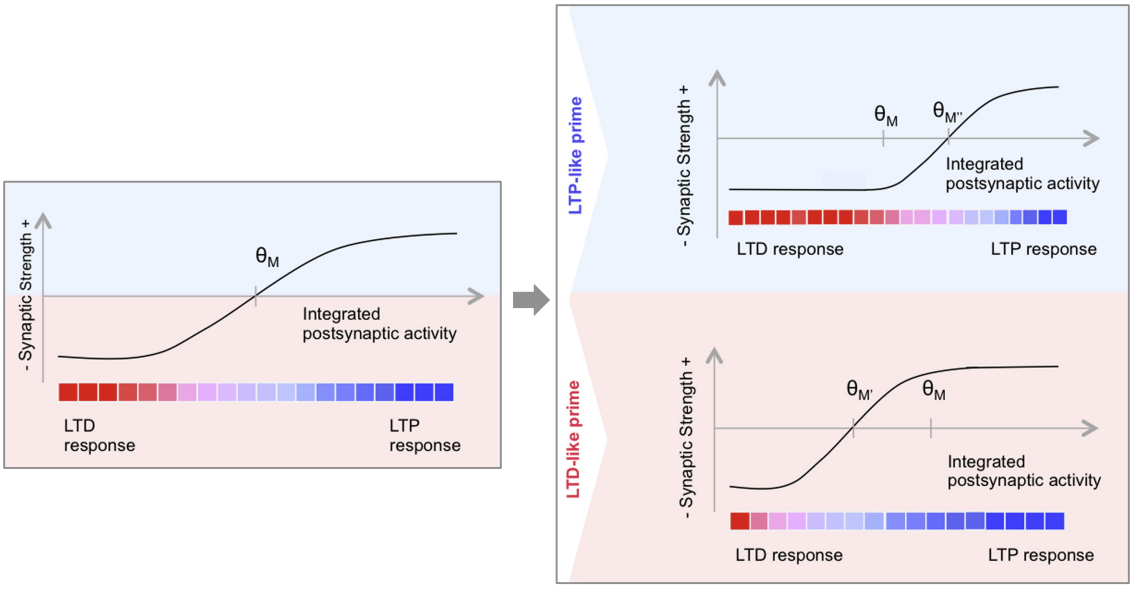


Figure 1.9 The bidirectional shift of LTP-LTD induction curve predicted by the BCM theory

The LTD-LTP crossover point (θ_M; left) slides to the right on the x-axis if the preceding neuronal activity is high ($\theta_{M''}$; top right), and to the left if preceding activity is low ($\theta_{M'}$; bottom right). (Adapted from Karabanov et al 2015)

In the human M1, homeostatic plasticity has been induced using non-invasive stimulation techniques (Siebner et al 2004; Nitsche et al 2007; Müller et al 2007; Batsikadze et al 2013). In these studies, homeostatic patterns have been examined using a priming-test approach, consisting of a priming stimulation protocol that triggers a homeostatic response in M1 and a test stimulation protocol that captures the response (Karabanov et al 2015; Müller-Dahlhaus and Ziemann 2015). Priming activity is usually implemented some time before the application of the test protocol. However, a break between the two stimulation protocols is not always necessary to induce homeostatic-like effects (Mockett et al 2002; Gentner et al 2008; Rothkegel et al 2010). For example, continuous theta burst stimulation (cTBS) applied to the human M1 led to an increase in corticospinal excitability, but the opposite effect was observed when the stimulation duration was doubled (Gentner et al 2008).

1.5 Aims

The primary aim of this thesis is to investigate the mechanisms underlying human motor cortical β- and γ-frequency oscillations. To this end, I will employ novel multimodal approaches involving a combined tACS-TMS and tACS-7T MRS, as well as a sequential MEG-TMS design.

In Chapter 2 I will describe the transcranial stimulation techniques applied in this thesis, whereas in Chapter 3 I will outline details of the neuroimaging techniques used. The first experimental chapter (Chapter 4) will examine the effects of driving β and γ oscillatory activities using tACS on TMS-assessed physiological measures in M1. In particular, I will test the hypothesis that β tACS leads to an increase in local synaptic $GABA_A$ activity and γ tACS has the opposite effect. Further, I will aim to assess whether tACS-induced changes in $GABA_A$ inhibition are related to individual differences in motor learning performance. Chapter 5 will build upon this work, further exploring the mechanisms underlying the exogenously driven β activity. To this end, I will examine the effects of β tACS on various physiological measures, as assessed by TMS applied at different phases of tACS, both at rest and during movement preparation.

In Chapter 6, the effects of driving β oscillatory activity will be directly evaluated by measuring local changes in concentrations of GABA and glutamate *in vivo* in M1 using 7T MRS. Finally, in Chapter 7 I will employ a sequential MEG-TMS design to investigate whether the spontaneous and movement-related cortical β and γ oscillations are related to various TMS-assessed physiological measures. As a secondary objective, the relationship between motor cortical β and γ activity and an individual's performance in a motor learning task will be assessed.

CHAPTER

2

Transcranial stimulation techniques

The work within this thesis relies upon two non-invasive stimulation techniques: transcranial alternating current stimulation (tACS) and transcranial magnetic stimulation (TMS). In this Chapter, tACS and TMS are discussed as valuable tools to modulate cortical activity and measure physiological changes, respectively. Moreover, the concurrent use of both techniques is discussed with the main focus on the human primary motor cortex.

2.1 Transcranial alternating current stimulation (tACS)

2.1.1 Background

Transcranial electrical stimulation is the overarching term for a class of non-invasive brain stimulation techniques that induce neuromodulatory effects on the human cortex through the use of electric current applied via scalp electrodes. Among these techniques, transcranial direct current stimulation (tDCS) has received the most study and attention in the recent years (Paulus 2011). Because of the positive results shown by tDCS studies, attention has recently also turned to a new parameter of transcranial electric stimulation (tES), namely stimulation with alternating currents (AC). Although the idea of using tES with AC is not new (Zaghi et al 2010a), it is a low-intensity AC consisting of biphasic waves that has witnessed a renaissance in the past decade due to its ability to modulate physiologically relevant brain oscillations in a frequency-specific manner. Following the application of low-intensity AC via a similar montage as that used in tDCS by Antal and colleagues, this type of stimulation has started been appropriately referred to as transcranial alternating current stimulation (tACS) (Antal et al 2008).

2.1.2 Basic principles

tACS can induce sinusoidal fluctuations of the membrane potential by the alternating current between the two electrodes (Reato et al 2013) (Figure 2.1). Modern tACS utilises a very low amplitude alternating current of up to 2 mA (peak-to-peak) generated by a battery-powered device and applied via two or more scalp electrodes. Much like tDCS, it is possible to use many different electrode placements on the head, as well as high-definition tACS in order to stimulate more focal brain regions (Heise et al 2016).

For studies involving the motor system, the optimal placement of the M1 electrode is often identified by TMS localisation of the motor hotspot.

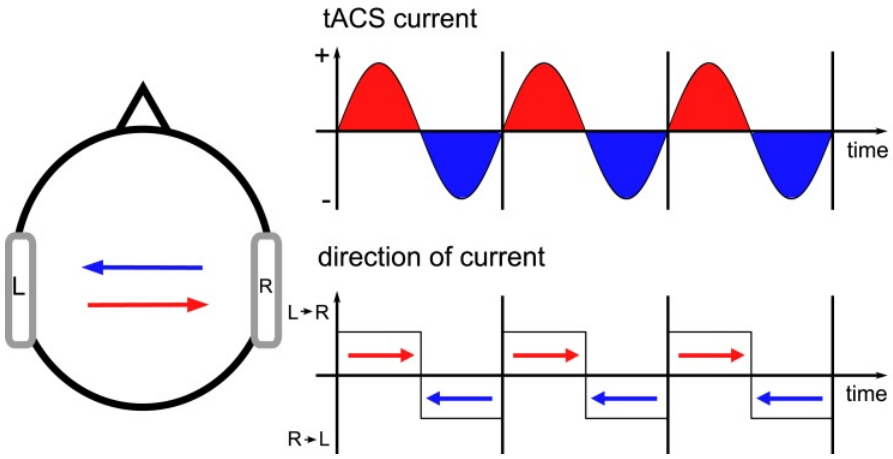


Figure 2.1 Current flow during tACS

When current is applied sinusoidally, the direction of current flow alternates back and forth by 180° for every half-wave. As illustrated here, during the positive half-wave, the left stimulation electrode represents the anode of tDCS with variable amplitude. During the negative half-wave, the direction of current flow suddenly flips by 180°. During each half-wave the direction remains stable but the strength of the current flow varies. Stimulation electrodes are depicted in grey. (Figure adapted from Neuling et al 2012).

The effects of tACS are strongly dependent on several major parameters, such as current density, duration and frequency of stimulation, as well as the underlying cortical activity, as will be discussed later.

2.1.3 Modelling and validating current flow

A number of modelling studies investigated how much current arrives intracranially as a result of extracranial electric stimulation (Neuling et al 2012b; Heise et al 2016; Huang et al 2017). For example, based on a fine-grained finite element model, it was shown that 1 mA of tACS/tDCS applied to the human visual cortex via two electrodes (size: 7 cm × 5 cm) results in an intracranial current density of 0.1 A/m^2 amounting to a cortical electric field of ~0.4 V/m (Neuling et al 2012b). The focality of the stimulation,

however, can be significantly enhanced by using the so-called 4 × 1 ring electrode configuration (Datta et al 2009; Heise et al 2016) (Figure 2.2).

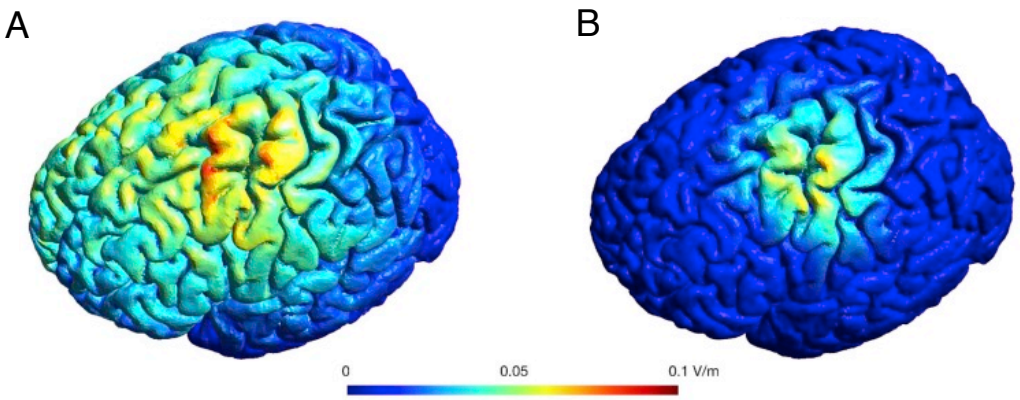


Figure 2.2 Electrical field simulation for the classic and the ring montage

Electrical field simulation for exemplary participant for the classic montage (**A**) and for the ring montage (**B**) with 20 Hz tACS of 400 µA intensity. (Adapted from Heise et al 2016)

Importantly, an *in vivo* intracranial recording was recently performed in humans to directly validate the computational models (Huang et al 2017). Transcranial sinusoidal alternating current was applied to ten patients (undergoing invasive monitoring for epilepsy surgery) through two electrodes placed medially over the frontal and occipital regions. The maximal electric field magnitude of approximately 0.4 V/m was reported when applying 2 mA transcranially, which is at the lower limit of effectiveness in animal studies. This is approximately half as strong as previous predictions using computational models. For the specific electrode montage tested, peak intensities were achieved under the stimulation electrodes and in deep midline structures, where current was shunted to through highly conductive cerebrospinal fluid (CSF).

2.1.4 Stimulation parameters

2.1.4.1 Frequency

In the majority of tACS studies, behavioural and electrophysiological amplification has been typically only elicited at a single stimulation frequency, which tends to be the frequency that dominates electrophysiological recordings of un-stimulated subjects during similar behavioural states. The case where the stimulation frequency is matched to the frequency of the neural oscillation is the most relevant scenario for controlled interaction with the underlying oscillator, representing an ideal condition for entrainment (Thut et al 2011).

The frequency-specificity of tACS effects has been demonstrated in a large number of human (Pogosyan et al 2009; Feurra et al 2011b; Feurra et al 2011a; Joundi et al 2012a; Cabral-Calderin et al 2015; Guerra et al 2016; Nakazono et al 2016), animal (*in vivo* and in slices) (Reato et al 2010; Reato et al 2013) and simulation studies (Fröhlich and McCormick 2010; Merlet et al 2013; Ali et al 2013). For example, Feurra and colleagues showed that tACS applied to the motor cortex at β-frequency, but not at other frequencies, directly influenced motor cortex physiology (Feurra et al 2011a). Further, in the somatosensory and visual systems, tACS only elicited behavioural effects at frequencies similar to those recorded from the cortex during analogous sensory stimulation (Kanai et al 2008; Feurra et al 2011b). Therefore, it is clear that the choice of stimulation frequency relative to the endogenous oscillations frequency plays a key role in determining the effect of stimulation.

2.1.4.2 Power of endogenous oscillations

Recently, it has also been demonstrated that the power of endogenous oscillations has a critical impact on tACS efficacy (Neuling et al 2013). Neuling and colleagues modulated the power of endogenous occipital α oscillations via tACS applied at individual α-frequency. They showed that under conditions of low endogenous α power, tACS enhanced α power, whereas under conditions of high endogenous α power, tACS failed to influence α power. One possible explanation proposed was that under conditions of high endogenous α power, the oscillatory activity at this frequency could not be further enhanced by tACS due to ceiling effects. Another explanation would suggest that low-intensity oscillating currents introduced to the brain by tACS are not strong enough to modulate high-power endogenous oscillations, but only low-power endogenous oscillations. Application of 1 mA of tACS results in the similar amount of an electric field in occipital areas as the amount of α power measured during intracranial recordings taken from the visual cortex of wake behaving monkeys during eyes open (Bollimunta et al 2008; Neuling et al 2012b), which most likely represented the case of low endogenous α power. With eyes closed, the power of endogenous α oscillations are increased by more than twice compared with the power with eyes open (Könönen and Partanen 1993). Based on these findings, it was further argued that stimulation intensities more than twice as high as used in the study by Neuling and colleagues would be required to enhance α power under conditions of high endogenous α power. In conclusion, a neuronal network with strong oscillatory power should not be as prone to a certain external periodic force as a network with weaker oscillatory power.

2.1.4.3 Intensity

The effect of tACS intensity on physiological parameters and behaviour has not been systematically assessed. A recent experiment showed that changes in corticospinal excitability depend non-linearly upon the intensity of tACS (Moliadze et al 2012). M1 was stimulated with tACS at 140 Hz and single-pulse motor evoked potentials (MEPs) were recorded at various time points after stimulation offset. Low stimulation intensities of 0.2 mA resulted in a decreased corticospinal excitability, high intensities of 1 mA had the opposite effect, whereas intermediate intensities of 0.6 and 0.8 mA had no effect. This suggests that the stimulation at lower intensity may have preferentially activated intracortical inhibitory networks of corticospinal neurons, thus resulting in net inhibition of MEP amplitude. However, the possibility that stimulation at lower intensity may have inhibited intracortical facilitatory influences of corticospinal motor neurons cannot be excluded. At intermediate intensities, inhibitory and excitatory effects may have cancelled each other out. In addition, this study only assessed the after-effect of different intensities of 140 Hz tACS. It remains to be tested whether these results could be replicated also during stimulation and, importantly, at lower frequencies (< 100 Hz) of stimulation.

From a broader neuronal network perspective, it was demonstrated that at higher stimulation intensities an increasingly larger population of neurons was recruited and the range of stimulation frequencies that successfully entrained the network broadened (Ozen et al 2010; Merlet et al 2013; Ali et al 2013; Schmidt et al 2014), suggesting that the ability of stimulation to drive network activity may be less constrained by the natural frequency of an area at higher intensities. However, this concept remains to be directly tested in human experiments.

2.1.5 Mechanism of action

Significant progress has been made in our understanding of the mechanisms that underlie the effects of tACS, though these are not yet completely clarified. The most significant data will be discussed below, with a focus on human studies.

2.1.5.1 Entrainment by a periodic external drive – general concepts

According to a conceptual approach that originated from physics, oscillating elements, including neuronal oscillators, can become synchronised to or, in other words, entrained by, an external force (Winfree 1980; Pikovsky et al 2003). tACS is a rhythmic type of stimulation and can be considered as an example of the external force. The effects of the external force on ongoing oscillations depend on: the amplitude of the stimulation (relative to the amplitude of the endogenous oscillation), the phase of the stimulation (relative to the phase of the endogenous oscillation), the duration of stimulation, and the frequency of stimulation (relative to the frequency of ongoing neural oscillation) (Thut et al 2011). An ideal condition for entrainment occurs when the stimulation frequency is matched to the frequency of the neural oscillation. In this scenario, on the level of the populations of oscillators (as recordable with EEG/MEG), in-phase adjustment as well as amplitude increase would occur (Figure 2.3). This phenomenon has been demonstrated in a number of computational, animal and human studies, as discussed in the subsequent sections.

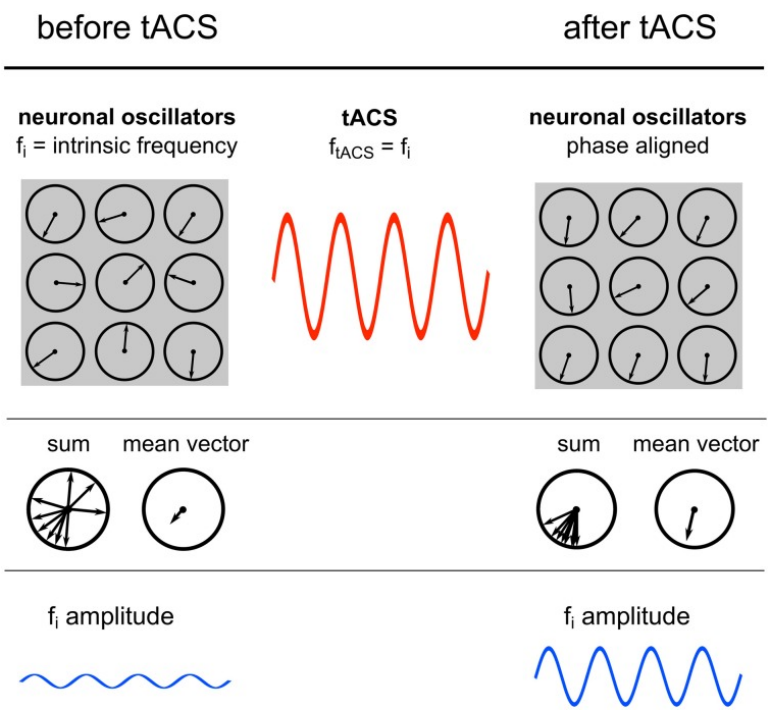


Figure 2.3 Power increase by synchronisation

Upper row: Single neuronal oscillators, depicted as vectors on a unit circle, with a specific intrinsic frequency synchronise to an external sinusoidal force with the same frequency. Middle row: The mean resultant vector of the single oscillating elements represents the amplitude of the oscillations. Due to phase alignment of each single oscillator to the external oscillation, the length of this mean vector increases and likewise the amplitude. Lower row: Schematic illustration of the mean amplitude signal resulting from the neural oscillators. (Adapted from Neuling et al 2013)

2.1.5.2 Animal and computational modelling studies

In vitro and *in vivo* animal studies have demonstrated that sinusoidal AC electric fields generate periodic states of depolarization and hyperpolarization relative to the resting membrane potential, polarizing neurons proportionally with field intensity (Deans et al 2007; Fröhlich and McCormick 2010). The cell susceptibility to polarization was reported to be inversely proportional to the applied field frequency (Deans et al 2007), indicating a decrease in membrane response to increasing stimulation frequency. The same mechanism should be assumed for tACS, which induces oscillations in resting membrane potential towards more depolarized and more hyperpolarized states.

The effect of AC electric fields on individual neurons is relatively weak compared with its effect on network dynamics. Computational simulations and animal studies support hypothesis that tACS can entrain neuronal networks in a frequency-specific manner through network resonance (Deans et al 2007; Fröhlich and McCormick 2010; Ozen et al 2010; Reato et al 2010; Herrmann et al 2013; Reato et al 2013; Merlet et al 2013; Ali et al 2013; Ni et al 2017), defined in this context as the preference of a network to oscillate in a narrow frequency band in response to periodic stimulation (Hutcheon and Yarom 2000). According to these studies, stimulation with an oscillating current increases the number of individual neurons, which start to synchronise with the external oscillation, resulting in a power increase of the whole network (Figure 2.3).

2.1.5.3 MEG/EEG studies

A number of studies have combined tACS with electroencephalography (EEG) and magnetoencephalography (MEG) in order to clarify whether and to what extent tACS affects endogenous oscillations in humans. Initially, only after-effects of tACS on oscillatory activity were investigated using these methods, due to the large amplitude stimulation artefact. For example, tACS applied over the occipital cortex at individual α-frequency was shown to selectively elevate the endogenous α power (Zaehle et al 2010; Neuling et al 2013; Vossen et al 2015) for up to 70 min after stimulation offset (Kasten et al 2016). Similarly, tACS applied at lower-γ frequency (40 Hz) to extra-striate visual cortex modulated γ coherence after stimulation for up to 20 min (Helfrich et al 2014a). One important question with relation to these findings is to what extent tACS after-effects on endogenous oscillatory activity relate to entrainment effects observed during stimulation (Veniero et al 2015). To start to address it, Vossen and colleagues employed a novel, intermittent tACS protocol to test to what extent plasticity can account for tACS-induced after-effects. Their results showed that plasticity

mechanisms were sufficient to explain after-effects on endogenous α oscillatory activity in response to α-frequency tACS (Vossen et al 2015). However, the mechanisms set in motion by online entrainment as prerequisite to the observed effects cannot be excluded. Moreover, no consistent, predictable after-effects of tACS on brain oscillations were found across studies (Veniero et al 2015), supporting the view that after-effects can be at least partially dissociated from online, frequency-specific (entrainment) effects during tACS.

Importantly, tACS has been applied concurrently with EEG and MEG in order to demonstrate its ability to synchronise cortical oscillators in humans with similar intrinsic frequencies to the entrainment frequency (Soekadar et al 2013; Helfrich et al 2014b; Helfrich et al 2014a; Neuling et al 2015; Witkowski et al 2015; Neuling et al 2016). However, the efficiency of current artefact rejection methods remains questionable (Noury et al 2016), and further research is needed to establish standards in artefact rejection methods.

Finally, it is worth noting that although most tACS studies are designed to modulate endogenous brain oscillations in a frequency-specific manner, recent evidence suggests that tACS may also modulate cross-frequency interactions (Wach et al 2013a; Pahor and Jaušovec 2014; Helfrich et al 2014a; Herrmann et al 2016).

2.1.5.4 TMS studies

In the past decade, a number of studies have been performed to explore the effects of tACS on various measures of motor cortical excitability, as assessed using TMS (Table 2.1).

Study	Frequency of tACS (Hz)	tACS parameters	TMS measures	Results
Antal *et al.* 2008	1, 10, 15, 30, 45	**M:** M1-CO **C:** 0.16-0.25 A/m^2 **D:** 5-10 min	Single MEP (offline)	No effect
Zaghi *et al.* 2010b	15	**M:** C3-C4 **C:** 0.8 A/m^2 **D:** 20 min	Single MEP, SICI, ICF (offline)	Reduction in single MEP and ICF amplitude
Moliadze *et al.* 2010	80, 140, 250	**M:** C3-Fp1/Fp2 **C:** 0.25 A/m^2 **D:** 10 min	Single MEP, I-O curve, SICI, ICF, LICI, CSP (online and offline)	Increase in single MEP amplitude and IO curve; reduction in SICI by 140 Hz tACS
Feurra *et al.* 2011a	5, 10, 20, 40	**M:** C3-Pz **C:** 0.29 A/m^2 **D:** 90 sec	Single MEP (online and offline)	Increase in single MEP amplitude by 20 Hz tACS (no offline effect)
Schutter and Hortensius 2010	5-20, 10	**M:** C3-C4 **C:** 0.29 A/m^2 **D:** 5-10 min	Single MEP (offline)	Increase in single MEP amplitude by 5-20 Hz tACS
Moliadze *et al.* 2012	140	**M:** C3-CO **C:** 0.125-0.63 A/m^2 **D:** 10 min	Single MEP (offline)	Reduction in single MEP amplitude by 0.4 mA tACS; no effect of 0.6-0.8 mA tACS; increase by 1 mA tACS
Wach *et al.* 2013b	10, 20	**M:** C3-CO **C:** 0.29 A/m^2 **D:** 10 min	Single MEP, CSP (offline)	Reduction in CSP by 10 Hz tACS
Feurra *et al.* 2013	5, 10, 20, 40	**M:** C3-Pz **C:** 0.29 A/m^2 **D:** 90 sec	Single MEP (online)	Increase in single MEP by 20 Hz tACS at rest and by 5 Hz during motor imagery
Tecchio *et al.* 2013	10, 20	**M:** Personalised **C:** 0.1 A/m^2 **D:** 1.5 min	Single MEP (online)	Reduction in single MEP by 20 Hz tACS
Cancelli *et al.* 2015	20	**M:** C3-C4 **C:** 0.25-0.63 A/m^2 **D:** 1.5 min	Single MEP (online)	Reduction and increase in single MEP by low and high current densities, respectively; increased single MEP only with centre-ring montage
Heise *et al.* 2016	20	**M:** C3-Fp2; C3-centre ring montage **C:** 0.1-0.4 A/m^2 **D:** 10 min	Single MEP (online and offline)	

Table 2.1. Effects of tACS on TMS-assessed motor excitability measures

Summary of combined tACS-TMS studies, which assessed the effects of tACS (online and/or offline) on M1 excitability measures. Abbreviations: C; current density; CSP, cortical silent period; D, duration of tACS; ICF, intracortical facilitation; I-O curve, input-output curve; LICI, long interval intracortical inhibition, M, montage; SICI, short interval intracortical inhibition.

What emerges from these studies are very mixed results, highly dependent on stimulation parameters. In addition, of these, the vast majority only examined the effects of tACS on a single MEP amplitude, which reflects general corticospinal excitability (see Section 2.2.3), with little work performed so far to investigate the effects of stimulation on paired-pulse TMS protocols, which allow for the assessment of various aspects of intracortical excitability. Moreover, none of the studies summarised in Table 2.1 controlled for the phase of tACS, which is a crucial factor in the modification of neuronal activity and behaviour (Ozen et al 2010; Neuling et al 2012a; Ali et al 2013; Helfrich et al 2014b; Riecke et al 2015). More recently, a few groups have started to address this factor. For example, 20 Hz tACS was found to modulate the amplitude of a single MEP, SICI and ICF (Guerra et al 2016; Nakazono et al 2016) in a phase-dependent manner. However, another study reported no phase-dependent modulation of a single MEP amplitude by 20 Hz tACS, despite matching stimulation frequency to individual β peak frequency (Braun et al 2017). More efforts are required to determine optimal stimulation parameters, which will lead to an improvement in the effectiveness of this technique and increase its value as a tool to study both oscillatory activities *per se* and oscillations-behaviour relationship.

2.1.5.5 fMRI studies

Recent studies have combined tACS with functional magnetic resonance imaging (fMRI) to investigate how stimulation affects blood oxygen level-dependent (BOLD) activity. This novel approach allows for quantifying any stimulation-induced changes in

neural activity both at the site of stimulation and at anatomically remote projection areas with a high spatial resolution, both during ongoing or after stimulation (Saiote et al 2013). So far, the majority of studies have focused on examining the effects of α-frequency tACS applied to occipital region, reporting a reduction in the task-related BOLD response to visual targets in occipital and other brain areas, both during and after stimulation offset (Vosskuhl et al 2015; Cabral-Calderin et al 2015; Alekseichuk et al 2015).

In the motor domain, β- and γ-frequency tACS-induced motor performance enhancements were related to changes in BOLD activity in the stimulated area (M1) and were shown to modulate the neural activity in the dorsomedial prefrontal cortex in a frequency- and task-specific manner (Moisa et al 2016). Further, β tACS was capable of changing the connectivity pattern of the stimulated M1, without changing overall local activity or network connectivity, as examined using resting-state MRI (Weinrich et al 2017). The concurrent tACS-fMRI approach has also been successful in providing causal evidence that synchronised power fluctuations contribute to the formation of fMRI-based resting state networks (Bächinger et al 2017). Overall, the above studies demonstrate the value of combined tACS-fMRI approach in elucidating the causal link between brain oscillations, neural systems, and behaviour.

2.1.6 Behavioural effects of tACS

In the past decade, tACS has become a valuable tool to manipulate brain oscillations and examine the consequences of such manipulations on sensorimotor and cognitive processes, thus offering the advantage to demonstrate a causal nature of oscillation-behaviour relationship. tACS has been shown to modulate various aspects of behaviour, including perception (Kanai et al 2008; Feurra et al 2011b; Laczó et al 2012;

Neuling et al 2012a; Strüber et al 2014; Helfrich et al 2014a; Márquez-Ruiz et al 2016; Stonkus et al 2016); motor (Pogosyan et al 2009; Joundi et al 2012a; Wach et al 2013a; Pollok et al 2015; Davide et al 2016; Brinkman et al 2016; Moisa et al 2016; Santarnecchi et al 2017; Varlet et al 2017) and cognitive processes (Sela et al 2012; Polanía et al 2012; Santarnecchi et al 2013; Jaušovec and Jaušovec 2014; Antonenko et al 2016), in many cases establishing for the first time the causal relationship between specific oscillatory activities and behaviour.

A number of neurological and psychiatric disorders have been associated with abnormal neuronal synchronisation, including, but not limited to, Parkinson's disease, schizophrenia, stroke and Alzheimer's disease (Brown 2003; Uhlhaas et al 2006; Uhlhaas and Singer 2010; Rossiter et al 2012; Rossiter et al 2014a). Therefore, tACS may be of therapeutic value. In fact, first successes in using this technique for therapeutic purposes have already been reported in Parkinson's disease (Brittain et al 2013), dystonia (Angelakis et al 2013), stroke (Wu et al 2016; Naros and Gharabaghi 2017) and schizophrenia (Kallel et al 2016). Further studies exploring the potential of tACS in the treatment of disorders characterised by abnormal neuronal synchronisation are warranted.

2.1.7 Safety of tACS

tACS is a relatively new technique and so there have been far fewer papers on its safety issues or adverse effects as compared with other non-invasive brain stimulation techniques, such as TMS and tDCS. The most common adverse effect reported are phosphenes, the perception of which peaks at stimulation frequency of 10 and 20 Hz, is absent beyond 40 Hz, and is stronger when electrode montages are closer to the retina (Antal et al 2008; Kanai et al 2008; Schutter and Hortensius 2010; Moliadze et al

2010; Chaieb et al 2011; Turi et al 2013; Chaieb et al 2014; Raco et al 2014; Matsumoto and Ugawa 2017). Dizziness and skin sensations were also reported in some participants (Raco et al 2014; Matsumoto and Ugawa 2017). Overall, the reported adverse effects are mild and disappear soon after stimulation.

2.2 Transcranial magnetic stimulation (TMS)

Transcranial magnetic stimulation (TMS) is a technique that has been widely used to study causal brain-behaviour relations, functional brain connectivity and has potential clinical utility in various disorders such as stroke, epilepsy and chronic pain (Pascual-Leone et al 2000; Hallett 2007; Chen et al 2008). The work within this thesis, however, focuses on the use of TMS as a powerful tool for studying human motor physiology (Chen 2000; Hallett 2000). When TMS is applied to the motor cortex, different TMS paradigms can be used to study various components of motor excitability and provide insight into the function of different neurotransmitter systems.

2.2.1 Underlying principles

TMS, introduced by Anthony Barker in 1985, is a cutting-edge non-invasive stimulation technique, based on the Faraday's principle of electromagnetic induction (Barker et al 1985). Stimulation is produced by passing pulses of electric current through a magnetic coil placed tangentially over the scalp. This generates a rapidly changing magnetic field (with peak strengths of 1–2.5 Tesla) that undergoes minimal attenuation in the skull tissues while inducing smaller, focally directed electric currents within the brain (Barker et al 1987; Dhuna et al 1991) (Figure 2.4). The depth of penetration of TMS is limited because the strength of the magnetic field decreases exponentially with increasing distance from the coil. TMS of the primary motor had area is effective at relatively low stimulus intensities since this region is large and located at the hemispherical surface.

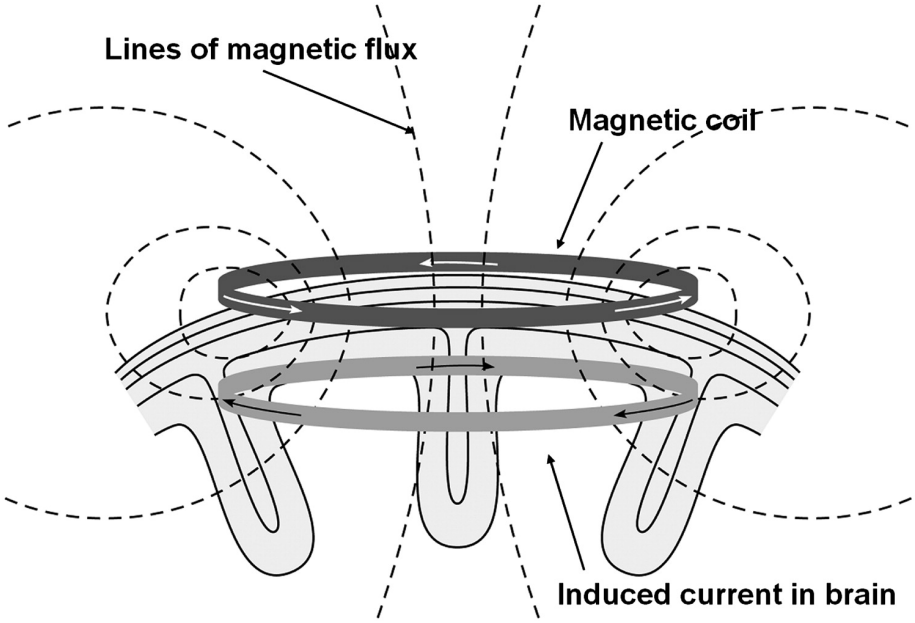


Figure 2.4 Illustration of direction of current flow in a magnetic coil and the induced current in the brain (Adapted from Hallett 2000)

TMS stimulates axons since cell bodies have a much longer electrical time constant and higher threshold (Burke et al 2000; Rossini et al 2015). Moreover, axonal bending has been indicated as an important feature that determines the susceptibility of cortical neurons to TMS since the change in electric field at these points is greatest (Maccabee et al 1993).

2.2.2 The physiological basis of TMS

When a single pulse TMS is delivered to the human M1 at gradually increasing intensities of stimulation, an increasing number of highly synchronised orthodromic action potentials is induced in fast-conducting large diameter axons of corticospinal neurons making direct monosynaptic connections with spinal motor neurons. The first volley, referred to as D-wave or direct-wave, results from direct excitation of the corticospinal neuron at its axon hillock and has the shortest latency. Later waves,

known as I-waves or indirect-waves, are induced at intervals of 1.2-2.0 ms and result from indirect trans-synaptic corticospinal excitation via different sets of intracortical neurons that project onto the pyramidal neurons (Figure 2.5 A, B). Dependent on coil orientation, TMS of the motor cortex evokes a wave corresponding to the I1 wave, and the D-wave is only recruited at intensities much greater than threshold (Di Lazzaro et al 2004). Each descending corticospinal volley leads to glutamate release from cortico-motoneuronal synapses, resulting in a depolarization at the post-synaptic cell membrane. If temporal and spatial summation of excitatory post-synaptic potentials exceeds the firing threshold, an action potential is generated in the spinal motor neurons. The action potentials propagate along the peripheral motor axons inducing a motor response that can be recorded as the motor evoked potential (MEP) from corresponding muscles (Figure 2.5 C).

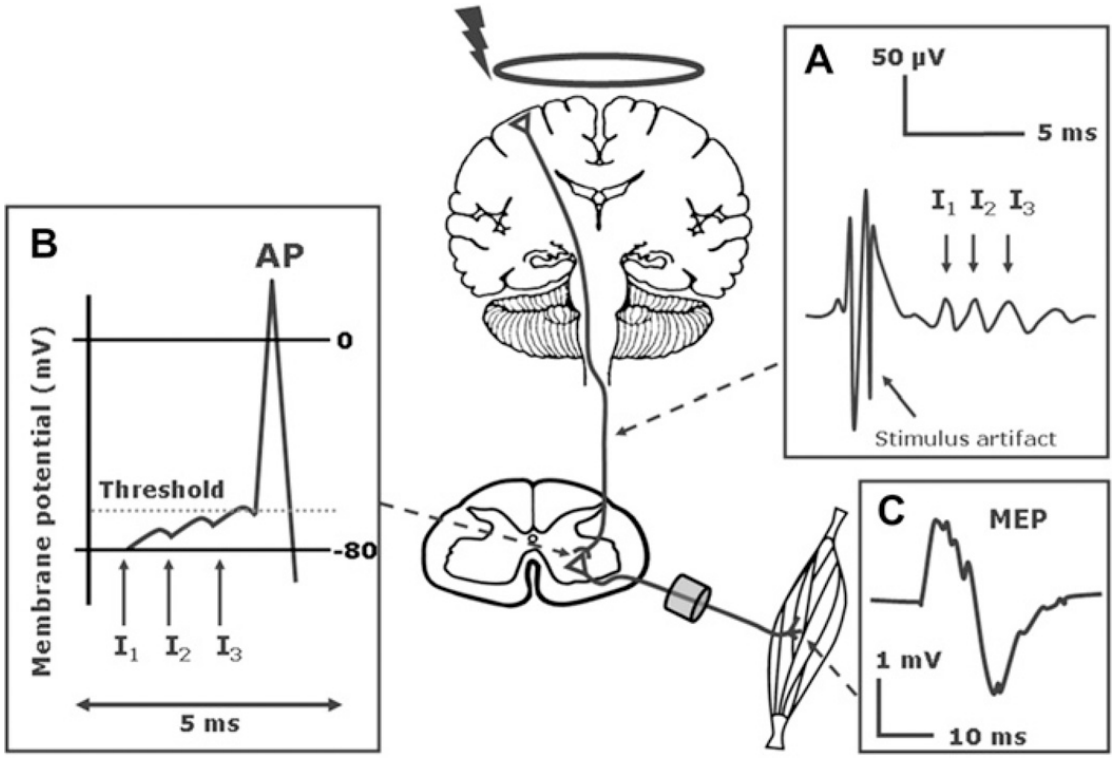


Figure 2.5 Neurophysiological basis of MEP

A. TMS-induced activation of the corticospinal neurons with a main contribution by I-waves. **B.** Temporo-spatial summation at the cortico-motoneuronal synapses. **C.** Motor evoked potential (MEP). (Adapted from Groppa et al 2012)

2.2.3 Single-pulse TMS

A single TMS pulse delivered over the hand area in M1 elicits a MEP in the contralateral hand muscles, as measured by EMG. The lowest TMS intensity required to evoke a MEP of more than 50 μV peak-to-peak amplitude in at least 50% of successive trials is referred to as motor threshold (MT) (Kobayashi and Pascual-Leone 2003). MEPs and MTs can be used to evaluate global excitability of the corticospinal pathway (Mathiowetz et al 1985).

Single TMS pulses of progressively increasing intensity applied to the motor cortex can also be used to generate a recruitment curve (RC), also referred to as input-output curve. RC depicts the rise of MEP amplitude to increasing intensity of TMS pulses and is dependent on neuronal membrane excitability (Ziemann et al 1996a; Chen et al 2008), as well as synaptic mechanisms (Boroojerdi et al 2000; Di Lazzaro et al 2003). The slope of the MEP RC serves often as an index of excitability within a wider region of the cortex with steeper slopes reflecting increased cortical excitability. The relationship between MEP RC slope and neurotransmitter concentration is not completely elucidated, but may be due, at least in part, to increased glutamatergic activity (Di Lazzaro et al 2003).

The cortical silent period (CSP) is another important measure stemming from single-pulse TMS protocols. The CSP occurs following the application of a single suprathreshold TMS pulse to the motor cortex during voluntary muscle contraction and is manifested as a pause in the EMG activity after the MEP (Kobayashi and Pascual-Leone 2003). The CSP, thought to be mediated mainly by $GABA_B$ receptors, has been used as a measure of the intracortical inhibition (Siebner et al 1998; Sanger et al 2001).

2.2.4 Paired-pulse TMS

Paired pulse TMS has been most frequently used to examine intracortical inhibitory and facilitatory mechanisms as well as interhemispheric interactions. The former ones are of particular interest in this thesis and therefore are going to be discussed in greater detail.

Paired-pulse TMS protocols involve the application of two TMS pulses to the same region of the cortex through a single coil. The inhibitory intracortical mechanisms have been studied in the intact human primary motor cortex using primarily two protocols: short interval intracortical inhibition (SICI) and long interval intracortical inhibition (LICI). SICI and LICI involve the application of a subthreshold (SICI) and suprathreshold (LICI) conditioning stimulus (CS) followed by the test stimulus (TS) over M1 at an inter-stimulus interval (ISI) of 2-4 ms (SICI) or 50-200 ms (LICI), respectively (Valls-Solé et al 1992; Kujirai et al 1993). In both cases a distinct inhibition of the conditioned test stimulus compared with an unconditioned stimulus occurs. SICI is thought to reflect mainly $GABA_A$-synaptic mediated inhibition (Ziemann et al 1996a; Di Lazzaro et al 2000; Ilic et al 2002). However, there is a possibility that some enhanced intracortical facilitation masks normal inhibition. For example, glutamate antagonists lead to an apparent enhancement of SICI (Ziemann et al 1998a; Schwenkreis et al 1999). In addition, SICI can be affected by various neuromodulators (Ziemann 2004b). Another type of inhibition can be measured when using a SICI protocol with an ISI of 1 ms. This inhibition is known to be GABAergic (Ni et al 2007), it is largely unaffected by neurotransmitter or neuromodulator systems in those studies which differentiated between SICI at 1 ms versus longer intervals of 2-4 ms (Ziemann 2004), and most likely it is mediated by extrasynaptic $GABA_A$ receptors (Stagg et al 2011b). LICI represents a long-lasting inhibition, which is distinct from SICI (Sanger et al 2001) but similar to the previously described CSP (Valls-Solé et al 1992). Several lines of

evidence suggest that LICI reflects $GABA_B$-mediated inhibition (Valls-Solé et al 1992; Werhahn et al 1999; McDonnell et al 2006).

The application of a first CS at subthreshold intensities followed by a second suprathreshold TS, with an ISI of 10-15 ms or longer, results in a physiological increase of cortical excitability (Kujirai et al 1993). This protocol is referred to as intracortical facilitation (ICF) and is thought to reflect principally, but not exclusively, glutamatergic neurotransmission (Ziemann 2004). For example, $GABA_A$ agonists decrease ICF, supporting a contribution of inhibition through the $GABA_A$ receptor to the magnitude of ICF (Ziemann et al 1995; Ziemann et al 1996b).

2.2.5 Movement-related TMS

General corticospinal excitability, as assessed using a single MEP, and certain paired-pulse TMS measures of intracortical excitability, i.e., those with sufficiently short ISI, can be evaluated in association with performance of a voluntary movement and are also referred to as event-related TMS or pre-movement TMS measures. In healthy subjects, preparation to move is accompanied by increased corticospinal excitability and reduced motor cortical $GABA_A$ inhibition (disinhibition) (Rossini et al 1988; Chen and Hallett 1999; Reynolds and Ashby 1999; Zaaroor et al 2003). Further, pre-movement inhibition is related to performance in complex manual motor tasks and shows age-related changes (Heise et al 2013). In addition, changes in pre-movement TMS measures have been reported in certain neurological disorders, including stroke and Tourette's syndrome (Hummel et al 2009; Heise et al 2010), thus pointing to the importance of these event-related parameters of motor excitability not only in healthy but also in clinical populations.

In a typical pre-movement paradigm, participants perform a simple response time (RT) task in the absence of TMS in order to characterise each individual's RT. Next, the RT task is performed while single-pulse and paired-pulse TMS measures are delivered at different time-points (selected by a researcher) preceding movement onset, with the timing of TMS pulses adjusted based on individual's RT (Hummel et al 2009).

2.2.6 Coil types

There are a variety of coil types available for TMS. The two most commonly used are: a figure-of-eight shaped coil and a circular coil. For the experiments within this thesis, a figure-of-eight coils will be used, as in this type of coil the induced electrical field is maximal at the intersection of the two round components, allowing for a relatively focal stimulation of a distinct cortical region, with the resolution of approximately 5 mm (Ueno et al 1988; Cohen et al 1990).

2.2.7 Safety of TMS

TMS is generally considered to be a safe technique (Anand and Hotson 2002; Hirshberg et al 2005; Rossi et al 2009). The most serious acute adverse effect reported is induction of seizures, mainly reported following the use of repetitive TMS (rTMS; not used in this thesis) prior to the definition or outside safety limits and/or in high-risk individuals, e.g., those with a history or family history of seizures or those taking drugs that could lower seizure threshold (Wassermann 1998; Rossi et al 2009). Because of these potential risks, all TMS experiments carried out within this thesis were performed in accordance with the current guidelines (Rossi et al 2009). To ensure that the risks are minimised, participants were required to fill out a TMS safety screening form before participating to rule out contraindications to TMS. Single- and paired-pulse TMS protocols are generally well tolerated and reported as painless. However, they may

occasionally cause syncope, transient headaches and discomfort (Wassermann 1998; Rossi et al 2009). Therefore, it will be ensured that all the participants are fully informed and comfortable with the procedure before the beginning.

CHAPTER

3

Neuroimaging methods

This Chapter describes the neuroimaging methods used in this thesis: electroencephalography (EEG), magnetoencephalography (MEG), and magnetic resonance spectroscopy (MRS). The basic principles underlying these techniques, advantages and some of the technical challenges are discussed.

3.1 Electroencephalography (EEG) and magnetoencephalography (MEG)

At the end of 19th century, Richard Caton, an English scientist, discovered electrical properties of the brain by recording activity from the brains of animals using a sensitive galvanometer. In 1924, Hans Berger, a German psychiatrist, pioneered the electroencephalography (EEG), which allowed for the first time to record electrical activity arising from the human brain. A few decades later (~1960s), the journey to unravel the electrical properties of the brain took an interesting detour when David Cohen, the physicist at MIT, successfully performed a recording of the tiny magnetic fields produced by the brain in a magnetically shielded room (magnetoencephalography, MEG). The quality of MEG recordings was greatly improved in subsequent years by the development of SQUIDs (superconducting quantum interference devices). At very low temperatures, SQUIDS are extremely sensitive to magnetic field change, which can be recorded and converted into digital signal (the process known as quantisation; the principles of quantum physics underlying the function of SQUIDs are beyond the scope of this thesis). While in the case of EEG, the electrodes are placed on the scalp, present-day MEG sensor arrays are enveloped in a helmet-shaped dewar of cooling liquid helium that typically contains ~300 sensors, providing whole-head coverage.

Both EEG and MEG are brain-wide imaging techniques with high temporal resolution, capable of resolving events with millisecond precision. Unlike EEG measures, however, the magnetic fields recorded by MEG pass through dura, skull and scalp relatively unaltered.

3.1.1 Biophysical events measurable with EEG/MEG

Neurons generate spatially and time-varying electrical currents when activated. EEG and MEG reflect mainly the summation of postsynaptic potentials: the excitatory (EPSPs) and the inhibitory (IPSPs) potentials. The positive electric current is directed towards the intracellular medium in the case of an EPSP, and towards the extracellular medium in the case of an IPSP (Figure 3.1). Synaptic activity at a given site of the soma-dendrite membrane of a neuron causes a sink-source configuration in the extracellular medium around neurons, which can be viewed as a current dipole.

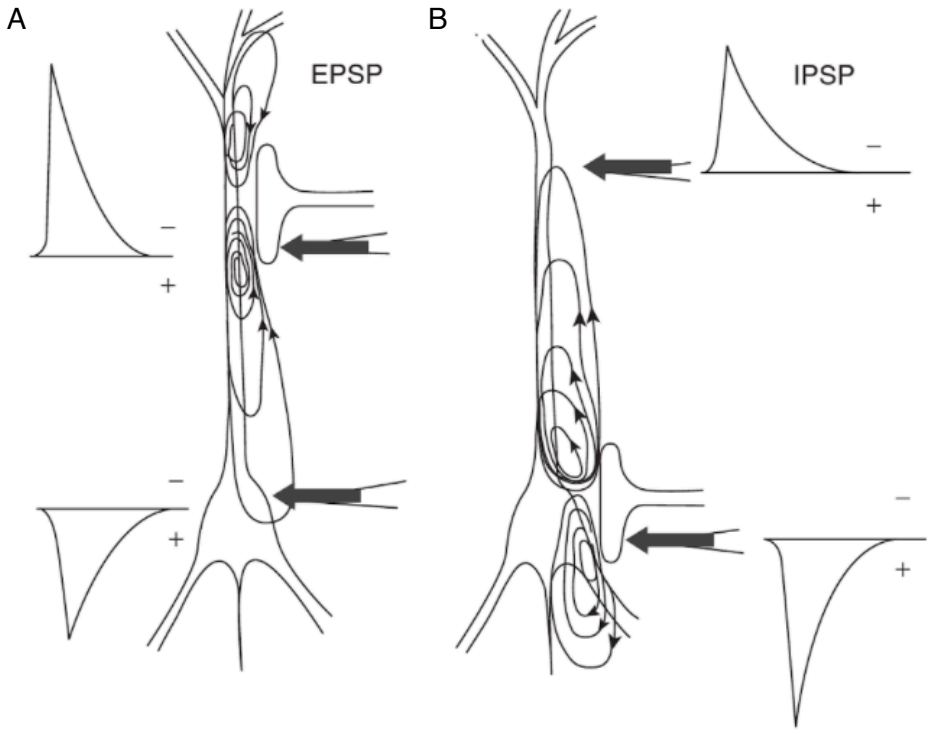


Figure 3.1 Intra- and extracellular current flow in a pyramidal neuron due to synaptic activation

A. Excitatory synapse at the level of the apical dendrite. A current of positive ions flows inwards, causing depolarization of the membrane, which results in an active sink at the level of synapse. The extracellularly measured EPSP has a negative polarity at the level of the synapse. At the soma there exists a distributed passive source resulting in an extracellular potential of positive polarity. **B.** Inhibitory synapse at the level of the soma. A current of negative ions flows inwards, causing hyperpolarization of the membrane; this results in an active source at the level of the synapse. The extracellularly measured IPSP has a positive polarity at the level of the synapse. At the level of the distal apical dendrite there is a distributed passive sink, and the potential has a reversed polarity. (Adapted from Niedermeyer and Lopes da Silva, 2005)

The folding of the cortex and the orientation of neurons with respect to the skull are particularly relevant when discussing the biophysical events measurable with EEG and MEG. The populations of pyramidal neurons located at the top of a gyrus have apical dendrites that are perpendicular to the overlying skull, whereas those that are on the wall of a sulcus have apical dendrites that are parallel to the skull. MEG can detect only those magnetic fields that have a component perpendicular to the skull, i.e., the magnetic fields generated by neuronal currents that have a component oriented tangentially to the skull. In contrast, EEG can detect both tangential and radial sources and is maximally sensitive to radial sources on gyral crowns (Figure 3.2).

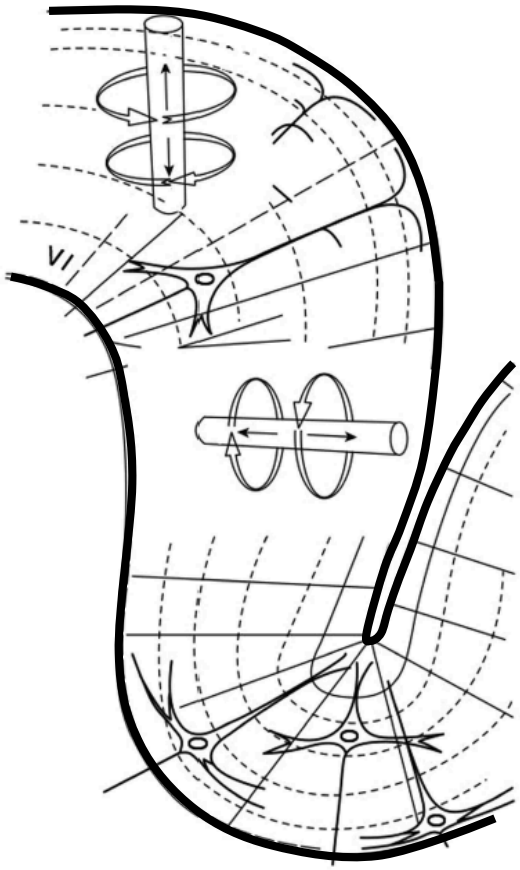


Figure 3.2 Schematic drawing showing the direction of the intracellular electric current and the resulting magnetic fields around the apical dendrites within the crown of a gyrus and a sulcus

Sources at the top of a gyrus cause radial fields that are detectable mainly by EEG. Conversely, MEG is maximally sensitive to the tangential sources, located within the sulcal bank, since they generate magnetic fields which project beyond the skull surface. (Modified and adapted from Hansen et al 2010).

It was estimated that around 10,000-15,000 neurons, mainly in superficial cortical layers (covering a cortical surface area of approximately ~0.9 mm diameter) need to be simultaneously active in order to be detectable by EEG or MEG (Murakami and Okada 2006).

An important point to consider is a high-frequency oscillatory activity (> 60 Hz), which is challenging to measure with EEG/MEG since it overlaps entirely with the spectral bandwidth of muscle activity (~20–300 Hz) and generally has low power. In comparison to EEG, however, the spatial topography of MEG data is visually less smeared and distorted since the magnetic fields are unimpeded by the differing conductance across the brain, skull, and scalp. This allows for a clearer interpretation of MEG sensor topography in terms of putative anatomical locations of its underlying brain sources (Baillet 2017). It also helps separate the contributions of brain signals from physiological contaminants, such as muscle artefacts (Whitham et al 2008; Yuval-Greenberg et al 2008), which can be confounded with high-frequency brain signals in EEG but are more clearly distinguished with MEG on the basis of their distinctive sensor topography (Muthukumaraswamy 2013; Baillet 2017).

3.2 Magnetic resonance spectroscopy (MRS)

Magnetic resonance spectroscopy (MRS) is an *in vivo* non-invasive method used to detect and quantify neurochemicals within the brain. MRS of the human brain has developed rapidly since its first observation in the 1980s (Cady et al 1983; Bottomley et al 1985) and has been increasingly utilised within the clinical and basic neuroscience to study the role of various chemicals in normal brain function and the pathophysiology of disease.

MRS is based on the same basic physical principles and uses similar equipment as magnetic resonance imaging (MRI). Therefore, the first part of this section will discuss basic concepts of MRI that are also relevant for MRS. Moreover, since the vast majority of brain MRI and MRS techniques are based on imaging the hydrogen nucleus (^{1}H, a single proton), including the work described in this thesis, the remainder of this chapter will focus on ^{1}H-MRI and ^{1}H-MRS.

3.2.1 Basic concepts of MRI

MRI is founded on the physical phenomenon, known as nuclear magnetic resonance (NMR), which was first experimentally demonstrated by the physicists Edward M. Purcell and Felix Bloch in 1940s (Purcell et al 1946; Bloch 1946). The discovery of a specific property of sub-atomic particles known as spin and its interaction with a magnetic field has had a huge impact on our understanding of magnetic resonance phenomena and the development of MRI.

3.2.1.1 The magnetic property of a nucleus

Hydrogen nuclei possess a positive charge and therefore exhibit a nuclear magnetic moment, or vector through their axis of spin. In a free environment, protons spin around their own, randomly oriented, axes (Figure 3.3 A). In a magnetic field, however, most protons will line up with the direction of the magnetic field (B_0) (parallel), and some will also line up against it (anti-parallel) (Figure 3.3 B), precessing (resonating) around the direction of the net magnetic field. The balance between parallel and anti-parallel nuclei is termed the net magnetization (M_0). The frequency at which the magnetic moment of a nucleus precesses about the direction of the main magnetic field is referred to as angular frequency (ω_0). This precessional frequency can be described by the Larmor equation. When placed in a magnetic field, the atomic nucleus of an element will precess at a frequency, which is described by the gyromagnetic ratio of the element (γ) and the strength of the magnetic field, in accordance with the following equation:

$$\omega_0 = \gamma B_0$$

Nuclear isotopes have unique gyromagnetic ratios (depending on the size and shape of the nucleus), which means that different nuclei resonate at different frequencies in the same magnetic field B_0. Because the hydrogen's nucleus contains no neutrons, it has a gyromagnetic ratio much higher than, for example, phosphorus and carbon. In addition, hydrogen atoms are also present at high concentrations in the brain, making the hydrogen the best candidate for an MR-sensitive isotope for imaging of the brain.

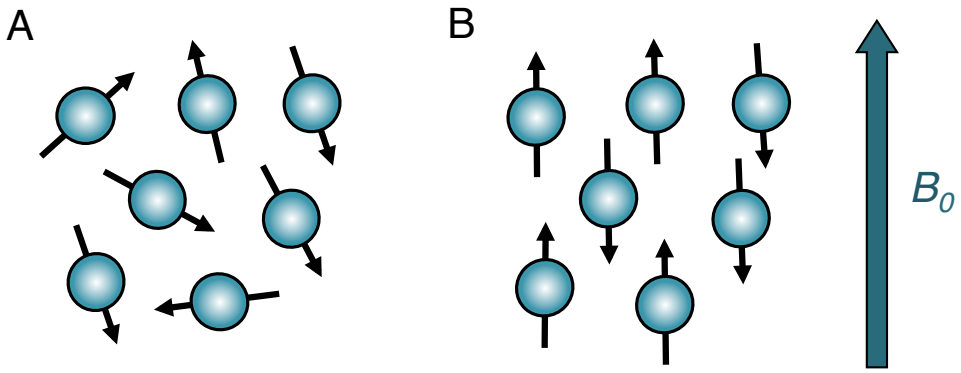


Figure 3.3 Nuclear spins in the absence and in the presence of a magnetic field

A. Randomly oriented protons in the absence of a magnetic field (B_0). **B.** Protons aligned to B_0.

3.2.1.2 Excitation and relaxation

The M_0 is aligned parallel to the B_0 field (along the z-axis) and since it has no component in the transverse plane (x, y) it cannot precess and generate a signal. In order to generate an MR signal, M_0 must be tipped away from B_0 to the transverse plane. To achieve this, the spins are exposed to an alternating magnetic field (B_1) applied in the transverse plane using a radiofrequency (RF) pulse that is matched to the Larmor frequency of the nucleus (Figure 3.4).

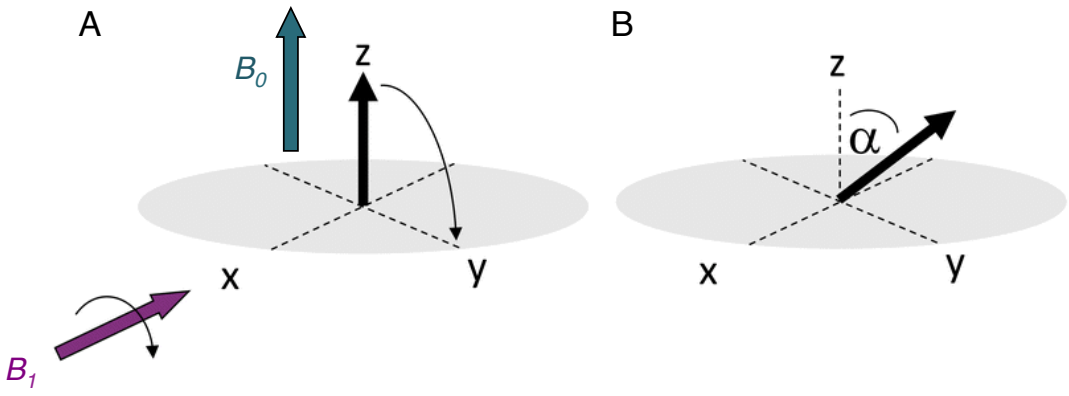


Figure 3.4 The effect of an RF pulse on net magnetization

A. The effect of an RF pulse (B_1) on the net magnetization is to rotate the magnetization about the axis along which B_1 is applied. **B.** The angle of rotation of the net magnetization (the flip angle) is denoted as alpha (α).

As a result of this excitation, the hydrogen nucleus absorbs the energy of the pulse. The amount by which M_0 is rotated during application of an RF pulse is referred to as the flip angle. An excitation of the equilibrium system by an RF pulse leads to an unstable high-energy anti-parallel state of the system. Next, individual spins realign to a low-energy parallel state, releasing energy at the resonant frequency from each atom. This is observed as an oscillating signal in the xy-plane, referred to as the free induction decay (FID; “free” relates to free precession, “induction” is the process where a varying magnetic field produces a current in a coil, and “decay” indicates the loss of signal). The processes of return of the longitudinal (M_z) and the transverse components (M_{xy}) of the magnetization to their equilibrium values can be described with relaxation times T1 and T2, respectively. The T1 relaxation time is the time constant defining the rate of recovery of magnetization along the longitudinal axis following an RF pulse (i.e., the net magnetization rotates back to align itself with the z-axis), whereas the T2 relaxation time is the time constant defining the irreversible loss of magnetization, and therefore signal, in the transverse plane following excitation. The actual decay of the FID following an RF pulses is more rapid due to local magnetic field inhomogeneities

and is referred to as the T2* relaxation time. The magnetic susceptibility variations are particularly evident in and around blood vessels, where the level of deoxyhaemoglobin (dHb) in the blood affects the T2* in the tissue around the blood vessels. This effect is the basis of the blood oxygenation level-dependent signal (BOLD) used in functional MRI (fMRI).

3.2.1.3 Data acquisition: repetition time (TR) and echo time (TE)

An important part of MRI data acquisition is a pulse sequence, which is composed of RF pulses, periods of recovery (that generate the MR image), and the signal readout. Two important components of the pulse sequence are the repetition time (TR) and echo time (TE). The TR is defined as the time between the repeated RF excitations of the magnetization, whereas TE refers to the time between the RF excitation pulse and the acquisition of the signal. By using various TR and TE values, it is possible to change the contrast between different tissues in an MR image, based on either the T1 or the T2 properties of the tissues (Figure 3.5).

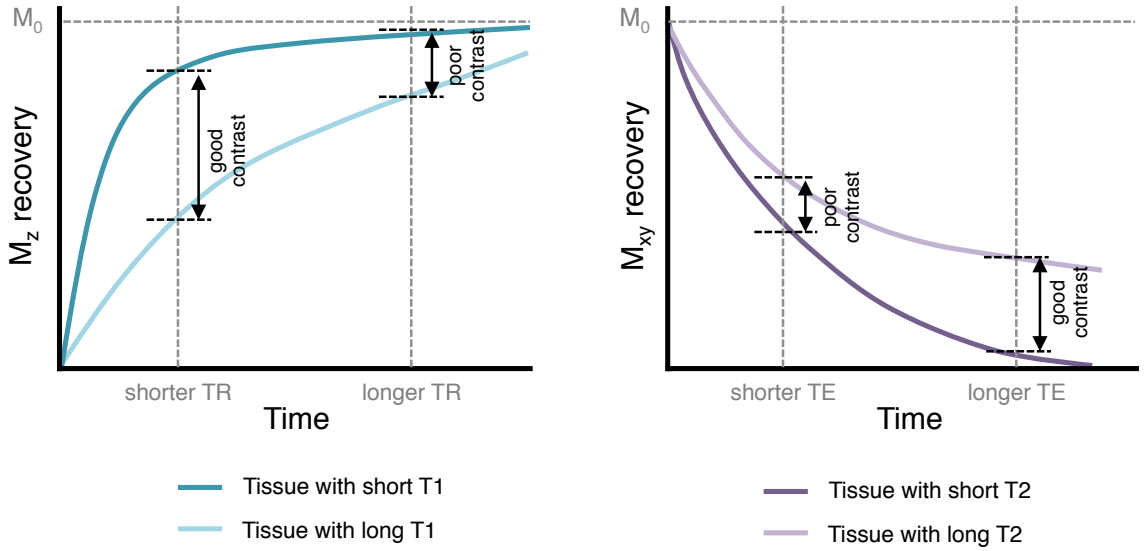


Figure 3.5 T1- and T2-weighting

A. In tissues with different T1 relaxation times, selecting a short TR will increase the T1 contrast between tissues (T1-weighting), as the magnitudes of their recovered longitudinal magnetizations will be different. By selecting a longer TR, longitudinal magnetization of both tissues will recover significantly, and there will be a smaller difference between the magnitudes of their recovered magnetization vector, resulting in little T1 tissue contrast. **B.** In tissues with different T2 relaxation times, selecting a short TE will result in the poor T2 contrast between the tissues (T2-weighting), because there is no major difference between the loss of their transverse magnetizations. Selecting a longer TE will allow a significant difference to develop between the amount of transverse magnetization of the two tissues, resulting in better T2 contrast.

3.2.2 Basic principles of *in vivo* MRS

^{1}H-MRS detects radiofrequency signals that arise from hydrogen nuclear spins within tissue metabolites. ^{1}H nuclei exhibit minute variations in their resonance frequencies. The field variations causing these frequency shifts are determined by two factors: chemical shift and J-coupling.

The chemical shift depends on the electrical environment around the atomic nucleus, i.e., the number of electrons orbiting near the nucleus. Therefore, nuclei in different molecular environments give rise to signals at different frequencies. The spectrum is a plot of signal intensity (roughly proportional to metabolite concentration) against

chemical shift (Figure 3.6 A). Chemical shift is reported in the dimensionless unit ppm (parts per million of the proton frequency). If the resonance frequency is calculated relative to a reference frequency, the derived chemical shift becomes independent of the applied B_0, which facilitates comparison of spectra at different B_0 field strengths (Stagg, C., Rothman 2014).

In addition to the surrounding chemical environment, the spins of neighbouring nuclei also affect the electronic shielding of the nucleus. J-coupling provides information on the connectivity of molecules and describes the interaction between two nuclear spins that is mediated through the chemical bonds that connect them.

3.2.3 Analysis and quantification of MR spectra

The signal of an MRS resonance, corresponding to the area of its spectral peak, is proportional to the concentration of a metabolite. If the chemical has more than one resonating nucleus, more than one peak is observed in the spectrum (Figure 3.6 B). The metabolite specific combination of chemical shifts and J-couplings gives rise to the "spectral fingerprint", which is unique to each molecule. The acquired spectra contain a sum of individual spectroscopic patterns of all observable metabolites (Figure 3.6 A). However, the reliable identification of individual metabolites is challenging due to the limited spectral dispersion and the broad linewidths, which lead to severe spectral overlap (Stagg, Rothman 2014).

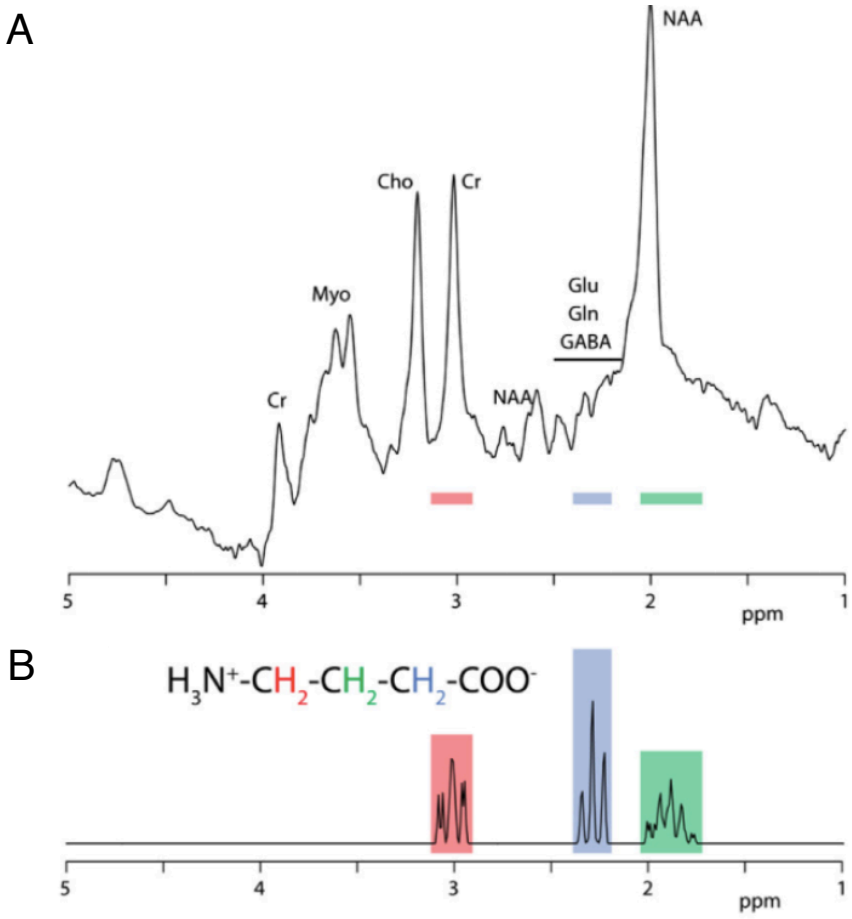


Figure 3.6 ^{1}H-MR spectrum

A. ^{1}H-MR spectrum of the human brain acquired at 3T showing peaks for various metabolites. Coloured bars correspond to the simulated peak locations for GABA shown in B. **B.** Simulated MR spectrum of GABA, showing the assignments to the GABA CH_2 spins. Abbreviations: Cho, choline-containing compounds; Cr, creatine; Glu, glutamate; Gln, glutamine; Myo, myoinositol. (Adapted from Puts and Edden 2012)

Since the experimentally measured spectrum is considered the sum of the individual metabolite contributions, various quantification methods have been developed, which aim to reproduce the overall spectrum by using an appropriately scaled linear combination of the potential, individual metabolite concentrations (Stagg, Rothman 2014). One of the more widely used methods for spectral quantification in recent years is the LCModel (Figure 3.7) (Provencher 1993; Provencher 2001). The software analyses *in vivo* MRS data as a linear combination of model spectra, also known as basis spectra, i.e., the spectral patterns of the potentially detected metabolites. The

prior knowledge of the basis spectra is required for the analysis. They can be derived experimentally by MRS measurements of metabolites in solution or by numerical simulation based on the spectroscopic characteristics of the metabolites, e.g., the chemical shifts and the J-coupling. The basis spectra are specific for the particular MRS experiment, as they rely on the scanner B_0 field strength and other acquisition parameters, such as RF pulses, sequence timing and voxel geometry.

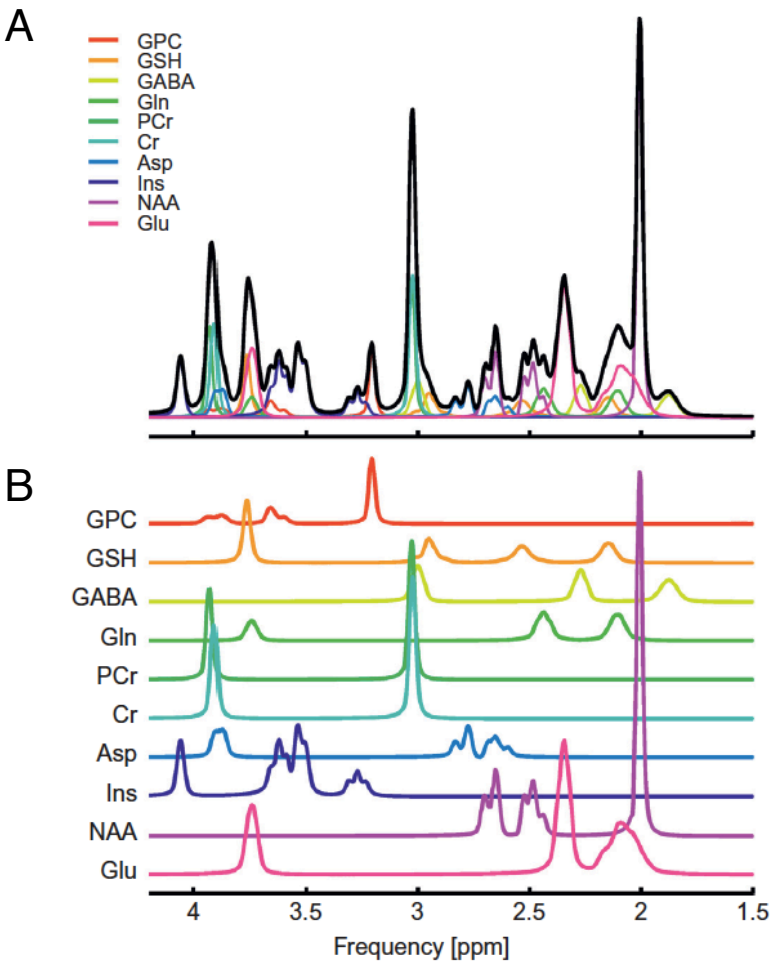


Figure 3.7 Quantification of ^{1}H-MR spectra as linear combination of model spectra (LCModel)

A. *In vivo* ^{1}H spectra consist of a sum of signals from the apparent neurochemical profile. **B.** The quantification aims at reproducing the spectrum at hand as a scaled combination of the spectral patterns from individual metabolites. For each substance, the necessary scaling corresponds to the apparent concentration. (Adapted from Stagg, Rothman 2014)

Since repeated MRS measurements are generally not performed due to the high cost of MRI scan and lack of time, the uncertainty on a metabolite measurement is usually estimated using Cramer-Rao lower bounds (CRLB) of variance. The CRLB is a measure of the minimum possible variance on a fit parameter, assuming that the model is an accurate representation of the data (Cavassila et al 2001).

A given metabolite can be quantified by comparing its signal intensity with a reference compound signal. If the concentration of the reference compound is known, then the absolute concentration of the metabolite of interest can be calculated based on the relative peak intensities. The two most popular reference approaches include internal and external referencing.

The external reference method applies identical settings of an *in vivo* experiment on an *in vitro* solution that contains metabolites of known concentrations. Since the reference signal is acquired from a different spatial location, the reference signal intensity will be affected by B_1 (RF field) inhomogeneities. To account for it, RF field simulations or additional scans to map the RF field inhomogeneity need to be performed. The internal reference method involves choosing a metabolite or water to serve as the reference compound. The most commonly used reference metabolites are the total creatine (creatine [Cr] + phosphocreatine [PCr]) and N-acetylaspartate (NAA). The total creatine is a reflection of cellular adenosine triphosphate (ATP) metabolism, whereas NAA level is thought to reflect neural density and viability. The concentration of both metabolites is relatively stable under normal physiological conditions (Pouwels and Frahm 1998). The internal referencing method is considered a relative (not absolute) quantification technique, i.e., the concentrations of metabolites of interest are expressed as a ratio to the reference compound, with the signal intensity of the metabolite in the numerator, and the signal intensity of the reference metabolite in the denominator. The total creatine was used as a reference in the MRS experiment performed as part of this

thesis.

3.2.3.1 Water and outer volume suppression

In the healthy human brain, water is the most prevalent $_1$H-containing compound; its concentration is estimated to be 83 % for the gray matter and 70 % for the white matter (McIlwain and Bachelard 1985). In contrast, brain metabolites detectable by MRS are 10^3 times and 10^4 times smaller, i.e., in the millimolar to micromolar concentration range. Therefore, efficient water suppression is vital for the reliable observation and measurement of these neurochemicals. To this end, differences in the chemical shifts of water and brain metabolites are used in order to achieve a frequency-selective RF excitation of the water resonance (Figure 3.8 A). The water signal is then minimized by phase-spoiling gradients, while the metabolite signals remain unaffected (Figure 3.8 B).

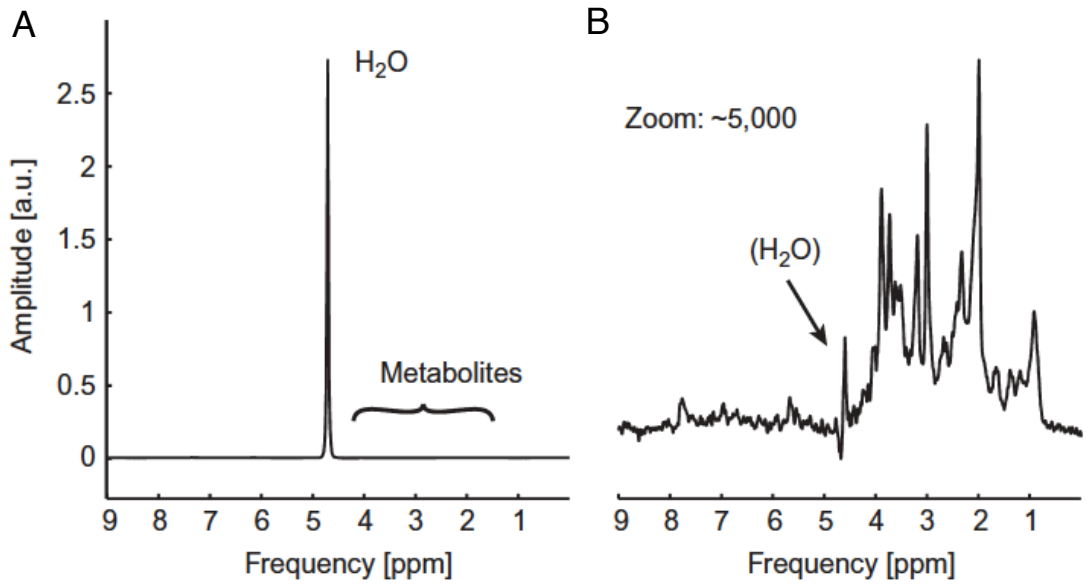


Figure 3.8 Water unsuppressed and water suppressed ^{1}H spectra

A. Unsuppressed spectrum showing a prominent water peak that overwhelms metabolite signals. **B.** Water suppressed spectrum revealing metabolite signals. (Adapted from Stagg, Rothman 2014)

In the healthy human brain, lipids are generally MR invisible since they immobile and are held tightly in bilayer membranes. However, when the voxel of interest is placed too close to the skull, extracranial lipid signals can strongly contaminate the spectrum (Figure 3.9) (Rothman 1994). Therefore, a voxel placement in proximity of dura matter that surrounds the brain is frequently avoided. In addition, spatial outer volume suppression (OVS) is commonly used to minimise lipid signals. The OVS employs a frequency-selective RF pulse in the presence of a magnetic field gradient to excite the unwanted magnetization from the spatial slice (outside the voxel of interest) before it is erased by phase spoiling (Duyn et al 1993).

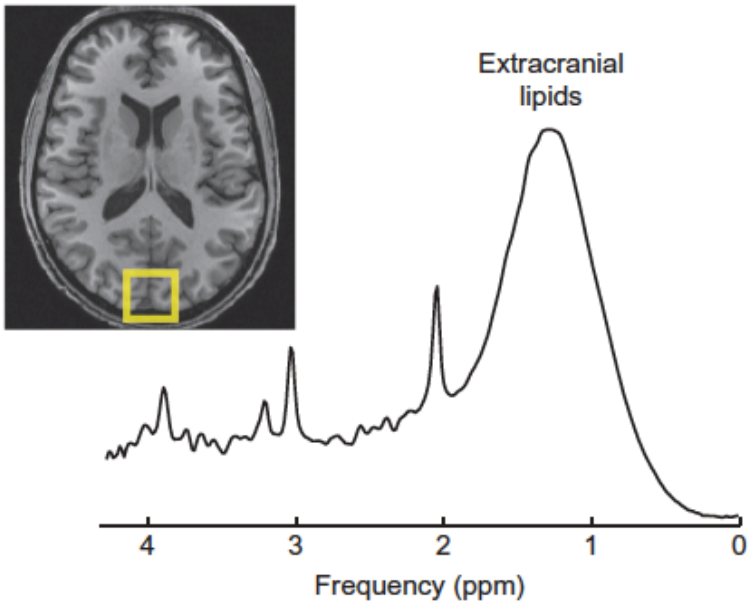


Figure 3.9 Lipid resonances in the human brain

Extracranial lipids are observed if the voxel of interest (yellow box) is placed too close to the scalp. (Adapted from Stagg, Rothman 2014)

3.2.4 The neurochemical profile detected by MRS

At high magnetic fields (7T and above), a neurochemical profile of more than 20 metabolites can be detected in the brain with *in vivo* ^{1}H-MRS (Figure 3.10). In general, ^{1}H-MRS can detect metabolites existing in a concentration above 0.5 mM (Duarte et al

2012). Moreover, the neurochemical profile is dependent on brain region (Pouwels and Frahm 1998; Tkáč et al 2003; Emir et al 2012), functional state (Mangia et al 2007) and is affected by pathological conditions (Abdallah et al 2015; Chiapponi et al 2016; Godlewska et al 2017).

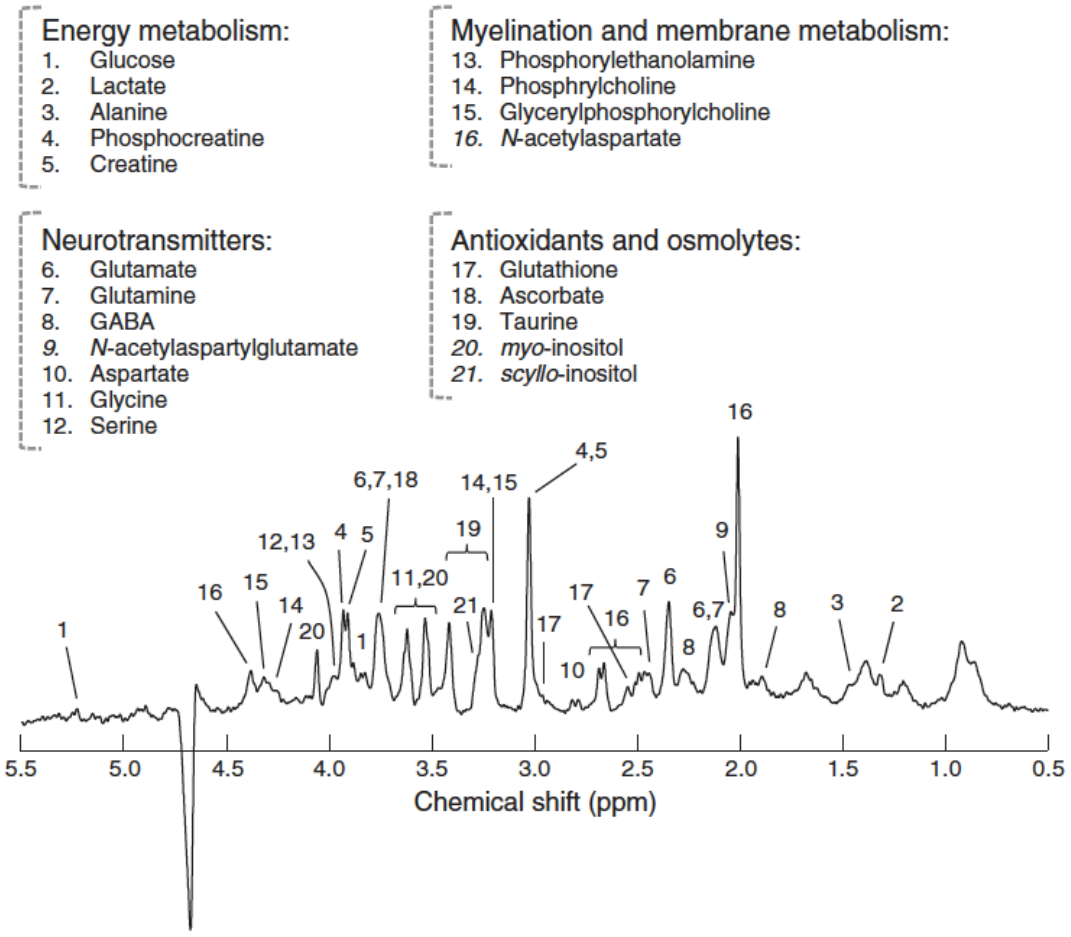


Figure 3.10 Compounds detected in the brain with *in vivo* ^{1}H-MRS

Spectrum was acquired from the rat hippocampus at 14.1 T. (Adapted from Duarte et al 2012)

The primary metabolites of interest in this thesis are the neurotransmitters glutamate (Glu) and GABA. Glutamate is the primary excitatory neurotransmitter in the brain. At 1.5 T, there is almost complete overlap of Glu and glutamine (Gln), and they are detected as a composite "Glx" peak. At higher magnetic field strengths (3.0 T and above), Glu and Gln become better resolved and can be quantified individually with

good accuracy (Tkác et al 2001). Glu level is quantified from a prominent multiplet between 2.35 and 2.04 ppm, and a doublet-of-doublets at 3.74 ppm (Govindaraju et al 2000) and its concentration varies between 5-13 mM, depending on the brain region (Govindaraju et al 2000; Tkác et al 2001; Garwood and DelaBarre 2001; Emir et al 2012).

GABA, the major inhibitory neurotransmitter in the brain, is only present at a very low concentration (~1–2 mM) compared with the other metabolites that dominate the MR spectrum (Novotny et al 2003). In addition, all three GABA resonances (i.e., 3.01 ppm, 2.28 ppm, 1.88 ppm) overlap with stronger signals originating from Glu, NAA, Cr, PCr, and macromolecules (e.g., DNA, RNA, phospholipids). These aspects make reliable quantification of GABA difficult with conventional MRS sequences. One of the most widely applied methods to quantify GABA is the "MEGA-PRESS" (Mescher-Garwood Point-Resolved Spectroscopy) sequence, which dephases unwanted transverse magnetisation at specific frequency and allows editing of GABA (Mescher et al 1998; Floyer-Lea et al 2006).

3.2.4.1 What does MRS-assessed GABA reflect?

In the past few years, there has been much debate on whether the GABA measured using MRS represents all pools of GABA available for measurement (i.e., metabolic, intracellular, and extracellular). Recent studies demonstrated no relationship between MRS-assessed GABA concentration and TMS measures of synaptic $GABA_A$ and $GABA_B$ activity (Stagg et al 2011b; Tremblay et al 2013; Dyke et al 2017), suggesting that GABA concentrations measured with MRS reflect tonic rather than phasic inhibition. This view was supported by the report showing that MRS-assessed GABA levels are related to $SICI_{1ms}$, a TMS measure proposed to reflect tonic extrasynaptic

$GABA_A$ activity (Stagg et al 2011b). However, recent study was unable to replicate these findings (Dyke et al 2017), which indicates that the previously observed relationship between $SICI_{1ms}$ and MRS-GABA may be unreliable.

3.2.5 Ultra-high field MRS

The advantages of performing MRS at ultra-high field (UHF) include increased signal-to-noise ratio (SNR) and better spectral, spatial and temporal resolution, allowing a more accurate metabolite identification and quantification. For example, the differentiation of Glu and Gln signals is difficult at field strengths of 3 T or less due to spectral overlapping, and Glx is reported instead. By contrast, Glu and Gln become separable at field strengths of 7 T and above. Moreover, increased detection sensitivity and efficiency of metabolites, especially those with low concentration such as GABA, can be gained at UHF strengths (Tkáč et al 2009; Puts and Edden 2012). The improved quality of spectral information, however, is not without several limiting factors. The main technical challenges include increased B_0 shimming (optimising B_0 homogeneity over the region of interest) and RF power requirements (for a review, see Di Costanzo et al 2003). In addition, it may be difficult to achieve the desired flip angles in the "MEGA-PRESS", for example. To address these issues, adiabatic excitation or refocusing pulses have been implemented in techniques such as "LASER" (localised by adiabatic selective refocusing) (Garwood and DelaBarre 2001) or its simplified version "semi-LASER" (Scheenen et al 2008; Zhu and Barker 2011).

CHAPTER

4

The physiological effects of driving β and γ oscillations and their behavioural relevance

In this first experimental Chapter I investigated the effects of driving β- and γ-frequency oscillations on various TMS-assessed measures of motor excitability. In addition, I assessed whether the physiological changes induced as a result of driving motor cortical oscillations are behaviourally relevant.

4.1 Introduction

Over the past decades, there has been an increasing understanding of the importance of oscillatory neural activity in underpinning behaviour. In the motor domain, synchronised oscillations in the beta- (β; 15–30 Hz) and gamma-frequency bands (γ; 60–90 Hz) are known to be of particular importance. Specifically, β-band oscillations are the dominant oscillatory activity in the primary motor cortex (M1) at rest (Murthy and Fetz 1992; Salmelin and Hari 1994b), and a reduction in β oscillatory power is routinely observed immediately prior to and during transient voluntary movements (movement-related β desynchronisation [MRBD]) (Baker et al 1997; Pfurtscheller and Lopes da Silva 1999; Hall et al 2011). Conversely, an increase in γ power occurs shortly before movement onset and during movement execution (movement-related γ synchronisation [MRGS]) and has been suggested to reflect the initial activation of primary motor neurons subserving movement (Crone et al 1998; Pfurtscheller and Lopes da Silva 1999; Pfurtscheller et al 2003; Cheyne et al 2008; Muthukumaraswamy 2010; Cheyne 2013; Gaetz et al 2013). Recently, it has been shown in humans that driving γ oscillations facilitates, and driving β oscillations inhibits, motor performance (Pogosyan et al 2009; Joundi et al 2012a), thus demonstrating a causal role of these brain rhythms in motor control.

At a mechanistic level, a growing body of research supports a link between oscillatory activity in both the β- and γ-bands and the balance of excitation and inhibition within reciprocally connected networks of inhibitory GABAergic interneurons and excitatory glutamatergic pyramidal cells within M1 (Whittington et al 1995; Yamawaki et al 2008; Atallah and Scanziani 2009; Gaetz et al 2011; Hall et al 2011; Buzsáki and Wang 2012; Guerra et al 2016). In humans, however, more

research is needed to advance our understanding of the physiological basis underlying these motor rhythms and their behavioural relevance.

tACS is a non-invasive tool which allows the frequency-specific modulation of neural oscillations (Zaehle et al 2010; Feurra et al 2011b; Ali et al 2013) and has been a valuable approach for demonstrating the causal nature of the oscillation-behaviour relationship (Pogosyan et al 2009; Thut et al 2012; Helfrich et al 2014b). Mounting evidence suggests that tACS modulates intrinsic brain oscillations via direct entrainment (Zaehle et al 2010; Herrmann et al 2013; Ali et al 2013; Helfrich et al 2014b; Fröhlich 2015; Witkowski et al 2015), so that its effect is most pronounced when stimulation frequency matches the natural frequency of the stimulated neuronal elements (frequency-tuning) (Zaehle et al 2010; Fröhlich and McCormick 2010; Reato et al 2010; Thut et al 2011; Reato et al 2013; Ali et al 2013). For example, Fröhlich and McCormick (2010) studied the effect of AC stimulation *in vitro* and showed that the frequency of the applied field determined the degree of entrainment of the neural oscillations. If the driving frequency was close to the intrinsic frequency, membrane voltages showed strong periodic fluctuations. In contrast, if the external field differed significantly from the intrinsic frequency, no such entrainment was observed. In a recent human study, the entrainment of selected interneurons by β-frequency tACS has also been supported by demonstrating that tACS that was EEG frequency matched to the individual β peak resulted in a more consistent phase modulation of short interval intracortical inhibition (SICI) (Guerra et al 2016). Overall, these findings suggest that frequency tuning allows for at least some degree of specificity when targeting endogenous network oscillations and highlight the potential of tACS to be used to study local oscillatory activity *in vivo*.

To this end, TMS was employed to evaluate the neurophysiological basis of driving oscillatory activity *in vivo* using tACS. Specifically, the effects of β- and γ-frequency

tACS applied over the M1 for 20 minutes were examined. The effects of tACS on resting physiological measures were studied and, due to the well-recognised patterns of changes in β- and γ-frequency power during movement preparation, the after-effects of tACS on pre-movement physiological measures were also evaluated. Moreover, given the converging evidence demonstrating the critical role of $GABA_A$ inhibition in both motor cortical oscillations and learning (Gaetz et al 2011; Stagg et al 2011a; Hall et al 2011; Pollok et al 2014), I addressed the question of whether the magnitude of tACS-induced changes in $GABA_A$ activity could be related to individual differences in motor learning. I hypothesised that β tACS would increase, and γ tACS decrease, $GABA_A$ inhibition, as assessed via SICI, and, further, that these changes would be related to the degree to which an individual could learn a motor task.

4.2 Methods

4.2.1 Participants

Twenty healthy subjects (age 24.9 years, range: 21–30 years; 9 male) gave their informed consent to participate in the study in accordance with Central University Research Ethics Committee approval (University of Oxford; MSD-IDREC-C2-2014-026 and MS-IDREC-C1-2015-010). All subjects were right-handed as assessed by the Edinburgh Handedness Inventory (Oldfield 1971) and had no history of neurological or psychiatric disorders; no metal implants, and reported no other contraindications to tACS, TMS and MEG.

4.2.2 Experimental design and procedure

Subjects participated in four experimental sessions separated by at least one week and performed at approximately the same time of the day for each subject (Figure 4.1A). In session 1, all subjects had a MEG measurement in order to determine peak β and γ frequency within the left M1 for subsequent tACS sessions. After the MEG recording, participants performed an explicit sequence learning task. In the remaining sessions (2-4), subjects received tACS over the left M1 at β-frequency (individual β-frequency [IBF] or 20 Hz), γ-frequency (75 Hz; see below) or sham stimulation, with the order of sessions counterbalanced across subjects. At the start of each tACS session, participants performed a visually cued response time (RT) task.

Measures of corticospinal excitability, intracortical facilitation and inhibition in left M1 were acquired during eyes-open at rest (in the absence of a task) before (baseline), during (online) and after tACS (post) using TMS (these are referred to as resting-state measures). In addition, in conjunction with a response time task performed with

the right hand, corticospinal excitability and intracortical inhibition were investigated during the pre-movement period before and after tACS (Figure 4.1 B, C).

All subjects had MEG recording and completed the explicit sequence learning task as well as the β tACS and sham sessions. Due to scheduling constraints, eighteen subjects completed the γ tACS session. Data from one β and one γ tACS session were excluded due to difficulties with TMS data acquisition.

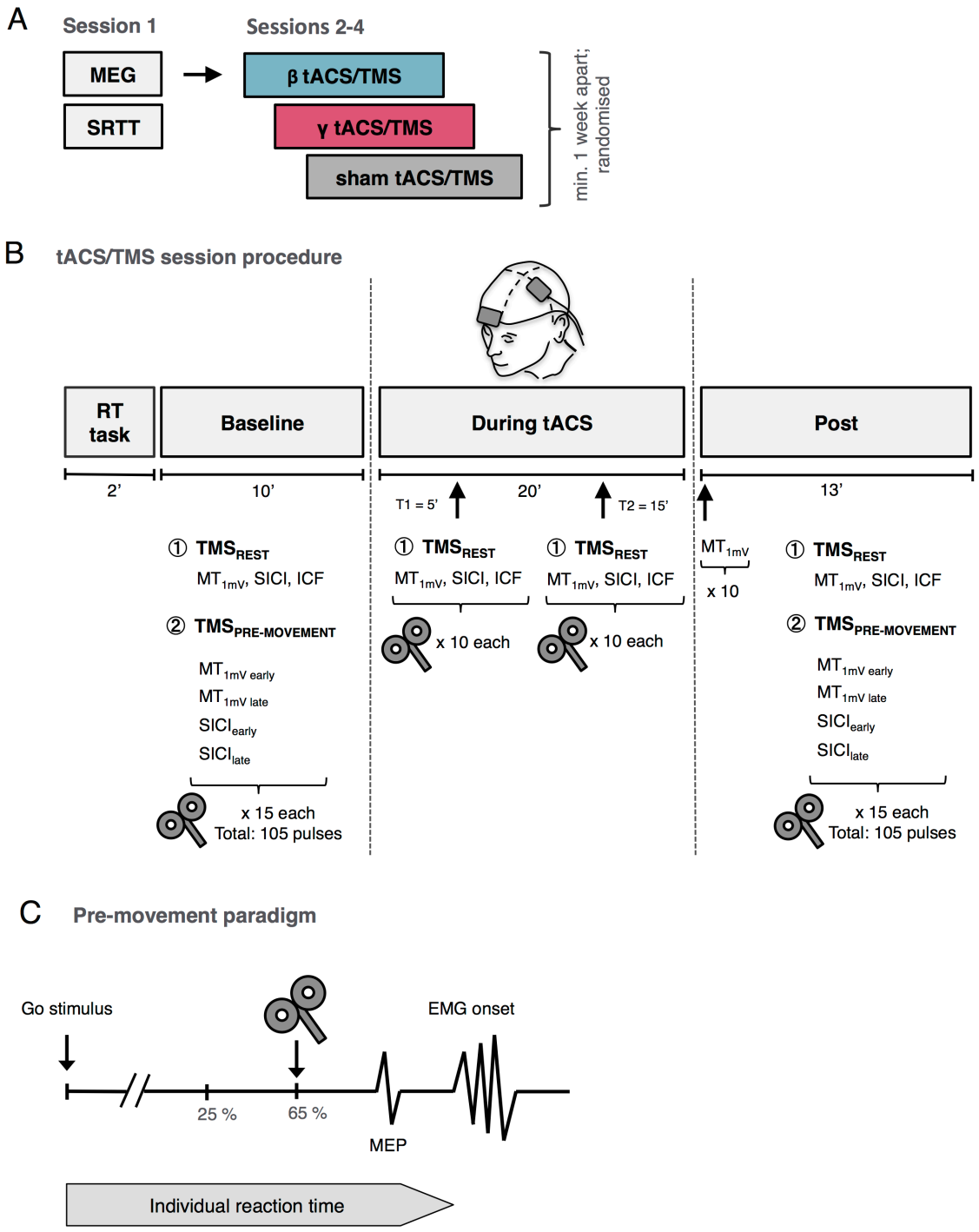


Figure 4.1 Study outline and experimental design

A. Study outline. **B.** Summary of tACS/TMS session procedure. Resting-state TMS measures (MT_{1mV}, SICI, ICF) were applied at baseline, during (at T1 = 5 min and at T2 = 15 min) and after tACS. Event-related TMS measures ($MT_{1mV\ early}$, $MT_{1mV\ late}$, $SICI_{early}$, $SICI_{late}$) were applied at baseline and after tACS. **C.** Pre-movement paradigm. TMS measures were delivered at two time-points during pre-movement period: early (at 25 % iRT) and late (at 65 % of iRT) (see **C**). Abbreviations: ICF, intracortical facilitation; MT_{1mV}, 1 mV motor threshold; iRT, individual response time; SICI, short interval intracortical inhibition; SRTT, serial response time task

4.2.3 MEG

The primary goal of the MEG recording was to acquire resting-state and motor task-related data for the purpose of identification of the peak β and γ frequency, respectively, for subsequent tACS sessions.

4.2.3.1 MEG data acquisition

MEG data were acquired with a whole-head 306-channel Elekta Neuromag system (204 planar gradiometers, 102 magnetometers). Concurrent surface electromyography (EMG) of the right extensor digitorum communis (EDC) and first dorsal interosseous (FDI) muscle were recorded using bipolar surface electrodes. Both MEG and EMG data were sampled at 1000 Hz with a band-pass filter of 0.03–330 Hz, and stored for offline analysis. Head position was continuously monitored with respect to the MEG sensors using four head-position (HPI) coils. The locations of HPI coils and of three anatomical fiducials (the nasion and two preauricular points) were digitized using a 3D tracking system (Polhemus, EastTrach 3D) to define the subject-specific Cartesian head coordinate system. In addition, vertical and horizontal electrooculogram (EOG) electrodes were used to allow for detection and removal of eye-blink artefacts.

MEG data were acquired during a single session consisting of resting-state (8 min; eyes open) and a Go/NoGo task. In the Go/NoGo task, a blue circle cue, presented for 200 ms, instructed participants to prepare for an abduction of the index finger of their right hand. The cue was then replaced by a fixation cross for 1000 ms (cue-stimulus interval; CSI). A subsequent visual stimulus presented for 200 ms (coloured circle: green for Go or red for NoGo) indicated whether they should perform (Go) or withhold (NoGo) the prepared response. Participants were instructed to respond as quickly as possible on the Go trials. The stimulus was then replaced by a fixation

cross for a duration that varied randomly between 2000-4000 ms (inter-trial interval) (Figure 4.2). The task consisted of a total of 70 trials and lasted approximately 5 min. NoGo trials (20 % of all trials) were introduced to encourage participants' attention to the task.

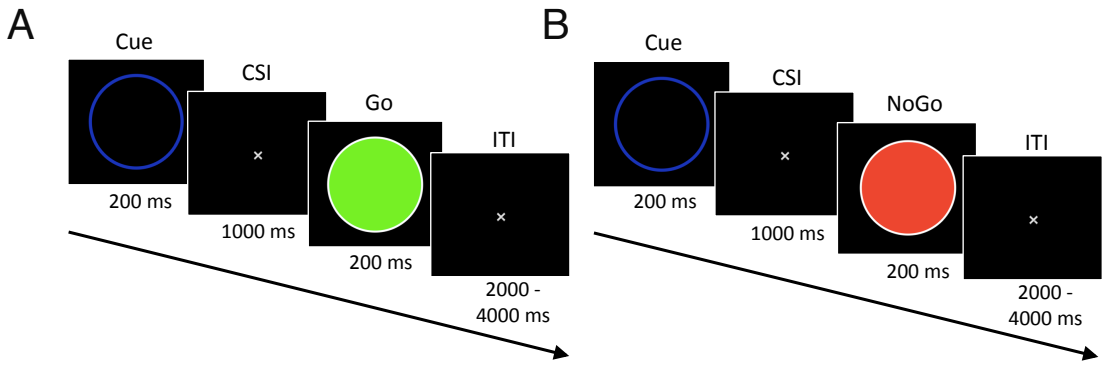


Figure 4.2 Go/NoGo task

Schematic of a Go (A) and NoGo (B) trial. Abbreviations: CSI, cue-stimulus interval; ITI, inter-trial interval.

Stimuli were generated using the MATLAB Psychophysics Toolbox v.3.0 package (Brainard 1997) and back-projected (Panasonic DLP Projector, PT D7700E) onto a screen at a viewing distance of 120 cm with a spatial resolution of 1024 by 768 pixels and a refresh rate of 60 Hz.

4.2.3.2 MEG data analysis

MEG data were analysed using the OHBA Software Library (OSL), Fieldtrip (Oostenveld et al 2011), and Elekta software.

MEG data preprocessing. The raw MEG data were first visually inspected to remove channels with high levels of noise and then the temporal extension of Maxfilter Signal Space Separation (tSSS) method was applied, together with the detection of statistically bad channels and head movement compensation (Taulu and

Simola 2006). Next, continuous data were downsampled to 250 Hz. Physiological artefacts of ocular or cardiac origin were identified via independent component analysis (ICA), and regressed out of the data. The analysis was performed in sensor space. Twelve planar gradiometers covering the left sensorimotor cortex were selected for the analysis of both resting-state and task data (Figure 4.3 A).

The onset of EMG activity was determined in Go trials. This was defined as the first point after the Go stimulus onset where EMG signal exceeded the critical value (calculated as the mean of pre-stimulus activity [-1 s to 0 s] + 3*SD). The cleaned data were then epoched with respect to the onset of EMG (from – 1.5 to + 1.5 s). Any Go trials in which no response was made were rejected. In a final step, data were imported into Fieldtrip and visually inspected using the semi-automatic rejection tool to eliminate any remaining trials with excessive variance in the frequency band of interest (< 2 % of all trials).

Time-frequency analysis of Go/NoGo data. A time-frequency representation of power was computed using a short-time Fourier transform, with a sliding time window of 400 ms that was advanced over the data in 80 ms steps. Power estimates were calculated for frequencies from 2 to 100 Hz in 2-Hz steps. We used a multi-taper method (Percival and Walden, 1993) to achieve frequency smoothing of ± 4 Hz. Baseline correction was applied by subtracting the mean power values between 0 and -1 s relative to onset of the Go stimulus. The Go trials were averaged, and then grand averaged across participants (Figure 4.3 C, left).

Due to the absence of consistent movement-related γ activity (60–90 Hz range) and a distinct peak at this frequency in more than half of subjects, the grand mean time-frequency representation was plotted and, based on that, 75 Hz was selected as stimulation frequency (Figure 4.3C, left). The topographies of the movement-related γ synchronisation (MRGS) (frequency range: 60–90 Hz) and movement-related β desynchronisation (MRBD) (frequency range: 15–30 Hz) for the movement period

(time window: 0 to 0.5 s) are shown in Figure 4.3 C, right. The temporal and spatial pattern of these oscillatory activities is consistent with that reported in previous studies (Cheyne et al 2008; Gaetz et al 2011; Kilavik et al 2013; Cheyne and Ferrari 2013).

Peak detection. The detection of individual oscillatory peaks in the β range (15–30 Hz) was performed on cleaned resting-state MEG data using an in-house script. Oscillatory activity was estimated using a fast Fourier transform. Smoothing was achieved using a Savitzky-Golay filter with the order of 3 and window length of 3 Hz. The peak frequencies were detected by first identifying zero-crossings in the differential of each participant's spectrum before linear interpolation of the differential around the zero was used to locate the peak maximum (Figure 4.3 B). Eleven subjects showed a distinct β-band peak, ranging from 16 to 23 Hz.

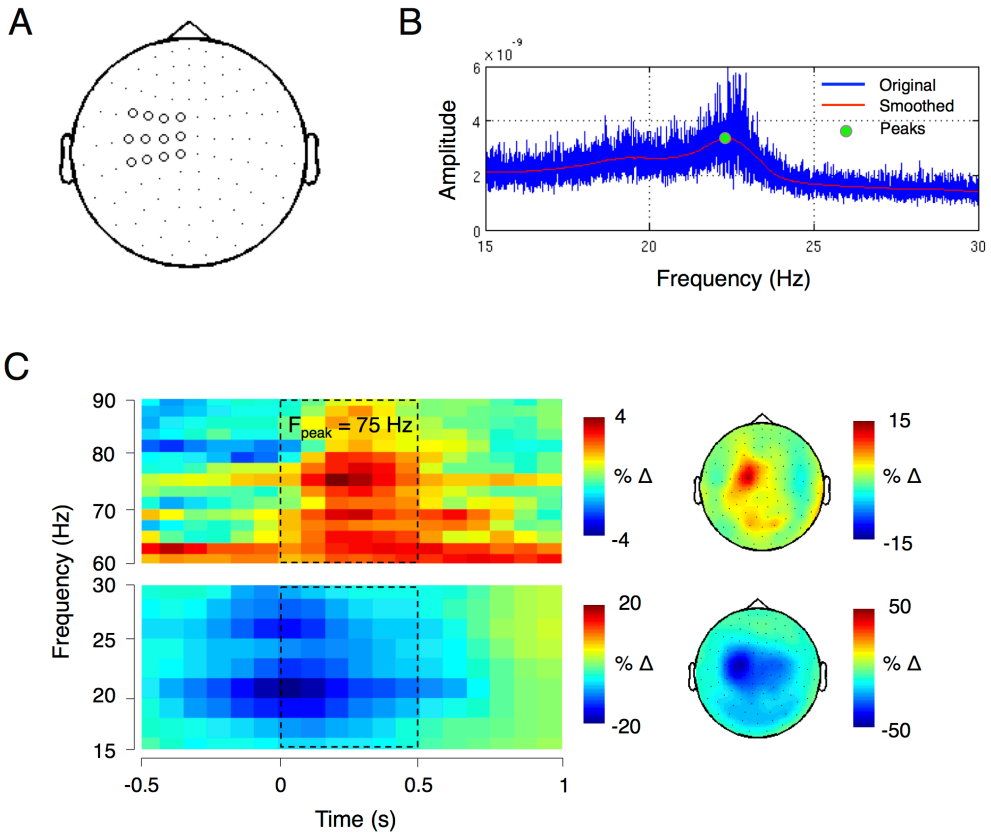


Figure 4.3 MEG analysis results

A. Sensor selection for left sensorimotor cortex. **B.** Amplitude spectrum of one example subject who showed a clear β peak. **C.** (Left) Grand mean time-frequency representation time-locked to the onset of EMG activity (at 0 s) for all subjects. The dashed rectangles denote approximate movement period (0-0.5 s). F_{peak} indicates the mean peak frequency. (Right) Topography in the γ-band (60–90 Hz) (top) and β-band (15–30 Hz) (bottom) over the time-frequency window marked with dashed rectangles on the left. Power is expressed as a percentage change from a 1 s pre-stimulus baseline (i.e. [[power - baseline] / baseline] * 100).

4.2.4 Explicit motor learning task

Subjects performed an explicit, visually cued sequence-learning task after the MEG recording (session 1). As described previously (Stagg et al 2011a), four horizontal bars were displayed on the screen, each of which corresponded to a key on the keyboard. When a bar changed into an asterisk, subjects were instructed to press the corresponding key as quickly and accurately as possible. The task included fifteen sequence blocks consisting of three repeats of a ten-item sequence, and two

random blocks (the first and the fifteenth block) consisting of 30 visual cues presented in a random order.

Response time (RT) was calculated as the time from cue onset to a correct button press. Anticipatory responses, i.e., those that occurred prior to the cue, were discarded. RTs outside of the mean value ± 2 SD for each block were also excluded. One participant was excluded from analysis due to misunderstanding the instructions.

A motor learning score was calculated for each subject as a percentage change from the RT in the first sequence block (Block 2) to blocks 10-14 (i.e., $[RT_{(10\text{-}14)} – RT_{(2)}) / RT_{(2)}] * 100$ %), when the learning plateaued (Stagg et al 2011a).

The overall pattern of reduction in RT would not necessarily indicate that sequence learning occurred as other generic factors, such as comfort with the task, could also lead to a reduction in RT. Therefore, it was important to demonstrate that the observed changes in RT resulted from sequence-specific learning. To this end, it was examined whether RT changed across successive sequence blocks and the two random blocks. If generic factors, such as comfort with the task, affected task performance, a decrease in RT would be expected in both sequence and random blocks.

4.2.5 Response time task

At the start of each tACS/TMS session (sessions 2-4), subjects performed a simple response time task consisting of 20 trials in the absence of TMS in order to characterise their individual RT. 25 % and 65 % of mean individual RT were calculated. The same RT task was then performed in conjunction with TMS before and after tACS. TMS protocols were applied at 25 % and at 65 % of mean individual RT in order to examine M1 excitability at early and late time-points during movement preparation, respectively (see section 4.2.7.5 for more details). Subjects were

instructed to respond to a visual Go signal (coloured green circle) by performing an index finger abduction of the right hand as quickly as possible. Visual stimuli appeared at random intervals (5-7 sec) and the subjects were instructed to avoid anticipation of the Go signal and to relax their hand while the fixation cross was displayed on the screen. Stimuli were generated using the MATLAB Psychophysics Toolbox v.3.0 package (Brainard 1997).

4.2.5.1 Response time data analysis

EMG data acquired during RT task performed in the absence of TMS were analysed online using Signal software v.3.13 (Cambridge Electronic Design Ltd, Cambridge, UK). RT was defined as the time interval (in milliseconds) between the Go signal and the onset of EMG activity in the FDI muscle. The onset of EMG was identified in each trial as the first data point in which the signal exceeded 0.1 mV. The identified RT was then used in the remainder of that experimental session to calculate the timing of the pre-movement TMS pulses.

The data from RT task performed in conjunction with TMS before and after tACS were analysed offline using MATLAB (MathWorks, Inc., Natick, MA, USA). The onset of EMG was identified in each trial as the time when the signal exceeded a threshold of 3 SD of the EMG activity in the 150 ms period preceding the onset of TMS artefact. RT was defined as the time interval between the Go signal and the onset of EMG activity in the FDI muscle and RTs outside mean ± 2 SD for each block were excluded.

4.2.6 Transcranial alternating current stimulation (tACS)

tACS was delivered via a DC stimulator (NeuroConn GmbH, Germany) through a pair of conductive rubber electrodes (5 × 7 cm^2). Chloride free conductive gel was

used as a conducting medium between the scalp and the electrodes. One electrode was centred over the TMS-derived FDI hotspot of left M1 (see below); the other was positioned on the contralateral supraorbital ridge.

tACS was administered in a within-subject design. Subjects participated in two active sessions, with different tACS frequency applied at each session, and one sham session. All sessions were separated by at least 1 week. Subjects received tACS at: (i) β-frequency (individual β-frequency [IBF], n = 11; if no distinct β peak was identified, tACS was applied at group average β-frequency [mean 20.1 Hz, SD = 2.07], n = 9); (ii) γ-frequency (75 Hz), and (iii) sham stimulation.

Stimulation intensity was determined on a subject-by-subject basis and was set to be the highest amplitude that did not elicit phosphenes or discomfort. This resulted in an average stimulation intensity (peak-to-peak) of 0.69 ± 0.11 mA for β-frequency and 1.3 ± 0.36 mA (mean ± SD) for γ-frequency tACS. Given different tACS intensities used, the contribution of intensity to stimulation-induced changes in motor excitability measures was examined (see section 4.3.2.6).

Current was ramped up and down over the first and last 5 s of stimulation. The total duration of stimulation was 20 min for active sessions and 10 s for the sham session. Impedance was kept below 5 kΩ. Subjects were blind to the stimulation condition used.

4.2.7 TMS

4.2.7.1 TMS data acquisition

All TMS data were acquired using a monophasic BiStim machine, connected to a 70 mm figure-of-eight coil (Magstim Co., Whitland, Dyfield, UK). The left M1 was stimulated in all subjects. The optimal scalp position to elicit MEPs (referred to as the motor hotspot) in the right FDI muscle was determined before each session, with the

TMS coil held at 45° to the mid-sagittal line with the handle pointing posteriorly. The hotspot was marked on a tight fitting cap to ensure reproducible coil positioning and TMS pulses were delivered through the M1 electrode. For the duration of the sessions the subjects were seated comfortably in an armchair with their eyes open.

Surface EMG was recorded via disposable neonatal electrocardiogram (ECG) electrodes (Henley's Medical Ltd, Welwyn Garden City, UK) from the FDI of the right hand, using a belly-tendon montage with a ground electrode over the ulnar styloid process. Signals were sampled at 5 kHz, amplified, filtered (10 Hz–1 kHz) and recorded using a CED 1902 amplifier, a CED micro1401 A/D converter and Signal software v.3.13 (Cambridge Electronic Design Ltd, Cambridge, UK).

4.2.7.2 Motor thresholds

The resting 1 mV motor threshold (MT_{1mV}) and active motor threshold (aMT) were determined at the beginning of each tACS/TMS session. The MT_{1mV} was defined as the minimum stimulus intensity required for eliciting an MEP of ~1 mV peak-to-peak amplitude in at least 5 out of 10 consecutive trials in the relaxed FDI muscle. The active motor threshold was defined as the minimum stimulus intensity necessary to evoke a 200 μV peak-to-peak MEP in at least 5 out of 10 consecutive trials while subjects maintained approximately 30 % of the maximum contraction of the FDI.

4.2.7.3 Paired-pulse TMS protocols

Two paired-pulse protocols were performed in the study: short interval intracortical inhibition (SICI) with an ISI of 2.5 ms to assess $GABA_A$ synaptic activity (Kujirai et al 1993; Di Lazzaro et al 2005), and intracortical facilitation (ICF) with an ISI of 12 ms as a measure of NMDA receptor activity (Ziemann et al 1996). The conditioning stimulus (CS) was set at 70 % of aMT and the test stimulus (TS) was set at MT_{1mV} for

both protocols. An ISI of 2.5 ms was selected for SICI in order to avoid contamination with superimposed short interval (I-wave) facilitation (Peurala et al 2008).

4.2.7.4 Rest measures

Resting-state MT_{1mV}, SICI and ICF were measured before, during (at T1 = 5 min and at T2 = 15 min following tACS onset) and after tACS. 15 trials per condition were applied before and after tACS and 10 trials per condition were applied during tACS. Due to potential changes in motor cortex excitability after tACS, 10 single pulse MEPs were recorded at the original intensity immediately after stimulation had ceased. If the amplitude of the resulting MEP differed markedly from 1 mV, the stimulation intensity was altered accordingly (Nitsche et al 2005; Amadi et al 2015) before other post-tACS measures were taken. MT_{1mV}, SICI and ICF were delivered in a pseudo-randomised order (Figure 4.1B).

4.2.7.5 Pre-movement measures

MT_{1mV} and SICI were also measured during the pre-movement period in a simple RT paradigm before and after tACS. To avoid any potential interactions between tACS and task performance, pre-movement measures were not performed during stimulation. The TMS measures were performed in a pseudo-randomised order at two different timings during movement preparation: early time-point (25 % of mean individual RT) and late time-point (65 % of mean individual RT), resulting in four different pre-movement protocols: $MT_{1mV\ early}$, $MT_{1mV\ late}$, $SICI_{early}$ and $SICI_{late}$. 25 % and 65 % RT were adjusted to each subject's mean RT according to a previously described procedure (Murase et al 2004; Hummel et al 2009). 15 trials per condition and time-point were recorded (Figure 4.1 B).

4.2.7.6 MEP data analysis

Trials were excluded if the test pulse alone failed to elicit a reliable MEP (amplitude < 0.1 mV), there was pre-contraction in the target FDI muscle (EMG amplitude > 0.1 mV in the 80 ms preceding the pulse) or, for the pre-movement TMS measures, EMG onset coincided with TMS pulse, or no response was made. The peak-to-peak amplitude for each MEP was then calculated. Any MEPs which were outside 2 SD of the mean for each condition for each block were rejected. Next, a single iteration of Grubbs' test with a significance level of 0.05 was performed for each TMS condition separately and any significant outliers excluded. Collectively, these rejection criteria resulted in the exclusion of less than 5 trials per subject in any condition (a minimum of 10 trials were analysed per subject in any condition).

Given that pre-contraction at very low EMG levels can affect MEP amplitudes, the above exclusion criterion may not be sufficient to detect such sub-threshold fluctuations in the signal. To further control for background EMG activity, we calculated the root mean square (RMS) of the EMG signal in the 80 ms preceding the TMS pulse. A repeated measures (RM) ANOVA with one factor of session (β, γ, sham tACS), one factor of protocol (rest protocols or pre-movement protocols) and one factor of time (pre, post or T1, T2) showed no significant main effects or interactions ($p < 0.05$), suggesting that there were no differences in EMG activity between the experimental conditions.

SICI and ICF were expressed as a ratio of the mean conditioned MEP amplitude to the mean unconditioned MEP amplitude (MT_{1mV}).

For the pre-movement data, the TMS measures were analysed separately for each pre-movement time-point (0.25 and 0.65 RT). SICI values were expressed as a ratio of the mean conditioned MEP amplitude to the mean unconditioned MEP amplitude at that specific time-point.

Finally, to investigate the offline effect of tACS on dynamic changes in corticospinal excitability and intracortical inhibition over the pre-movement time span, a linear function was fitted to each subject's MT_{1mV} and SICI amplitudes (expressed as a ratio of the mean conditioned stimulus to the unconditioned stimulus amplitude [MT_{1mV}] occurring temporally closest to it) against the position in the pre-movement period when the TMS pulse was delivered. The effect of tACS on the slope of this function was then assessed. The steeper the slope the higher the increase in dynamic MT_{1mV} and SICI modulation (less inhibition) approaching movement.

4.2.8 Statistical analysis

Statistical analyses were performed using MATLAB 8 software (version R2014b; The MathWorks, Inc., Natick, MA, USA), GraphPad Prism (version 7, GraphPad Software Inc., San Diego, CA, USA) and SPSS (version 22.0; IBM).

Normality of data distribution was tested by D'Agostino-Pearson omnibus normality test. All MEP and RT data passed the normality test. Data were analysed using RM ANOVA. In the case of significant effects, *post hoc* analyses with paired t-tests (two-tailed) were applied. Mauchly's test was used to test for assumption of sphericity and Greenhouse–Geisser corrections were applied as necessary. Effect size estimates were computed using partial eta squared (η2*p*) for RM ANOVAs and Cohen's d_z for t-tests. Correlations were assessed using the Spearman's rank correlation method (ρ), and the obtained correlation coefficients were converted into z-values with Fisher's r-to-z transformation. Paired t-tests (two-tailed) were then used to test for differences between correlations. In order to prevent a bias, only the subjects for whom the data were available for all sessions were considered for correlational analyses. The significance level for all tests was set at $p < 0.05$.

4.3 Results

4.3.1 Quality assessment

First, it was important to ensure that there were no systematic differences between the sessions at baseline. For each metric, a RM ANOVA with one factor of session (β, γ, sham tACS) was performed on the baseline data. There was no difference in motor thresholds between stimulation sessions (MT_{1mV}: $F_{(2,34)}$ = 0.564, p = 0.574; aMT: $F_{(2,34)}$ = 0.398, p = 0.675) (Table 4.1).

	β tACS	γ tACS	sham tACS
MT_{1mV}	62.7 ± 11.4	63.6 ± 11.7	62.3 ± 11.3
aMT	40.4 ± 7.5	39.8 ± 7.1	40.2 ± 7.5

Table 4.1 Mean motor thresholds (± SD)

Further, there were no differences between sessions in MEP amplitude resulting from any of the protocols performed at rest (MT_{1mV}: $F_{(2,30)}$ = 0.356, p = 0.703; SICI: $F_{(2,26)}$ = 2.064, p = 0.147; ICF: $F_{(2,30)}$ = 0.356, p = 0.703) or during movement preparation ($MT_{1mV\ early}$: $F_{(2,30)}$ = 0.165, p = 0.849; $MT_{1mV\ late}$: $F_{(2,30)}$ = 0.669, p = 0.520; $SICI_{early}$: $F_{(2,32)}$ = 2.195, p = 0.128; $SICI_{late}$: $F_{(2,30)}$ = 0.493, p = 0.616) (Figure 4.4). Finally, there was no difference in baseline mean RT values between sessions ($F_{(2,30)}$ = 0.207, p = 0.814).

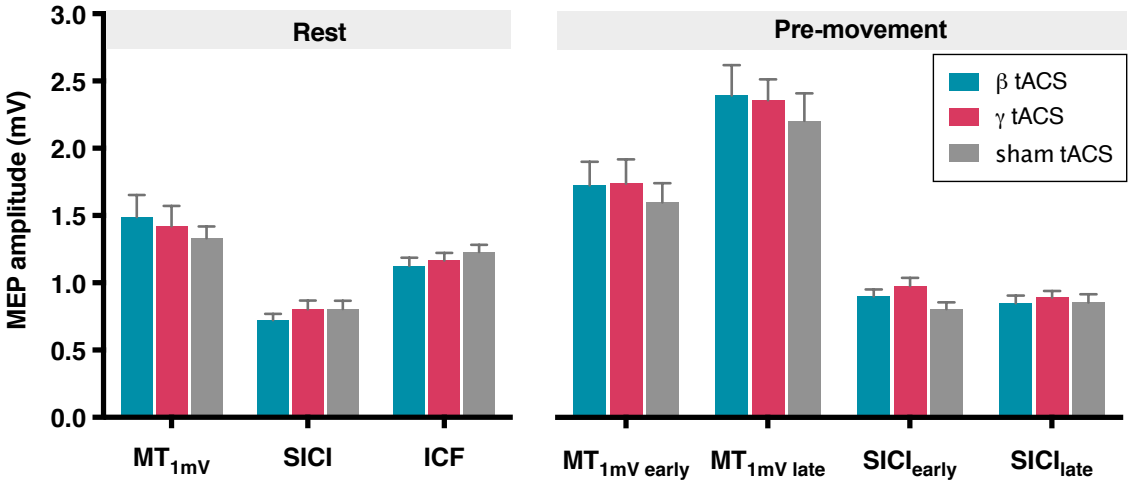


Figure 4.4 Average baseline MEP amplitude values

Average baseline MEP amplitude values (± SEM) for resting-state and pre-movement TMS protocols for each tACS session.

Next, to confirm that there was no difference between the amplitude of MT_{1mV} at baseline and the amplitude of MT_{1mV} adjusted post-stimulation, a RM ANOVA with one factor of session (β, γ, sham tACS) and one factor of time (baseline, post) was performed. There was no main effect of time ($F_{(1,14)}$ = 0.594, p = 0.158) or session ($F_{(2,28)}$ = 0.462, p = 0.635) and no session × time interaction ($F_{(2,28)}$ = 3.182, p = 0.057).

Finally, to verify that the paired-pulse protocols elicited the expected inhibition and facilitation at rest, a RM ANOVA with one factor of session (β, γ, sham tACS) and one factor of protocol (MT_{1mV} and paired-pulse TMS protocol) was performed on the mean baseline values. A significant main effect of protocol was found when MT_{1mV} was compared against SICI ($F_{(1,14)}$ = 8.582, p = 0.011) and ICF ($F_{(1,15)}$ = 12.977, p = 0.003). *Post hoc* analyses showed that, as expected, the SICI protocol led to a significant inhibition, and ICF to a significant facilitation, of MEP amplitudes in all sessions (Figure 4.5).

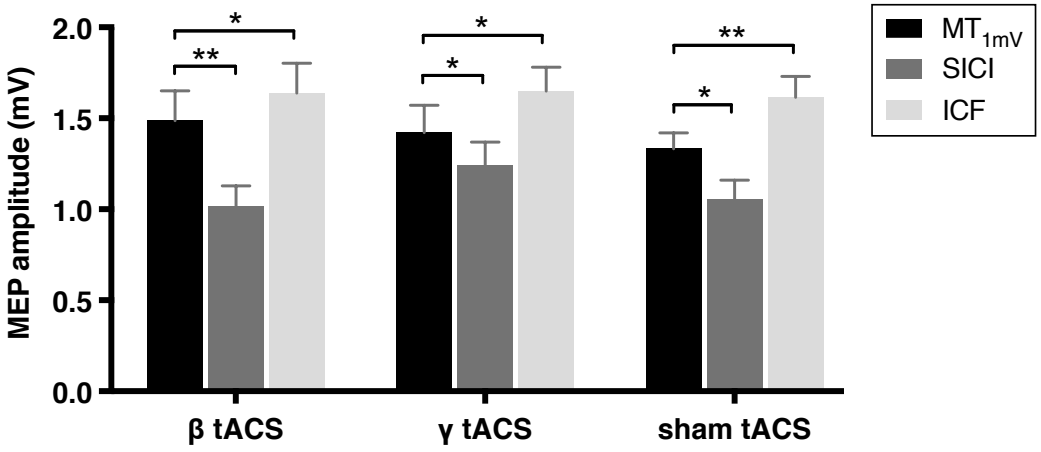


Figure 4.5. Effectiveness of paired-pulse TMS protocols at baseline

Average baseline MEP amplitude values (± SEM) for resting-state TMS protocols for each tACS session. *$p < 0.05$, **$p < 0.005$

4.3.2 Effects of tACS on physiological measures at rest

Having confirmed that there were no systematic differences between sessions and that the TMS protocols employed in this study had the expected effects, I then wished to examine the effects of driving oscillatory activity on resting cortical physiology.

4.3.2.1 tACS does not affect corticospinal excitability

First, the effects of driving cortical oscillations on corticospinal excitability, as reflected by a single MEP amplitude (MT_{1mV}), were examined. A RM ANOVA with one factor of session (β, γ, sham tACS) and one factor of time (baseline, T1, T2, post) revealed no significant effect of tACS on corticospinal excitability (no main effect of time [$F_{(3,33)} = 0.179$, $p = 0.910$, $\eta 2p = 0.016$] or session [$F_{(2,22)} = 2.421$, $p = 0.112$, $\eta 2p = 0.180$] and no significant session × time interaction [$F_{(6,66)} = 0.754$, $p = 0.526$, $\eta 2p = 0.064$]) (Figure 4.6 A).

4.3.2.2 tACS does not affect glutamatergic activity

Next, the effects of tACS on glutamatergic activity, as reflected by ICF, were examined. In line with the lack of effect on single-pulse MEPs, which are also thought to partly reflect glutamatergic activity, a RM ANOVA with one factor of session (β, γ, sham tACS) and one factor of time (baseline, T1, T2, post) revealed no main effect of time ($F_{(3,42)}$ = 0.650, p = 0.587, η2p = 0.044) or session ($F_{(2,28)}$ = 0.035, p = 0.966, η2p = 0.002) and no significant session × time interaction ($F_{(6,84)}$ = 1.598, p = 0.158, η2p = 0.102) (Figure 4.6 B).

4.3.2.3 Frequency-matched β tACS does not affect motor excitability measures

Since the effects of tACS are more pronounced when the stimulation frequency coincides with the natural resonance frequency of local neural circuits (Zaehle et al 2010; Fröhlich and McCormick 2010; Reato et al 2010; Romei et al 2016; Guerra et al 2016), the analysis was performed specifically on the subset of participants who received β tACS that was matched to their individual β peak frequency (IBF tACS group; n = 11). A RM ANOVA with one factor of session (IBF tACS, sham tACS) and one factor of time (baseline, T1, T2, post) was performed for each resting-state protocol (MT_{1mV}, SICI, ICF). The results revealed no significant effect of IBF tACS on any of the protocols as compared with the sham session ($p > 0.05$).

4.3.2.4 γ tACS modulates $GABA_A$ inhibition in a duration-dependent manner

I then went on to investigate the effects of tACS on local $GABA_A$ inhibition, as reflected by SICI. A RM ANOVA with one factor of session (β, γ, sham tACS) and one factor of time (baseline, T1, T2, post) was performed. The analysis revealed no

main effect of time ($F_{(3,39)}$ = 1.484, p = 0.234, η2p = 0.102) or session ($F_{(2,26)}$ = 0.542, p = 0.588, η2p = 0.040) but a significant session × time interaction ($F_{(6,78)}$ = 3.191, p = 0.007, η2p = 0.197).

Follow-up RM ANOVAs with one factor of session (active stimulation, sham tACS) and one factor of time (baseline, T1, T2, post) revealed a significant change in SICI in the γ session as compared with sham (no main effect of time [$F_{(3,42)}$ = 2.267, p = 0.095, η2p = 0.139] or session [$F_{(1,14)}$ = 0.305, p = 0.589, η2p = 0.021] but a significant session × time interaction [$F_{(3,42)}$ = 5.122, p = 0.004, η2p = 0.268]). SICI in the γ session was also significantly different when compared with SICI in the β session (no main effect of time [$F_{(3,39)}$ = 1.451, p = 0.243, η2p = 0.100] or session [$F_{(1,13)}$ = 0.831, p = 0.379, η2p = 0.060] but a significant session × time interaction [$F_{(3,39)}$ = 4.107, p = 0.013, η2p = 0.240]). There was no significant difference between the β and sham sessions.

Post hoc t-tests demonstrated a significant decrease in SICI during γ tACS as compared with sham at T1 ($t_{(15)}$ = 3.820, p = 0.002, Cohen's d_z = 0.955), but not at T2 ($t_{(16)}$ = -1.432, p = 0.171, Cohen's d_z = -0.347) (Figure 4.6 C). SICI at T1 in the γ session was also significantly smaller than at baseline ($t_{(15)}$ = 2.343, p = 0.033, Cohen's d_z = 0.586) and at T1 in the β session ($t_{(15)}$ = 3.317, p = 0.005, Cohen's d_z = 0.829), whereas SICI in the sham session increased significantly compared with baseline ($t_{(17)}$ = -2.437, p = 0.026, Cohen's d_z = -0.574). Within-session analyses revealed that SICI at T1 in the γ session was significantly smaller than at T2 ($t_{(16)}$ = 4.359, p < 0.001, Cohen's d_z = 1.057). In contrast, no difference was observed between SICI at T1 and T2 in the sham session (T2: $t_{(17)}$ = -1.959, p = 0.067, Cohen's d_z = -0.462).

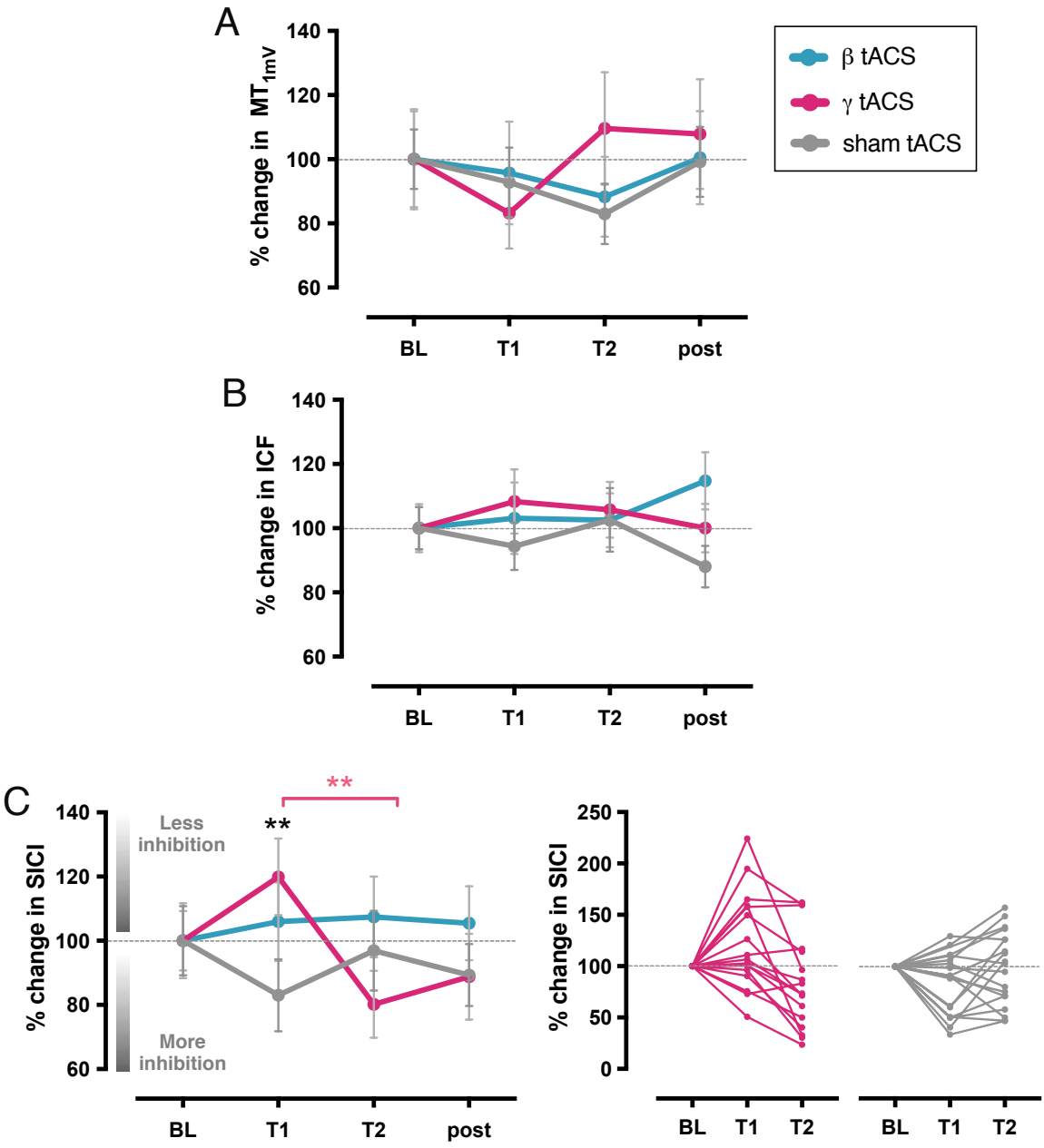


Figure 4.6 The effect of tACS on resting-state motor excitability measures

Average MEP amplitude (± SEM) values for MT_{1mV} (**A**), SICI (**B**) and ICF (**C**, left) at baseline (BL), T1 (5 min) and T2 (15 min) and after tACS for all sessions: β, γ, sham tACS. (**C**, right), Individual subject data showing MEP amplitude values for SICI at BL, T1 and T2 in γ and sham sessions. MEP amplitudes are given relative to baseline (set as 100 %). SICI amplitude was increased at T1 by γ tACS as compared with sham session (black asterisks) and as compared with T2 in γ session (pink asterisks). *$p < 0.05$, **$p < 0.005$

4.3.2.5 γ tACS-induced change in $GABA_A$ activity is unrelated to change in corticospinal excitability

Although the results showed that a significant γ tACS-induced change in $GABA_A$ inhibition at T1 was not accompanied by a significant change in corticospinal excitability (a single MEP amplitude), I also examined whether these two metrics of motor excitability could be directly linked. No correlation was found between MT_{1mV} and SICI amplitude at T1 ($\rho = -0.246$, $p = 0.375$) or at T2 ($\rho = -0.189$, $p = 0.498$).

4.3.2.6 γ tACS-induced change in $GABA_A$ activity is not related to current intensity

Due to the experimental procedures employed in this study, a significantly higher peak-to-peak current amplitude was used for γ tACS compared with β tACS. I therefore wished to examine whether the effects seen due to γ stimulation could be directly attributed to the higher current intensity. First, correlation analysis was performed to assess whether there was a relationship between γ tACS-affected $SICI_{T1}$ and stimulation intensity. No significant correlation was found ($\rho = -0.129$; $p = 0.630$). Second, I used a median split procedure in which participants within each active stimulation session were divided into two groups, low and high stimulation intensity. Next, $SICI_{T1}$ measures in γ session, low stimulation group, were compared separately against those in β session, high stimulation group. Similarly, $SICI_{T1}$ measures in γ session, high stimulation group, were compared against those in β session, low stimulation group. None of the group comparisons performed was significant ($p > 0.05$).

4.3.2.7 Baseline pre-movement $GABA_A$ activity is related to γ tACS-induced changes in resting $GABA_A$ inhibition

Finally, I wished to explore the potential mechanism underlying the γ tACS-induced decrease in $GABA_A$ activity. Specifically, I hypothesised that if γ tACS engages endogenous circuits then the magnitude of the $GABA_A$ decrease in response to tACS should be related on a subject-by-subject basis to the magnitude of $GABA_A$ release in the pre-movement period, close to movement onset, when an endogenous engagement of local interneuronal circuits that are central to the generation and maintenance of γ oscillations would be expected.

To this end, I performed correlations between pre-movement $SICI_{late}$ at baseline and resting-state SICI changes recorded during stimulation (at T1 = 5 min and T2 = 15 min) for each session. The results revealed a positive association between baseline pre-movement $SICI_{late}$ and change in $SICI_{T1}$ in γ session ($\rho = 0.692$, $p = 0.003$) but not in β or sham sessions (β tACS: $\rho = 0.088$, $p = 0.744$; sham tACS: $\rho = -0.269$, $p = 0.295$; γ versus sham tACS: $Z = 3.12$, $p = 0.002$; β versus sham tACS: $Z = 0.97$, $p = 0.333$) (Figure 4.7).

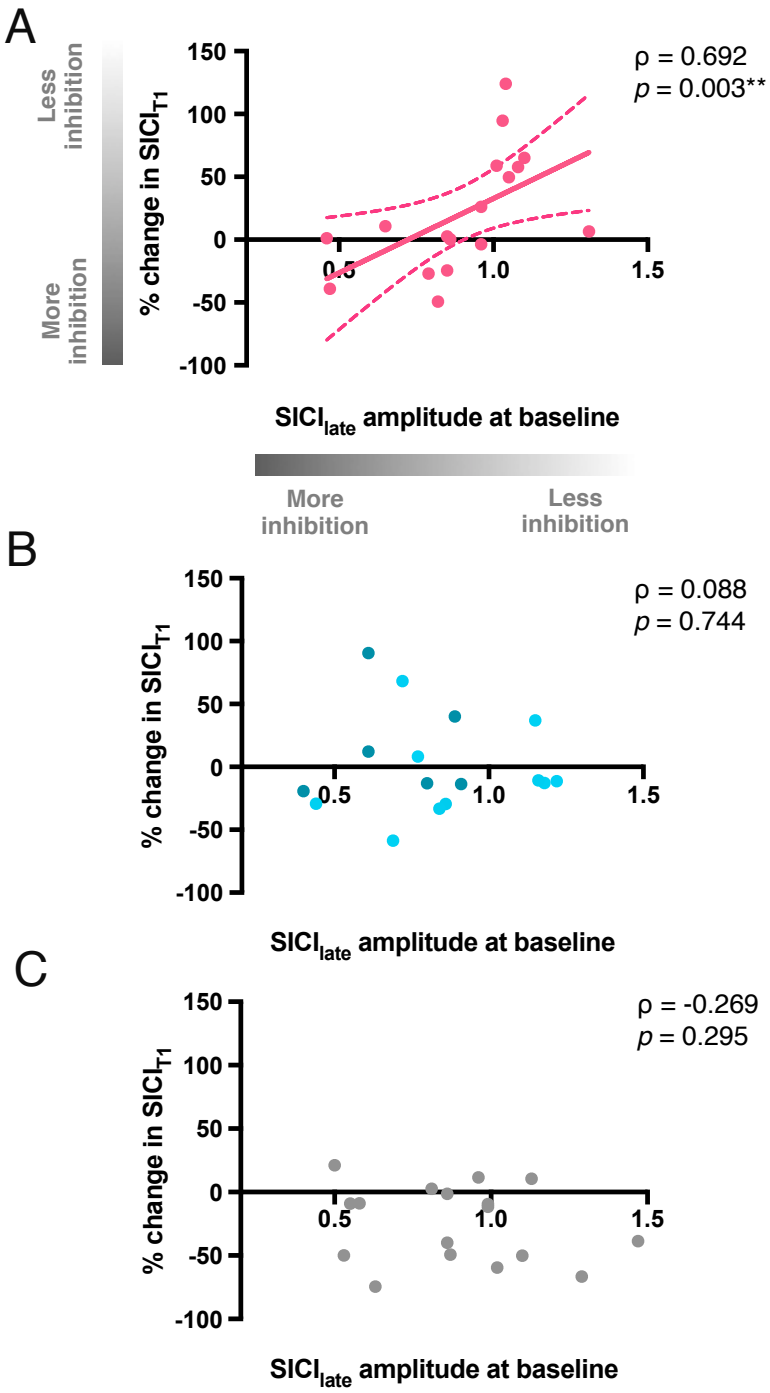


Figure 4.7 Relationship between the magnitude of baseline SICI$_{late}$ and the magnitude of tACS-induced change in SICI$_{T1}$

Correlation between pre-movement SICI$_{late}$ prior to stimulation and % change in resting-state SICI at early time-point during stimulation (SICI$_{T1}$) relative to baseline in γ tACS (**A**), β tACS (**B**) and sham sessions (**C**). Light blue circles in correlations for β session (**B**) represent participants who received IBF tACS. *p < 0.05, **p < 0.005

4.3.2.8 γ tACS-induced modulation of $GABA_A$ inhibition predicts an individual's ability to learn a motor task

Finally, given the converging evidence demonstrating the critical role of $GABA_A$ inhibition in both motor cortical oscillations and motor learning (Gaetz et al 2011; Stagg et al 2011a; Hall et al 2011; Pollok et al 2014), I set out to determine whether tACS-induced changes in $GABA_A$ inhibition were related to individual differences in motor learning performance.

First, I determined whether subjects were able to learn the task. As expected, response time (RT) significantly decreased across successive sequence blocks ($F_{(14,140)} = 9.972$; $p < 0.001$). By contrast, there was no significant difference in mean RT between the two random blocks ($t_{(16)} = 0.548$; $p = 0.591$), whereas there was a significant difference between Block 14 (the final learning block) and Block 15 (the second random block) ($t_{(13)} = -9.611$; $p < 0.001$), suggesting that improvements in RT occurred via learning of a specific sequence and not generic skill learning. There was also no significant difference between the RT from blocks 10-14, which were on the plateau of the learning curve ($F_{(4,48)} = 0.984$; $p = 0.425$).

A strong correlation was identified between motor learning performance and the change in $SICI_{T1}$ and, to a lesser extent, a change in $SICI_{post}$ induced by γ tACS (T1: ρ = 0.804, $p < 0.001$; post: ρ = 0.564, $p = 0.031$) (Figure 4.8 A, D). Specifically, it was observed that individuals who exhibited a greater increase in $GABA_A$ inhibition at an early time-point during and after γ tACS performed better in the motor learning task. No significant association was detected between motor learning and tACS-induced change in SICI in β (T1: ρ = 0.282, $p = 0.307$; post: ρ = -0.279, $p = 0.314$) (Figure 4.8 B, E) or sham sessions (T1: ρ = -0.014, $p = 0.964$; post: ρ = -0.114, $p = 0.686$) (Figure 4.8 C, F). In addition, the correlation between motor learning and γ tACS-

induced change in $SICI_{T1}$ was significantly different as compared with sham (Z = 2.76, p = 0.006) but not when compared with β session (Z = 1.92, p = 0.055).

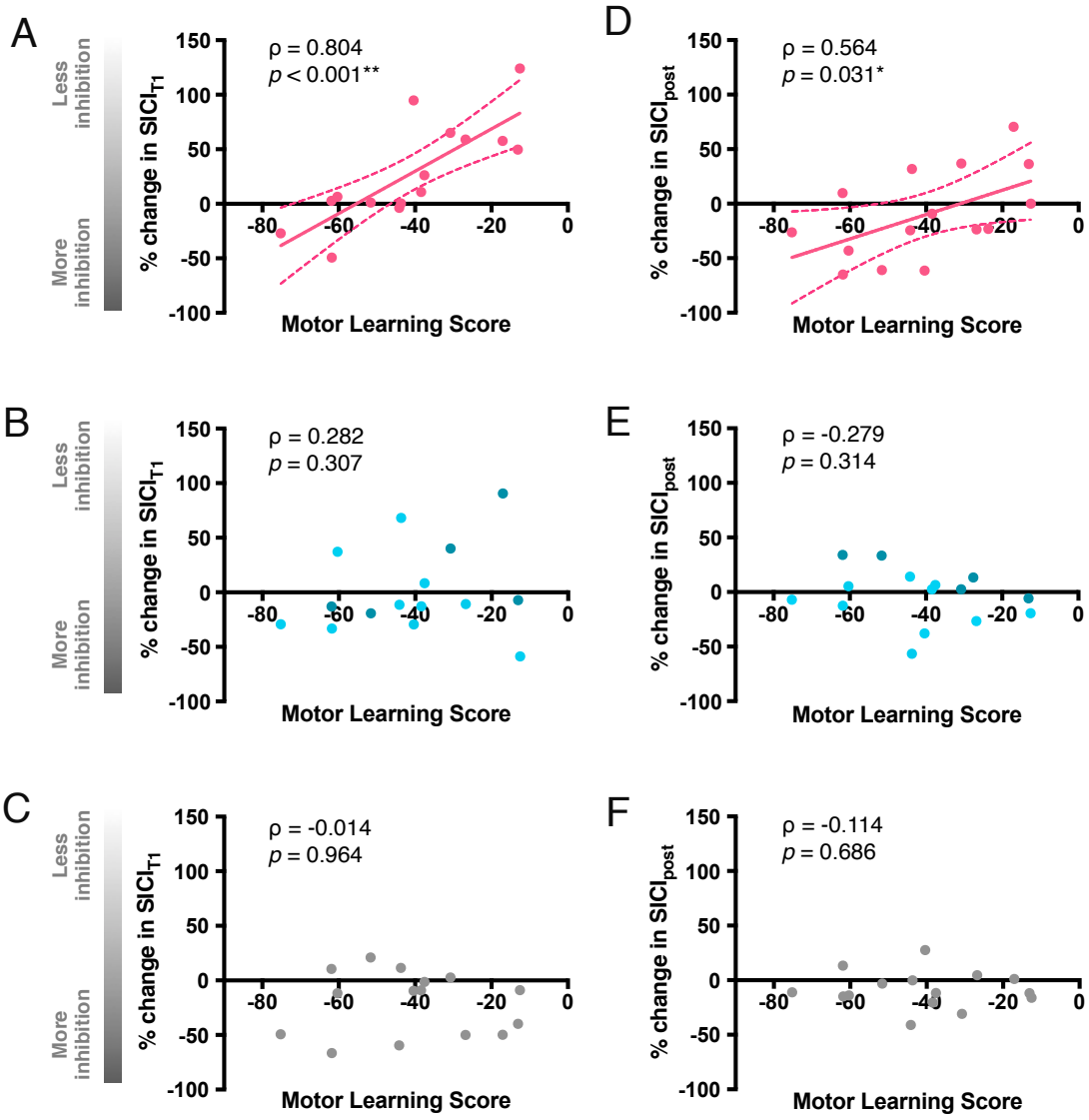


Figure 4.8 Relationship between motor learning score and tACS-induced change in SICI

Correlations between motor learning score and stimulation-induced change in SICI at early time-point during ($SICI_{T1}$, left) and after stimulation ($SICI_{post}$, right) in γ (**A**, **D**), β (**B**, **E**), and sham sessions (**C**, **F**). Light blue circles in correlations for β session (**B**, **E**) represent participants who received IBF tACS. *p < 0.05, **p < 0.005

4.3.3 tACS has no after-effects on pre-movement physiological measures

Based on the well-recognised distinct patterns of changes in β- and γ-frequency power during movement preparation, in parallel to changes in motor excitability, it was of interest to examine whether tACS had any after-effects on pre-movement physiological measures. First, the distribution of TMS protocols (both MT_{1mV} and SICI) was plotted across pre-movement period for each session in order to find out whether the pulses delivered at an early time-point (0.25 RT) were separate from those delivered at a later time-point (0.65 RT) (Figure 4.9).

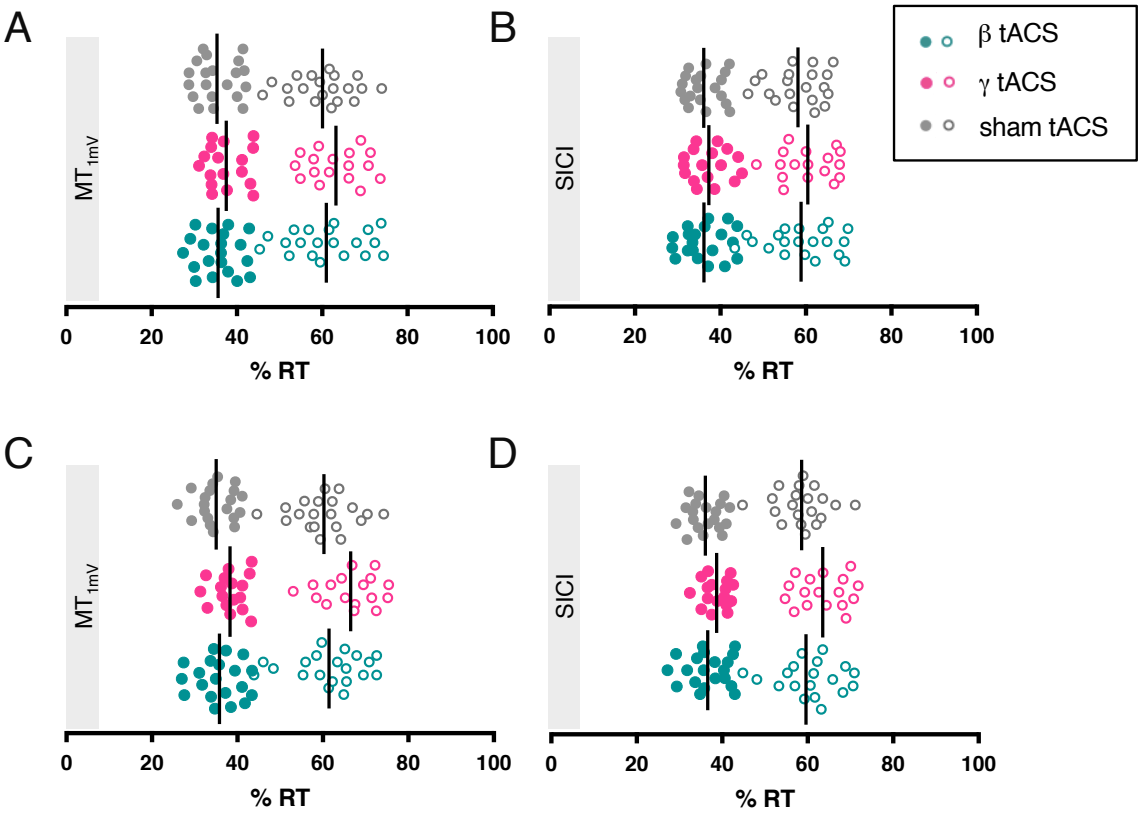


Figure 4.9 Distribution of TMS measures during pre-movement period

Distribution of TMS measures during pre-movement period at baseline (**A**, **B**) and after tACS (**C**, **D**), shown as % of RT. Each dot represents one participant. The filled dots represent TMS measures applied at early time-point during pre-movement period ($MT_{1mV\ early}$, $SICI_{early}$) and empty dots show TMS measures applied at late time-point during pre-movement period ($MT_{1mV\ late}$, $SICI_{late}$). The black vertical line represents the mean.

Given the distribution of the TMS protocols during the pre-movement period, MT_{1mV} and SICI measures were analysed separately for early and late pre-movement time-points. RM ANOVAs with the factor of session (β, γ, sham tACS) and time (baseline, post) were performed for each pre-movement protocol ($MT_{1mV\ early}$, $MT_{1mV\ late}$, $SICI_{early}$, $SICI_{late}$). No effect of tACS on any of the pre-movement protocols was found ($p > 0.05$) (Figure 4.10).

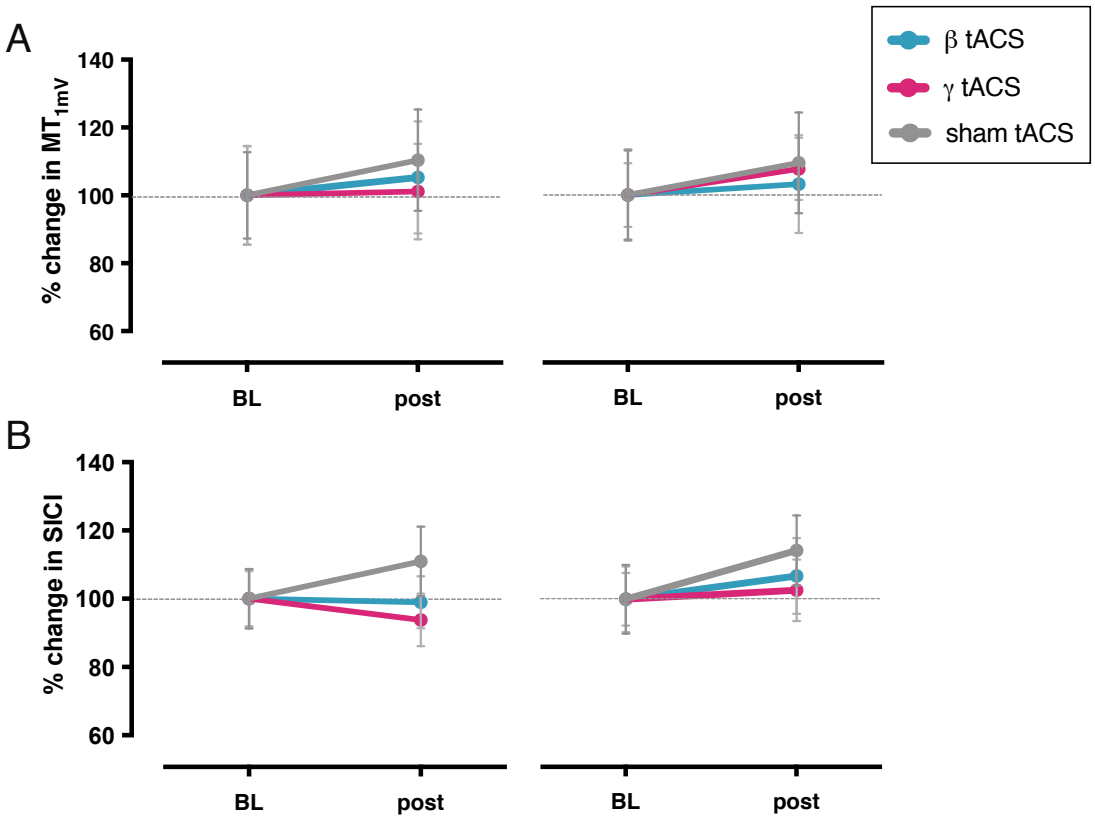


Figure 4.10 The effect of tACS on pre-movement motor excitability measures

Average MT_{1mV} (**A**) and SICI amplitude values (± SEM) (**B**) at baseline (BL) and after tACS for early time-point (left) and late time-point (right) during pre-movement period for each session. MEP amplitudes are given relative to baseline (set as 100%).

Next, the after-effect of tACS on dynamic changes in MT_{1mV} and SICI over the pre-movement time span were examined (see section 4.2.7.6 in Methods for details). RM ANOVAs with the factor of session revealed no differences between any of the

sessions in pre-movement MT_{1mV} modulation (slope) ($F_{(2,30)}$ = 0.695, p = 0.507, η2p = 0.044) nor in SICI modulation ($F_{(2,26)}$ = 2.660, p = 0.089, η2p = 0.170) (Figure 4.11).

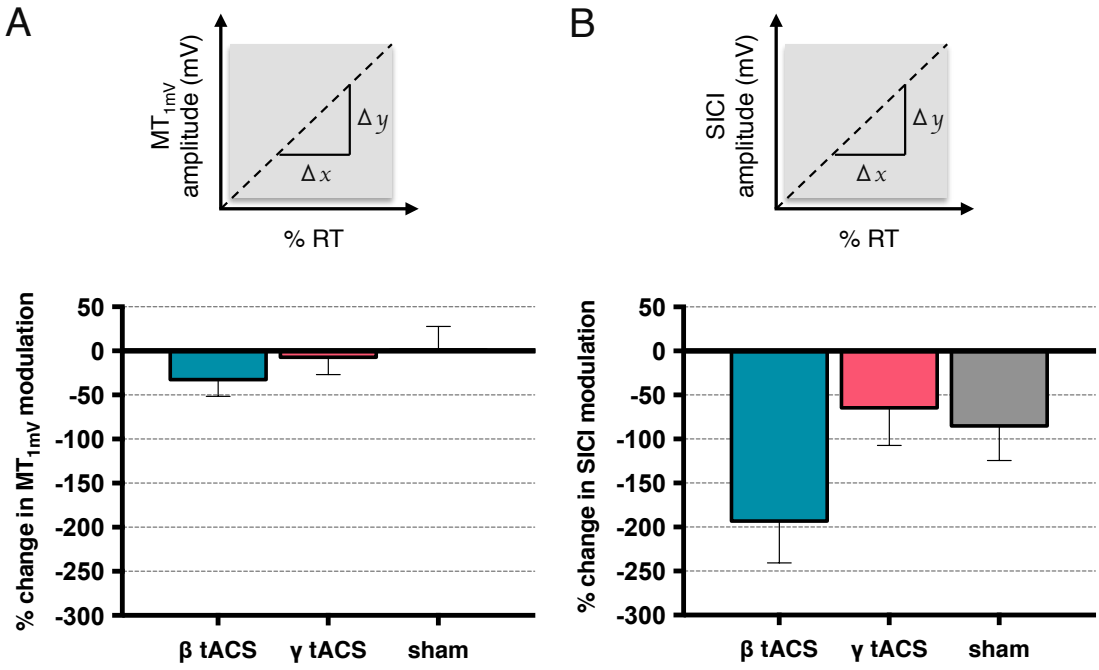


Figure 4.11 The effect of tACS on dynamic MT_{1mV} and SICI modulation

Change in pre-movement MT_{1mV} (**A**) and SICI modulation (**B**) (linear slope normalised to baseline slope) for each session. The values are expressed as % change ± SEM.

4.3.4 tACS has no after-effects on response time

Based on the previously proposed anti- and prokinetic role of β and γ oscillations, respectively (Pogosyan et al 2009; Joundi et al 2012; Gonzalez Andino 2004), I aimed to investigate whether prolonged application of oscillatory currents at β- and γ-frequencies had any after-effect on response time (RT). A RM ANOVA with one factor of session (β, γ, sham tACS) and one factor of time (baseline, post) revealed no significant change in RT after stimulation had ceased (no main effect of time [$F_{(1,15)}$ = 2.586, p = 0.129, η2p = 0.147] or session [$F_{(2,30)}$ = 0.711, p = 0.499, η2p =

0.045] and no significant session × time interaction [$F_{(2,30)}$ = 0.968, p = 0.391, η2p = 0.061]) (see Table 4.2 for summary of mean RTs for all sessions; Figure 4.12 A).

	β tACS	**γ tACS**	**Sham**
Baseline	207.7 ± 0.04	200.0 ± 0.03	209.0 ± 0.04
Post	205.8 ± 0.04	192.0 ± 0.03	207.3 ± 0.03

Table 4.2 Mean response times (± SD) at baseline and post-tACS for each session

In addition, the effect of tACS on variability of RT was assessed. A RM ANOVA with one factor of session (β, γ, sham tACS) and one factor of time (baseline, post) revealed no significant change in standard deviation of RT (no main effect of time [$F_{(1,16)}$ = 2.652, p = 0.123, η2p = 0.142] or session [$F_{(2,32)}$ = 2.412, p = 0.106, η2p = 0.131] and no significant session × time interaction [$F_{(2,32)}$ = 0.061, p = 0.941, η2p = 0.004]).

Further, to investigate the stability of tACS-induced effects on RT over the 10-min post-stimulation period, the slope of RT in the real stimulation sessions was compared with sham. A RM ANOVA with one factor of session (β, γ, sham tACS) and one factor of time (baseline, post) revealed no significant change in the slope of RT (no main effect of time [$F_{(1,15)}$ = 0.041, P = 0.9841, η2p = 0.003] or session [$F_{(2,30)}$ = 0.356, P = 0.633] and no significant session × time interaction [$F_{(2,30)}$ = 0.483, P = 0.622]) (Figure 4.12 B).

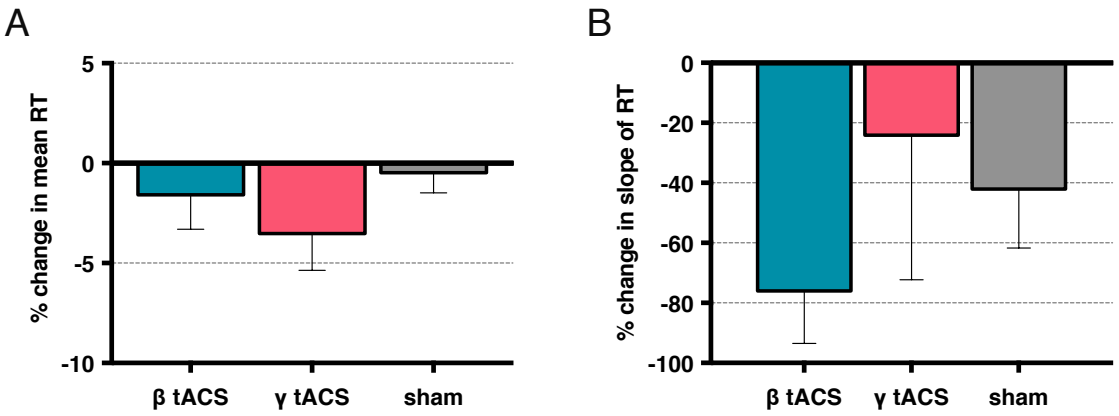


Figure 4.12 The effect of tACS on response time

A. The mean % change (± SEM) in RT from baseline for each session. **B.** The mean % change in linear slope of RT from baseline (± SEM) for each session.

4.3.4.1 β tACS-induced changes in response time are related to changes in corticospinal excitability

Given the substantial inter-individual variability in behavioural responses after tACS, I aimed to explore the underlying physiological basis of any tACS-associated contribution to the variability of behavioural responses between individuals. The results showed that β tACS-induced changes in response time were associated with changes in corticospinal excitability during the late pre-movement period in the β session ($\rho = 0.712$, $p = 0.003$), but not in the γ ($\rho = 0.296$, $p = 0.283$) or sham sessions ($\rho = 0.118$, $p = 0.676$) (Figure 4.13).

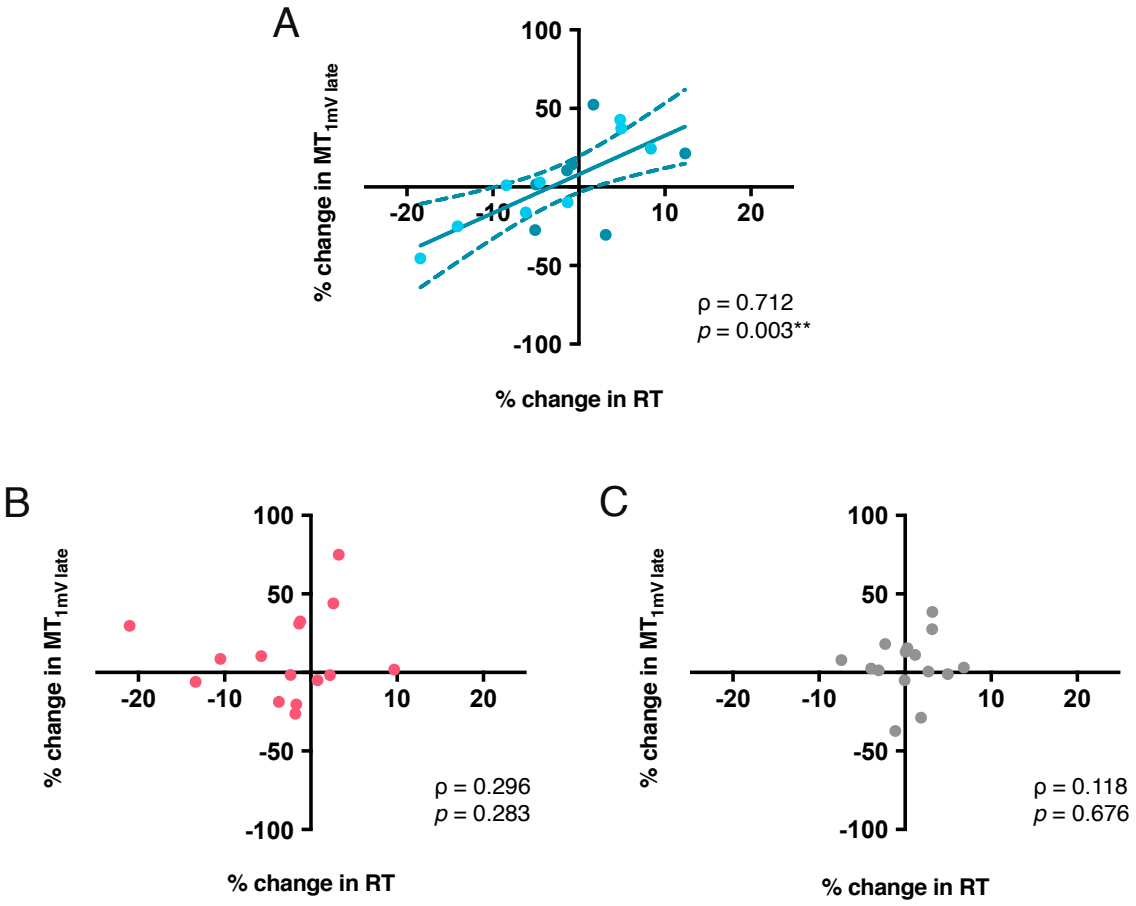


Figure 4.13 Relationship between tACS-induced change in response time and corticospinal excitability

Correlations between stimulation-induced change in RT and change in $MT_{1mV\ late}$ in β tACS (**A**), γ tACS (**B**) and sham sessions (**C**). The values are expressed as % change from baseline. *$p < 0.05$, **$p < 0.005$

4.4 Discussion

This study was performed to investigate the physiological basis and functional significance of driving oscillatory activity in the primary motor cortex (M1) using tACS. As hypothesised, γ-frequency tACS led to a significant reduction in $GABA_A$ inhibition, as assessed by SICI. Interestingly, a reversal of this effect was observed at a later stimulation period, which, to my knowledge, may constitute the first-time evidence of homeostatic changes induced by prolonged application of oscillatory currents. Further, the change in magnitude of resting $GABA_A$ inhibition due to γ tACS was positively related to the magnitude of $GABA_A$ inhibition observed during task-related synchronisation of oscillations in inhibitory interneuronal circuits, supporting the hypothesis that tACS engages endogenous oscillatory circuits. Finally, the change in inhibition was strongly related to an individual's ability to learn a motor task.

4.4.1 γ tACS modulates $GABA_A$ inhibition during stimulation

The results show that γ tACS significantly modulated $GABA_A$ inhibition during stimulation. There is broad consensus from the animal and human literature that γ oscillations reflect underlying GABAergic activity (Towers et al 2004; Mann and Paulsen 2007; Gaetz et al 2011). In agreement with the initial hypothesis, the exogenous application of a prokinetic γ rhythm reduced $GABA_A$ inhibition early during stimulation. It is worth noting that although the predominant oscillatory activity in the sensorimotor cortex at rest is at β-frequency (Salmelin and Hari 1994b), different types of neurons differ in the degree to which they are intrinsically responsive to γ-band synchrony in their inputs (Cardin et al 2009; Otte et al 2010). It is therefore conceivable that local inhibitory subnetworks that exhibit γ-frequency oscillations, despite being disengaged at rest, are more susceptible to the exogenously applied oscillatory current at this frequency, as it is closest to their resonant frequency. The

changes induced in the affected circuits may then manifest as, for example, changes in $GABA_A$ inhibition, as shown here. Further, it can be speculated that the affected inhibitory neurons are likely to be parvalbumin (PV)-expressing fast-spiking (FS) interneurons, which are implicated in generating γ oscillations in the cortex (Cardin et al 2009; Sohal et al 2009).

In addition, it is worth noting that tACS was applied at individualised amplitude, i.e., below individual phosphene and/or discomfort threshold. The phosphene and cutaneous perception threshold was different for β and γ tACS, in agreement with previous studies (Kanai et al 2008; Chaieb et al 2011; Turi et al 2013), which, in turn resulted in the use of different stimulation intensities for different frequencies of tACS. However, to the best of my analysis, the effects reported above were not related to the stimulation intensity. Nonetheless, the use of the same intensity for all stimulation sessions would have been preferred to unequivocally establish the frequency-specificity of the findings presented here.

4.4.2 β tACS has no effect on motor excitability measures

Despite the initial hypothesis that β tACS would increase TMS-assessed $GABA_A$ inhibition, no effect of β tACS on this measure was found. It is difficult to know how to interpret this lack of an effect, especially given the extensive animal and simulation literature that strongly suggests a role for $GABA_A$ interneurons in β oscillations (Jensen et al 2005; Roopun et al 2006; Yamawaki et al 2008; Hall et al 2010a). It is possible that β tACS was delivered at insufficient intensity in the present study (Moliadze et al 2012; Cancelli et al 2015). However, it is worth noting that a recent study also found no effect of β tACS on SICI when the phase of tACS was not controlled for, despite using a higher stimulation intensity (Guerra et al 2016).

In addition, no effect of β tACS on corticospinal excitability was found. Other studies exploring the effect of β tACS on this measure have reported mixed results (Feurra et al 2011a; Tecchio et al 2013; Feurra et al 2013; Cancelli et al 2015; Guerra et al 2016). For example, while one study showed an increase in a single MEP amplitude (Feurra et al 2011a), another study found no net stimulation phase-independent change in the amplitude of a single MEP, despite using the same stimulation parameters (Guerra et al 2016). Moreover, β tACS-induced changes in corticospinal excitability were shown to be dependent upon current density, i.e., low current densities decreased MEP amplitudes while high current densities had the opposite effect. Finally, the differences in the electrode montage used in the present study (left M1-contralateral forehead) compared with the above-mentioned studies (left M1-Pz or bilateral M1) make inter-study comparisons difficult. Future research will focus on establishing optimised stimulation parameters to increase the value of tACS as a tool to study oscillatory activity and also its therapeutic potential.

One final point worth considering is a phase of stimulation. Aside from power and frequency, brain oscillations are also characterised by their instantaneous phase. There is mounting evidence suggesting that phase dynamics reflects cyclic fluctuations of neural excitability and the phase of β oscillations is vital for cortical and corticospinal computations (Mäki and Ilmoniemi 2010; Miller et al 2012; Berger et al 2014; Romei et al 2016). Moreover, the motor excitability, as indexed by TMS of the sensorimotor cortex, is characterised by large variability. The instantaneous phase of cortical oscillations at the time of the stimulation has been suggested as a possible source of this variability. It is plausible that the effects of β tACS in the present study and other similar work may have been under-estimated. In fact, the evidence to support this claim has been provided by the recent study, which showed that β tACS phase selectively modulated the amplitude of a single MEP, SICI and ICF, yet no net stimulation phase-independent change in the amplitude of these

measures was observed (Guerra et al 2016). Thus future studies aiming at examining the effects of tACS may benefit from delivering TMS pulses at the desired phase of tACS (Goldsworthy et al 2016; Raco et al 2016).

4.4.3 tACS-induced change in resting $GABA_A$ inhibition is related to $GABA_A$ change in a period of γ recruitment

Whether tACS is capable of driving activity in circuits that are not engaged is still an open question. To start to address this point, I investigated the relationship between the physiological changes in response to β and γ tACS, and the physiological changes (prior to stimulation) during the pre-movement period, i.e., when endogenous γ activity is increasing, and β activity decreasing. A positive association between the magnitude of γ tACS-induced change in $GABA_A$ inhibition and the magnitude of late pre-movement $GABA_A$ activity was found, supporting the hypothesis that tACS engages local inhibitory interneuronal circuits involved in the generation of γ-frequency oscillations. In addition, these findings may be of importance for clinical stimulation protocols as they may allow us to probe stimulation efficacy before therapeutic application.

4.4.4 γ tACS-induced modulation of $GABA_A$ inhibition predicts motor learning

The next question I sought to address was whether γ tACS was able to modulate intracortical neuronal circuits in a behaviourally relevant manner. I observed a strong association between γ tACS-induced change in $GABA_A$ inhibition and the degree of motor learning, such that subjects who demonstrated a greater increase in $GABA_A$ inhibition at early time-point during and after stimulation also showed faster short-term learning. Although these findings provide clear evidence for the behavioural relevance of physiological changes induced by γ oscillatory current in the motor

domain, the question remains as to why stimulation-induced modulation of inhibition is related to performance in the motor learning task. While speculative at this point, a stronger inhibition due to γ tACS may reflect a higher inhibitory capacity at an individual level, which, in turn, has been shown to be related to increased precision in $GABA_A$ergic transmission and better manual motor performance (Stinear and Byblow 2004; Beck et al 2009; Heise et al 2013). This is also in agreement with a recent study demonstrating that greater pre-movement inhibition is related to successful performance in the motor learning task (Dupont-Hadwen et al, unpublished observations). Importantly, the association between γ tACS-induced modulation of $GABA_A$ activity within local interneuronal circuits and the degree of motor learning suggests that the inhibitory circuits involved in γ oscillations in M1 may also be important for motor learning. However, this remains to be directly tested in humans.

4.4.5 Duration-dependent effects of γ tACS – evidence for homeostatic plasticity?

One striking aspect of γ tACS-induced changes in $GABA_A$ activity, as quantified using SICI, is the opposite pattern of responses early (5 min) as opposed to later time-point (15 min) during stimulation. Although not previously reported in the context of tACS, time-dependent reversal of physiological effects have been frequently documented in studies of homeostatic plasticity in human M1, induced by other non-invasive brain stimulation techniques (Siebner et al 2004; Nitsche et al 2007; Müller et al 2007; Batsikadze et al 2013). In these studies, homeostatic patterns were examined using a priming-test approach, consisting of a priming stimulation protocol that triggers a homeostatic response in M1 and a test stimulation protocol that captures the response (Karabanov et al 2015; Müller-Dahlhaus and Ziemann 2015). In light of this work, the key question is whether the experimental protocol used in the current study could have elicited homeostatic-like changes. Firstly, in experimental studies on

synaptic plasticity, priming activity is usually implemented some time before the application of the test protocol, whereas in the present study tACS was applied continuously for 20 min. Importantly, though, a break between the two stimulation protocols is not always necessary to induce homeostatic-like effects (Mockett et al 2002; Gentner et al 2008; Rothkegel et al 2010). For example, continuous theta burst stimulation (cTBS) applied to the human M1 led to an increase in corticospinal excitability, but the opposite effect was observed when the stimulation duration was doubled (Gentner et al 2008). Secondly, in the majority of human studies, single-pulse MEPs have been used as read-out to trace homeostatic metaplasticity, whereas the present work also shows duration-dependent effect of γ tACS on SICI. According to the recent evidence, however, homeostatic effects are likely to exist in other intracortical circuits as well, including those mediating SICI and LICI (Murakami et al 2012; Amadi et al 2015; reviewed in Karabanov et al 2015). Murakami and colleagues (2012) applied 'facilitatory' intermittent theta-burst stimulation (iTBS) or 'inhibitory' cTBS to induce a homeostatic response in intracortical inhibitory circuits. All four TBS→TBS interventions consistently revealed homeostatic regulation of corticospinal excitability. Intriguingly, yet somewhat in agreement with the present study, only when a priming TBS protocol was followed by identical test TBS protocol (the iTBS→iTBS or cTBS→cTBS protocol), a homeostatic modulation of SICI was observed. Apart from stimulation duration-dependent changes in a single MEP and SICI amplitude, there was no parallel change in the size of ICF, which primarily probes the excitability of intracortical glutamatergic neurons. On first sight, this contrasts with the influential model of homeostatic plasticity, i.e., Bienenstock-Cooper-Munro (BCM) model, according to which homeostatic plasticity occurs via modifications in synaptic mechanisms and is well characterised for glutamatergic changes (Pozo and Goda 2010; Lee et al 2010). However, facilitatory circuits within M1 have been sparsely studied and no consistent homeostatic effects have been demonstrated so far on ICF (Fricke et al 2011; Doeltgen and Ridding 2011). In

addition, it might be argued that a different population of glutamatergic neurons is important for homeostatic effects from that explored using ICF protocol.

Finally, it is worth noting that although the duration-dependent changes reported here appear to have a homeostatic character, they don't outlast stimulation offset. Therefore, further research is needed to investigate the duration-dependency of exogenously applied oscillatory currents and their potential therapeutic implications.

4.4.6 tACS has no after-effects on pre-movement physiological measures

Based on the state- and frequency-dependency of tACS effects (Neuling et al 2013; Santarnecchi et al 2013; Feurra et al 2013) and the well-recognised distinct patterns of changes in β- and γ-frequency power and motor excitability during movement preparation (Reynolds and Ashby 1999; Pfurtscheller and Lopes da Silva 1999; Zaaroor et al 2003; Muthukumaraswamy 2010), here, for the first time, I also evaluated whether externally driving oscillatory activity at these frequencies can lead to plastic changes in motor excitability, as indexed during movement preparation. No after-effect of tACS on these measures was found. It is plausible that any potential tACS-driven event-related physiological changes did not outlast the stimulation period.

Pre-movement TMS measures were not performed during tACS in order to avoid potential interactions between stimulation and movement, which might then have influenced the physiological changes measured post-stimulation. Therefore, it was not possible to assess the relationship between tACS-driven oscillatory activity and the underlying motor excitability changes that accompany the movement preparation period online to stimulation. Nonetheless, the ability to evaluate the effects of exogenously applied oscillatory current on motor excitability in an event-related

paradigm, as shown here, opens the door to new investigations in the motor domain, which are likely to provide important new data on the relationship between oscillatory activity and underlying cortical and corticospinal excitability.

4.4.7 tACS has no after-effects on response time

Here, no after-effects of β or γ tACS on response time were observed. While there is a possibility that potential behavioural effects did not outlast the stimulation period, it is worth noting that previous studies also found no online effect of β- (20 Hz) or γ-frequency (70 Hz) tACS on response time, but instead reported a significant effect on initial and peak movement velocity (Antal et al 2008; Pogosyan et al 2009; Joundi et al 2012) and on sequence acquisition in a serial reaction time task (Pollok et al 2015).

4.5 Conclusions

The findings presented in this Chapter demonstrate that driving γ-frequency oscillations using tACS leads to significant, duration-dependent changes in $GABA_A$ inhibition. In addition, the results show for the first time a clear relationship between the change in magnitude of resting $GABA_A$ inhibition induced by stimulation and the magnitude of $GABA_A$ inhibition measured during task-related synchronisation of oscillations in inhibitory interneuronal circuits, supporting the hypothesis that tACS engages endogenous oscillatory circuits. Further, γ tACS-induced change in inhibition was closely related to an individual's ability to learn a motor task. The findings presented here contribute to our understanding of the neurophysiological basis of motor rhythms, and suggest that tACS modulates local endogenous circuits in a behaviourally relevant manner, offering the possibility of developing tACS as a potential therapeutic tool.

CHAPTER

5

The physiological effects of driving β oscillations at rest and during movement preparation: a tACS-TMS study

The previous chapter reported the significant physiological effects of driving motor γ- but not β-frequency oscillations. In this Chapter I employed different stimulation parameters to examine the effects of driving β oscillations on corticospinal excitability and intracortical GABA-mediated inhibition during different brain states. To this end, I combined tACS at motor resonance (20Hz) with TMS protocols triggered at different tACS phases both at rest and during movement preparation.

5.1 Introduction

Beta (β) oscillations (15–30 Hz) are the dominant oscillatory activity in the primary motor cortex (M1) at rest (Murthy and Fetz 1992; Salmelin and Hari 1994b). The power of this oscillatory activity is reduced during the preparation and execution of movements, the phenomenon known as movement-related β desynchronisation (MRBD) (Jasper and Penfield 1949; Baker et al 1997; Pfurtscheller and Lopes da Silva 1999; Hall et al 2011). The spatial and temporal characteristics of MRBD are relatively well characterised: it is typically observed in both contralateral and ipsilateral sensorimotor cortices during unimanual movements (Stancák and Pfurtscheller 1995) and its onset varies with the onset of motor preparation (Kaiser et al 2001; Alegre et al 2003; Kilner et al 2005). Changes in β oscillatory activity have been reported during development (Gaetz et al 2010), ageing (Rossiter et al 2014b; Heinrichs-Graham and Wilson 2016), in diseases such as Parkinson's disease (Brown 2003; Brown 2007; Little and Brown 2014), and in recovery after stroke (Rossiter et al 2014a).

At a mechanistic level, there is evidence that β oscillations in M1 are generated at least in part as a consequence of sustained excitation of inhibitory interneurons (Yamawaki et al 2008). This view has been corroborated by a number of pharmacological studies. For example, the administration of benzodiazepines to healthy human subjects resulted in increased β-band activity (Jensen et al 2005), whereas the application of picrotoxin, a $GABA_A$ receptor antagonist, to motor cortical slices *in vitro* eliminated β-frequency oscillations (Yamawaki et al 2008). Overall, however, it is likely that the complex interplay between both phasic and tonic inhibition plays an important role in network oscillatory activity, including β-frequency oscillations (Prokic et al 2015).

In addition, a range of TMS studies have shown that the excitability of corticospinal neurons is increased prior to and during movement (Chen and Hallett 1999; Reynolds and Ashby 1999; Zaaroor et al 2003), that is during the time interval when MRBD occurs in the same cortical area. Importantly, a number of studies have shown that β-band power (both spontaneous and movement-related) is closely related to both corticospinal excitability and intracortical inhibition (Aono et al 2013; Schulz et al 2014a; Takemi et al 2015)

Recently, a range of studies have shown that tACS is not only a valuable tool to study the causal nature of the oscillation-behaviour relationship (Pogosyan et al 2009; Thut et al 2012; Helfrich et al 2014b) but also a useful technique to study the local oscillatory activity *in vivo* (Guerra et al 2016; Nowak et al 2017). Recent evidence from humans suggests the involvement of selected GABAergic interneuronal populations in local resonance at β-frequency band, as demonstrated using a combined tACS-TMS approach (Guerra et al 2016).

The present study aimed to extend these findings in a number of important ways. Namely, I wished to examine the effects of driving motor cortical β oscillations on corticospinal excitability as well as on two distinct local GABAergic inhibitory phenomena, as assessed by TMS applied at different phases of tACS. Importantly, the physiological effects of driving β oscillations were evaluated both at rest and also, for the first time, during movement preparation, when desynchronisation of endogenous β activity occurs.

5.2 Methods

5.2.1 Participants

Eighteen healthy subjects (age 24.5 years, range: 20–29 years; 9 male) gave their informed consent to participate in the study in accordance with Central University Research Ethics Committee approval (University of Oxford; MSD-IDREC-C2-2014-026). All subjects were right-handed as assessed by the Edinburgh Handedness Inventory (Oldfield 1971), had no history of neurological or psychiatric disorders and reported no other contraindications to tACS or TMS.

5.2.2 Experimental design and procedure

Subjects participated in two experimental sessions: β (20 Hz) tACS stimulation session and sham stimulation session, with the order of sessions counterbalanced across subjects. The sessions were separated by at least one week and performed at approximately the same time of the day for each subject.

At the start of each session, EEG was recorded with eyes open for 2 min. Next, participants performed a visually cued response time (RT) task. Resting-state and pre-movement TMS measures of corticospinal excitability and intracortical inhibition in left M1 were acquired at baseline (in the absence of tACS) and during tACS (online; Figure 5.1 A & B). During β tACS, TMS pulses were triggered at one of the four phases of the tACS sinusoidal waveform (0°, 90°, 180°, 270°) (Figure 5.1C). Fourteen MEPs were collected for each protocol and for each phase in a randomised order.

Data from two subjects were excluded due to a delivery of TMS pulses at incorrect phases of tACS.

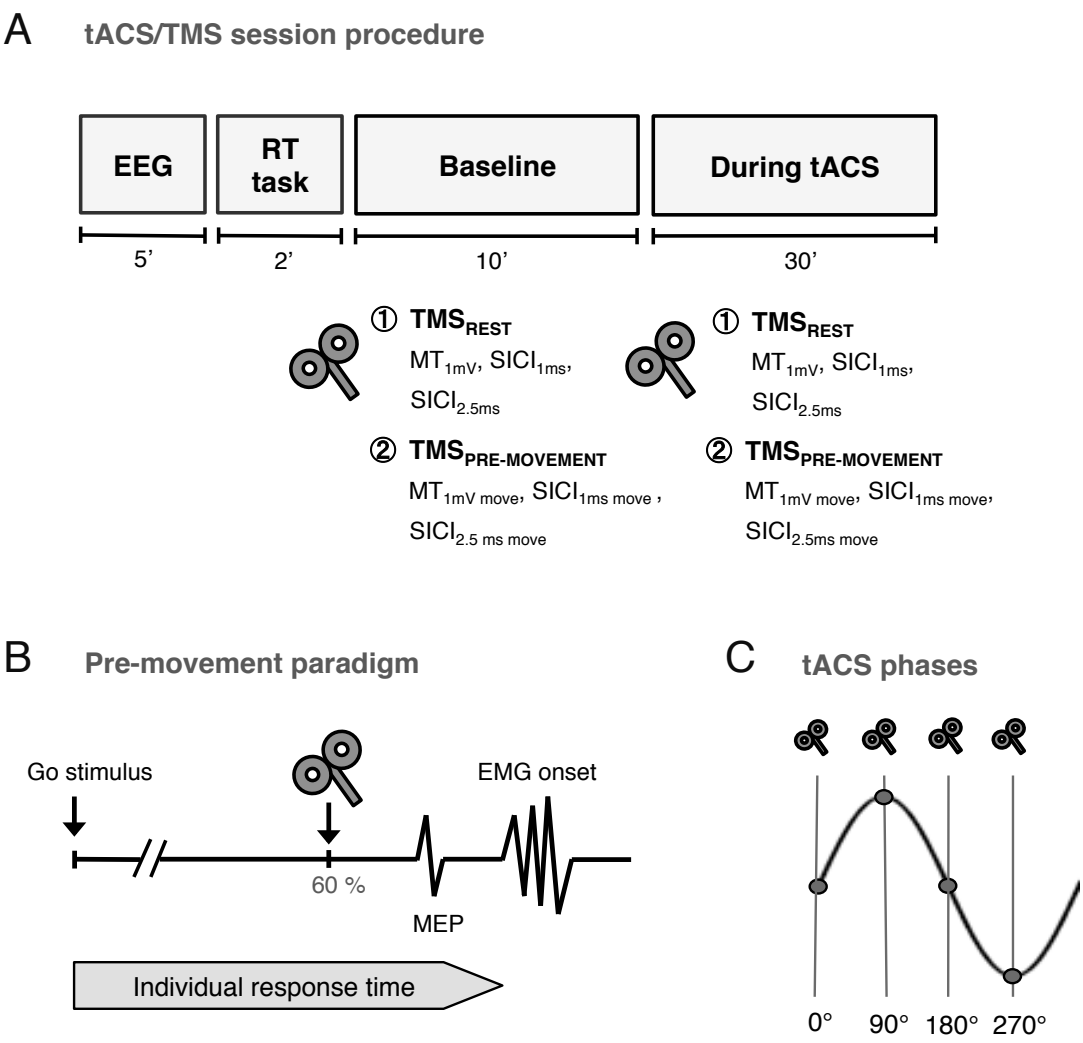


Figure 5.1 Experimental design

A. Summary of tACS/TMS session procedure. Resting-state (MT_{1mV}, $SICI_{1ms}$, $SICI_{2.5ms}$) and event-related TMS measures ($MT_{1mV\ move}$, $SICI_{1ms\ move}$, $SICI_{2.5ms\ move}$) were applied at baseline and during tACS. **B.** Pre-movement paradigm. TMS measures were delivered at one time-point during pre-movement period: at 60 % of iRT. **C.** TMS during tACS. The tACS signal was recorded and its instantaneous phase was calculated in real time. 14 TMS stimuli were triggered at each of the four tested phases (0º, 90º, 180º, 270º) in a random order. Abbreviations: MT_{1mV}, 1 mV motor threshold; RT, response time; SICI, short interval intracortical inhibition.

5.2.3 EEG

EEG signals were sampled at 2048 Hz, amplified (x 20) using Porti32 amplifier (Twente Medical Systems International, Oldenzaal, The Netherlands) and recorded using an in-house software (RecEEG©, developed by A. Pogosyan, Oxford). Following skin preparation with Nuprep gel (Weaver and Company), Ag/AgCl electrodes were placed over: Fz, C3, Cz, C4 and Pz, according to the International 10–20 EEG system of electrode placement. Electrodes were affixed using Ten20 conductive paste gel (Weaver and Company) and recorded in an average reference configuration.

5.2.3.1 EEG data analysis

Signals were edited using a custom-made software (EditEEG©, developed by A. Pogosyan, Oxford). The raw EEG data was inspected for artefacts and high-pass filtered at 1 Hz. Recordings were then imported into Spike2 software v7.12b (Cambridge Electronic Design Ltd, Cambridge, UK). Fourier analysis was used to calculate power spectra with frequency resolution of 0.5 Hz (2048 bins per channel). Channel C3 (overlying the stimulated M1 area) was selected and the individual peak frequency for β oscillatory activity was found, defined as the frequency with the largest power in the window 15–30 Hz.

5.2.4 Response time task

At the start of each tACS-TMS session, subjects performed a simple response time (RT) task consisting of 20 trials in the absence of TMS in order to determine their individual RT. The same RT task was also performed in conjunction with TMS before and during tACS. Subjects were instructed to respond to a visual Go signal (coloured

green circle) by performing an index finger abduction of the right hand as quickly as possible. Visual stimuli appeared at random intervals (5-7 sec) and the subjects were instructed to avoid anticipation of the Go signal and to relax their hand while the fixation cross was displayed on the screen. Stimuli were generated using the MATLAB Psychophysics Toolbox v.3.0 package (Brainard 1997).

5.2.4.1 Response time data analysis

EMG data acquired during RT task performed in the absence of TMS were analysed online using RecEEG© software. RT was defined as the time interval (in milliseconds) between the Go signal and the onset of EMG activity in the FDI muscle. The onset of EMG was identified in each trial as the first data point in which the signal exceeded 0.1 mV. The identified RT was then used in the remainder of that experimental session to calculate the timing of the pre-movement TMS pulses.

The data from RT task performed in conjunction with TMS before and during tACS were analysed offline using a customised Spike2 script. The onset of EMG was identified in each trial as the time when the signal first exceeded a threshold of 3 SD of the EMG activity in the 100 ms period preceding the onset of TMS artefact. RT was defined as the time interval between the Go signal and the onset of EMG activity in the FDI muscle and trials with RTs below 100 ms were excluded from further analyses. In total, there were 42 pre-movement trials recorded at baseline and during sham session and 168 pre-movement trials recorded during β tACS (42 at each of 4 phases of stimulation). In the analysis of RT data, an equal number of trials were considered, i.e., all 42 trials from baseline and during sham recordings and the first 42 out of 168 trials recorded during beta session. In addition, the last 42 trials from the β session were analysed and compared with baseline and sham session in order to examine whether RT has changed over time during this session.

Baseline-corrected RT data were analysed. Data from two participants were excluded from the analysis (due to a high number of anticipatory responses in one participant, the insufficient data quality and the inability to mark precisely the onset of RT in another participant).

5.2.5 Transcranial alternating current stimulation (tACS)

tACS was delivered was delivered via a DC stimulator (NeuroConn GmbH, Germany) through a pair of conductive rubber electrodes (5 × 7 cm^2) enclosed in saline-soaked sponges. One electrode was centred over the TMS-derived FDI hotspot of left M1; the other electrode was positioned on the midline parietal region (Pz; International 10–20 system). The electrode positions were adopted according to the previous studies that demonstrated region-, frequency- and phase-specific tACS effects on M1 excitability (Feurra et al 2011a; Feurra et al 2013; Guerra et al 2016; Nakazono et al 2016), and to avoid phosphenes (Schutter and Hortensius 2010; Turi et al 2013). tACS was administered in a within-subject design. Subjects participated in two sessions in which they received tACS at β-frequency (20 Hz) or sham stimulation. The sessions were separated by at least one week. In Chapter 4, the aim was to individually adjust both the tACS frequency and intensity. Since a distinct β peak could not be reliably detected in all participants, I elected not to match tACS frequency to individual β peak frequency. This offered the opportunity to examine whether β tACS-induced changes in motor excitability were dependent on the match between the frequency of tACS (20 Hz) and an individual's own spontaneous β frequency. Similarly, due to considerable variation in stimulation intensities used in Chapter 4, here all participants received the stimulation at a peak-to-peak amplitude of 1 mA (with no direct current offset). This also allowed for easier comparisons with results of previous tACS-TMS studies (for example, Feurra et al 2011a; Guerra et al 2016). Current was ramped up and down over the first and last 5 s of stimulation.

The total duration of stimulation was ~30 min for beta session and 10 s for sham session. Impedance was kept below 10 kΩ. Subjects were blind to the stimulation condition used. No participant reported phosphenes or skin sensations during stimulation.

The estimation of the instantaneous phase of tACS and delivery of TMS pulses at specific phases was performed according to the previously described procedure (Guerra et al 2016). Namely, the sequencer's capabilities in Spike2 v.7.17 (Cambridge Electronic Design Ltd, Cambridge, UK) connected with a Power1401 data acquisition interface (Cambridge Electronic Design Ltd) were used. The sequencer allows for monitoring data in real time and for precisely timed generation of digital pulses. tACS signal was recorded with a 1 kΩ resistance connected sequentially to the tACS stimulator and to ADC port 1 of the Power1401. Using the sequencer, polarity-dependent zero crossings were found and digital outputs (TTL) for triggering TMS were delivered after a time delay corresponding to the appropriate phase. In our experimental setup, the sequencer clock tick interval, dt, was set to 0.01 ms, which resulted in a phase precision of $2*\pi*f*dt = 0.00125$ rad = 0.072° with tACS at frequency f = 20 Hz.

5.2.6 TMS

5.2.6.1 TMS data acquisition

All TMS data were acquired using a monophasic BiStim machine, connected to a 70 mm figure-of-eight coil (Magstim Co., Whitland, Dyfield, UK). The left M1 was stimulated in all subjects. The optimal scalp position to elicit MEPs (referred to as the motor hotspot) in the right FDI muscle was determined before each session, with the TMS coil held at 45° to the mid-sagittal line with the handle pointing posteriorly. The

hotspot was marked on a tight fitting cap to ensure reproducible coil positioning and TMS pulses were delivered through the M1 electrode. For the duration of the sessions the subjects were seated comfortably in an armchair with their eyes open. Surface EMG was recorded via Ag–AgCl disks filled with conductive gel from the FDI of the right hand, using a belly-tendon montage. EMG signals were sampled at 2048 Hz, amplified (x 20) and band-pass filtered at 1-250 Hz using Porti32 amplifier.

5.2.6.2 Motor thresholds

The resting 1 mV motor threshold (MT_{1mV}) and active motor threshold (aMT) were determined at the beginning of each tACS-TMS session. The MT_{1mV} was defined as the minimum stimulus intensity required for eliciting an MEP of ~1 mV peak-to-peak amplitude in at least 5 out of 10 consecutive trials in the relaxed FDI muscle. The active motor threshold was defined as the minimum stimulus intensity necessary to evoke a 200 μV peak-to-peak MEP in at least 5 out of 10 consecutive trials while subjects maintained approximately 30 % of the maximum contraction of the FDI.

5.2.6.3 Paired-pulse TMS protocols

Two distinct measures of local inhibitory activity were acquired: short interval intracortical inhibition (SICI) with an ISI of 1 ms ($SICI_{1ms}$) and 2.5 ms ($SICI_{2.5ms}$). $SICI_{2.5ms}$ is a relatively specific measure of synaptic $GABA_A$ activity (Kujirai et al 1993; Di Lazzaro et al 2005). Less is understood about $SICI_{1ms}$, but it is also GABA-dependent (Ni et al 2007) and has been suggested to reflect extrasynaptic GABA tone (Stagg et al 2011b). The Conditioning Stimulus (CS) was set at 70 % of aMT and the Test Stimulus (TS) was set at MT_{1mV} for both protocols. During stimulation, it was the first stimulus, i.e., the CS, that was aligned to the specific phase of the tACS sinewave.

5.2.6.4 Rest measures

Resting-state MT_{1mV}, $SICI_{1ms}$ and $SICI_{2.5ms}$ were measured before and during tACS. 14 trials per protocol and phase were applied. All protocols were delivered in a randomised order (Figure 5.1 A).

5.2.6.5 Pre-movement measures

The TMS protocols ($MT_{1mV\ move}$, $SICI_{1ms\ move}$ and $SICI_{2.5ms\ move}$) were also applied during the pre-movement period in a simple RT paradigm before and during tACS. The TMS measures were performed in a randomised order at one time-point during movement preparation: at 60 % of RT. 60 % RT was adjusted to each subject's mean RT according to a previously described procedure (Murase et al 2004; Hummel et al 2009). 14 trials per protocol and phase were recorded (Figure 5.1 A).

5.2.6.6 MEP data analysis

Trials were excluded if: the test pulse alone failed to elicit a reliable MEP (amplitude < 0.1 mV); there was pre-contraction in the target FDI muscle (EMG amplitude > 0.1 mV in the 100 ms preceding the pulse); or, for the pre-movement TMS measures: EMG onset coincided with TMS pulse; no response was made; or TMS was delivered at an incorrect phase. The peak-to-peak amplitude for each MEP was then calculated. Any MEPs which were outside 3 SD of the mean within the block were rejected. Collectively, these rejection criteria resulted in the exclusion of 4.86 % of all trials. Next, a single iteration of Grubbs' test with a significance level of 0.05 was performed for each block separately and any significant outliers were excluded.

Both resting-state and pre-movement $SICI_{1ms}$ and $SICI_{2.5ms}$ were expressed as a ratio of the mean conditioned MEP amplitude to the mean unconditioned MEP amplitude (MT_{1mV}).

To explore phase-independent tACS effects on M1 excitability, an equal number of MEPs was considered for each condition, i.e., 14 MEPs at baseline in sham and β tACS sessions were compared against first 14 MEPs during sham and β tACS (random phases), aiming to limit any cumulative effects of prolonged tACS stimulation. To test the phase-dependent variations of MEP amplitude within each TMS protocol (i.e., MT_{1mV}, $SICI_{1ms}$ and $SICI_{2.5ms}$) in the β tACS session, the mean MEP amplitude for each phase was normalised to intra-protocol mean amplitude (the average of all four phases, i.e., 56 trials in total).

Finally, the stability of MEP amplitude during β tACS was evaluated for each protocol by comparing the first 14 pulses against the last 14 pulses.

5.2.7 Statistical analysis

Statistical analyses were performed using GraphPad Prism (version 7, GraphPad Software Inc., San Diego, CA, USA) and SPSS (version 22.0; IBM).

Normality of data distribution was tested by D'Agostino-Pearson omnibus normality test. Data were analysed using a repeated measures (RM) ANOVA. In the case of significant effects, *post hoc* analyses with paired t-tests (two-tailed) were applied. Mauchly's test was used to test for assumption of sphericity and Greenhouse–Geisser corrections were applied as necessary. Effect size estimates were computed using partial eta squared (η2*p*) for RM ANOVAs and Cohen's d_z for t-tests.

To examine whether the modulation of motor excitability measures during β tACS was dependent on how closely the applied stimulation frequency (20 Hz) matched an individual's own spontaneous β frequency (IBF) (match between stimulation

frequency and IBF = IBF – 20 Hz), the difference between the stimulation frequency and IBF was correlated for each individual with: (i) the average MEP amplitude (based on the first 14 trials [random phases]) for each protocol; (ii) the average MEP amplitude for each tested phase for each protocol normalised to intra-protocol overall average (the average of all four phases, i.e., 56 trials in total). Correlations were assessed using the Spearman's rank correlation method (ρ). The significance level for all tests was set at $p < 0.05$.

5.3 Results

5.3.1 Quality assessment

To ensure that there were no systematic differences between the sessions at baseline, baseline motor threshold and MEP values were compared for each protocol. There was no difference in motor thresholds between sessions (MT_{1mV}: $t_{(15)}$ = 1.625, p = 0.125; aMT: $t_{(15)}$ = 0.502, p = 0.623) (Table 5.1).

	β tACS	sham tACS
MT_{1mV}	62.4 ± 7.2	60.8 ± 6.4
aMT	37.8 ± 6.9	37.3 ± 6.5

Table 5.1 Mean motor thresholds (± SD)

There were no differences in mean MEP amplitude between the two experimental sessions for any TMS protocols performed at rest (MT_{1mV}: $t_{(13)}$ = -0.903, p = 0.378; $SICI_{1ms}$: $t_{(15)}$ = -0.277, p = 0.786; $SICI_{2.5ms}$: $t_{(15)}$ = 0.106, p = 0.917). There were also no differences between paired-pulse protocols performed during movement preparation ($SICI_{1ms}$: $t_{(15)}$ = -0.832, p = 0.418; $SICI_{2.5ms}$: $t_{(15)}$ = 0.114, p = 0.911) However, there was a significance difference in MT_{1mV} amplitude ($t_{(15)}$ = -2.444, p = 0.027) (Figure 5.2).

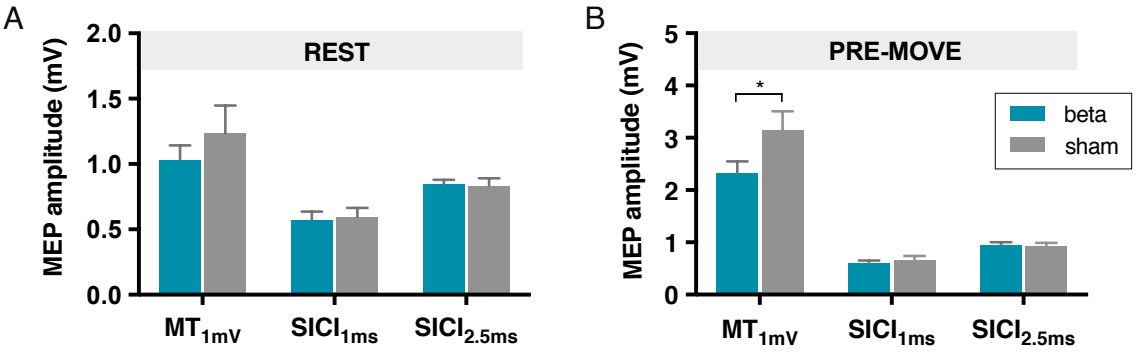


Figure 5.2 Average baseline MEP amplitude values

Average baseline MEP amplitude (± SEM) values for resting-state (**A**) and pre-movement (**B**) TMS protocols for β tACS and sham sessions. *$p < 0.05$

To verify that the paired-pulse protocols elicited the expected inhibition and facilitation at rest, a RM ANOVA with one factor of session (β, sham tACS) and one factor of protocol (MT_{1mV}, $SICI_{1ms}$, $SICI_{2.5ms}$) was performed on the mean baseline values. A significant main effect of protocol was found ($F_{(2,26)} = 36.583$, $p < 0.001$) but no main effect of session ($F_{(1,13)} = 0.409$, $p = 0.534$) or session × protocol interaction ($F_{(2,26)} = 0.838$, $p = 0.444$). *Post hoc* t-tests showed that, as expected, $SICI_{1ms}$ and $SICI_{2.5ms}$ protocols led to a significant inhibition of MEP amplitude values in β and sham sessions ($p < 0.001$) (Figure 5.3).

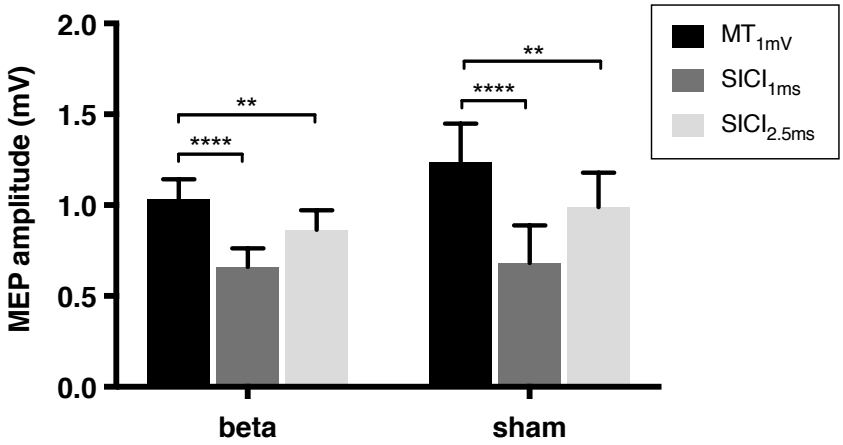


Figure 5.3 Inhibition of MEP amplitude values in SICI protocols

Average baseline MEP amplitude (± SEM) values for resting-state TMS protocols for β tACS and sham sessions. *$p < 0.05$, **$p < 0.005$, ***$p < 0.0005$, ****$p < 0.00005$

Finally, there was no difference in baseline mean response time values between β tACS and sham sessions ($t_{(13)}$ = 0.807, p = 0.434).

5.3.2 Comparison between baseline resting-state and pre-movement motor excitability measures

Next, I wished to test for the characteristic increase in corticospinal excitability observed during movement-related desynchronisation (Reynolds and Ashby 1999; Zaaroor et al 2003) and to explore the potential changes in intracortical inhibition associated with this process. To this end, a RM ANOVA with one factor of protocol (MT_{1mV}, $SICI_{1ms}$, $SICI_{2.5ms}$) and one factor of state (rest, pre-movement) was performed on baseline measures collapsed across β and sham sessions. A significant main effect of protocol ($F_{(2,28)}$= 56.351, p < 0.005, η2p = 0.801), state ($F_{(1,14)}$= 43.688, p < 0.005, η2p = 0.757), and protocol × state interaction ($F_{(2,28)}$= 29.557, p < 0.005, η2p = 0.679) was observed. *Post hoc* t-tests identified a significant increase in MT_{1mV} ($t_{(14)}$ = -5.980, p < 0.005) and $SICI_{2.5ms}$ amplitude ($t_{(15)}$ = -2.230, p = 0.041) but no significant change in $SICI_{1ms}$ ($t_{(15)}$ = -1.487, p = 0.158) (Figure 5.4).

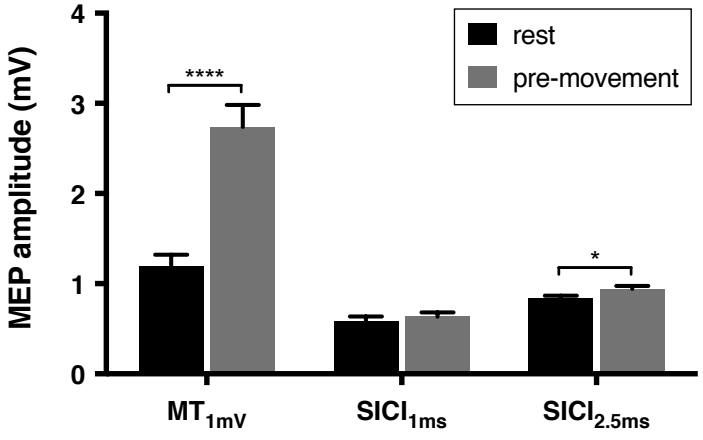


Figure 5.4 Average baseline rest and pre-movement MEP amplitude values

Average baseline MEP amplitude (± SEM) values for resting-state and pre-movement TMS protocols. *p < 0.05, **p < 0.005, ***p < 0.0005, ****p < 0.00005

5.3.3 Exploring the stability of MEP amplitude during prolonged stimulation

β tACS was applied for ~30 min. The resting-state TMS measures (total of 168 trials) were always performed in the first 15 min and the pre-movement TMS measures (total of 168 trials) were applied in the remaining 15 min. To explore the stability of MEP amplitudes over time, a RM ANOVA with one factor of protocol (MT_{1mV}, $SICI_{1ms}$, $SICI_{2.5ms}$) and one factor of time (first 14 versus last 14 trials of each protocol) was performed on both resting-state and pre-movement TMS measures in the β session. In the case of resting-state TMS measures, there was a significant main effect of protocol ($F_{(2,28)}$= 16.340, p < 0.001, η2p = 0.539) and time ($F_{(1,14)}$= 6.733, p = 0.021, η2p = 0.325) but no significant protocol × time interaction ($F_{(2,28)}$= 0.289, p = 0.667, η2p = 0.020). A RM ANOVA performed on pre-movement TMS measures revealed a significant main effect of protocol ($F_{(2,30)}$= 74.029, p < 0.001, η2p = 0.832) but no main effect of time ($F_{(1,15)}$= 0.428, p = 0.523, η2p = 0.028) or protocol × time interaction ($F_{(2,30)}$= 1.070, p = 0.333, η2p = 0.067). *Post hoc* t-tests were performed to further examine the stability of MEP amplitude in all TMS protocols. The results showed a significant increase in the resting-state $SICI_{1ms}$ magnitude (less inhibition) over time during β tACS session ($t_{(15)}$ = -2.284, p = 0.037) but no change in other resting-state or pre-movement TMS protocols (p > 0.05).

5.3.4 β tACS has no phase-independent effects on motor excitability at rest

Next, I wished to investigate whether 20 Hz tACS had any overall effect on motor excitability measures, regardless of tACS phase. A RM ANOVA with one factor of session (β, sham tACS) and one factor of time (baseline, during) was performed on mean MEP amplitudes for each resting-state TMS protocol. There was no significant effect of β tACS on any of the motor excitability measures at rest as compared with the sham session (MT_{1mV}: no main effect of session [$F_{(1,13)}$= 1.247, p = 0.284, η2p =

0.088] or time [$F_{(1,13)}$= 0.028, p = 0.089, η2p = 0.207] and no session × time interaction [$F_{(1,13)}$= 0.028, p = 0.871, η2p = 0.002]; $SICI_{1ms}$: no main effect of session [$F_{(1,15)}$= 0.205, p = 0.657, η2p = 0.014] or time [$F_{(1,15)}$= 0.009, p = 0.925, η2p = 0.001] and no session × time interaction [$F_{(1,15)}$= 0.198, p = 0.663, η2p = 0.013]; $SICI_{2.5ms}$: no main effect of session [$F_{(1,15)}$= 0.128, p = 0.726, η2p = 0.008] or time [$F_{(1,15)}$= 3.624, p = 0.076, η2p = 0.195] and no session × time interaction [$F_{(1,15)}$= 0.188, p = 0.671, η2p = 0.012]) (Figure 5.5).

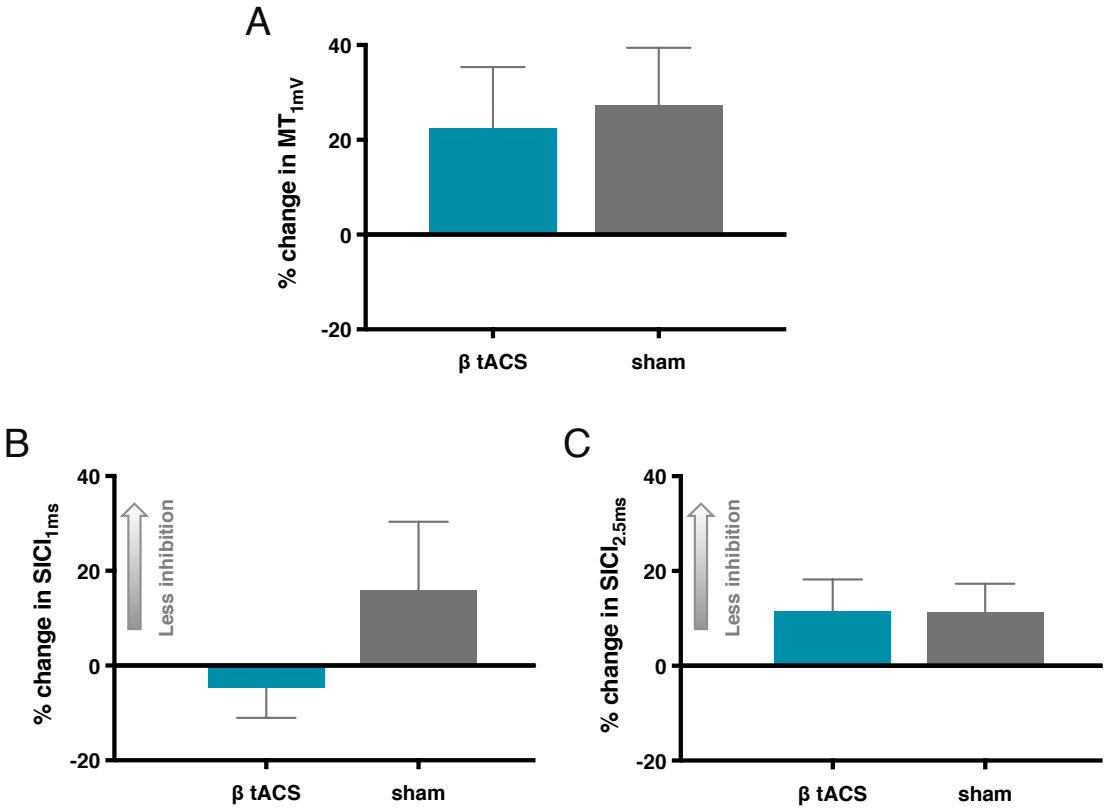


Figure 5.5 Average resting-state MEP amplitude values

Average MEP amplitude (± SEM) values for resting-state MT_{1mV} (**A**), $SICI_{1ms}$ (**B**), $SICI_{2.5ms}$ (**C**) for β tACS and sham sessions. MEP amplitudes are given relative to baseline (set at 0 %).

5.3.5 β tACS affects pre-movement $SICI_{1ms}$ in a phase-independent manner

To investigate phase-independent effects of tACS on pre-movement motor excitability, a RM ANOVA with one factor of session (β, sham tACS) and one factor of time (baseline, during) was performed on the mean MEP amplitudes for each pre-movement TMS protocol. There was no significant effect of β tACS on pre-movement MT_{1mV} (no main effect of session [$F_{(1,15)}$= 2.863, p = 0.111, η2p = 0.160] or time [$F_{(1,15)}$ = 2.046, p = 0.173, η2p = 0.120] and no significant session × time interaction [$F_{(1,15)}$ = 3.982, p = 0.064, η2p = 0.210]) or $SICI_{2.5ms}$ (no main effect of session [$F_{(1,14)}$ = 1.654, p = 0.219, η2p = 0.106] or time [$F_{(1,14)}$ = 0.125, p = 0.729, η2p = 0.009] and no session × time interaction [$F_{(1,14)}$ = 3.473, p = 0.083, η2p = 0.199]). However, there was a significant effect of β tACS on $SICI_{1ms}$ (no main effect of session [$F_{(1,14)}$ = 0.904, p = 0.358, η2p = 0.061] or time [$F_{(1,14)}$ = 0.785, p = 0.391, η2p = 0.053] but a significant session × time interaction [$F_{(1,14)}$ = 12.347, p = 0.003, η2p = 0.469]).

Post hoc t-tests demonstrated a significant decrease in $SICI_{1ms}$ during β tACS as compared with sham ($t_{(14)}$ = 2.208, p = 0.044, Cohen's d_z = 0.570). $SICI_{1ms}$ was also decreased during β tACS session when compared with baseline ($t_{(15)}$ = -2.776, p = 0.014, Cohen's d_z = -0.694) (Figure 5.6).

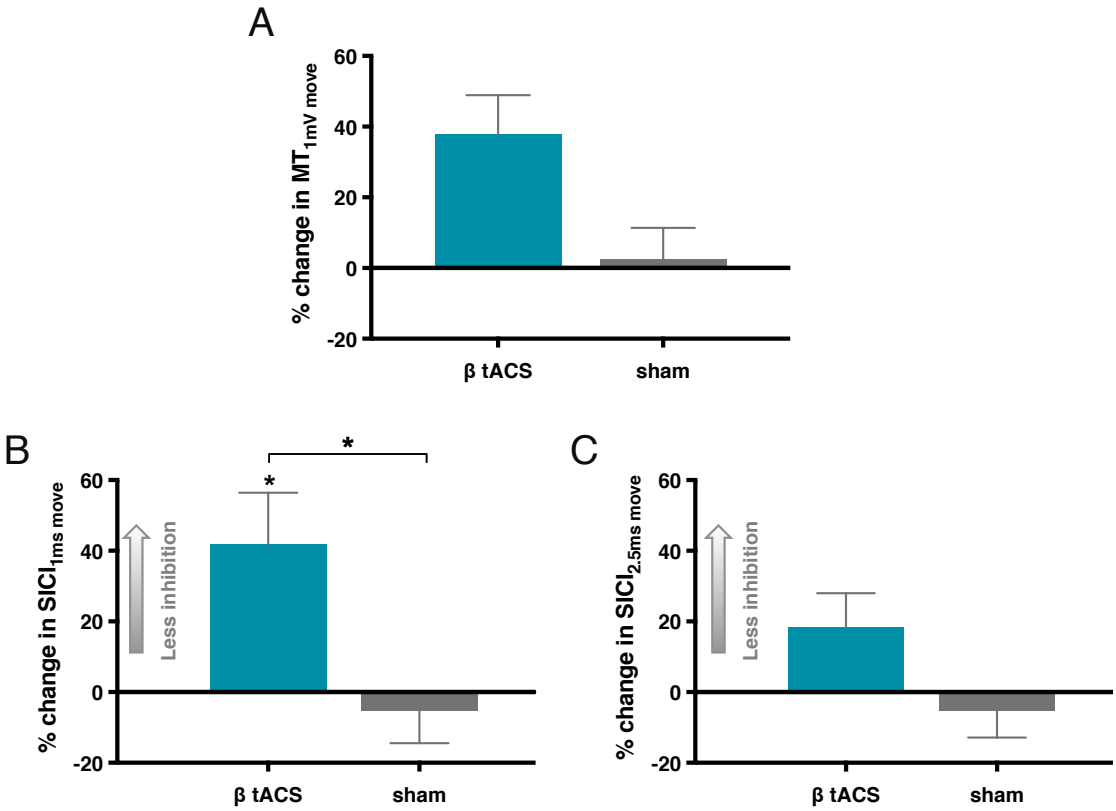


Figure 5.6 Average pre-movement MEP amplitude values

Average MEP amplitude (± SEM) values for pre-movement TMS protocols: $MT_{1mV\ move}$ (**A**), $SICI_{1ms\ move}$ (**B**), $SICI_{2.5ms\ move}$ (**C**). $SICI_{1ms}$ amplitude was increased by β tACS compared with baseline and sham (*p < 0.05). MEP amplitudes are given relative to baseline (set at 0 %). *p < 0.05

5.3.6 β tACS has no phase-dependent effects on motor excitability at rest

In order to explore the phase dependency of the response of motor cortical areas at rest to β-frequency stimulation, a RM ANOVA with one factor of protocol (MT_{1mV}, $SICI_{1ms}$, $SICI_{2.5ms}$) and one factor of phase (0º, 90º, 180º, 270º) was performed. There was no main effect of protocol ($F_{(2,26)}$= 1.596, p = 0.229, η2p = 0.109) or phase ($F_{(3,39)}$= 0.403, p = 0.752, η2p = 0.030) and no significant protocol × phase interaction ($F_{(6,78)}$= 0.817, p = 0.494, η2p = 0.059). Given recent evidence demonstrating phase-dependent effects of β tACS at rest (Guerra et al 2016), I then wished to perform exploratory analyses to help clarify what effects β tACS has on corticospinal

excitability and intracortical measures of inhibition. A follow up RM ANOVA with the factor of phase performed for each resting-state protocol revealed no effect of phase in any of the protocols (MT_{1mV}: $F_{(3,45)}$= 2.338, p = 0.086, η2p = 0.135; $SICI_{1ms}$: $F_{(3,45)}$= 0.457, p = 0.713, η2p = 0.030; $SICI_{2.5ms}$: $F_{(3,39)}$= 0.837, p = 0.482, η2p = 0.060). The results were followed up further with *post hoc* t-tests, summarised in Figure 5.7.

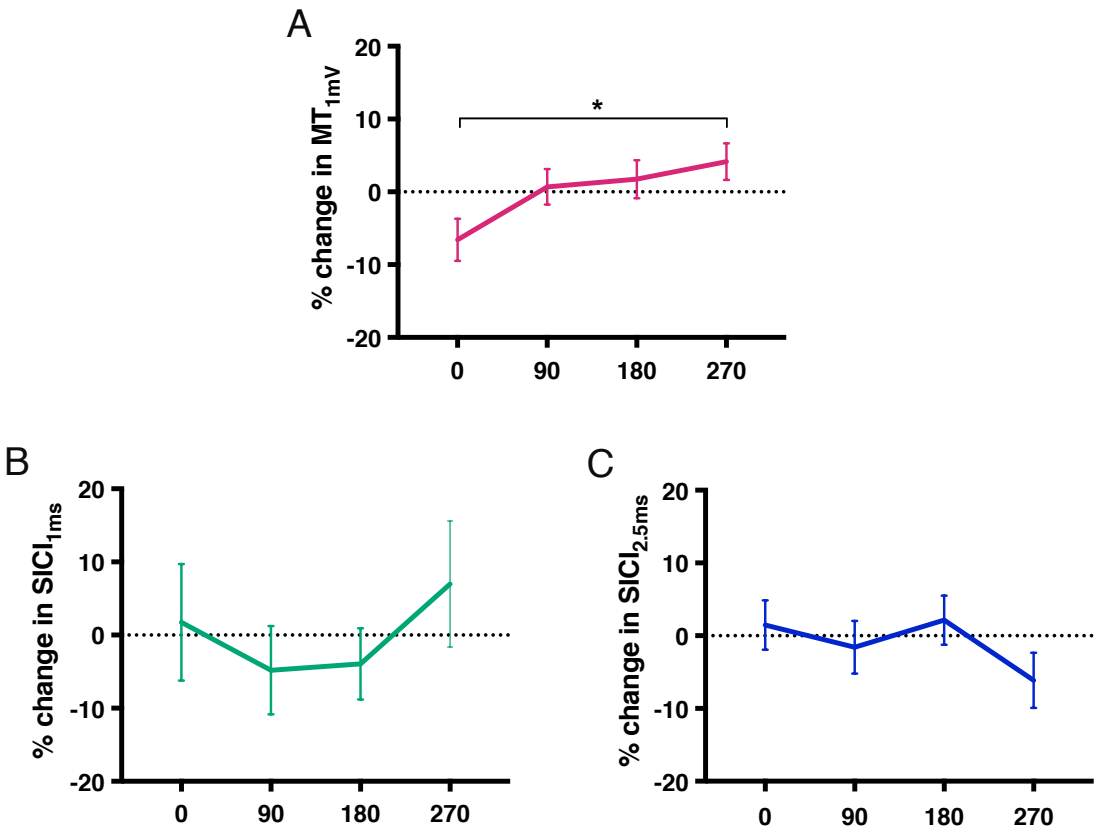


Figure 5.7 Phase dependency of β tACS effects on motor excitability at rest

Average MEP amplitude (± SEM) values for resting-state TMS protocols: $MT_{1mV\ move}$ (**A**), $SICI_{1ms\ move}$ (**B**), $SICI_{2.5ms\ move}$ (**C**) during β tACS according to the stimulation phase (0°, 90°, 180°, or 270°). MEP amplitude values are given relative to the mean MEP amplitude of all four phases. *p < 0.05

5.3.7 β tACS affects pre-movement motor excitability in a phase-dependent manner

In order to explore the phase dependency of the response of motor cortical areas during movement preparation to β-frequency stimulation, a RM ANOVA with one factor of protocol ($MT_{1mV\ move}$, $SICI_{1ms\ move}$, $SICI_{2.5ms\ move}$) and one factor of phase (0º, 90º, 180º, 270º) was performed. There was no main effect of protocol ($F_{(2,26)}$= 2.177, p = 0.134, η2p = 0.143) or phase ($F_{(3,39)}$= 1.185, p = 0.328, η2p = 0.084) but there was a significant protocol × phase interaction ($F_{(6,78)}$= 2.319, p = 0.041, η2p = 0.151). A further RM ANOVA was therefore performed for each protocol separately. MEPs were significantly modulated in a phase-dependent manner for $MT_{1mV\ move}$ ($F_{(3,45)}$= 4.728, p = 0.006, η2p = 0.240), but not for $SICI_{1ms\ move}$ ($F_{(3,45)}$= 1.578, p = 0.208, η2p = 0.095) or $SICI_{2.5ms\ move}$ ($F_{(3,39)}$= 1.192, p = 0.325, η2p = 0.084) (Figure 5.8). *Post hoc* t-tests showed a significant decrease in $MT_{1mV\ move}$ amplitude at 0º phase ($t_{(15)}$ = 3.086, p = 0.008) and a significant increase in $MT_{1mV\ move}$ amplitude at 180º phase relative to the mean MEP amplitude of all four phases ($t_{(15)}$ = -2.454, p = 0.027). $MT_{1mV\ move}$ amplitude at 0º phase was also significantly smaller than $MT_{1mV\ move}$ amplitude at 90º ($t_{(15)}$ = -2.628, p = 0.019) and 180º phase ($t_{(15)}$ = -3.340, p = 0.004) (Figure 5.8 A).

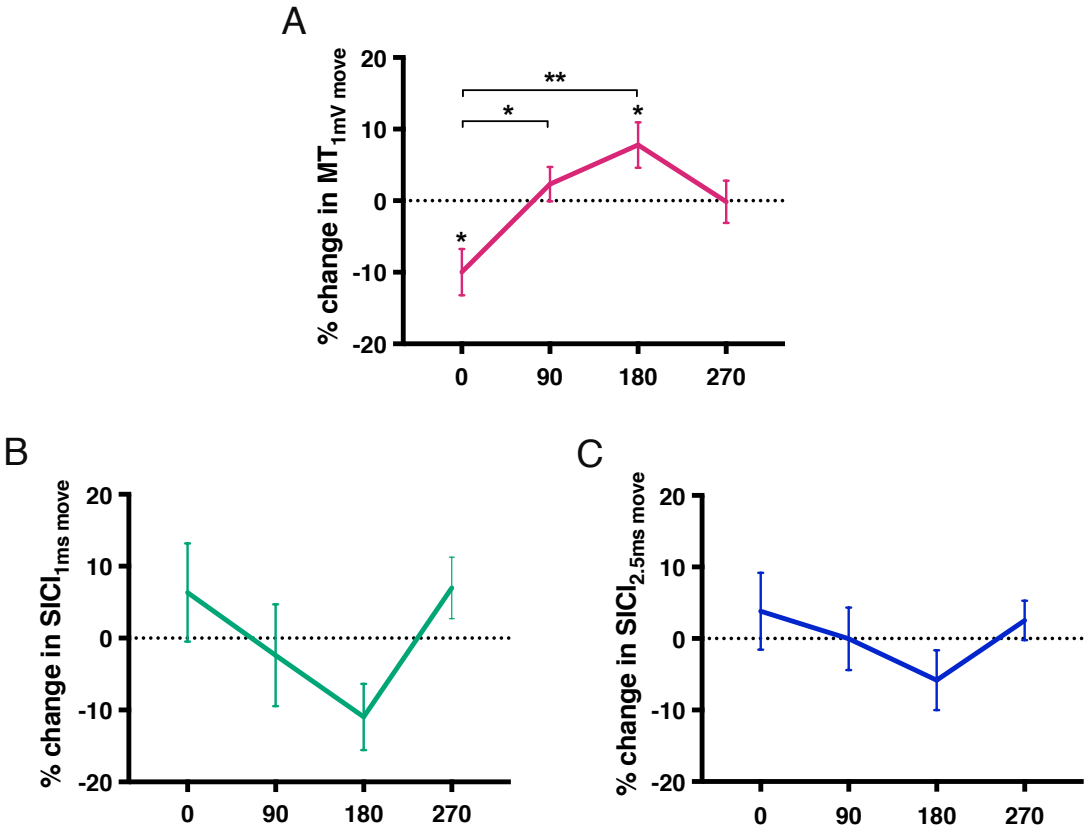


Figure 5.8 Phase dependency of β tACS on pre-movement motor excitability

Average MEP amplitude (± SEM) values for pre-movement TMS protocols: $MT_{1mV\ move}$ (**A**), $SICI_{1ms\ move}$ (**B**), $SICI_{2.5ms\ move}$ (**C**) during β tACS according to the stimulation phase (0°, 90°, 180°, or 270°). MEP amplitude values are given relative to the mean MEP amplitude of all four phases. *p < 0.05, *p < 0.05

5.3.8 Variable effects of tuning individual spontaneous EEG on motor excitability measures

The individual β peak frequency (IBF) was estimated based on resting-state EEG recording prior to tACS-TMS session (Figure 5.9 A). The individual peaks in the β-band were within 0.5-4.5 Hz of the tACS frequency (20 Hz) (5.9 B).

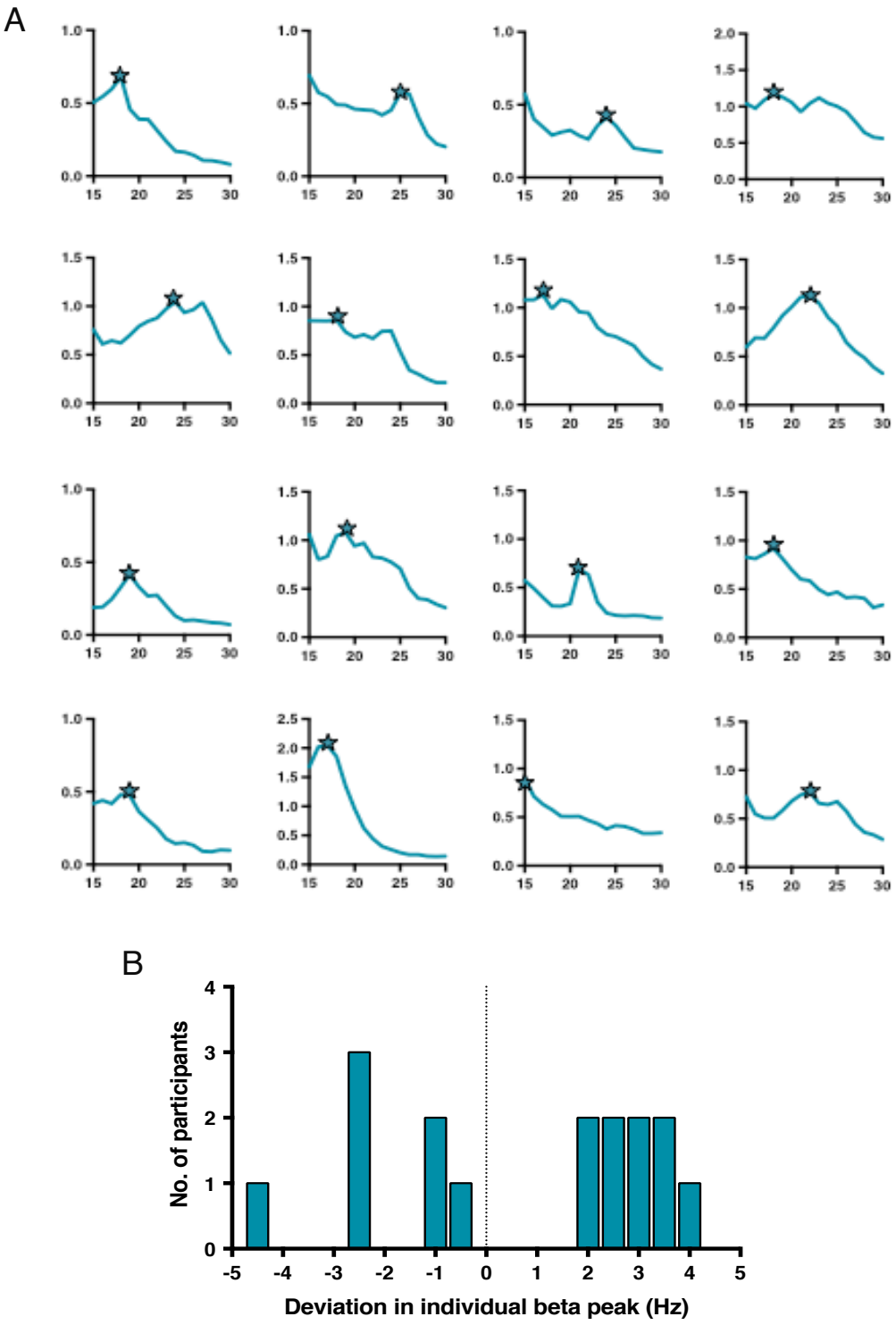


Figure 5.9 Individual β peak frequencies

A. Individual β peak frequency (highlighted by stars), defined as the frequency with the largest power in the window 15–30 Hz, was estimated for all 16 subjects based on channel C3. **B.** Deviation of individual β peak frequency from stimulation frequency (20 Hz).

First, I aimed to examine whether β tACS-induced changes in motor excitability were dependent on how well the applied β (20 Hz) tACS matched an individual's own spontaneous β frequency. To this end, the normalised MEP values (see Methods section 5.2.7 for more details) for each protocol during β tACS were correlated with the absolute deviation of stimulation frequency from IBF. When averaged values were taken into account for each individual and each TMS protocol (independent of phase), no resting-state or pre-movement TMS measures showed stronger β tACS-induced change with better match between stimulation frequency and IBF ($p > 0.05$).

When correlations were performed separately for each phase of each protocol, a significant positive relationship was found between β tACS-induced effects and absolute deviations of stimulation frequency from IBF for the following resting-state measures: MT_{1mV} at 0º phase ($\rho = 0.533$, $p = 0.035$), MT_{1mV} at 180º phase ($\rho = 0.533$, $p = 0.05$) and $SICI_{2.5ms}$ at 0º phase ($\rho = 0.533$, $p = 0.045$). In terms of pre-movement measures, a significant inverse relationship was found between stronger β tACS-induced effects and greater absolute deviations of stimulation frequency from IBF for $SICI_{2.5ms\ move}$ at 90º phase ($\rho = -0.577$, $p = 0.027$), such that a stronger effect of β tACS on this protocol was observed with better match between stimulation frequency and IBF.

In addition, the motor excitability values were correlated with the relative deviation of stimulation frequency from IBF. A significant relationship was only found between stronger β tACS-induced effects and greater relative deviations of stimulation frequency from IBF for resting-state MT_{1mV} at 180º phase ($\rho = 0.610$, $p = 0.014$). In contrast, no relationship was found β tACS-induced effects and relative deviations of stimulation frequency from IBF for pre-movement TMS measures.

5.3.9 β tACS slows down response time

Based on the previously proposed antikinetic role of β oscillations (Pogosyan et al 2009; Joundi et al 2012; Gonzalez Andino 2004), I aimed to investigate whether driving motor cortical β-frequency oscillations had any effect on response time (RT). There was a significant increase in response time in β session as compared with sham: both when the first ($t_{(13)}$ = 3.834, p = 0.002) and the last 42 trials ($t_{(13)}$ = 2.242, p = 0.043) of the β session were considered (Figure 5.10).

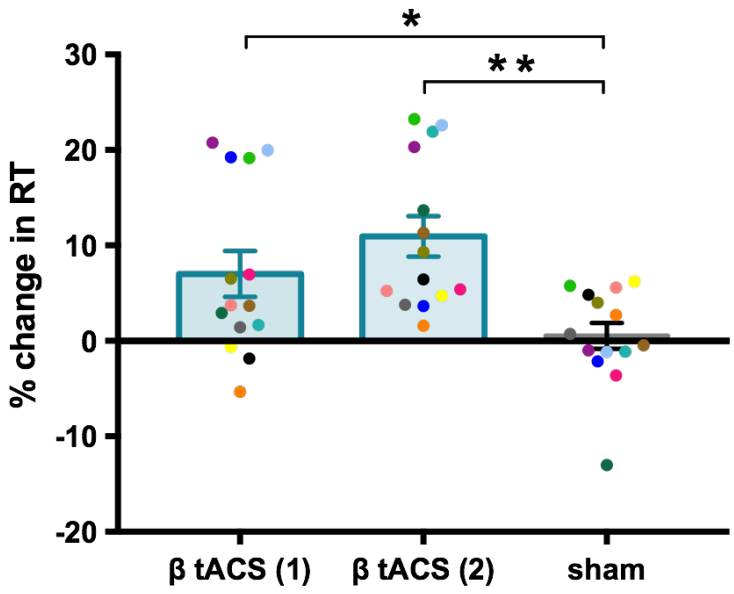


Figure 5.10 The effect of tACS on response time

The mean % change (± SEM) in RT from baseline for the first 42 trials and the last 42 trials of β tACS session (β tACS (1) and β tACS (2), respectively) and sham session. Data points for each subject are shown with different colour.

The inherent variability in participant's RT meant that TMS would sometimes occur during or after the onset of RT and therefore coincide with its corresponding burst in EMG activity. These trials were excluded from the analysis (11.7 % of all pre-movement trials). Since excluding the trials with faster responses could have affected an individual's average RT more in one session than the other, the % of excluded

trials in each session (both at baseline and during) was calculated and a RM ANOVA with one factor of session (β, sham tACS) and one factor of time (baseline, during) was performed. No significant difference between the number of trials rejected was found (no main effect of session [$F_{(1,13)} = 1.419$, $p = 0.255$, $\eta 2p = 0.098$] or time [$F_{(1,13)} = 0.613$, $p = 0.448$, $\eta 2p = 0.045$] and no significant session × time interaction [$F_{(1,13)} = 2.610$, $p = 0.130$, $\eta 2p = 0.167$]).

Additionally, I examined whether β tACS-induced changes in RT were related to the stimulation-induced changes in resting-state and pre-movement TMS measures. No relationship was found ($p > 0.05$).

5.4 Discussion

This study was performed to investigate the physiological basis and functional significance of driving β-frequency oscillations in the M1. The results demonstrate that driving cortical β oscillations led to a phase-independent modulation of pre-movement $SICI_{1ms}$, thought to reflect extrasynaptic $GABA_A$ tonic inhibition. Furthermore, corticospinal excitability during movement preparation was affected by β tACS in a stimulation phase-dependent manner. Finally, β tACS slowed down response time, further supporting the antikinetic role of β oscillatory activity in motor control.

5.4.1 Comparison between baseline resting-state and pre-movement motor excitability measures

As expected, a strong increase in corticospinal excitability and a reduction in $SICI_{2.5ms}$ (which corresponds to reduced synaptic $GABA_A$ inhibition as a subject prepares to move) were observed here, in agreement with previous studies (Aono et al 2013; Schulz et al 2014b; Takemi et al 2015).

5.4.2 β tACS has no phase-independent effects on resting-state motor excitability measures

In the present study, no significant phase-independent change in any of the resting-state measures of motor excitability was observed during β tACS. In terms of corticospinal excitability, other studies exploring the effect of 20 Hz tACS on this measure have reported mixed results (Feurra et al 2011a; Tecchio et al 2013; Feurra et al 2013; Cancelli et al 2015; Guerra et al 2016). The results also showed no effect of β tACS on the measures of local inhibitory activity: $SICI_{2.5ms}$, which is a relatively specific measure of synaptic $GABA_A$ activity (Kujirai et al 1993; Ilic et al 2002; Di

Lazzaro et al 2005), and $SICI_{1ms}$, which has been previously suggested to reflect extrasynaptic GABA tone (Stagg et al 2011b). In agreement with our findings, a recent study by Guerra et al. reported no phase-independent effects of 20 Hz tACS on TMS-assessed corticospinal excitability and synaptic $GABA_A$ activity (Guerra et al 2016). The reasons for the lack of consistent findings in the literature are not clear, but may be in part due to the relatively low intensity of tACS used.

5.4.3 Pre-movement $SICI_{1ms}$ is modulated by β tACS in a phase-independent manner

Tonic conductance mediated by extrasynaptic $GABA_A$ receptors is likely to exert a powerful control over network oscillatory activity, including β-frequency oscillations (Semyanov et al 2003; Mann and Mody 2010; Manseau et al 2010; Hall et al 2014; Prokic et al 2015). The inhibitory interneurons, which mediate tonic inhibition in the cortex (Semyanov et al 2003), have a vital role in β oscillations (Gonzalez-Burgos and Lewis 2008) and have been shown to control both synchronisation and desynchronisation processes in cortical networks (Manseau et al 2010). Therefore, one of the aims of the present study was to find out whether β tACS leads to a modulation of $SICI_{1ms}$, which has been suggested to reflect extrasynaptic $GABA_A$ tonic inhibition (Stagg et al 2011b). While no effect of driving cortical β oscillations on $SICI_{1ms}$ at rest was found, the results showed that β tACS reduced $SICI_{1ms}$ during movement preparation, when MRBD occurs. If TMS-assessed tonic $GABA_A$ inhibition was important in the process of event-related desynchronisation, β tACS would be expected to cause, via entrainment, a decrease in MRBD, which, in turn, should be represented by the reduced $SICI_{1ms}$, as demonstrated here. Despite this, other findings presented in the current study argue against this hypothesis. Firstly, if $SICI_{1ms}$ is important in the process of event-related desynchronisation, one would expect a modulation of this measure during movement preparation as compared with the resting-state at baseline.

Yet, no change in this measure between these two different brain states was found. In addition, if the β tACS-induced changes in inhibitory circuits (the activity of which $SICI_{1ms}$ reflects) were entrainment-dependent, the modulation of this measure might be expected to show stimulation-phase dependency or dependency on proximity of stimulation frequency (20 Hz) to the individual β peak frequency. Neither of these, however, was demonstrated for $SICI_{1ms}$ protocol. Therefore, it is conceivable that the changes observed in $SICI_{1ms}$ are a reflection of online tACS-induced plasticity effects, especially since the pre-movement TMS measures were performed during 15-min of tACS applied continuously. It remains to be investigated whether the suggested here plasticity effects are dependent on entrainment and to what extent.

5.4.4 β tACS has no phase-dependent effects on resting-state motor excitability measures

No phase-dependent modulation of motor excitability measures was found during β tACS at rest. These findings are in disagreement with the recent study (Guerra et al 2016), which employed the same tACS parameters and reported phase-dependent changes in both TMS-assessed corticospinal excitability and synaptic $GABA_A$-mediated inhibition. It is worth noting that in the study performed by Guerra and colleagues, 3 ms inter-stimulus interval was used for SICI protocol, whereas in the present study 2.5 ms inter-stimulus interval was used. In addition, the deviation of stimulation frequency (20 Hz) from individual β peak frequency, measured prior to tACS-TMS procedure, was also assessed. Our results show that only three participants displayed the frequency of the highest peak in the β-band that was within ± 1.5 Hz of the tACS frequency (20 Hz), whereas in the study performed by Guerra and colleagues, the majority of the participants' individual β peak was closer to the stimulation frequency. Since entrainment is more pronounced when the stimulation frequency matches the natural frequency of the stimulated neuronal elements (Zaehle et al 2010; Fröhlich and

McCormick 2010; Reato et al 2010; Thut et al 2011; Reato et al 2013; Ali et al 2013), it is possible that the entrainment of the activity within corticospinal and interneuronal circuits at rest in the present study was less effective. Accordingly, the lack of adjustment of stimulation frequency to individual endogenous β-frequency could have compromised the ability of tACS to entrain β oscillatory activity. Further, it was previously demonstrated that under conditions of high endogenous α power, tACS failed to influence α power (Neuling et al 2013), suggesting that α power reached a maximum (ceiling effect) or that tACS applied at low intensity (~ 1 mA) is not strong enough to influence high endogenous oscillations. Similarly, it can be speculated that β tACS employed in the present study did not effectively entrain endogenous β activity since the underlying neuronal motor cortical network has strong oscillatory β power and therefore may not be as prone to an external periodic force.

Finally, it is difficult to provide support to the above discussion based on the correlation results exploring the relationship between tACS-induced changes and the match between stimulation frequency and individual β peak frequency, since the findings are inconclusive and were not corrected for multiple comparisons.

Overall, the lack of consistency of tACS effects was reported in recent studies (Braun et al 2017; Veniero et al 2017), emphasising the importance of optimising the stimulation parameters for establishing the robustness and reliability of electrical stimulation effects.

5.4.5 β tACS modulates corticospinal excitability during movement preparation in a phase-dependent manner

The results demonstrate that β tACS led to stimulation phase-dependent modulation of corticospinal excitability during movement preparation, i.e., the period when MRBD occurs. Since endogenous resonance at β-frequency is much weaker as compared with the resting state, it is plausible that it was easier to drive local oscillatory activity by exogenous rhythm, despite the fact that it was not matched to the resonance frequency of the cortex. Another possibility is that corticospinal circuits during movement preparation are simply affected by weak up and down states induced by β tACS, which is then reflected in MEP amplitude.

The results show that β tACS decreased corticospinal excitability during movement preparation specifically at the rising flank of sine wave (0°) and increased it at the falling flank of sine wave (180°). Anodal (positive) current leads to depolarisation of the membrane potential, leading to an increase in neuronal excitability and more spontaneous cell firing, whereas cathodal (negative) current has the opposite effects (Nitsche and Paulus 2000). Since M1 would be exposed to anodal current during stimulation at 90° phase and to cathodal current during stimulation at 270° phase, the phase-dependent effects observed here cannot be trivially explained by the effect of anodal/cathodal currents as there is no difference in potential between the electrodes.

An alternative, albeit speculative, explanation of phase-dependent tACS effects observed here in a movement-related paradigm is that cortical circuits oppose the exogenous rhythm, trying to resist synchronisation in the β-frequency band and, therefore, the effects measured represent a compensatory cortical response to β tACS, rather than reflecting directly stimulation-induced phase-dependent modulation of motor excitability.

5.4.6 β tACS slows down response time

β tACS led to slower response times, consistent with the antikinetic role of β oscillations. Previous studies reported an increase in movement velocity induced by β tACS but no significant change in response times (Pogosyan et al 2009; Joundi et al 2012a). The latter finding is also consistent with the results reported in Chapter 4. It is worth noting, however, that different stimulation parameters were employed in these studies (montage and/or intensity), which could explain the difference in the observed effects of β tACS on this aspect of motor behaviour.

5.5 Conclusions

The present study demonstrated that driving β oscillatory activity in M1 at rest is capable of inducing a stimulation phase-independent modulation of $SICI_{1ms}$, thought to reflect extrasynaptic $GABA_A$ tonic inhibition. Moreover, β-frequency tACS affected corticospinal excitability during movement preparation in a stimulation phase-dependent manner. Finally, β tACS slowed down response time, further supporting the antikinetic role of this frequency band in motor control.

CHAPTER

6

The neurochemical effects of driving β oscillations: a tACS-7T MRS study

The previous two experimental Chapters have focused on investigating the effects of tACS-driven motor cortical oscillations on measures of excitatory/inhibitory mechanisms and their implicated neurotransmitter systems, as assessed indirectly using TMS. The goal of this Chapter is to directly evaluate the effects of driving β oscillatory activity by measuring local changes in the cortical concentrations of GABA and glutamate in M1 using ultra-high field (7T) Magnetic Resonance Spectroscopy (MRS).

6.1 Introduction

A growing body of evidence suggests a vital role of GABAergic and glutamatergic activity in motor cortical beta (β) oscillations (Jensen et al 2005; Yamawaki et al 2008; Hall et al 2010a; Hall et al 2011; Baumgarten et al 2016). The evidence from *in vitro* preparations shows that the primary motor cortex (M1) generates synchronous network oscillations preferentially at β-frequency, which, in turn, are dependent on fast synaptic (phasic) inhibition mediated by $GABA_A$ receptors, with a contribution from NMDA and $GABA_B$ receptors (Yamawaki et al 2008). In humans, the mechanisms underlying oscillatory activities have been mainly studied using pharmaco-MEG approach, which allows for determination of the spatial profile of neuronal network oscillatory power change in the region of interest or across the cortex following administration of a drug (Hall et al 2010a; Hall et al 2011). The administration of the benzodiazepine site agonist, diazepam, was shown to elicit large power increases in the β-band in the precentral gyrus (Hall et al 2010a), thus demonstrating that elevated β power is indicative of elevated local inhibitory network activity. However, since benzodiazepines affect both fast synaptic and slower, extra-synaptic, GABA-mediated inhibition (Semyanov et al 2003; Semyanov et al 2004; Prokic et al 2015), it has not been possible to determine which type of inhibition mediates their effect on oscillatory power using pharmaco-MEG approach alone. Recently, an important role for local synaptic $GABA_A$-mediated inhibition, quantified via the paired-pulse technique, short interval intracortical inhibition ($SICI_{3ms}$), has been demonstrated in human motor cortical β activity using a novel combined tACS-TMS approach (Guerra et al 2016). A similar approach was employed in the two previous experimental Chapters but no significant effect of driving motor cortical β oscillations on TMS-assessed measures of $GABA_A$-mediated inhibition or

glutamatergic facilitation was found, most likely due to differences in the stimulation parameters used.

Since TMS measures provide assessment only of specific aspects of underlying physiological activity, the primary goal of the present study was to drive motor cortical β oscillations using tACS while simultaneously performing direct *in vivo* quantification of neurochemicals of interest, i.e., GABA and glutamate, in M1 using ultra-high field (7T) MRS. Interestingly, increasing evidence suggests that GABA concentration measured using MRS largely represents pools of GABA that are linked to tonic rather than phasic inhibitory neurotransmission (Stagg et al 2011b; Dyke et al 2017), thus providing the opportunity to examine the role of this less-explored aspect of GABAergic inhibition in β-band activity. In addition, since the present study involved the application of β-frequency and sham tACS in the same session, the after-effect of stimulation was also assessed. Furthermore, given the high inter-individual variability in the effects of non-invasive brain stimulation paradigms, including tACS, I additionally aimed to examine the relationship between the magnitude of any tACS-induced modulation of M1 GABA and glutamate levels and the difference between the stimulation frequency (20 Hz) and spontaneous individual β peak frequency (IBF).

6.2 Methods

6.2.1 Participants

Eighteen healthy subjects (age 24.5 years, range: 20–29 years; 9 male) gave their informed consent to participate in the study in accordance with Central University Research Ethics Committee approval (University of Oxford; MS-IDREC-C2-2015-021). All subjects were right-handed as assessed by the Edinburgh Handedness Inventory (Oldfield 1971), had no history of neurological or psychiatric disorders and reported no other contraindications to tACS or MRS. The cohort of participants recruited for the study in Chapter 6 was recruited for the present study.

6.2.2 Experimental design and procedure

Subjects participated in one experimental session. At the start of the session, EEG was recorded with eyes open for 2 min in order to quantify individual β peak frequency in M1. Next, subjects were positioned comfortably in the scanner and were instructed to relax and to keep their eyes open throughout the experiment. A T1-weighted structural scan was acquired first. Participants received β (20 Hz) tACS stimulation and sham stimulation for 10 min each, with a 10 minute break between. The order in which the participants received the stimulation conditions was counterbalanced across subjects. MRS data were acquired before, during and immediately after β tACS and sham stimulation (Figure 6.1).

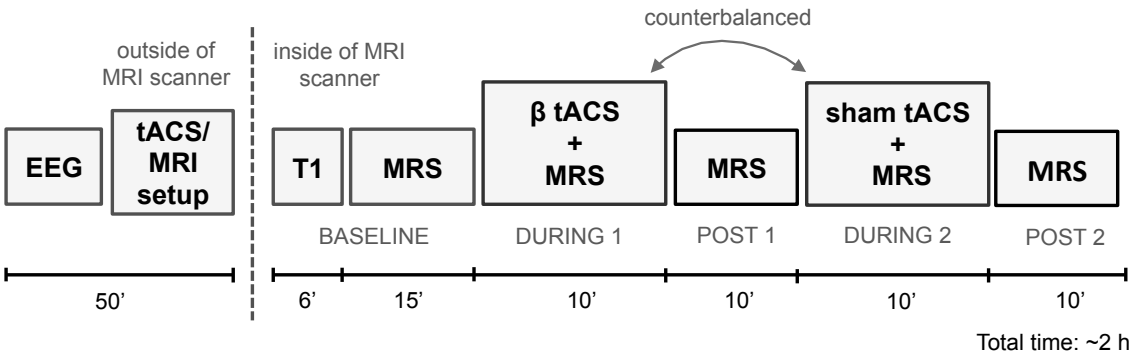


Figure 6.1 Experimental design

EEG was performed outside of the scanner at the start of the session. β and sham tACS were applied for the duration of 10 min, with the order of stimulation counterbalanced across subjects. MRS acquisitions were performed before ('baseline'), during and after ('post') β tACS and sham stimulation.

6.2.3 EEG

EEG signals were sampled at 2048 Hz, amplified (x 20) using Porti32 amplifier (Twente Medical Systems International, Oldenzaal, The Netherlands) and recorded using an in-house software (RecEEG©, developed by A. Pogosyan, Oxford). Following skin preparation with Nuprep gel (Weaver and Company), Ag/AgCl electrodes were placed over: Fz, C3, Cz, C4 and Pz, according to the International 10–20 EEG system of electrode placement. Electrodes were affixed using Ten20 conductive paste gel (Weaver and Company) and recorded in an average reference configuration.

6.2.3.1 EEG data analysis

Signals were edited using a custom-made software (EditEEG©, developed by A. Pogosyan, Oxford). The raw EEG data was inspected for artefacts and high-pass filtered at 1 Hz. Recordings were then imported into Spike2 software v7.12b (Cambridge Electronic Design Ltd, Cambridge, UK). Fourier analysis was used to calculate power spectra with frequency resolution of 0.5 Hz (2048 bins per channel).

Channel C3 (overlying the stimulated M1 area) was selected and the individual peak frequency for β oscillatory activity was found, defined as the frequency with the largest power in the window 15–30 Hz. No distinct peak at β-frequency was present in two participants.

6.2.4 Transcranial alternating current stimulation (tACS)

tACS was delivered by an MR compatible DC stimulator (NeuroConn GmbH, Germany) through a pair of conductive rubber electrodes (5 × 7 cm^2) (fitted with 5 kΩ resistors; Easycap, GmbH, Germany). The electrodes were positioned prior to entry into the scanner. Chloride-free conductive gel was used as a conducting medium between the scalp and the electrodes. One electrode was centred over the TMS-derived FDI hotspot of left M1; the other electrode was positioned on the midline parietal region (Pz; International 10–20 system). The electrode positions were adopted according to the previous studies that demonstrated region-, frequency- and phase-specific tACS effects on M1 excitability (Feurra et al 2011a; Feurra et al 2013; Guerra et al 2016; Nakazono et al 2016), and to avoid phosphenes (Schutter and Hortensius 2010; Turi et al 2013).

Stimulation was delivered with no direct current offset and at a peak-to-peak amplitude of 1 mA. Current was ramped up and down over the first and last 5 s of stimulation. The total duration of stimulation was 10 min for β session and 10 s for sham session. Impedance was kept below 10 kΩ. Subjects were blind to the stimulation condition used. No participant reported phosphenes or skin sensations during stimulation.

6.2.5 Magnetic resonance spectroscopy (MRS)

6.2.5.1 MRS data acquisition

MR data were acquired using a Siemens 7T Magnetom system with a 32-channel head coil. Dielectric pads (barium titanate: 13 × 14 × 0.5 cm^3) were positioned to increase B1 efficiency in the regions of interest for MRS acquisition (Lemke et al 2015). MRS data were acquired using a semi-LASER sequence (Scheenen et al 2008) (64 averages, TR 5000 ms, TE 50 ms, Voxel size 2 × 2 × 2 cm^3) using VAPOR (variable power RF pulses with optimised relaxation delays) water suppression (Tkác et al 2001). The voxel of interest (VOI) was manually positioned in the left M1, covering the whole hand knob structure (a landmark previously described to represent the hand area of the primary motor cortex [Yousry 1997]), avoiding contact with the dura to minimise significant macromolecule contamination (Figure 6.2).

Structural MRI data were acquired to aid MRS voxel placement using a magnetization-prepared rapid acquisition gradient echo (MPRAGE) sequence (TR 2200 ms, TE 2.82 ms, slice thickness 1.0 mm, in-plane resolution 1.0 × 1.0 mm^2, GRAPPA [generalised autocalibrating partial parallel acquisition] factor = 2).

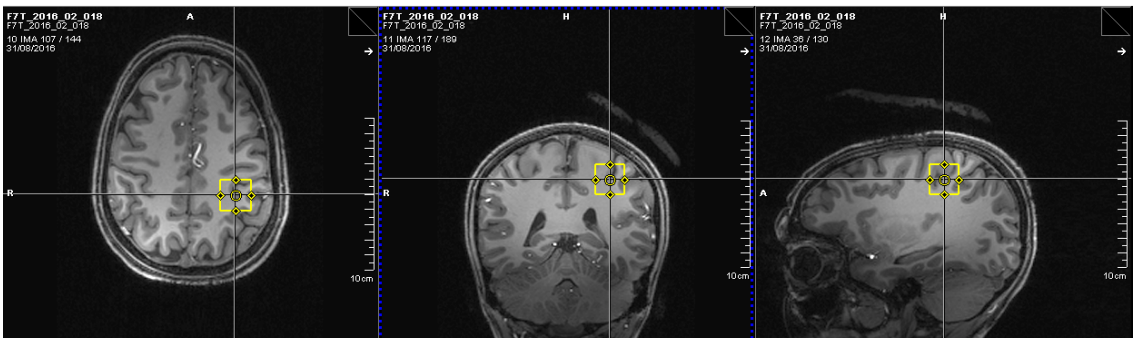


Figure 6.2 Typical placement of the VOI

Typical placement of the 2 × 2 × 2 cm^3 voxel of interest (VOI) in the left M1, shown in axial (left), coronal (middle) and sagittal (right) view.

6.2.5.2 MRS data analysis

Raw data were corrected using the unsuppressed water signal from the same VOI, eddy current correction, and a zero-order phasing of array coil spectra. Neurochemicals within the chemical shift range 0.5 to 4.2 ppm were quantified with LCModel analysis (Provencher 2001). GABA and glutamate values are reported as a ratio to total creatine (tCr, sum of creatine and phosphocreatine).

6.2.6 Statistical analysis

Statistical analyses were performed using SPSS (version 22.0; IBM) and GraphPad Prism (version 7, GraphPad Software Inc., San Diego, CA, USA).
Normality of data distribution was tested by D'Agostino-Pearson omnibus normality test. All MRS data passed the normality test. A single iteration of Grubbs' test with a significance level of 0.05 was performed for each MRS measures of GABA and glutamate for each stimulation type (β and sham tACS) separately and any significant outliers were excluded.

Since β tACS and sham stimulation were applied in the same session (counterbalanced across subjects), the MRS data acquired immediately prior to stimulation was used as a baseline measurement, i.e., the initial baseline measurement was used as a baseline for the stimulation type (β tACS or sham) performed first, whereas data acquired in the 'post 1' period (Figure 6.1) served as a baseline for the stimulation type applied second.

Data were analysed using a repeated measures (RM) ANOVA. In the case of significant effects, *post hoc* analyses with paired t-tests (two-tailed) were applied. Mauchly's test was used to test for assumption of sphericity and Greenhouse–

Geisser corrections were applied as necessary. Effect size estimates were computed using partial eta squared (η2*p*) for RM ANOVAs and Cohen's d_z for t-tests.

Correlations were assessed using the Spearman's rank correlation method (ρ). Specifically, I examined whether the modulation of GABA and glutamate levels during β tACS was dependent on how closely the applied stimulation frequency (20 Hz) matched an individual's own spontaneous β frequency (IBF) (match between stimulation frequency and IBF = IBF – 20 Hz). The significance level for all tests was set at $p < 0.05$.

6.3 Results

6.3.1 Driving β-band oscillations reduces M1 GABA levels

The first aim was to examine whether driving β-frequency oscillations affected MRS-measured GABA levels, suggested to reflect $GABA_A$-mediated tonic inhibition. A RM ANOVA with one factor of stimulation type (β tACS, sham) and one factor of time (baseline, during, post) showed a main effect of stimulation type ($F_{(1,17)}$ = 5.541, p = 0.031, η2p = 0.246), no main effect of time ($F_{(2,34)}$ = 0.798, p = 0.459, η2p = 0.045), and no stimulation type × time interaction ($F_{(2,34)}$ = 0.407, p = 0.563, η2p = 0.023).

Further exploration of the data with t-tests showed a significant reduction in M1 GABA during β tACS compared with sham stimulation ($t_{(17)}$ = -3.233, p = 0.005, Cohen's d_z = -0.762) (Figure 6.3 A). To examine whether the order of stimulation type alone affected the measures of M1 GABA, a RM ANOVA with one factor of stimulation order (1,2) and one factor of time (baseline, during, post) was performed. No main effect of stimulation order was found ($F_{(1,17)}$ = 2.686, p = 0.120, η2p = 0.136). In addition, no main effect of time ($F_{(2,34)}$ = 1.519, p = 0.234, η2p = 0.082) or stimulation type × time interaction ($F_{(2,34)}$ = 0.082, p = 0.865, η2p = 0.005) was observed.

Next, the effect of driving β-frequency oscillations on M1 glutamate levels was assessed. A RM ANOVA with one factor of stimulation type (β, sham tACS) and one factor of time (baseline, during, post) showed no main effect of stimulation type ($F_{(1,17)}$ = 3.421, p = 0.082, η2p = 0.168) or time ($F_{(2,34)}$ = 2.500, p = 0.097, η2p = 0.128), and no session × time interaction ($F_{(2,34)}$ = 1.942, p = 0.159, η2p = 0.103) (Figure 6.3 B).

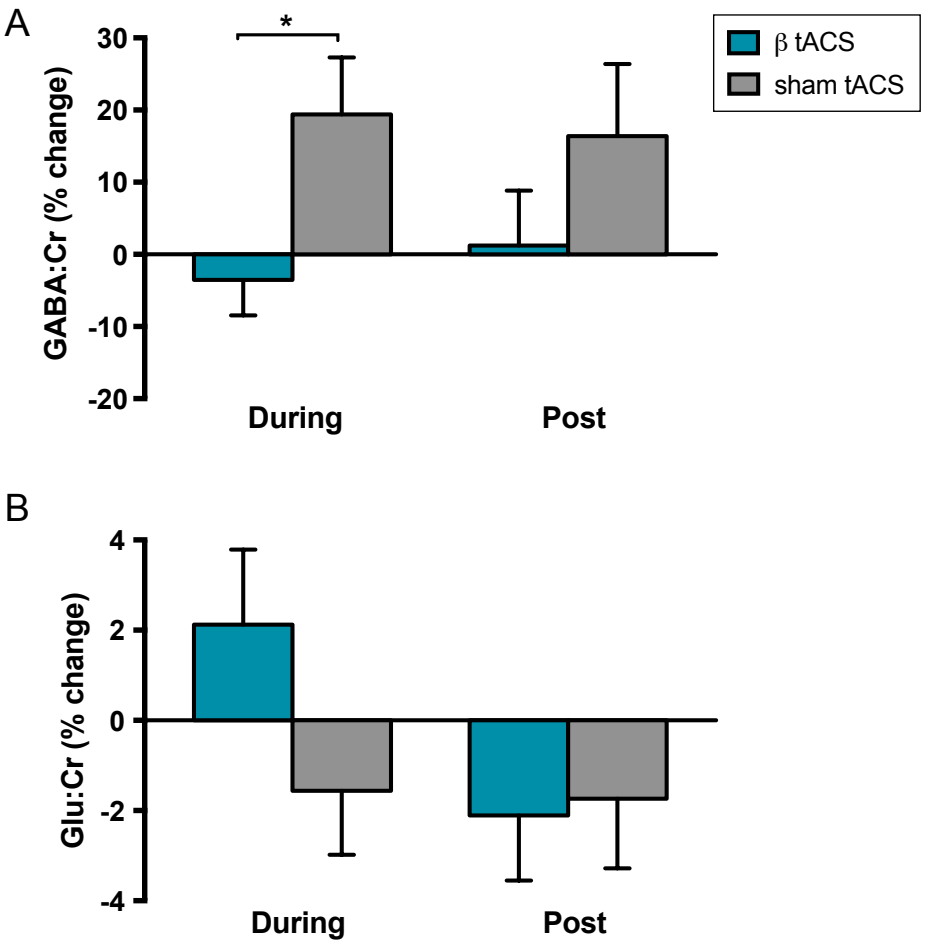


Figure 6.3 The effect of β and sham tACS on MRS-assessed M1 GABA and glutamate levels

A. M1 GABA levels during and after ('post') β tACS and sham stimulation. **B.** M1 glutamate levels during and after ('post') β tACS and sham stimulation. The data are shown as % change from baseline (± SEM). *$p < 0.05$

6.3.2 The relationship between stimulation frequency and spontaneous β-frequency affects β tACS-induced modulation of M1 GABA

To assess the dependence of β tACS-induced modulation of M1 GABA and glutamate on the match between stimulation frequency (20 Hz) and individual β peak frequency (IBF), a correlational analysis was performed. There was a significant association between β tACS-induced change in M1 GABA during stimulation and the deviation of stimulation frequency from IBF (calculated as IBF – 20 Hz; ρ = -0.533, *p*

= 0.041) (Figure 6.4 A). In contrast, there was no association between sham tACS-induced change in M1 GABA during stimulation and the relative deviation of stimulation frequency from IBF (ρ = -0.062, p = 0.735) (Figure 6.4 B). β tACS-induced modulation of M1 glutamate was not dependent on the match between stimulation frequency and IBF (p > 0.05).

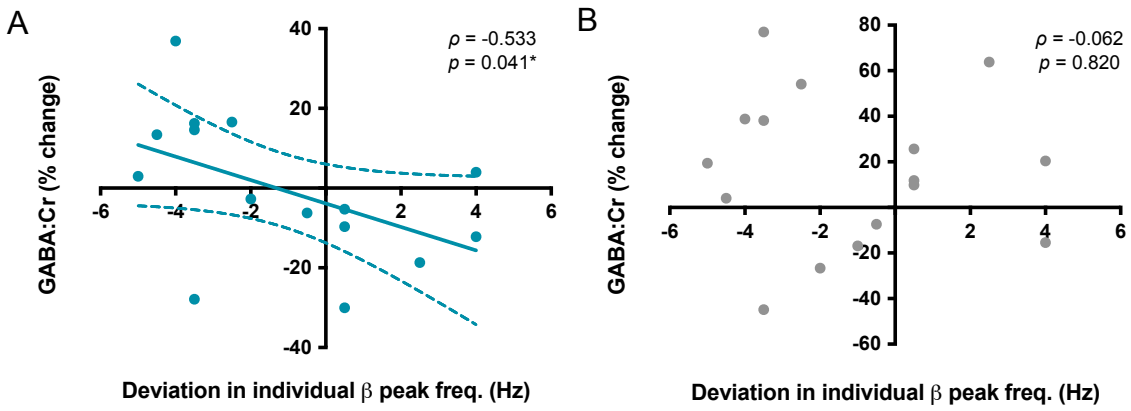


Figure 6.4 Relationship between tACS-induced change in M1 GABA and the match between stimulation frequency and individual β-frequency

Correlations between β tACS-induced (**A**) and sham tACS-induced (**B**) change in M1 GABA levels during stimulation and the relative deviation of stimulation frequency from an individual's β peak frequency. *p < 0.05

6.4 Discussion

The primary objective of this Chapter was to employ a novel tACS-7T MRS approach in order the study the neurochemical basis of motor cortical β oscillations. The findings presented here demonstrated that driving oscillatory activity in the β-frequency band leads to a reduction in M1 GABA levels during stimulation. Interestingly, β tACS-driven modulation of M1 GABA activity was dependent on the match between the frequency of stimulation (20 Hz) and an individual's spontaneous β peak frequency (IBF), such that participants who were stimulated at β-frequency that either matched or was slower than their IBF tended to show a reduction in M1 GABA, whereas participants who were stimulated at the frequency faster than their IBF showed the opposite effect.

6.4.1 Driving β-frequency oscillations reduces MRS-assessed M1 GABA levels

The main finding presented in this chapter suggests that driving β-frequency oscillations leads to a reduction in MRS-assessed M1 GABA. This observation is in agreement with the previous report showing a trend towards decreased M1 GABA levels during β tACS, as examined using 3T MRS (M. Nowak, C.J. Stagg, unpublished observations). There is a growing body of evidence from both animal and human studies showing the critical role of GABAergic activity in motor cortical β oscillations (Jensen et al 2005; Yamawaki et al 2008; Hall et al 2010a; Hall et al 2011; Baumgarten et al 2016). However, disentangling the role of different types of $GABA_A$-mediated types of inhibition (synaptic [phasic] vs. extrasynaptic [tonic]) in β oscillatory activity has been a challenge, particularly in human studies. Only recently, an important role of local synaptic $GABA_A$-mediated inhibition in motor β oscillations was demonstrated using a simultaneous tACS-TMS approach (Guerra et al 2016). Interestingly, increasing evidence suggests that GABA concentration measured using MRS largely

represents pools of GABA that are linked to tonic rather than phasic inhibitory neurotransmission (Stagg et al 2011b; Dyke et al 2017). Therefore, β tACS induced change in MRS-assessed M1 GABA demonstrated in this Chapter may constitute evidence of the role of extrasynaptic $GABA_A$-mediated activity in human motor cortical β oscillations. This finding is particularly interesting in light of recent evidence suggesting that extrasynaptic $GABA_A$ receptors mediating tonic inhibition exert powerful control over network activity (Semyanov et al 2003; Semyanov et al 2004; Mann and Mody 2010).

6.4.2 β tACS-induced change in M1 GABA levels depends on the match between stimulation frequency and an individual's spontaneous β frequency

Large inter-individual variability is one of the major challenges of transcranial stimulation approaches, including tACS. The present work provided evidence on the dependence of β tACS-induced change in M1 GABA on the relative deviation of stimulation frequency (20 Hz) from IBF. Specifically, driving β oscillations at the frequency that either matched (within ± 1 Hz) or was slower than IBF led to a reduction in M1 GABA, whereas stimulation at the frequency faster than IBF had the opposite effect. The importance of the match between stimulation frequency and an individual's spontaneous frequency on stimulation-induced effects has been demonstrated in a number of studies (Thut et al 2011; Ali et al 2013; Vossen et al 2015; Guerra et al 2016). For example, a recent report showed that the phase modulation of $SICI_{3ms}$ during stimulation was dependent on the convergence between the frequency of tACS and that of spontaneous activity in the β-band, such that the group in whom the frequency of the highest peak in the β-band was within ± 1.5 Hz of the tACS frequency (20 Hz) showed more effective modulation of $SICI_{3ms}$ as opposed to the group in whom the frequency was outside of this range (Guerra et al 2016). In contrast, the present findings show the relationship only between the relative, rather than absolute, deviation

of stimulation frequency from an individual's β peak frequency. This raises the possibility that β tACS-induced change in M1 GABA during stimulation found here may also reflect plastic changes rather than purely entrainment-related effects. In the absence of simultaneous EEG/MEG recording, it is not possible to directly assess the relationship between the observed biochemical changes and the extent of motor cortical β activity enhancement.

Furthermore, even in the absence of plastic changes, the relationship between β oscillatory activity and MRS-assessed M1 GABA in humans is likely to be complex. Of particular relevance here is a recent study which showed that low concentration of the benzodiazepine site agonist, zolpidem, augmented a tonic inhibitory $GABA_A$ receptor-mediated current in fast-spiking cells and subsequently reduced the power of pharmacologically-induced β oscillatory activity. In contrast, higher doses of the drug reduced the tonic current leading to an increase in β power in rat M1 (Prokic et al 2015). Overall, these findings show that changes in tonic inhibitory current can produce bidirectional modulation of β oscillatory power, suggesting a complex interplay between the inhibitory mechanisms and motor cortical β oscillations.

6.5 Conclusions

The findings presented in this Chapter demonstrate that driving oscillatory activity in the β-frequency band leads to a reduction in M1 GABA levels during stimulation. Moreover, the assessment of the relationship between the deviation of the stimulation frequency from individual β peak frequency (IBF) and tACS-induced changes in MRS measures has revealed that participants who were stimulated at β-frequency that either matched or was slower than their IBF tended to show a reduction in M1 GABA, whereas participants who were stimulated at the frequency faster than their IBF

showed the opposite effect. This finding helps explain variability in responses to β tACS and, importantly, may also provide evidence on the complex interaction between local MRS-assessed M1 GABA levels, suggested to reflect tonic extrasynaptic $GABA_A$ activity, and motor cortical β oscillations.

CHAPTER

7

Relationship between β- and γ-frequency oscillations, motor excitability and motor learning: a multimodal MEG and TMS study

The goal of this Chapter was to examine whether the spontaneous and movement-related cortical β and γ oscillations are related to various parameters of motor excitability. To this end, I employed MEG and subsequent TMS and performed within-subject comparisons between various measures acquired using these two different modalities. In addition, and to follow up on the findings from Chapter 4, I investigated whether performance in a motor learning task is dependent on motor cortical β- and γ-band oscillatory activities.

7.1 Introduction

Over the past two decades, an increasing number of studies have examined the relationship between motor cortical oscillations and TMS-assessed motor excitability measures (Zarkowski et al 2006; Mitchell et al 2007; Lepage et al 2008; Sauseng et al 2009; Mäki and Ilmoniemi 2010; Berger et al 2014). Most frequently, a simultaneous TMS-EEG approach has been employed to establish the link between corticospinal excitability, as assessed via a single MEP amplitude and oscillatory activity. This has previously been done either on a trial-by-trial basis (Zarkowski et al 2006; Mitchell et al 2007; Lepage et al 2008; Mäki and Ilmoniemi 2010), or by dividing the trials into two groups based on a single MEP amplitude and analysing the differences in spontaneous oscillatory activity between the groups (Mäki and Ilmoniemi 2010). A negative correlation between the amplitude of spontaneous oscillations in the midrange β-band (~12–20 Hz) measured over the stimulated (left) M1 and a single MEP amplitude, such that higher corticospinal excitability is related to less β-band activity, was previously demonstrated (Lepage et al 2008; Mäki and Ilmoniemi 2010). These results are in line with findings showing that the excitability of corticospinal neurons is increased during movement preparation and execution, i.e., during the time interval when β-band activity is reduced in the same cortical area (Chen and Hallett 1999; Reynolds and Ashby 1999; Zaaroor et al 2003; Kennefick et al 2014). However, it is worth noting that other studies have been unable to show a relationship between the amplitude of β oscillations and a single MEP amplitude, despite using a similar approach, i.e., concurrent TMS-EEG (Sauseng et al 2009; Berger et al 2014). The relationship between β-band oscillations and motor excitability therefore requires further investigation.

In terms of motor cortical γ oscillations, one study showed no relationship between spontaneous low (30–46 Hz) or high γ-band amplitude (46–70Hz) and a single MEP amplitude (Sauseng et al 2009), whereas another study, demonstrated that low γ-band (specified as the frequency range: 30–60 Hz; > 60 Hz activity was not examined) amplitude was positively associated with a single MEP amplitude (Zarkowski et al 2006). In general, few studies have assessed whether and how the amplitude of motor cortical γ activity is linked to TMS-assessed M1 excitability, probably due to multiple challenges associated with recording high-frequency activity using EEG (Yuval-Greenberg et al 2008; Muthukumaraswamy 2013; Baillet 2017). Further work, whether interventional (the main focus of the previous experimental chapters) or correlational (the main focus of this experimental chapter), is therefore important to help advance our understanding of the physiological mechanisms underlying motor cortical oscillatory activities.

To further investigate how motor cortical oscillations within the β- and γ- frequency bands are related to the TMS-assessed motor excitability, I adopted a sequential design, involving a MEG recording followed by TMS measurements in healthy young participants. This study extends our previous knowledge in a number of important ways. Firstly, a sequential design allowed for the correlation between the averaged measures of oscillatory activities and TMS-assessed motor excitability, both of which show large trial-by-trial fluctuations that cannot be fully accounted for in a concurrent experimental design, where on-going oscillations are inevitably disrupted by the applied TMS pulses. This type of study design is particularly relevant in light of recent findings demonstrating that both motor cortical β and γ oscillations are highly stable within individuals over time (Cheyne and Ferrari 2013; Espenhahn et al 2017). Secondly, for the first time, the relationship between oscillatory activities, both spontaneous and movement-related (movement-related beta desynchronisation [MRBD] and movement-related gamma synchronisation [MRGS]), and movement-

related motor excitability was evaluated. Thirdly, while the vast majority of previous studies have focused on recording single-pulse TMS-evoked MEPs, as an index of general corticospinal excitability, the present study additionally examined whether the aforementioned oscillatory activities are related to the paired-pulse TMS protocols: short interval intracortical inhibition (SICI) and intracortical facilitation (ICF), which primarily reflect local synaptic $GABA_A$-mediated inhibition and NMDA-mediated glutamatergic facilitation respectively.

Finally, given the findings reported in Chapter 4 showing that motor cortical γ-band activity may be both relevant and important for motor learning, I also examined whether motor cortical γ-band activity could be directly related to an individual's performance in a motor learning task.

Understanding how motor cortical β- and γ-frequency spectral "fingerprints" are related to local physiological measures and motor behaviour will help further unravel the underlying mechanisms and functional significance of these oscillatory activities in humans.

7.2 Methods

7.2.1 Participants

Thirty healthy subjects (age 24.9 years, range: 21–30 years; 14 male) gave their informed consent to participate in the study in accordance with Central University Research Ethics Committee approval (University of Oxford; MSD-IDREC-C2-2014-026 and MS-IDREC-C1-2015-010). These volunteers included 20 subjects that participated in the tACS-TMS study described in Chapter 4. All subjects were right-handed as assessed by the Edinburgh Handedness Inventory (Oldfield 1971) and had no history of neurological or psychiatric disorders; no metal implants, and reported no other contraindications to TMS and MEG.

7.2.2 Experimental design and procedure

Subjects had a MEG recording, followed by a TMS session and then performed an explicit sequence learning task, the serial response time task (SRTT), all performed on the same day (Figure 7.1 A). The primary goal of the MEG recording was to acquire resting-state and motor task-related data. Measures of corticospinal excitability, intracortical facilitation and inhibition in left M1 were acquired during eyes-open at rest (in the absence of a task) using TMS (these are referred to as resting-state measures). In addition, in conjunction with a response time (RT) task performed with the right hand, corticospinal excitability and intracortical inhibition were investigated during the pre-movement period (Figure 7.1 B, C).

All subjects had MEG recording and completed the SRTT. Four MEG datasets were excluded due to a difficulty with data acquisition and/or an insufficient quality. It was not possible to obtain MEPs from six subjects due to a high TMS threshold and a

discomfort caused by stimulation. Data from six further subjects were excluded due to missing data that resulted from technical difficulties during data acquisition.

The TMS and motor learning data were acquired and analysed in an identical manner as described in Chapter 4 and this has also been described below for ease of reading.

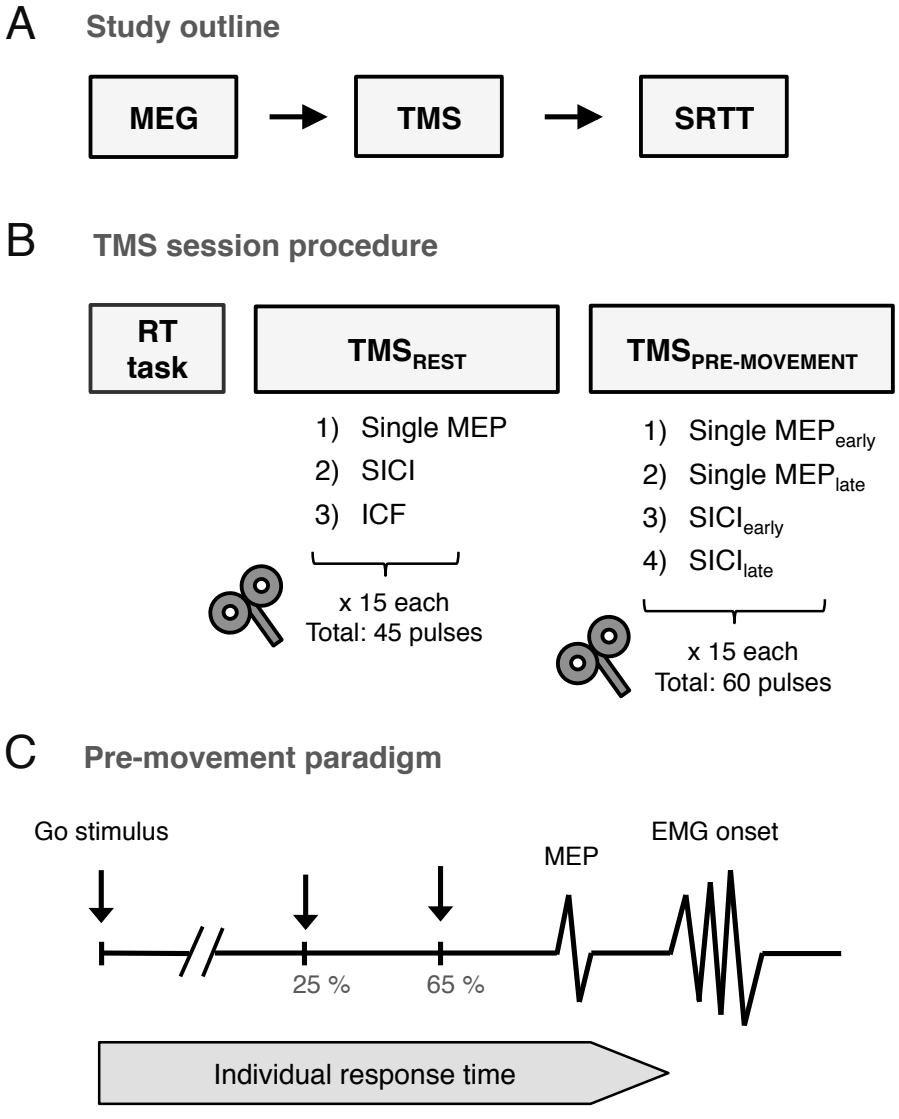


Figure 7.1 Study outline and experimental design

A. Study outline. **B.** Summary of TMS session procedure. Resting-state (single MEP, SICI, ICF) and event-related TMS measures (single MEP_{early}, single MEP_{late}, $SICI_{early}$, $SICI_{late}$) were performed in a pseudo-randomised order. **C.** Pre-movement paradigm. TMS measures were delivered at two time-points during pre-movement period: early (at 25 % iRT) and late (at 65 % of iRT). Abbreviations: iRT, individual response time; ICF, intracortical facilitation; MEP, motor evoked potential; SICI, short interval intracortical inhibition; SRTT, serial response time task.

7.2.3 MEG

7.2.3.1 MEG data acquisition

MEG data were acquired with a whole-head 306-channel Elekta Neuromag system (204 planar gradiometers, 102 magnetometers). Concurrent surface electromyography (EMG) of the right extensor digitorum communis (EDC) and first dorsal interosseous (FDI) muscle were recorded using bipolar surface electrodes. Both MEG and EMG data were sampled at 1000 Hz with a band-pass filter of 0.03–330 Hz, and stored for offline analysis. Head position was continuously monitored with respect to the MEG sensors using four head-position (HPI) coils. The locations of HPI coils and of three anatomical fiducials (the nasion and two preauricular points) were digitized using a 3D tracking system (Polhemus, EastTrach 3D) to define the subject-specific Cartesian head coordinate system. In addition, vertical and horizontal electrooculogram (EOG) electrodes were used to allow for detection and removal of eye-blink artefacts.

MEG data were acquired during a single session consisting of resting-state (8 min; eyes open) and a Go/NoGo task. In the Go/NoGo task, a blue circle cue, presented for 200 ms, instructed participants to prepare for an abduction of the index finger of their right hand. The cue was then replaced by a fixation cross for 1000 ms (cue-stimulus interval; CSI). A subsequent visual stimulus presented for 200 ms (coloured circle: green for Go or red for NoGo) indicated whether they should perform (Go) or withhold (NoGo) the prepared response. Participants were instructed to respond as quickly as possible on the Go trials. The stimulus was then replaced by a fixation cross for a duration that varied randomly between 2000-4000 ms (inter-trial interval). The task consisted of a total of 70 trials and lasted approximately 5 min. NoGo trials (20 % of all trials) were introduced to encourage participants' attention to the task.

Stimuli were generated using the MATLAB Psychophysics Toolbox v.3.0 package (Brainard 1997) and back-projected (Panasonic DLP Projector, PT D7700E) onto a

screen at a viewing distance of 120 cm with a spatial resolution of 1024 by 768 pixels and a refresh rate of 60 Hz.

7.2.3.1 MEG data analysis

MEG data were analysed using the OHBA Software Library (OSL), Fieldtrip (Oostenveld et al 2011), and Elekta software.

MEG data preprocessing. The raw MEG data were first visually inspected to remove channels with high levels of noise and then the temporal extension of Maxfilter Signal Space Separation (tSSS) method was applied, together with the detection of statistically bad channels and head movement compensation (Taulu and Simola 2006). Next, continuous data were downsampled to 250 Hz. Physiological artefacts of ocular or cardiac origin were identified via independent component analysis (ICA), and regressed out of the data. Only signals from planar gradiometers were analysed (204 channels) since they are sensitive to activity directly underneath the sensors. All analyses were performed in sensor space.

In the task data, the onset of EMG activity was determined in Go trials. This was defined as the first point after the Go stimulus onset where EMG signal exceeded the critical value (calculated as the mean of pre-stimulus activity [-1 s to 0 s] + 3*SD). The cleaned data were then epoched with respect to the onset of EMG (from -1.5 to +1.5 s). Any Go trials in which no response was made were rejected. In a final step, data were imported into Fieldtrip and visually inspected using the semi-automatic rejection tool to eliminate any remaining trials with excessive variance in the frequency band of interest (< 2 % of all trials).

Similarly to the MEG analysis performed in Chapter 4, 12 sensors overlying the left sensorimotor cortex were selected as the primary region of interest (ROI) for all MEG analyses. In the case of resting-state data, the main focus of the analysis was β-

frequency oscillatory activity (15–30 Hz), as γ-band activity cannot be easily detected.

Analysis of resting-state data. The data were segmented into 2-second epochs (240 data points) and visually inspected using the semi-automatic rejection tool to eliminate any remaining trials with excessive variance in the frequency band of interest (< 2 % of all trials). Individual data were normalized using z-scoring (with variability calculated across time points). Power estimates were calculated for frequencies from 2 to 100 Hz in 1-Hz steps. The data were transformed into the frequency domain using a multi-taper fast Fourier transform. The amount of smoothing was set at ± 4 Hz. Next, two orthogonal sensors of each gradiometer pair were combined, resulting in 102 gradiometers. For each subject, the power spectra were averaged over trials, sensors within the sensor group of interest and the frequency range.

The detection of individual oscillatory peaks in the β-frequency range was performed using an in-house script. Smoothing was achieved using a Savitzky-Golay filter with the order of 3 and window length of 3 Hz. Individual peak frequency was detected by first identifying zero-crossings in the differential of each participant's spectrum before linear interpolation of the differential around the zero was used to locate the peak maximum. Twenty-three subjects showed a distinct β-band peak, ranging from 16 to 23 Hz. The data from these participants were considered for correlational analyses.

Analysis of task data. A time-frequency representation of power was computed using a short-time Fourier transform, with a sliding time window of 400 ms that was advanced over the data in 80 ms steps. Power estimates were calculated for frequencies from 2 to 100 Hz in 1-Hz steps. A multi-taper method (Percival and Walden, 1993) was used to achieve frequency smoothing of ± 3 Hz. Next, two orthogonal sensors of each gradiometer pair were combined, resulting in 102

gradiometers. For each subject, the power spectra were averaged over trials and sensors within the left motor ROI. The data were normalised by subtracting the mean power values from the pre-movement baseline period (from -1.5 to -1 s time period relative to EMG onset) and are expressed as a percentage change from this reference period (P_{ref}):

$$\% \text{ power} = (\text{power} - P_{ref}) / P_{ref} * 100$$

This normalisation allowed task-related power fluctuations to be readily visualised in sensor space. The time-frequency plots of mean spectral density within the frequency bands of interest (i.e., β- [15–30 Hz] and γ-frequency range [60–90 Hz]) were generated for each subject (Figure A1, Appendix). Subsequently, for each individual subject, mean percentage decrease in β power (MRBD) and increase in γ power (MRGS) were extracted from the time window set to 0–500 ms (approx. the time period encompassing movement). The peak frequency for the MRBD and MRGS were determined as frequencies with the largest mean change in spectral power observed within the 0 to 500 ms time window (collapsing over time), for the 15–30 Hz and 60–90 Hz bands, respectively.

In total, six different oscillatory measures were used for subsequent analyses: resting-state (spontaneous) β activity (power [z-scored] and peak frequency), MRBD (relative power and peak frequency) and MRGS (relative power and peak frequency).

7.2.4 Motor learning task

Subjects performed a visually cued response time task after the MEG recording (session 1). As described previously (Stagg et al 2011a; Nowak et al 2017), four horizontal bars were displayed on the screen, each of which corresponded to a key on the keyboard. When a bar changed into an asterisk, subjects were instructed to press the corresponding key as quickly and accurately as possible. The task included

sequence blocks consisting of three repeats of a ten-item sequence. The first and fifteenth blocks consisted of 30 visual cues presented in a random order.

Response Time (RT) was calculated as the time from cue onset to a correct button press. Anticipatory responses, i.e., those that occurred prior to the cue, were discarded. RTs outside of the mean value ± 2 SD for each block were also excluded.

A motor learning score was calculated for each subject as a percentage change from the RT in the first sequence block (Block 2) to blocks 10-14 (i.e., $[RT_{(10\text{-}14)} - RT_{(2)}) / RT_{(2)}] * 100$ %), when the learning plateaued (Stagg et al 2011a).

Five subjects who did not learn the task (motor learning score > 0) were excluded from further analysis.

7.2.5 Response time task

At the start of TMS recording, subjects performed a simple response time task consisting of 20 trials in the absence of TMS in order to characterise their individual RT. The same RT task was also performed in conjunction with TMS in order to measure corticospinal and intracortical excitability during movement preparation. Subjects were instructed to respond to a visual Go signal (coloured green circle) by performing an index finger abduction of the right hand as quickly as possible. Visual stimuli appeared at random intervals (5-7 sec) and the subjects were instructed to avoid anticipation of the Go signal and to relax their hand while the fixation cross was displayed on the screen. Stimuli were generated using the MATLAB Psychophysics Toolbox v.3.0 package (Brainard 1997).

EMG data acquired during RT task performed in the absence of TMS were analysed online using Signal software v.3.13 (Cambridge Electronic Design Ltd, Cambridge, UK). RT was defined as the time interval (in milliseconds) between the Go signal and the onset of EMG activity in the FDI muscle. The onset of EMG was identified in each trial as the first data point in which the signal exceeded 0.1 mV. The identified RT

was then used in the remainder of that experimental session to calculate the timing of the pre-movement TMS pulses.

7.2.6 TMS

7.2.6.1 TMS data acquisition

All TMS data were acquired using a monophasic BiStim machine, connected to a 70 mm figure-of-eight coil (Magstim Co., Whitland, Dyfield, UK). The left M1 was stimulated in all subjects. The optimal scalp position to elicit MEPs (referred to as the motor hotspot) in the right FDI muscle was determined before each session, with the TMS coil held at 45° to the mid-sagittal line with the handle pointing posteriorly. The hotspot was marked on a tight fitting cap to ensure reproducible coil positioning and TMS pulses were delivered through the M1 electrode. For the duration of the sessions the subjects were seated comfortably in an armchair with their eyes open.

Surface EMG was recorded via disposable neonatal electrocardiogram (ECG) electrodes (Henley's Medical Ltd, Welwyn Garden City, UK) from the FDI of the right hand, using a belly-tendon montage with a ground electrode over the ulnar styloid process. Signals were sampled at 5 kHz, amplified, filtered (10 Hz–1 kHz) and recorded using a CED 1902 amplifier, a CED micro1401 A/D converter and Signal software v.3.13 (Cambridge Electronic Design Ltd, Cambridge, UK).

7.2.6.2 Motor thresholds

The resting 1 mV motor threshold (MT_{1mV}) and active motor threshold (aMT) were determined at the beginning of TMS session. The MT_{1mV} was defined as the minimum stimulus intensity required for eliciting an MEP of ~1 mV peak-to-peak amplitude in at least 5 out of 10 consecutive trials in the relaxed FDI muscle. The

active motor threshold was defined as the minimum stimulus intensity necessary to evoke a 200 μV peak-to-peak MEP in at least 5 out of 10 consecutive trials while subjects maintained approximately 30 % of the maximum contraction of the FDI.

7.2.6.3 Paired-pulse TMS protocols

Two paired-pulse protocols were performed in the study: short interval intracortical inhibition (SICI) with an ISI of 2.5 ms to assess $GABA_A$ synaptic activity (Kujirai et al 1993; Di Lazzaro et al 2005), and intracortical facilitation (ICF) with an ISI of 12 ms as a measure of NMDA receptor activity (Ziemann et al 1996). The conditioning stimulus (CS) was set at 70 % of aMT and the test stimulus (TS) was set at MT_{1mV} for both protocols. An ISI of 2.5 ms was selected for SICI in order to avoid contamination with superimposed short interval (I-wave) facilitation (Peurala et al 2008).

7.2.6.4 Rest measures

Three measures were performed at rest in a pseudo-randomised order: a single MEP, SICI and ICF. 15 trials per condition were applied (Figure 7.1).

Motor studies primarily rely on change in MEP amplitude, evoked by TMS, as a measure reflecting biological change in corticospinal excitability. Since a resting-state single MEP measure taken in this study represents an absolute measure, elicited by a specific TMS stimulus intensity adjusted in order to induce a MEP amplitude of ~1 mV (as described in Section 7.2.6.2), it cannot be regarded as a reliable measurement of corticospinal excitability and was not considered for subsequent analysis.

7.2.6.5 Pre-movement measures

A single MEP and SICI were also measured during the pre-movement period in a simple RT paradigm. These TMS measures were performed in a pseudo-randomised order at two different timings during movement preparation: early time-point (25 % of mean individual RT) and late time-point (65 % of mean individual RT), resulting in four different pre-movement protocols: a single MEP_{early}, a single MEP_{late}, $SICI_{early}$ and $SICI_{late}$. 25 % and 65 % RT were adjusted to each subject's mean RT according to a previously described procedure (Murase et al 2004; Hummel et al 2009). 15 trials per condition and time-point were recorded (Figure 7.1).

7.2.6.6 MEP data analysis

Trials were excluded if the test pulse alone failed to elicit a reliable MEP (amplitude < 0.1 mV), there was pre-contraction in the target FDI muscle (EMG amplitude > 0.1 mV in the 80 ms preceding the pulse) or, for the pre-movement TMS measures, EMG onset coincided with TMS pulse, or no response was made. The peak-to-peak amplitude for each MEP was then calculated. Any MEPs which were outside 2 SD of the mean for each condition for each block were rejected. Next, a single iteration of Grubbs' test with a significance level of 0.05 was performed for each TMS condition separately and any significant outliers excluded.

SICI and ICF were expressed as a ratio of the mean conditioned MEP amplitude to the mean unconditioned MEP amplitude (a single MEP).

For the pre-movement data, the TMS measures were analysed separately for each pre-movement time-point (0.25 and 0.65 RT). SICI values were expressed as a ratio of the mean conditioned MEP amplitude to the mean unconditioned MEP amplitude at that specific time-point.

7.2.7 Statistical analysis

Statistical analyses were performed using MATLAB 8 software (version R2014b; The MathWorks, Inc., Natick, MA, USA), GraphPad Prism (version 7, GraphPad Software Inc., San Diego, CA, USA) and SPSS (version 22.0; IBM). Associations between oscillatory activities, motor excitability measures and performance in the motor learning task were determined using Pearson correlation test. The results were not corrected for multiple comparisons and therefore have to be interpreted with caution.

7.3 Results

7.3.1 Spontaneous (resting-state) and movement-related patterns of oscillatory activity

First, I wished to ensure that the expected patterns of motor β and γ oscillatory activities were observed. The topographical map of spontaneous β activity showed a clear activity in this frequency band distributed bilaterally over the M1 regions (Figure 7.2).

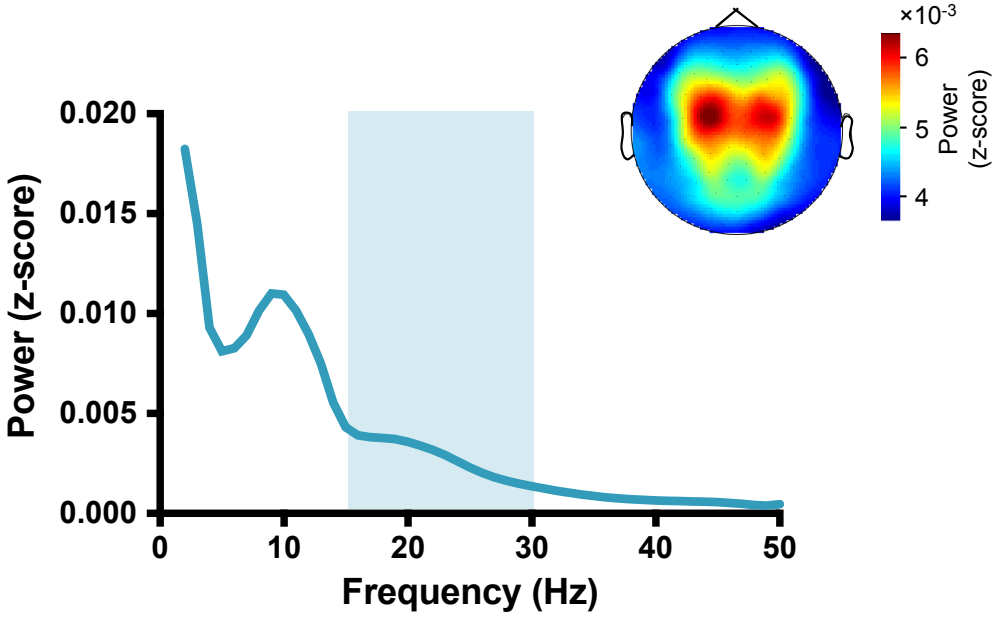


Figure 7.2 The grand average power spectrum of the left motor ROI and topographical map of spontaneous (resting-state) β activity

The grand average power spectrum of the left motor ROI with the frequency range of interest (β-band: 15–30 Hz) highlighted. Inset: Topographical map of β-band activity.

Similarly, a grand mean time-frequency (TFR) representation and topographical maps of task data revealed clear movement-related β desynchronisation (MRBD) and movement-related γ synchronization (MRGS), consistent with previous reports (Cheyne et al 2008; Gaetz et al 2011; Hall et al 2011; Kilavik et al 2013; Cheyne and Ferrari 2013) (Figure 7.3; individual TFR plots are illustrated in Figure A1, Appendix).

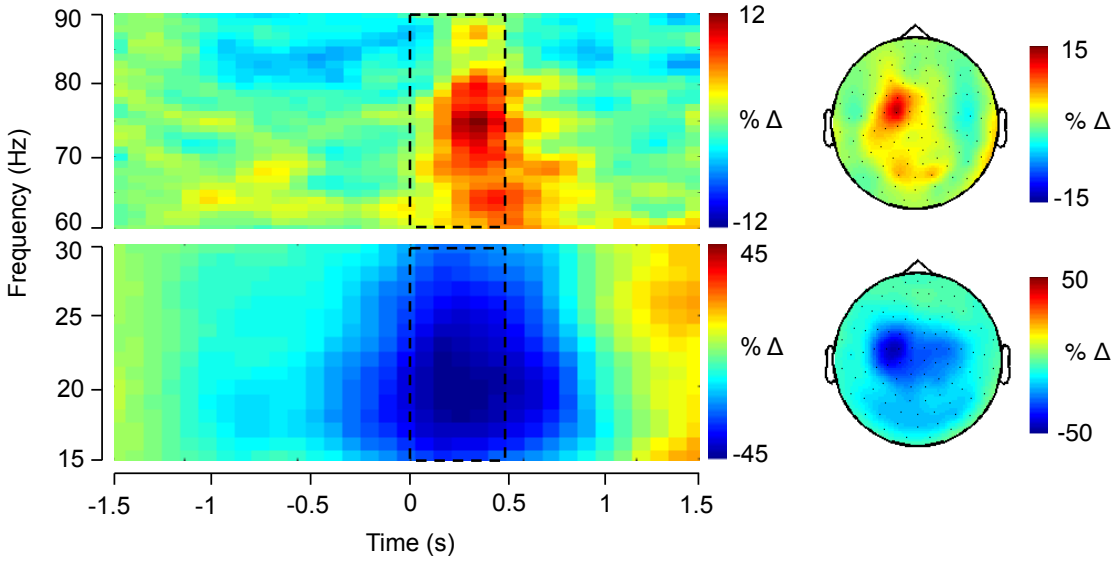


Figure 7.3 Grand mean time-frequency representation of task data and topographical maps of MRBD and MRGS

Grand mean time-frequency representation locked to the onset of EMG activity (at 0 s) for frequency bands of interest (15–30 and 60–90 Hz) in the left motor ROI. Topographies of MRBD (bottom right) and MRGS (top right) over the time-frequency window marked with dashed rectangles on the left. Power is expressed as a percentage change from baseline (-1.5 to -1 s) as follows: (power-baseline) / baseline * 100.

7.3.2 β power is inversely correlated with corticospinal excitability

To test the relationship between β power and corticospinal excitability, a correlational analysis was performed between (i) spontaneous β power and pre-movement corticospinal excitability, and (ii) MRBD and pre-movement corticospinal excitability. A negative relationship was found between spontaneous β power and pre-movement corticospinal excitability measures (single MEP_{early}: r = -0.557, p = 0.013; single MEP_{late}: r = -0.525, p = 0.037), such that greater β power was related to lower corticospinal excitability on a subject-by-subject basis (Figure 7.4 A, B). In addition, a correlation was found between MRBD and pre-movement corticospinal excitability (single MEP_{early}: r = 0.700, p = 0.003; single MEP_{late}: r = 0.721, p = 0.004) (Figure 7.4 C, D). However, that this association was not statistically significant when the most extreme case was removed (single MEP_{early}: r = 0.439, p = 0.102; single MEP_{late}: r =

0.386, p = 0.192), and thus requires further investigation. Further, the peak frequencies of spontaneous β oscillatory activity and MRBD were found to be unrelated to pre-movement corticospinal excitability measures (p > 0.05).

Next, the relationship between β activity and local synaptic $GABA_A$ activity, as quantified by SICI, was evaluated. No association was observed between spontaneous β activity (power and peak frequency) and SICI measures (resting-state and pre-movement) (p > 0.05). Similarly, MRBD (power and peak frequency) was not related to any of the SICI measures (p > 0.05).

Finally, the relationship between β activity (power and peak frequency) and local glutamatergic facilitation, as indexed using ICF performed at rest, was examined. A significant negative correlation was observed between β-frequency peak at rest and ICF (r = -0.500, p = 0.035) (Figure 7.4 E). No other measures of β oscillatory activity (spontaneous β power, MRBD power or frequency peak) were found to be related to ICF (p > 0.05).

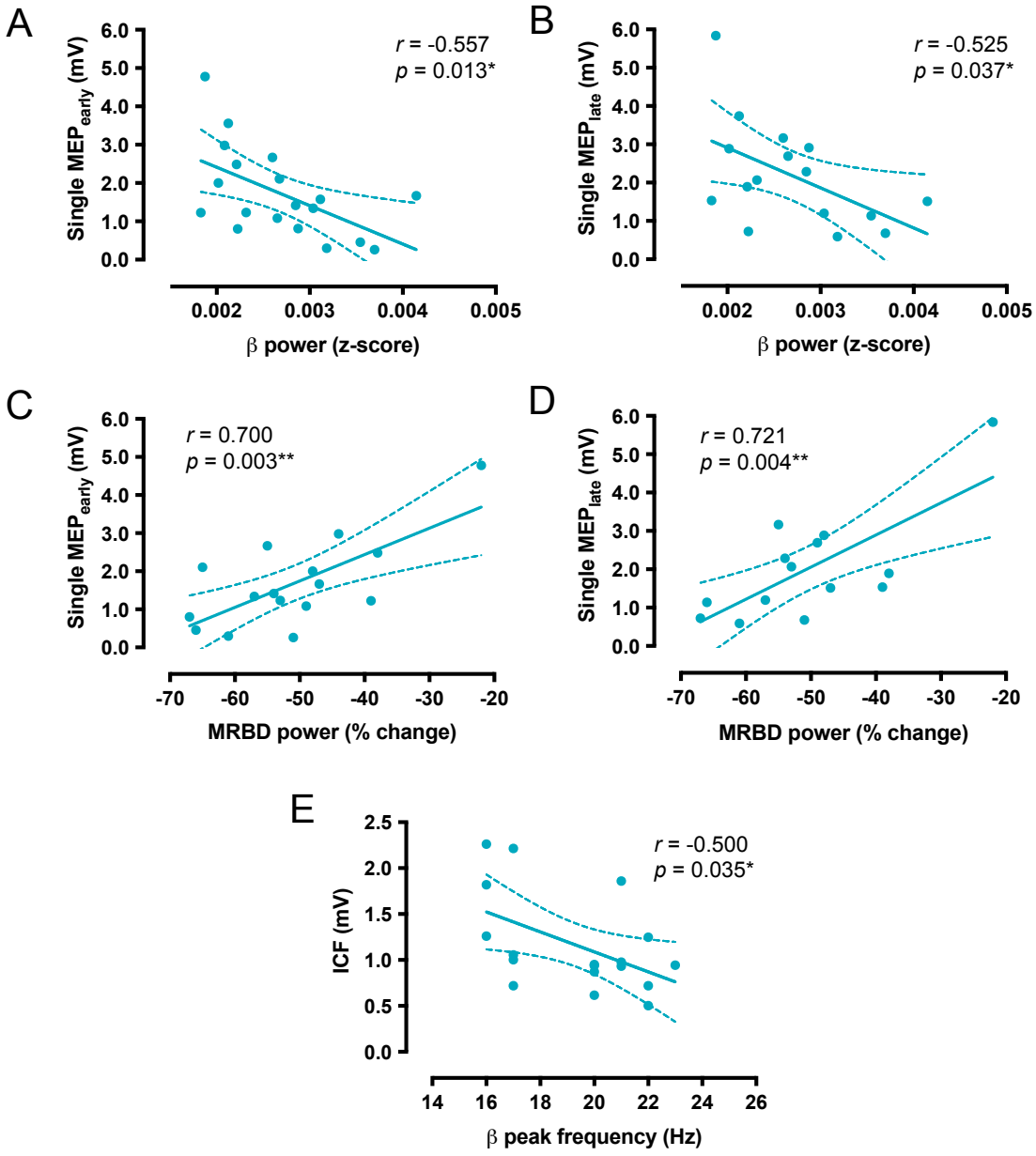


Figure 7.4 Correlations between β activity and motor excitability measures

Correlations between: (**A**) spontaneous β power and early pre-movement corticospinal excitability, (**B**) spontaneous β power and late pre-movement corticospinal excitability, (**C**) MRBD and early pre-movement corticospinal excitability, (**D**) MRBD and late pre-movement corticospinal excitability, (**E**) spontaneous β peak frequency and local glutamatergic facilitation. *$p < 0.05$, **$p < 0.05$

7.3.3 MRGS peak frequency is related to motor excitability

Next, I examined whether MRGS activity (power and peak frequency) was related to motor excitability measures. No association was found between MRGS power and any of the motor excitability measures ($p > 0.05$). However, there was a significant negative correlation between MRGS peak frequency and late pre-movement corticospinal excitability ($r = -0.571$, $p = 0.033$) (Figure 7.5 A). In addition, there was a trend towards a negative relationship between MRGS and local glutamatergic facilitation ($r = -0.400$, $p = 0.081$) (Figure 7.5 B).

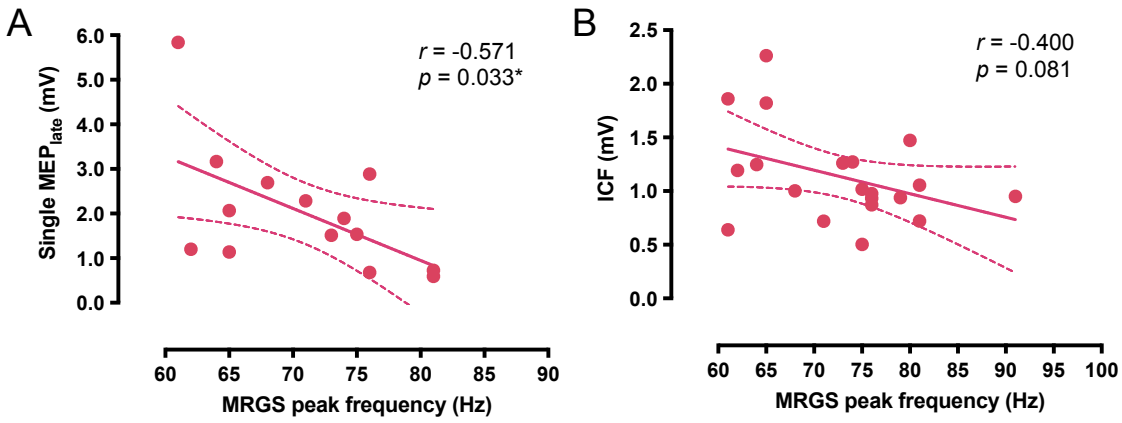


Figure 7.5 Correlations between MRGS peak frequency and motor excitability measures

Correlations between: (**A**) MRGS peak frequency and late pre-movement corticospinal excitability, and (**B**) MRGS peak frequency and ICF. *$p < 0.05$

No significant relationships were found between MRGS peak frequency and the measures of local $GABA_A$-mediated inhibition ($p > 0.05$).

7.3.4 MRGS peak frequency is related to performance in motor learning task

In Chapter 4, I demonstrated that γ tACS-induced changes in motor excitability are related to an individual's performance in a motor learning task. Here, I aimed to

follow up on these findings and examine directly whether there is an association between γ oscillatory activity, as measured using MEG, and performance in a motor learning task.

Firstly, it was important to determine that subjects were able to learn the task. As expected, RT decreased significantly across successive sequence blocks ($F_{(14,336)}$ = 9.015; p < 0.001). In contrast, there was no significant difference in mean RT between the two random blocks ($t_{(32)}$ = 0.885; p = 0.383), whereas there was a significant difference between block 14 (the final learning block) and block 15 (the second random block) ($t_{(28)}$ = -6.899; p < 0.001), suggesting that improvements in RT occurred via learning of a specific sequence and not generic skill learning. There was also no significant difference between the RT from blocks 10-14, which were on the plateau of the learning curve ($F_{(4,108)}$ =0.440; p = 0.780).

Next, a correlational analysis between MRGS (power and peak frequency) and an individual's performance in a motor learning task was performed. There was a positive relationship between MRGS peak frequency and a motor learning score, such that subjects who had a lower MRGS peak frequency were the ones who performed better in a motor learning task (r = 0.503, p = 0.024) (Figure 7.6).

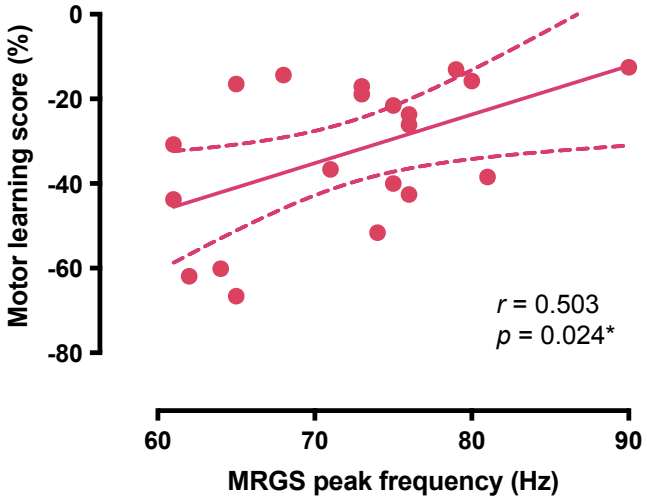


Figure 7.6 Correlation between MRGS peak frequency and motor learning score

Given that there was also a significant association between MRGS peak frequency and late pre-movement corticospinal excitability, as well as a trend towards a significant correlation with local glutamatergic facilitation, I examined whether any of these measures contribute to the significant relationship observed between MRGS peak frequency and performance in a motor learning task. To this end, partial correlations between MRGS peak frequency and motor learning score were performed while controlling for the motor excitability measures. There was still a significant association between MRGS peak frequency and motor learning score when late pre-movement corticospinal excitability (single MEP_{late}: r = 0.620, p = 0.042) or local glutamatergic facilitation were controlled for (ICF: r = 0.520, p = 0.032). Given the findings presented in Chapter 4 showing a significant relationship between γ tACS-induced changes in local $GABA_A$ activity and motor learning score, I also aimed to investigate whether a relationship between MRGS peak frequency and motor learning score persists after controlling for SICI measures (SICI at rest, $SICI_{early}$, $SICI_{late}$). The relationship was no longer significant when $SICI_{late}$ was used as a covariate in partial correlation between MRGS peak frequency and motor learning score (r = 0.377, p = 0.253).

Finally, to examine the frequency-specificity of the observed association between MRGS peak frequency and an individual's motor learning performance, I also tested whether this behavioural measure was related to spontaneous β activity (power and peak frequency) and MRBD (power and peak frequency). No association was found between any of the β oscillatory measures and how well the subjects performed in a motor learning task ($p > 0.05$).

7.4 Discussion

This study employed a sequential MEG-TMS design to investigate whether and how mean measures of motor cortical β and γ oscillations are related to motor excitability measures on an individual subject basis. As expected, there was an inverse relationship between β oscillatory power and corticospinal excitability. In addition, MRGS peak frequency was inversely related to late pre-movement corticospinal excitability. Further, my results provide evidence on the relationship between motor cortical MRGS peak frequency and an individual's performance in a motor learning task. Further analysis suggests that, consistent with findings presented in Chapter 4, local $GABA_A$-mediated inhibition may play an important role in this association.

7.4.1 β power and corticospinal excitability are inversely related

A negative correlation between spontaneous β power and movement-related corticospinal excitability was found. This finding is in agreement with the previous TMS-EEG studies. For example, it has been shown that the amplitude of spontaneous β oscillations measured over the left M1 is, on average, smaller before stimuli producing large MEPs than before stimuli producing small MEPs (Mäki and Ilmoniemi 2010). However, no consistent relationship has been revealed between these measures when they were correlated on a single-trial basis, most likely due to a large variability of oscillatory and MEP amplitudes over time (Zarkowski et al 2006; Mitchell et al 2007; Lepage et al 2008; Mäki and Ilmoniemi 2010; Berger et al 2014). This speaks in favour of the sequential approach used in the present study, in which mean measures of oscillatory activities and motor excitability were correlated.

Further, no relationship has been found between β oscillatory activity and local synaptic $GABA_A$-mediated inhibition, as measured by SICI. At first glance, this might

seem surprising given the importance of $GABA_A$ activity in motor cortical oscillations (Jensen et al 2005; Hall et al 2011). One reason for this may be that SICI reflects only a specific aspect of this type of inhibition rather than providing a complete measure of it. For example, it has been shown previously that SICI is not mediated by the α1-subunit-bearing subtype of the $GABA_AR$ but by those bearing either the α2- or α3-subunit (Di Lazzaro et al 2006).

7.4.2 MRGS peak frequency is inversely related to pre-movement corticospinal excitability

The results in this Chapter show that MRGS peak frequency is negatively related to the movement-related corticospinal excitability, specifically to the measure performed close to the movement onset. There is a large body of evidence showing that MRGS occurs shortly prior to and during movement execution (Crone et al 1998; Pfurtscheller and Lopes da Silva 1999; Pfurtscheller et al 2003; Cheyne et al 2008; Muthukumaraswamy 2010; Cheyne 2013; Gaetz et al 2013). A separate line of evidence has demonstrated that the excitability of corticospinal neurons is increased prior to and during movement (Chen and Hallett 1999; Reynolds and Ashby 1999; Zaaroor et al 2003). Based on these findings, a positive relationship between MRGS power and movement-related corticospinal excitability would be expected. In contrast, since lower frequency is associated with higher power, an inverse relationship between MRGS peak frequency and motor excitability might be expected. Here, MRGS peak frequency, but not power, showed a significant inverse correlation with movement-related motor excitability. It is worth noting that MRGS was not consistently observed in our participants (potentially due to the low trial number), which may explain the absence of relationship between the power in this frequency band and other measures of motor excitability or motor learning (see below).

7.4.3 MRGS peak frequency is related to performance in a motor learning task

The final question I sought to address was whether MRGS was directly related to an individual's performance in a motor learning task. In Chapter 4, I demonstrated a strong association between γ tACS-induced change in $GABA_A$ inhibition and motor learning score. Here, I found that the subjects who have a lower MRGS peak frequency also show faster short-term learning. Importantly, this significant relationship was absent when the individual level of movement-related $GABA_A$-mediated inhibition was controlled for.

These findings are particularly interesting in light of recent animal studies demonstrating the role of γ-frequency oscillations in learning outside the motor network (Tort et al 2009; Kendrick et al 2011). In the near future, it will be important to test whether there is a causal relationship between motor γ activity and motor learning in humans.

7.5 Conclusions

To summarise, the results demonstrate that, as expected, the average β oscillatory power is inversely related to movement-related corticospinal excitability. In addition, the presented findings provide first time evidence on the relationship between motor cortical γ peak frequency and an individual's performance in a motor learning task. In agreement with the findings presented in Chapter 4, local $GABA_A$-mediated inhibition may play an important role in this association.

CHAPTER

8

Conclusions, limitations, and future directions

This Chapter summarises the main findings presented in this thesis and draws the relevant conclusions. Moreover, limitations and suggestions for future work are briefly discussed, followed by the general conclusions.

8.1 Thesis overview

The primary aim of this thesis was to investigate the mechanisms underlying human motor cortical oscillations - the line of research motivated by a strong and growing interest in the role of brain oscillations in healthy and clinical populations. To this end, I employed a novel multimodal approach involving a combined tACS-TMS and tACS-7T MRS to examine the neurophysiological and neurochemical basis of driving β- and γ-frequency oscillations *in vivo* in the primary motor cortex (M1). Moreover, a sequential MEG-TMS study was performed with the primary objective of exploring the relationship between motor cortical oscillations and M1 excitability measures. Lastly, the behavioural relevance of the reported findings was assessed, where possible.

The primary objective of Chapter 4 was to examine the physiological basis of driving β and γ oscillatory activity using tACS. I demonstrated that driving γ-frequency oscillations led to a significant, duration-dependent decrease in local resting-state $GABA_A$ inhibition in M1, as quantified by an inhibitory TMS protocol ($SICI_{2.5ms}$). The magnitude of this effect was positively correlated with the magnitude of $GABA_A$ decrease during movement preparation, when γ activity in motor circuitry is known to increase. In addition, γ tACS-induced change in $GABA_A$ inhibition was closely related to performance in a motor learning task, suggesting that local inhibitory circuits involved in γ oscillations in M1 may also be involved in motor learning. Overall, the findings presented in this Chapter contribute to our understanding of the neurophysiological basis of motor rhythms and suggest that tACS may have similar physiological effects to endogenously driven local oscillatory activity.

Given the absence of β tACS-induced physiological effects in Chapter 4, the main focus of the subsequent Chapter 5 was to further examine the physiological

mechanisms underlying the exogenously driven β activity. To this end, a different electrode montage (left M1–Pz rather than left M1–contralateral forehead montage) and stimulation intensity (1 mA) were used, and the phase of stimulation was controlled for. The results showed that β tACS led to stimulation phase-dependent modulation of corticospinal excitability during movement preparation, i.e., the period when movement-related β desynchronisation occurs. While these changes may result from entrainment within corticospinal neurons, the imposition of alternating up and down states by β tACS cannot be excluded, particularly given that no conclusive evidence for the dependence of these effects on match between stimulation frequency and individual β frequency (IBF), as assessed using EEG, was observed. Moreover, β tACS reduced $SICI_{1ms}$ (a TMS measure suggested to reflect extrasynaptic $GABA_A$ tonic inhibition) during movement preparation. Further analyses suggested that this change is likely to reflect tACS-induced plasticity effects, rather than an entrainment-driven reduction in MRBD. Finally, β tACS slowed down response time, supporting the antikinetic role of β activity in motor control. This behavioural effect, however, was not related to any reported stimulation-induced changes in physiological measures.

Chapter 6 aimed at directly evaluating the effects of driving β oscillatory activity by measuring local changes in the cortical concentrations of GABA and glutamate *in vivo* in M1 using ultra-high field (7T) Magnetic Resonance Spectroscopy (MRS). In addition, the dependence of stimulation-induced changes on match between stimulation frequency and IBF was examined. The findings demonstrated that β tACS did not affect glutamate levels within M1 but led to a reduction in MRS-assessed M1 GABA concentration (suggested to largely represent pools of GABA that are linked to tonic rather than phasic inhibition) during stimulation, the findings which may constitute evidence of the role of extrasynaptic $GABA_A$-mediated activity in human motor cortical β oscillations. Interestingly, β tACS-driven modulation of M1 GABA activity was dependent on the match between the frequency of stimulation and IBF, such that

participants who were stimulated at β-frequency that either matched or was slower than their IBF tended to show a reduction in M1 GABA, whereas participants who were stimulated at the frequency faster than their IBF showed the opposite effect. These results may be a reflection of a complex relationship between local tonic inhibitory activity and β oscillations.

In Chapter 7, a sequential MEG-TMS design was employed to investigate whether the spontaneous and movement-related cortical β and γ oscillations are related to various parameters of motor excitability. Moreover, in light of the findings reported in Chapter 4 showing that motor cortical γ-band activity may be both relevant and important for motor learning, I also examined whether motor cortical γ-band activity could be directly related to an individual's performance in a motor learning task. The results demonstrated that β oscillatory power was inversely related to movement-related corticospinal excitability. Moreover, the relationship between motor cortical movement-related gamma synchronisation (MRGS) peak frequency and an individual's performance in a motor learning task was found, such that subjects who had a lower MRGS peak frequency were the ones who performed better in a motor learning task. Further analysis suggested that, in agreement with the findings presented in Chapter 4, local synaptic $GABA_A$-mediated inhibition plays an important role in this association. Understanding how motor cortical β- and γ-frequency spectral "fingerprints" are related to local physiological measures and motor behaviour will help further unravel the underlying mechanisms and functional significance of these oscillatory activities in humans.

8.2 Limitations and future directions

8.2.1 tACS as a tool to study brain oscillations

The majority of the work presented in this thesis relied on tACS as a tool to drive endogenous cortical oscillations. This was based on the growing evidence supporting the hypothesis that tACS can influence neuronal networks, including entraining them in a frequency-specific manner (Deans et al 2007; Zaehle et al 2010; Fröhlich and McCormick 2010; Ozen et al 2010; Reato et al 2010; Neuling et al 2013; Herrmann et al 2013; Reato et al 2013; Merlet et al 2013; Ali et al 2013; Helfrich et al 2014b; Guerra et al 2016; Ni et al 2017). Several findings reported here suggest that tACS has similar physiological effects to endogenously driven local oscillatory activity, thus supporting the efficacy of this interventional approach as a tool to study cortical oscillations. For example, in Chapter 4, a positive association has been found between the magnitude of γ tACS-induced change in resting $GABA_A$ inhibition and the magnitude of M1 $GABA_A$ activity during late pre-movement period, i.e., when endogenous γ activity is increasing. This result supports the hypothesis that γ tACS engages local inhibitory interneuronal circuits involved in the generation of γ-frequency oscillations. Furthermore, there was a strong relationship between γ tACS-induced change in $GABA_A$ activity and learning ability on a subject-by-subject basis. Importantly, Chapter 7 has provided evidence on the relationship between MRGS peak frequency and an individual's performance in a motor learning task as well as the importance of movement-related $GABA_A$ inhibition in this association. These observations, based on MEG-measured endogenous γ activity, are at least partially consistent with the effects of artificially driven γ activity reported in Chapter 4. In addition, exogenously driving β oscillations led to stimulation phase-dependent modulation of movement-related corticospinal excitability (measured during the period when movement-related β desynchronisation [MRBD] occurs), as reported in Chapter 5. Similarly, the results

reported in Chapter 7 have shown that MEG-measured endogenous β oscillatory power is related to movement-related corticospinal excitability.

On the other hand, at least some of the reported tACS-induced physiological changes are likely to be a reflection of neural plasticity rather than entrainment of endogenous rhythms. For example, one of the main hypotheses put forward in Chapter 4 was γ tACS-induced reduction in local synaptic $GABA_A$ activity. As expected, γ tACS decreased $GABA_A$-mediated inhibition as measured at 5 min during stimulation. However, an opposite effect was observed at a later time-point during stimulation period (15 min after stimulation onset), potentially suggesting homeostatic-like changes set in motion by prolonged application of transcranial oscillatory currents. Similarly, β tACS-induced reduction in $SICI_{1ms}$ (a measure suggested to reflect extrasynaptic $GABA_A$ tonic inhibition) during movement preparation, reported in Chapter 5, was likely to reflect online tACS-induced plasticity effects rather than constitute evidence on the role of this measure in MRBD. These pieces of evidence pose a significant challenge to the interpretation of results since it is unclear to what extent one measures the effects arising purely as a result of entrainment and/or neural plasticity. Nevertheless, it is reasonable to assume that during prolonged stimulation periods, the early changes are more likely to be driven purely by entrainment and therefore represent more appropriate set of measures to be considered when the primary objective is to study the mechanisms underlying oscillatory activities. One solution would be to employ an intermittent tACS paradigm, similar to the ones recently employed in other tACS studies (Vossen et al 2015; Weinrich et al 2017), with longer windows of stimulation-free periods to reduce the chance of inducing plastic changes.

Finally, to provide unequivocal evidence on tACS-induced entrainment of endogenous cortical oscillations, it would have been necessary to supplement the studies described in this thesis with concurrent tACS-M/EEG investigations utilising the same stimulation

parameters. However, this line of research remains a non-trivial challenge due to uncertainties surrounding stimulation artefact removal methods (Soekadar et al 2013; Witkowski et al 2015; Noury et al 2016; Neuling et al 2016).

8.2.2 Individual variability of responses to tACS

The findings presented in Chapters 4, 5 and 6 show large individual differences in neurochemical and neurophysiological responses to tACS, as examined using TMS and 7T MRS, respectively. The high variability in responses to tACS and other non-invasive brain stimulation approaches is the rule rather than the exception in the field, thus raising concerns regarding the efficacy and reliability of these techniques (López-Alonso et al 2014; Ammann et al 2017). It has been demonstrated that differences in individual responses are driven by a large number of factors, including an individual's brain state (Kanai et al 2008; Feurra et al 2013), structural and functional anatomy (Datta et al 2012; Bikson et al 2012), underlying neurochemistry (Muthukumaraswamy et al 2009; O'Shea et al 2014) and a range of other factors, such as hormonal levels and circadian rhythm (Krause and Cohen Kadosh 2014). Therefore, it is unsurprising that tACS and other non-invasive brain stimulation methods can elicit different effects across, and even within, individuals, which currently limits attempts to explore their therapeutic potential. In light of these considerations, computational modelling studies aimed at guiding and optimising tACS and other non-invasive brain stimulation tools represent an important step forward towards more individualised stimulation approaches. In the past two decades, current-flow modelling tools have progressed from spherical models (Miranda et al 2006; Datta et al 2008; Dmochowski et al 2012) to accurate and detailed MRI-derived individual head models (Wagner et al 2007; Datta et al 2010; Minhas et al 2012). However, this vital aspect of research has long suffered from the lack of validation by experimental data from human subjects. Only this year, computational models of TCS have been for the first time thoroughly validated with *in*

vivo intracranial recordings in humans (Huang et al 2017). The study reported that 2-mA transcranial electric stimulation produces the intensities of electric field half as strong as previous predictions using computational models, i.e., 0.4 V/m. Moreover, individualised models were shown to provide a very accurate prediction of the spatial distribution of currents. Taking into account these findings, there is a possibility that current intensities higher than the ones used in the experiments presented in this thesis could have elicited stronger and less variable effects. Indeed, a recent study showed that tDCS at 2 mA, but not 1 mA, significantly increased corticospinal excitability at the group level, overall resulting in consistent intra- and inter-individual increases of M1 excitability (Ammann et al 2017). In addition, a recently reported and validated approach involving the stimulation of neurons by interference between multiple alternating electric fields will allow for the use of higher intensities (Grossman et al 2017).

8.2.3 Clinical applications of tACS

The findings presented in this thesis provide novel insights into the mechanisms underpinning motor cortical β- and γ-frequency oscillations. From a clinical perspective, these may be of importance for a number of reasons. Motor cortical β oscillations have been recently shown to reflect meaningful and reliable individual differences in the motor system (Espenhahn et al 2017) and their potential role as a neurophysiological marker of motor system function has been suggested in various clinical populations, including Parkinson's disease (Pollok et al 2012; Heinrichs-Graham et al 2014), stroke (Rossiter et al 2014a; Thibaut et al 2017) and ALS (Proudfoot et al 2017). In addition, β-frequency (20 Hz) tACS has been found to improve brain self-regulation-based neurofeedback in chronic stroke patients by reducing the intrinsic variance of sensorimotor β oscillations.

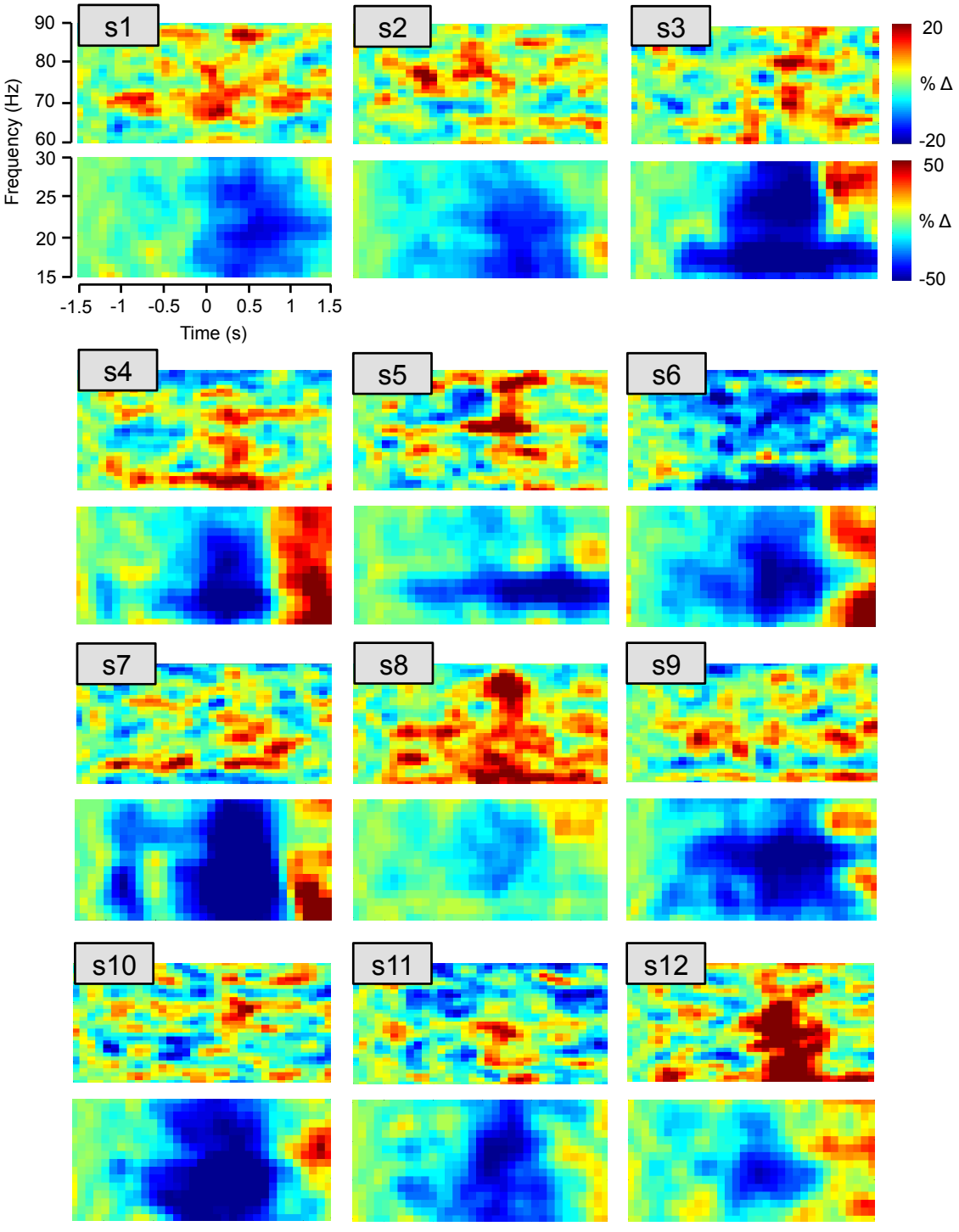
The findings presented in Chapter 4 have demonstrated that driving motor cortical γ rhythm modulates synaptic $GABA_A$ activity in the human M1, which in turn was strongly related to an individual's ability to learn a motor task (Nowak et al 2017). This is particularly interesting in light of the previous studies performed outside the motor system, suggesting that γ oscillations are a prime candidate for modulating synaptic plasticity (Bi and Poo 1998; Wespatat et al 2004) and can predict subsequent learning across a range of tasks (Sederberg et al 2003; Sederberg et al 2006; Headley and Weinberger 2011). Given that synaptic plasticity plays a vital role in motor learning and functional recovery after a brain injury, such as stroke (Wespatat et al 2004; Axmacher et al 2006; Dayan and Cohen 2011; Takeuchi and Izumi 2013), it is not unreasonable to suggest that driving motor cortical γ activity might be of potential benefit in promoting recovery after stroke.

8.3 General conclusions

Understanding the mechanisms and functional significance of human brain rhythms has been in the forefront of neuroscience research during the past few decades. The work in this thesis employed a novel multimodal approach involving a combined tACS-TMS and tACS-7T MRS, as well as a sequential MEG-TMS design, with the primary objective of studying the mechanisms underlying human cortical oscillations. The presented findings contribute to the understanding of the neurophysiological basis (in particular the underlying $GABA_A$-mediated inhibitory activity) of exogenously driven motor cortical β and γ rhythms. The results additionally provide the initial first-time evidence supporting the role of motor cortical γ oscillations in motor learning, opening an interesting avenue for further research in the motor domain. Finally, the work presented in this thesis raises a number of important considerations regarding the use of tACS as a tool to study oscillations and its inherent limitations. Further, it is hoped

that this work will help guide future experiments and encourage further efforts towards the development of more individualised and effective tACS-based approaches for the purpose of understanding the mechanisms underlying human brain oscillations and their functional significance.

Appendix



Continued on next page →

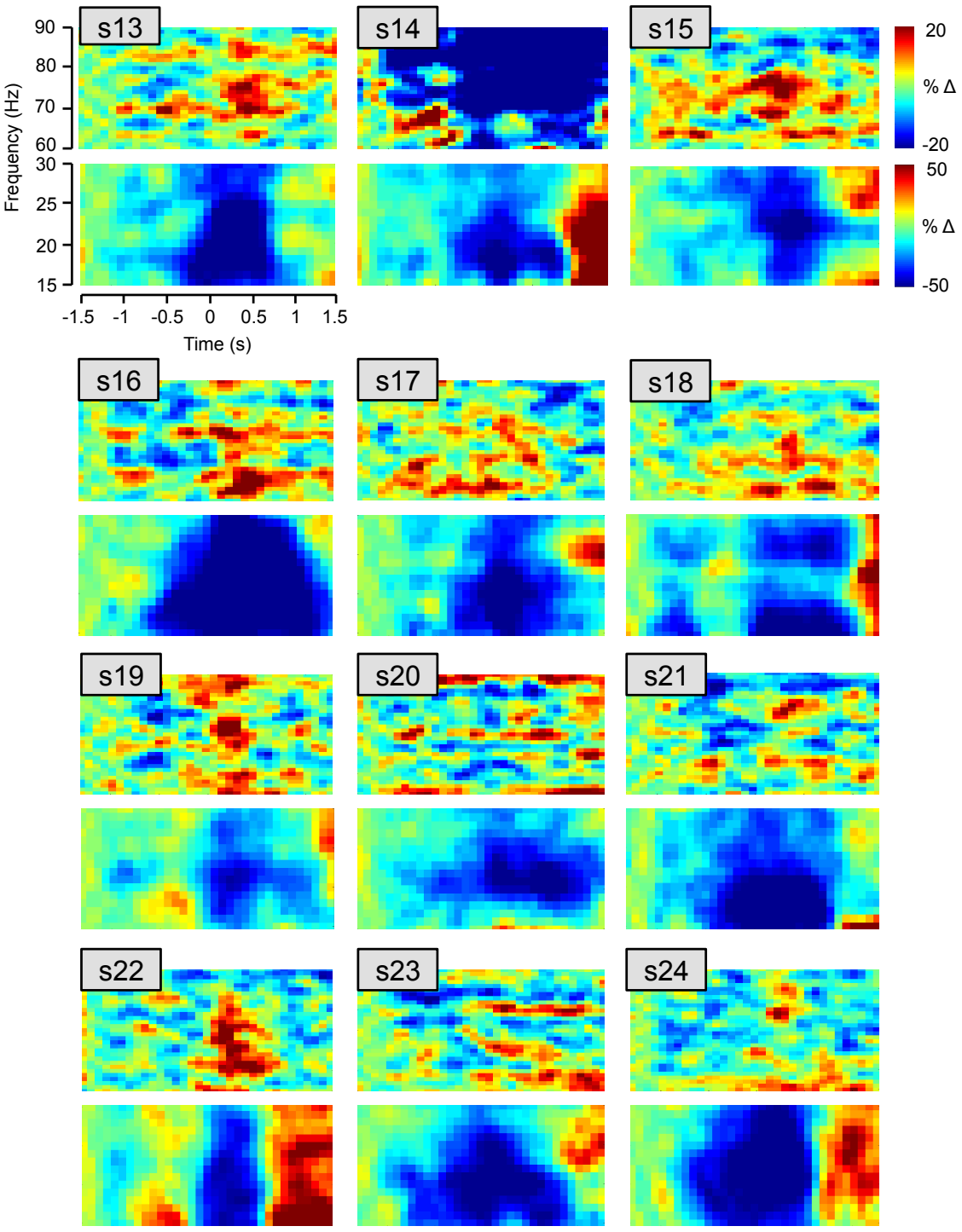


Figure A1. Individual TFR plots of task data

Mean time-frequency representation locked to the onset of EMG activity (at 0 s) for frequency bands of interest (15–30 and 60–90 Hz) in the left motor ROI for each individual subject. Power is expressed as a percentage change from baseline (-1.5 to -1 s) as follows: (power-baseline) / baseline * 100.

Bibliography

Abbott, L. F., & Nelson, S. B. (2000). Synaptic plasticity: taming the beast. *Nature Neuroscience*, *3 Suppl*, 1178–83.

Abdallah, C. G., Jackowski, A., Sato, J. R., Mao, X., Kang, G., Cheema, R., … Shungu, D. C. (2015). Prefrontal cortical GABA abnormalities are associated with reduced hippocampal volume in major depressive disorder. *European Neuropsychopharmacology*, *25*(8), 1082–1090.

Adjamian, P., Hadjipapas, A., Barnes, G. R., Hillebrand, A., Holliday, I. E., S., F. R., & J., R. H. (2008). Induced Gamma activity in primary visual cortex is related to luminance and not color contrast: An MEG study. *Journal of Vision*, *8*(7), 4.

Alegre, M., Alonso-Frech, F., Rodríguez-Oroz, M. C., Guridi, J., Zamarbide, I., Valencia, M., … Artieda, J. (2005). Movement-related changes in oscillatory activity in the human subthalamic nucleus: ipsilateral vs. contralateral movements. *The European Journal of Neuroscience*, *22*(9), 2315–2324.

Alegre, M., Gurtubay, I. G., Labarga, A., Iriarte, J., Malanda, A., & Artieda, J. (2003). Alpha and beta oscillatory changes during stimulus-induced movement paradigms: effect of stimulus predictability. *Neuroreport*, *14*(3), 381–5.

Alekseichuk, I., Diers, K., Paulus, W., & Antal, A. (2015). Transcranial electrical stimulation of the occipital cortex during visual perception modifies the magnitude of BOLD activity: A combined tES-fMRI approach. *NeuroImage*, *140*, 110-7.

Ali, M. M., Sellers, K. K., & Fröhlich, F. (2013). Transcranial alternating current stimulation modulates large-scale cortical network activity by network resonance. *The Journal of Neuroscience, 33*(27), 11262–75.

Amadi, U., Allman, C., Johansen-Berg, H., & Stagg, C. J. (2015). The Homeostatic Interaction Between Anodal Transcranial Direct Current Stimulation and Motor Learning in Humans is Related to GABAA Activity. *Brain Stimulation*, *8*(5), 898–905.

Ammann, C., Lindquist, M. A., & Celnik, P. A. (2017). Response variability of different anodal transcranial direct current stimulation intensities across multiple sessions. *Brain Stimulation*, *10*(4), 757–763.

Anand, S., & Hotson, J. (2002). Transcranial magnetic stimulation: Neurophysiological applications and safety. *Brain and Cognition*, *50*(3), 366–386.

Androulidakis, A. G., Doyle, L. M. F., Yarrow, K., Litvak, V., Gilbertson, T. P., & Brown, P. (2007). Anticipatory changes in beta synchrony in the human corticospinal system and associated improvements in task performance. *The European Journal of Neuroscience*, *25*(12), 3758–3765.

Angelakis, E., Liouta, E., Andreadis, N., Leonardos, A., Ktonas, P., Stavrinou, L. C., … Sakas, D. E. (2013). Transcranial alternating current stimulation reduces symptoms in intractable idiopathic cervical dystonia: A case study. *Neuroscience Letters*, 533(1), 39–43.

Antal, A., Boros, K., Poreisz, C., Chaieb, L., Terney, D., & Paulus, W. (2008). Comparatively weak after-effects of transcranial alternating current stimulation (tACS) on cortical excitability in humans. *Brain Stimulation*, *1*(2), 97–105.

Antonenko, D., Faxel, M., Grittner, U., Lavidor, M., & Flöel, A. (2016). Effects of Transcranial Alternating Current Stimulation on Cognitive Functions in Healthy Young and Older Adults. *Neural Plasticity*, *2016*, 1–13.

Aono, K., Miyashita, S., Fujiwara, Y., Kodama, M., Hanayama, K., Masakado, Y., &

Ushiba, J. (2013). Relationship between event-related desynchronization and cortical excitability in healthy subjects and stroke patients. *The Tokai Journal of Experimental and Clinical Medicine*, *38*(4), 123–8.

Atallah, B. V, & Scanziani, M. (2009). Instantaneous modulation of gamma oscillation frequency by balancing excitation with inhibition. *Neuron*, *62*(4), 566–77.

Aumann, T. ., & Fetz, E. . (2004). Oscillatory activity in forelimb muscles of behaving monkeys evoked by microstimulation in the cerebellar nuclei. *Neuroscience Letters*, *361*(1–3), 106–110.

Axmacher, N., Mormann, F., Fernández, G., Elger, C. E., & Fell, J. (2006). Memory formation by neuronal synchronization. *Brain Research Reviews*, *52*(1), 170–182.

Babiloni, C., Lizio, R., Marzano, N., Capotosto, P., Soricelli, A., Triggiani, A. I., … Del Percio, C. (2016). Brain neural synchronization and functional coupling in Alzheimer's disease as revealed by resting state EEG rhythms. *International Journal of Psychophysiology*, *103*, 88–102.

Bachelard, H. M. and H. S. (1985). *Biochemistry and the central nervous system*. London, England: Churchill Livingstone.

Bächinger, M., Zerbi, V., Moisa, M., Polania, R., Liu, Q., Mantini, D., … Wenderoth, N. (2017). Concurrent tACS-fMRI reveals causal influence of power synchronized neural activity on resting state fMRI connectivity. *The Journal of Neuroscience*, *37*(18), 4766-4777.

Baillet, S. (2017). Magnetoencephalography for brain electrophysiology and imaging. *Nature Neuroscience*, *20*(3), 327–339.

Baker, S. N., Olivier, E., & Lemon, R. N. (1997). Coherent oscillations in monkey motor cortex and hand muscle EMG show task-dependent modulation. *The Journal of Physiology*, *501*(Pt 1), 225–41.

Barker, A. T., Freeston, I. L., Jalinous, R., & Jarratt, J. A. (1987). Magnetic stimulation of the human brain and peripheral nervous system: an introduction and the results of an initial clinical evaluation. *Neurosurgery*, *20*(1), 100–109

Barker, A. T., Jalinous, R., & Freeston, I. L. (1985). Non-invasive magnetic stimulation of human motor cortex. *Lancet*, *1*(8437), 1106–7

Bartos, M., Vida, I., & Jonas, P. (2007). Synaptic mechanisms of synchronized gamma oscillations in inhibitory interneuron networks. *Nature Reviews. Neuroscience*, *8*(1), 45–56.

Batsikadze, G., Moliadze, V., Paulus, W., Kuo, M.-F., & Nitsche, M. A. (2013). Partially non-linear stimulation intensity-dependent effects of direct current stimulation on motor cortex excitability in humans. *The Journal of Physiology*, *591*(Pt 7), 1987–2000.

Battleday, R. M., Muller, T., Clayton, M. S., & Cohen Kadosh, R. (2014). Mapping the mechanisms of transcranial alternating current stimulation: a pathway from network effects to cognition. *Frontiers in Psychiatry*, *5*, 162.

Baumgarten, T. J., Oeltzschner, G., Hoogenboom, N., Wittsack, H.-J., Schnitzler, A., & Lange, J. (2016). Beta Peak Frequencies at Rest Correlate with Endogenous GABA+/Cr Concentrations in Sensorimotor Cortex Areas. *PLOS ONE*, *11*(6), e0156829.

Beck, S., Schubert, M., Richardson, S. P., & Hallett, M. (2009). Surround inhibition depends on the force exerted and is abnormal in focal hand dystonia. *Journal of Applied Physiology (Bethesda, Md. : 1985)*, *107*(5), 1513–8.

Berger, B., Minarik, T., Liuzzi, G., Hummel, F. C., & Sauseng, P. (2014). EEG

oscillatory phase-dependent markers of corticospinal excitability in the resting brain. *BioMed Research International*, *2014*, 936096.
Berke, J. D. (2009). Fast oscillations in cortical-striatal networks switch frequency following rewarding events and stimulant drugs. *The European Journal of Neuroscience*, *30*(5), 848–859.
Bi, G. Q., & Poo, M. M. (1998). Synaptic modifications in cultured hippocampal neurons: dependence on spike timing, synaptic strength, and postsynaptic cell type. *The Journal of Neuroscience*, *18*(24), 10464–72.
Bienenstock, E. L., Cooper, L. N., & Munro, P. W. (1982). Theory for the development of neuron selectivity: orientation specificity and binocular interaction in visual cortex. *The Journal of Neuroscience*, *2*(1), 32–48.
Bikson, M., Rahman, A., & Datta, A. (2012). Computational Models of Transcranial Direct Current Stimulation. *Clinical EEG and Neuroscience*, *43*(3), 176–183.
Bloch, F. (1946). Nuclear Induction. *Physical Review*, *70*(7–8), 460–474.
Bollimunta, A., Chen, Y., Schroeder, C. E., & Ding, M. (2008). Neuronal mechanisms of cortical alpha oscillations in awake-behaving macaques. *The Journal of Neuroscience*, *28*(40), 9976–88.
Börgers, C., & Kopell, N. (2003). Synchronization in Networks of Excitatory and Inhibitory Neurons with Sparse, Random Connectivity. *Neural Computation*, *15*(3), 509–538.
Boroojerdi, B., Prager, A., Muellbacher, W., & Cohen, L. G. (2000). Reduction of human visual cortex excitability using 1-Hz transcranial magnetic stimulation. *Neurology*, *54*(7), 1529–1531.
Bottomley, P. A., Edelstein, W. A., Foster, T. H., & Adams, W. A. (1985). In vivo solvent-suppressed localized hydrogen nuclear magnetic resonance spectroscopy: a window to metabolism? *Proceedings of the National Academy of Sciences of the United States of America*, *82*(7), 2148–52
Brainard, D. H. (1997). The Psychophysics Toolbox. *Spatial Vision*, *10*(4), 433–6
Braun, V., Sokoliuk, R., & Hanslmayr, S. (2017). On the effectiveness of event-related beta tACS on episodic memory formation and motor cortex excitability. *Brain Stimulation*, *10*(5), 910-918.
Brinkman, L., Stolk, A., Marshall, T. R., Esterer, S., Sharp, P., Dijkerman, H. C., … Toni, I. (2016). Independent Causal Contributions of Alpha- and Beta-Band Oscillations during Movement Selection. *The Journal of Neuroscience*, *36*(33), 8726–8733.
Brittain, J.-S., & Brown, P. (2014). Oscillations and the basal ganglia: Motor control and beyond. *NeuroImage*, *85*, 637–647.
Brittain, J.-S., Probert-Smith, P., Aziz, T. Z., & Brown, P. (2013). Tremor suppression by rhythmic transcranial current stimulation. *Current Biology : CB*, *23*(5), 436–40.
Brittain, J.-S., Sharott, A., & Brown, P. (2014). The highs and lows of beta activity in cortico-basal ganglia loops. *The European Journal of Neuroscience*, *39*(11), 1951–9.
Brodmann, K. (1909). *Broadmann's Localisation in the Cerebral Cortex*. New York: Springer.
Brown, P. (2003). Oscillatory nature of human basal ganglia activity: relationship to the pathophysiology of Parkinson's disease. *Movement Disorders*, *18*(4), 357–63.
Brown, P. (2007). Abnormal oscillatory synchronisation in the motor system leads to impaired movement. *Current Opinion in Neurobiology*, *17*(6), 656–64.

Brown, P., Oliviero, A., Mazzone, P., Insola, A., Tonali, P., & Di Lazzaro, V. (2001). Dopamine Dependency of Oscillations between Subthalamic Nucleus and Pallidum in Parkinson's Disease. *The Journal of Neuroscience*, *21*(3), 1033–1038

Brucke, C., Huebl, J., Schonecker, T., Neumann, W.-J., Yarrow, K., Kupsch, A., … Kuhn, A. A. (2012). Scaling of Movement Is Related to Pallidal Oscillations in Patients with Dystonia. *The Journal of Neuroscience*, *32*(3), 1008–1019.

Burke, D., Bartley, K., Woodforth, I. J., Yakoubi, A., & Stephen, J. P. (2000). The effects of a volatile anaesthetic on the excitability of human corticospinal axons. *Brain : A Journal of Neurology*, 992–1000.

Buzsáki, G., & Draguhn, A. (2004). Neuronal oscillations in cortical networks. *Science*, *304*(5679), 1926–9.

Buzsáki, G., & Wang, X.-J. (2012). Mechanisms of gamma oscillations. *Annual Review of Neuroscience*, *35*, 203–25.

Cabral-Calderin, Y., Anne Weinrich, C., Schmidt-Samoa, C., Poland, E., Dechent, P., Bähr, M., & Wilke, M. (2015). Transcranial alternating current stimulation affects the BOLD signal in a frequency and task-dependent manner. *Human Brain Mapping*. *37*(1), 94-121.

Cady, E. B., Costello, A. M., Dawson, M. J., Delpy, D. T., Hope, P. L., Reynolds, E. O., … Wilkie, D. R. (1983). Non-invasive investigation of cerebral metabolism in newborn infants by phosphorus nuclear magnetic resonance spectroscopy. *Lancet*, *1*(8333), 1059–62.

Cancelli, A., Cottone, C., Zito, G., Di Giorgio, M., Pasqualetti, P., & Tecchio, F. (2015). Cortical inhibition and excitation by bilateral transcranial alternating current stimulation. *Restorative Neurology and Neuroscience*, *33*(2), 105–14.

Cardin, J. A., Carlén, M., Meletis, K., Knoblich, U., Zhang, F., Deisseroth, K., … Moore, C. I. (2009). Driving fast-spiking cells induces gamma rhythm and controls sensory responses. *Nature*, *459*(7247), 663–667.

Cavassila, S., Deval, S., Huegen, C., van Ormondt, D., & Graveron-Demilly, D. (2001). Cramér-Rao bounds: an evaluation tool for quantitation. *NMR in Biomedicine*, *14*(4), 278–83.

Chaieb, L., Antal, A., & Paulus, W. (2011). Transcranial alternating current stimulation in the low kHz range increases motor cortex excitability. *Restorative Neurology and Neuroscience*, *29*(3), 167–75.

Chaieb, L., Antal, A., Pisoni, A., Saiote, C., Opitz, A., Ambrus, G. G., … Paulus, W. (2014). Safety of 5 kHz tACS. *Brain Stimulation*, *7*(1), 92–6.

Chen, R. (2000). Studies of human motor physiology with transcranial magnetic stimulation. *Muscle & Nerve. Supplement*, *9*, S26-32.

Chen, R., Cros, D., Curra, A., Di Lazzaro, V., Lefaucheur, J.-P., Magistris, M. R., … Ziemann, U. (2008). The clinical diagnostic utility of transcranial magnetic stimulation: report of an IFCN committee. *Clinical Neurophysiology, 119*(3), 504–32.

Chen, R., & Hallett, M. (1999). The time course of changes in motor cortex excitability associated with voluntary movement. *The Canadian Journal of Neurological Sciences, 26*(3), 163–9.

Chen, R., Yaseen, Z., Cohen, L. G., & Hallett, M. (1998). Time course of corticospinal excitability in reaction time and self-paced movements. *Annals of Neurology*, *44*(3), 317–325.

Chen, Z., Resnik, E., McFarland, J. M., Sakmann, B., & Mehta, M. R. (2011). Speed

Controls the Amplitude and Timing of the Hippocampal Gamma Rhythm. *PLoS ONE*, *6*(6), e21408.
Cheyne, D., Bakhtazad, L., & Gaetz, W. (2006). Spatiotemporal mapping of cortical activity accompanying voluntary movements using an event-related beamforming approach. *Human Brain Mapping*, *27*(3), 213–229.
Cheyne, D., Bells, S., Ferrari, P., Gaetz, W., & Bostan, A. C. (2008). Self-paced movements induce high-frequency gamma oscillations in primary motor cortex. *NeuroImage*, *42*(1), 332–42.
Cheyne, D., & Ferrari, P. (2013). MEG studies of motor cortex gamma oscillations: evidence for a gamma "fingerprint" in the brain? *Frontiers in Human Neuroscience*, *7*, 575.
Cheyne, D. O. (2013). MEG studies of sensorimotor rhythms: A review. *Experimental Neurology*, *245*, 27–39.
Chiapponi, C., Piras, F., Piras, F., Caltagirone, C., & Spalletta, G. (2016). GABA System in Schizophrenia and Mood Disorders: A Mini Review on Third-Generation Imaging Studies. *Frontiers in Psychiatry*, *7*, 61.
Chrobak, J. J., & Buzsáki, G. (1996). High-Frequency Oscillations in the Output Networks of the Hippocampal–Entorhinal Axis of the Freely Behaving Rat. *The Journal of Neuroscience*, *16*(9).
Citri, A., & Malenka, R. C. (2008). Synaptic Plasticity: Multiple Forms, Functions, and Mechanisms. *Neuropsychopharmacology*, *33*(1), 18–41.
Cobb, S. R., Buhl, E. H., Halasy, K., Paulsen, O., & Somogyi, P. (1995). Synchronization of neuronal activity in hippocampus by individual GABAergic interneurons. *Nature*, *378*(6552), 75–78.
Cohen, L. G., Roth, B. J., Nilsson, J., Dang, N., Panizza, M., Bandinelli, S., … Hallett, M. (1990). Effects of coil design on delivery of focal magnetic stimulation. Technical considerations. *Electroencephalography and Clinical Neurophysiology*, *75*(4), 350–357.
Cooper, L. N., & Bear, M. F. (2012). The BCM theory of synapse modification at 30: interaction of theory with experiment. *Nature Reviews Neuroscience*, *13*(11), 798–810.
Courtemanche, R., Fujii, N., & Graybiel, A. M. (2003). Synchronous, Focally Modulated β-Band Oscillations Characterize Local Field Potential Activity in the Striatum of Awake Behaving Monkeys. *Journal of Neuroscience*, *23*(37).
Crone, N. E., Miglioretti, D. L., Gordon, B., & Lesser, R. P. (1998). Functional mapping of human sensorimotor cortex with electrocorticographic spectral analysis. II. Event-related synchronization in the gamma band. *Brain*, *121*(12).
Datta, A., Bansal, V., Diaz, J., Patel, J., Reato, D., & Bikson, M. (2009). Gyri-precise head model of transcranial direct current stimulation: improved spatial focality using a ring electrode versus conventional rectangular pad. *Brain Stimulation*, *2*(4), 201–7, 207.e1.
Datta, A., Bikson, M., & Fregni, F. (2010). Transcranial direct current stimulation in patients with skull defects and skull plates: High-resolution computational FEM study of factors altering cortical current flow. *NeuroImage*, *52*(4), 1268–1278.
Datta, A., Elwassif, M., Battaglia, F., & Bikson, M. (2008). Transcranial current stimulation focality using disc and ring electrode configurations: FEM analysis. *Journal of Neural Engineering*, *5*(2), 163–174.
Datta, A., Truong, D., Minhas, P., Parra, L. C., Bikson, M., Hanajima, R., & al., et.

(2012). Inter-Individual Variation during Transcranial Direct Current Stimulation and Normalization of Dose Using MRI-Derived Computational Models. *Frontiers in Psychiatry*, *3*(0), 91.

Davide, C., Kevin, D., Gaëtan, G., John, R., & Patrizia, B. (2016). Effects of 10Hz and 20Hz Transcranial Alternating Current Stimulation on Automatic Motor Control. *Brain Stimulation*. *9*(4), 518-24

Dayan, E., & Cohen, L. G. (2011). Neuroplasticity subserving motor skill learning. *Neuron*, *72*(3), 443–54.

Deans, J. K., Powell, A. D., & Jefferys, J. G. R. (2007). Sensitivity of coherent oscillations in rat hippocampus to AC electric fields. *The Journal of Physiology*, *583*(2), 555–565.

Dhuna, A., Gates, J., & Pascual-Leone, A. (1991). Transcranial magnetic stimulation in patients with epilepsy. *Neurology*, *41*(7), 1067–71.

Di Costanzo, A., Trojsi, F., Tosetti, M., Giannatempo, G. M., Nemore, F., Piccirillo, M., … Scarabino, T. (2003). High-field proton MRS of human brain. *The European Journal of Radiology*, *48*(2), 146–153.

Di Lazzaro, V., Oliviero, A., Meglio, M., Cioni, B., Tamburrini, G., Tonali, P., & Rothwell, J. . (2000). Direct demonstration of the effect of lorazepam on the excitability of the human motor cortex. *Clinical Neurophysiology*, *111*(5), 794–799.

Di Lazzaro, V., Oliviero, A., Pilato, F., Saturno, E., Dileone, M., Mazzone, P., … Rothwell, J. C. (2004). The physiological basis of transcranial motor cortex stimulation in conscious humans. *Clinical Neurophysiology*, *115*(2), 255–66.

Di Lazzaro, V., Oliviero, A., Profice, P., Pennisi, M. A., Pilato, F., Zito, G., … Tonali, P. A. (2003). Ketamine increases human motor cortex excitability to transcranial magnetic stimulation. *The Journal of Physiology*, *547*(Pt 2), 485–96.

Di Lazzaro, V., Oliviero, A., Saturno, E., Dileone, M., Pilato, F., Nardone, R., … Tonali, P. (2005). Effects of lorazepam on short latency afferent inhibition and short latency intracortical inhibition in humans. *The Journal of Physiology*, *564*(Pt 2), 661–8.

Di Lazzaro, V., Pilato, F., Dileone, M., Ranieri, F., Ricci, V., Profice, P., … Ziemann, U. (2006). GABAA receptor subtype specific enhancement of inhibition in human motor cortex. *The Journal of Physiology*, *575*(Pt 3), 721–6.

Dmochowski, J. P., Bikson, M., & Parra, L. C. (2012). The point spread function of the human head and its implications for transcranial current stimulation. *Physics in Medicine and Biology*, *57*(20), 6459–6477.

Doeltgen, S. H., & Ridding, M. C. (2011). Low-intensity, short-interval theta burst stimulation modulates excitatory but not inhibitory motor networks. *Clinical Neurophysiology : Official Journal of the International Federation of Clinical Neurophysiology*, *122*(7), 1411–6.

Donner, T. H., Siegel, M., Fries, P., & Engel, A. K. (2009). Buildup of Choice-Predictive Activity in Human Motor Cortex during Perceptual Decision Making. *Current Biology*, *19*(18), 1581–1585.

Doyon, J., & Benali, H. (2005). Reorganization and plasticity in the adult brain during learning of motor skills. *Current Opinion in Neurobiology*, *15*(2), 161–167.

Duarte, J. M. N., Lei, H., Mlynárik, V., & Gruetter, R. (2012). The neurochemical profile quantified by in vivo 1H NMR spectroscopy. *NeuroImage*, *61*(2), 342–362.

Duque, J., Hummel, F., Celnik, P., Murase, N., Mazzocchio, R., & Cohen, L. G. (2005). Transcallosal inhibition in chronic subcortical stroke. *NeuroImage*, *28*(4), 940–6.

Duyn, J. H., Gillen, J., Sobering, G., van Zijl, P. C., & Moonen, C. T. (1993). Multisection proton MR spectroscopic imaging of the brain. *Radiology*, *188*(1), 277–282.

Düzel, E., Penny, W. D., & Burgess, N. (2010). Brain oscillations and memory. *Current Opinion in Neurobiology*, *20*(2), 143–149.

Dyke, K., Pépés, S. E., Chen, C., Kim, S., Sigurdsson, H. P., Draper, A., … Jackson, S. R. (2017). Comparing GABA-dependent physiological measures of inhibition with proton magnetic resonance spectroscopy measurement of GABA using ultra-high-field MRI. *NeuroImage*, *152*, 360–370.

Edden, R. A. E., Muthukumaraswamy, S. D., Freeman, T. C. A., & Singh, K. D. (2009). Orientation Discrimination Performance Is Predicted by GABA Concentration and Gamma Oscillation Frequency in Human Primary Visual Cortex. *Journal of Neuroscience*, *29*(50), 15721–15726.

Emir, U. E., Auerbach, E. J., Van De Moortele, P.-F., Marjańska, M., Uğurbil, K., Terpstra, M., … Oz, G. (2012). Regional neurochemical profiles in the human brain measured by ^{1}H MRS at 7 T using local B_1 shimming. *NMR in Biomedicine*, *25*(1), 152–60.

Engel, A. K., & Fries, P. (2010). Beta-band oscillations--signalling the status quo? *Current Opinion in Neurobiology*, *20*(2), 156–65.

Engel, A. K., Fries, P., & Singer, W. (2001). Dynamic predictions: Oscillations and synchrony in top–down processing. *Nature Reviews Neuroscience*, *2*(10), 704–716.

Ermentrout, G. B., & Kopell, N. (1998). Fine structure of neural spiking and synchronization in the presence of conduction delays. *Proceedings of the National Academy of Sciences of the United States of America*, *95*(3), 1259–64.

Espenhahn, S., de Berker, A. O., van Wijk, B. C. M., Rossiter, H. E., & Ward, N. S. (2017). Movement-related beta oscillations show high intra-individual reliability. *NeuroImage*, *147*, 175–185.

Eusebio, A., & Brown, P. (2009). Synchronisation in the beta frequency-band--the bad boy of parkinsonism or an innocent bystander? *Experimental Neurology*, *217*(1), 1–3.

Farrant, M., & Nusser, Z. (2005). Variations on an inhibitory theme: phasic and tonic activation of GABAA receptors. *Nature Reviews Neuroscience*, *6*(3), 215–229.

Feldman, D. E. (2012). The spike-timing dependence of plasticity. *Neuron*, *75*(4), 556–71.

Feurra, M., Bianco, G., Santarnecchi, E., Del Testa, M., Rossi, A., & Rossi, S. (2011). Frequency-dependent tuning of the human motor system induced by transcranial oscillatory potentials. *The Journal of Neuroscience*, *31*(34), 12165–70.

Feurra, M., Pasqualetti, P., Bianco, G., Santarnecchi, E., Rossi, A., & Rossi, S. (2013). State-dependent effects of transcranial oscillatory currents on the motor system: what you think matters. *The Journal of Neuroscience*, *33*(44), 17483–9.

Feurra, M., Paulus, W., Walsh, V., & Kanai, R. (2011). Frequency specific modulation of human somatosensory cortex. *Frontiers in Psychology*, *2*, 13.

Floyer-Lea, A., Wylezinska, M., Kincses, T., & Matthews, P. M. (2006). Rapid modulation of GABA concentration in human sensorimotor cortex during motor learning. *Journal of Neurophysiology*, *95*(3), 1639–44.

Foerster, O. (1926). “Die Pathogenese des epileptischen Krampfanfalles”. In: Deutsche Zeitschrift f. Nervenheilkunde 94.1 (pp. 15–53).

Fricke, K., Seeber, A. A., Thirugnanasambandam, N., Paulus, W., Nitsche, M. A., & Rothwell, J. C. (2011). Time course of the induction of homeostatic plasticity generated by repeated transcranial direct current stimulation of the human motor cortex. *Journal of Neurophysiology*, *105*(3), 1141–9.

Friedrich, E. V. C., Scherer, R., & Neuper, C. (2013). Stability of event-related (de-) synchronization during brain–computer interface-relevant mental tasks. *Clinical Neurophysiology*, *124*(1), 61–69.

Fries, P. (2005). A mechanism for cognitive dynamics: neuronal communication through neuronal coherence. *Trends in Cognitive Sciences*, *9*(10), 474–80.

Fries, P. (2015). Rhythms for Cognition: Communication through Coherence. *Neuron*, *88*(1), 220–35.

Fries, P., Nikolić, D., & Singer, W. (2007). The gamma cycle. *Trends in Neurosciences*, *30*(7), 309–316.

Fröhlich, F. (2015). Experiments and models of cortical oscillations as a target for noninvasive brain stimulation. *Progress in Brain Research*, *222*, 41–73.

Fröhlich, F., & McCormick, D. A. (2010). Endogenous electric fields may guide neocortical network activity. *Neuron*, *67*(1), 129–43.

Fulton, J. F. (1935). A NOTE ON THE DEFINITION OF THE “MOTOR” AND “PREMOTOR” AREAS. *Brain*, *58*(2), 311–316.

Gaetz, W., Edgar, J. C., Wang, D. J., & Roberts, T. P. L. (2011). Relating MEG measured motor cortical oscillations to resting γ-aminobutyric acid (GABA) concentration. *NeuroImage*, *55*(2), 616–21.

Gaetz, W., Liu, C., Zhu, H., Bloy, L., & Roberts, T. P. L. (2013). Evidence for a motor gamma-band network governing response interference. *NeuroImage*, *74*, 245–53.

Gaetz, W., MacDonald, M., Cheyne, D., & Snead, O. C. (2010). Neuromagnetic imaging of movement-related cortical oscillations in children and adults: Age predicts post-movement beta rebound. *NeuroImage*, *51*(2), 792–807.

Garwood, M., & DelaBarre, L. (2001). The Return of the Frequency Sweep: Designing Adiabatic Pulses for Contemporary NMR. *Journal of Magnetic Resonance*, *153*(2), 155–177.

Gentner, R., Wankerl, K., Reinsberger, C., Zeller, D., & Classen, J. (2008). Depression of human corticospinal excitability induced by magnetic theta-burst stimulation: evidence of rapid polarity-reversing metaplasticity. *Cerebral Cortex*, *18*(9), 2046–53.

Georgopoulos, A. P., Schwartz, A. B., & Kettner, R. E. (1986). Neuronal population coding of movement direction. *Science*, *233*(4771), 1416–9.

Gilbertson, T., Lalo, E., Doyle, L., Di Lazzaro, V., Cioni, B., & Brown, P. (2005). Existing motor state is favored at the expense of new movement during 13-35 Hz oscillatory synchrony in the human corticospinal system. *The Journal of Neuroscience*, *25*(34), 7771–9.

Godlewska, B. R., Pike, A., Sharpley, A. L., Ayton, A., Park, R. J., Cowen, P. J., & Emir, U. E. (2017). Brain glutamate in anorexia nervosa: a magnetic resonance spectroscopy case control study at 7 Tesla. *Psychopharmacology*, *234*(3), 421–426.

Goldsworthy, M. R., Vallence, A.-M., Yang, R., Pitcher, J. B., & Ridding, M. C. (2016). Combined transcranial alternating current stimulation and continuous theta burst stimulation: a novel approach for neuroplasticity induction. *The European Journal of Neuroscience*, *43*(4), 572–579.

Gonzalez-Burgos, G., & Lewis, D. A. (2008). GABA neurons and the mechanisms of network oscillations: implications for understanding cortical dysfunction in schizophrenia. *Schizophrenia Bulletin*, *34*(5), 944–61.

Govindaraju, V., Young, K., & Maudsley, A. A. (2000). Proton NMR chemical shifts and coupling constants for brain metabolites. *NMR in Biomedicine*, *13*(3), 129–53.

Groppa, S., Oliviero, A., Eisen, A., Quartarone, A., Cohen, L. G., Mall, V., … Siebner, H. R. (2012). A practical guide to diagnostic transcranial magnetic stimulation: report of an IFCN committee. *Clinical Neurophysiology*, *123*(5), 858–82.

Gross, J. (2014). Analytical methods and experimental approaches for electrophysiological studies of brain oscillations. *Journal of Neuroscience Methods*, *228*, 57–66.

Grossman, N., Bono, D., Dedic, N., Kodandaramaiah, S. B., Rudenko, A., Suk, H.-J., … Boyden, E. S. (2017). Noninvasive Deep Brain Stimulation via Temporally Interfering Electric Fields. *Cell*, *169*(6), 1029–1041.e16.

Guerra, A., Pogosyan, A., Nowak, M., Tan, H., Ferreri, F., Di Lazzaro, V., & Brown, P. (2016). Phase Dependency of the Human Primary Motor Cortex and Cholinergic Inhibition Cancelation During Beta tACS. *Cerebral Cortex, 26*(10), 3977-90

Gulyás, A. I., Megías, M., Emri, Z., & Freund, T. F. (1999). Total Number and Ratio of Excitatory and Inhibitory Synapses Converging onto Single Interneurons of Different Types in the CA1 Area of the Rat Hippocampus. *The Journal of Neuroscience*, *19*(22).

Hall, S. D., Barnes, G. R., Furlong, P. L., Seri, S., & Hillebrand, A. (2010). Neuronal network pharmacodynamics of GABAergic modulation in the human cortex determined using pharmaco-magnetoencephalography. *Human Brain Mapping*, *31*(4), 581–94.

Hall, S. D., Prokic, E. J., McAllister, C. J., Ronnqvist, K. C., Williams, A. C., Yamawaki, N., … Stanford, I. M. (2014). GABA-mediated changes in inter-hemispheric beta frequency activity in early-stage Parkinson's disease. *Neuroscience*, *281C*, 68–76.

Hall, S. D., Stanford, I. M., Yamawaki, N., McAllister, C. J., Rönnqvist, K. C., Woodhall, G. L., & Furlong, P. L. (2011). The role of GABAergic modulation in motor function related neuronal network activity. *NeuroImage*, *56*(3), 1506–10.

Hall, S. D., Yamawaki, N., Fisher, A. E., Clauss, R. P., Woodhall, G. L., & Stanford, I. M. (2010). GABA(A) alpha-1 subunit mediated desynchronization of elevated low frequency oscillations alleviates specific dysfunction in stroke – A case report. *Clinical Neurophysiology*, *121*(4), 549–555.

Hallett, M. (2000). Transcranial magnetic stimulation and the human brain. *Nature*, *406*(6792), 147–50.

Hallett, M. (2007). Transcranial Magnetic Stimulation: A Primer. *Neuron*, *55*(2), 187–199.

Hamada, M., Hanajima, R., Terao, Y., Okabe, S., Nakatani-Enomoto, S., Furubayashi, T., … Ugawa, Y. (2009). Primary motor cortical metaplasticity induced by priming over the supplementary motor area. *The Journal of Physiology*, *587*(20), 4845–4862.

Hammond, C., Bergman, H., & Brown, P. (2007). Pathological synchronization in Parkinson's disease: networks, models and treatments. *Trends in Neurosciences*, *30*(7), 357–64.

Hansen Peter, Kringelbach Morten, S. R. (2010). *MEG: an introduction to methods*. New York: Oxford University Press.

Hanslmayr, S., Gross, J., Klimesch, W., & Shapiro, K. L. (2011). The role of alpha oscillations in temporal attention. *Brain Research Reviews*, *67*(1–2), 331–343.
Hardwick, R. M., Rottschy, C., Miall, R. C., & Eickhoff, S. B. (2013). A quantitative meta-analysis and review of motor learning in the human brain. *NeuroImage*, *67*, 283–97.
Headley, D. B., & Weinberger, N. M. (2011). Gamma-band activation predicts both associative memory and cortical plasticity. *The Journal of Neuroscience, 31*(36), 12748–58.
Hebb, D. (1949). *The Organization of Behaviour*. New York: Wiley.
Heinrichs-Graham, E., & Wilson, T. W. (2015). Coding complexity in the human motor circuit. *Human Brain Mapping*, *36*(12), 5155–67.
Heinrichs-Graham, E., & Wilson, T. W. (2016). Is an absolute level of cortical beta suppression required for proper movement? Magnetoencephalographic evidence from healthy aging. *NeuroImage*, *134*, 514–521.
Heinrichs-Graham, E., Wilson, T. W., Santamaria, P. M., Heithoff, S. K., Torres-Russotto, D., Hutter-Saunders, J. A. L., … Gendelman, H. E. (2014). Neuromagnetic Evidence of Abnormal Movement-Related Beta Desynchronization in Parkinson's Disease. *Cerebral Cortex*, *24*(10), 2669–2678.
Heise, K.-F., Kortzorg, N., Saturnino, G. B., Fujiyama, H., Cuypers, K., Thielscher, A., & Swinnen, S. P. (2016). Evaluation of a Modified High-Definition Electrode Montage for Transcranial Alternating Current Stimulation (tACS) of Pre-Central Areas. *Brain Stimulation*, *9*(5), 700–704.
Heise, K.-F., Steven, B., Liuzzi, G., Thomalla, G., Jonas, M., Müller-Vahl, K., … Hummel, F. C. (2010). Altered modulation of intracortical excitability during movement preparation in Gilles de la Tourette syndrome. *Brain : A Journal of Neurology*, *133*(Pt 2), 580–90.
Heise, K.-F., Zimerman, M., Hoppe, J., Gerloff, C., Wegscheider, K., & Hummel, F. C. (2013). The aging motor system as a model for plastic changes of GABA-mediated intracortical inhibition and their behavioral relevance. *The Journal of Neuroscience, 33*(21), 9039–49.
Helfrich, R. F., Knepper, H., Nolte, G., Strüber, D., Rach, S., Herrmann, C. S., … Engel, A. K. (2014). Selective Modulation of Interhemispheric Functional Connectivity by HD-tACS Shapes Perception. *PLoS Biology*, *12*(12), e1002031.
Helfrich, R. F., & Schneider, T. R. (2013). Modulation of cortical network activity by transcranial alternating current stimulation. *The Journal of Neuroscienc*, *33*(45), 17551–2.
Helfrich, R. F., Schneider, T. R., Rach, S., Trautmann-Lengsfeld, S. a, Engel, A. K., & Herrmann, C. S. (2014). Entrainment of brain oscillations by transcranial alternating current stimulation. *Current Biology*, *24*(3), 333–9.
Hermes, D., Miller, K. J., Wandell, B. A., & Winawer, J. (2015). Gamma oscillations in visual cortex: the stimulus matters. *Trends in Cognitive Sciences*, *19*(2), 57–8.
Herrmann, C. S., Rach, S., Neuling, T., & Strüber, D. (2013). Transcranial alternating current stimulation: a review of the underlying mechanisms and modulation of cognitive processes. *Frontiers in Human Neuroscience*, *7*, 279.
Herrmann, C. S., Strüber, D., Helfrich, R. F., & Engel, A. K. (2016). EEG oscillations: From correlation to causality. *International Journal of Psychophysiology*, *103*, 12–21.
Hirshberg, L., Chiu, S., & Frazier, J. A. (2005). Emerging brain-based interventions for

children and adolescents: overview and clinical perspective. *Child and Adolescent Psychiatric Clinics of North America*, *14*(1), 1–19.
Hlustík, P., Solodkin, A., Gullapalli, R. P., Noll, D. C., & Small, S. L. (2001). Somatotopy in human primary motor and somatosensory hand representations revisited. *Cerebral Cortex*, *11*(4), 312–21.
Huang, Y., Liu, A. A., Lafon, B., Friedman, D., Dayan, M., Wang, X., … Parra, L. C. (2017). Measurements and models of electric fields in the *in vivo* human brain during transcranial electric stimulation. *eLife*, *6*, e18834.
Hummel, F. C., Steven, B., Hoppe, J., Heise, K., Thomalla, G., Cohen, L. G., & Gerloff, C. (2009). Deficient intracortical inhibition (SICI) during movement preparation after chronic stroke. *Neurology*, *72*(20), 1766–72.
Humphrey, D. R. (1986). Representation of movements and muscles within the primate precentral motor cortex: historical and current perspectives. *Federation Proceedings*, *45*(12), 2687–99.
Huntley, G. W. (1997). Correlation between patterns of horizontal connectivity and the extend of short-term representational plasticity in rat motor cortex. *Cerebral Cortex (New York, N.Y. : 1991)*, *7*(2), 143–56.
Hutcheon, B., & Yarom, Y. (2000). Resonance, oscillation and the intrinsic frequency preferences of neurons. *Trends in Neurosciences*, *23*(5), 216–22.
Ilic, T. V, Meintzschel, F., Cleff, U., Ruge, D., Kessler, K. R., & Ziemann, U. (2002). Short-interval paired-pulse inhibition and facilitation of human motor cortex: the dimension of stimulus intensity. *The Journal of Physiology*, *545*(1), 153–167.
Jacobs, K. M., & Donoghue, J. P. (1991). Reshaping the cortical motor map by unmasking latent intracortical connections. *Science*, *251*(4996), 944–7.
Jasper, H., & Penfield, W. (1949). Electrocorticograms in man: Effect of voluntary movement upon the electrical activity of the precentral gyrus. Article in *European Archives of Psychiatry and Clinical Neuroscience*, *183*(1–2), 163–174.
Jaušovec, N., & Jaušovec, K. (2014). Increasing working memory capacity with theta transcranial alternating current stimulation (tACS). *Biological Psychology*, *96*, 42–7.
Jenkinson, N., & Brown, P. (2011). New insights into the relationship between dopamine, beta oscillations and motor function. *Trends in Neurosciences*, *34*(12), 611–8.
Jenkinson, N., Kühn, A. A., & Brown, P. (2013). Gamma oscillations in the human basal ganglia. *Experimental Neurology*, *245*, 72–76.
Jensen, O., Goel, P., Kopell, N., Pohja, M., Hari, R., & Ermentrout, B. (2005). On the human sensorimotor-cortex beta rhythm: sources and modeling. *NeuroImage*, *26*(2), 347–55.
Joundi, R. A., Brittain, J.-S., Green, A. L., Aziz, T. Z., Brown, P., & Jenkinson, N. (2012). Oscillatory activity in the subthalamic nucleus during arm reaching in Parkinson's disease. *Experimental Neurology*, *236*(2), 319–326.
Joundi, R. A., Lopez-Alonso, V., Lago, A., Brittain, J.-S., Fernandez-Del-Olmo, M., Gomez-Garre, P., … Brown, P. (2012). The effect of BDNF val66met polymorphism on visuomotor adaptation. *Experimental Brain Research*, *223*(1), 43–50.
Joundi, R. a, Jenkinson, N., Brittain, J.-S., Aziz, T. Z., & Brown, P. (2012). Driving oscillatory activity in the human cortex enhances motor performance. *Current Biology*, *22*(5), 403–7.

Jurkiewicz, M. T., Gaetz, W. C., Bostan, A. C., & Cheyne, D. (2006). Post-movement beta rebound is generated in motor cortex: Evidence from neuromagnetic recordings. *NeuroImage*, *32*(3), 1281–1289.

Kaiser, J., Birbaumer, N., & Lutzenberger, W. (2001). Event-related beta desynchronization indicates timing of response selection in a delayed-response paradigm in humans. *Neuroscience Letters*, *312*(3), 149–52.

Kallel, L., Mondino, M., & Brunelin, J. (2016). Effects of theta-rhythm transcranial alternating current stimulation (4.5 Hz-tACS) in patients with clozapine-resistant negative symptoms of schizophrenia: a case series. *Journal of Neural Transmission*, *123*(10), 1213–1217.

Kanai, R., Chaieb, L., Antal, A., Walsh, V., & Paulus, W. (2008). Frequency-dependent electrical stimulation of the visual cortex. *Current Biology : CB*, *18*(23), 1839–43.

Karabanov, A., Ziemann, U., Hamada, M., George, M. S., Quartarone, A., Classen, J., … Siebner, H. R. (2015). Consensus Paper: Probing Homeostatic Plasticity of Human Cortex With Non-invasive Transcranial Brain Stimulation. *Brain Stimulation*, *8*(3), 442–54.

Kasten, F. H., Dowsett, J., & Herrmann, C. S. (2016). Sustained Aftereffect of α-tACS Lasts Up to 70 min after Stimulation. *Frontiers in Human Neuroscience*, *10*, 245.

Kempf, F., Brücke, C., Salih, F., Trottenberg, T., Kupsch, A., Schneider, G.-H., … Brown, P. (2009). Gamma activity and reactivity in human thalamic local field potentials. *The European Journal of Neuroscience*, *29*(5), 943–953.

Kendrick, K. M., Zhan, Y., Fischer, H., Nicol, A. U., Zhang, X., & Feng, J. (2011). Learning alters theta amplitude, theta-gamma coupling and neuronal synchronization in inferotemporal cortex. *BMC Neuroscience*, *12*(1), 55.

Kennefick, M., Maslovat, D., Carlsen, A. N., Ghosh, S., & Morris, I. (2014). The Time Course of Corticospinal Excitability during a Simple Reaction Time Task. *PLoS ONE*, *9*(11), e113563.

Kilavik, B. E., Zaepffel, M., Brovelli, A., MacKay, W. A., & Riehle, A. (2013). The ups and downs of beta oscillations in sensorimotor cortex. *Experimental Neurology*, *245*, 15–26.

Kilner, J., Bott, L., & Posada, A. (2005). Modulations in the degree of synchronization during ongoing oscillatory activity in the human brain. *The European Journal of Neuroscience*, *21*(9), 2547–2554.

Klimesch, W. (2012). α-band oscillations, attention, and controlled access to stored information. *Trends in Cognitive Sciences*, *16*(12), 606–17.

Kobayashi, M., & Pascual-Leone, A. (2003). Transcranial magnetic stimulation in neurology. *The Lancet Neurology*, *2*(3), 145–156.

Könönen, M., & Partanen, J. V. (1993). Blocking of EEG alpha activity during visual performance in healthy adults. A quantitative study. *Electroencephalography and Clinical Neurophysiology*, *87*(3), 164–6.

Kopell, N., Ermentrout, G. B., Whittington, M. A., & Traub, R. D. (2000). Gamma rhythms and beta rhythms have different synchronization properties. *Proceedings of the National Academy of Sciences*, *97*(4), 1867–1872.

Kramer, M. A., Roopun, A. K., Carracedo, L. M., Traub, R. D., Whittington, M. A., & Kopell, N. J. (2008). Rhythm Generation through Period Concatenation in Rat Somatosensory Cortex. *PLoS Computational Biology*, *4*(9), e1000169.

Krause, B., & Cohen Kadosh, R. (2014). Not all brains are created equal: the relevance of individual differences in responsiveness to transcranial electrical stimulation.

Frontiers in Systems Neuroscience, *8*, 25.
Kujirai, T., Caramia, M. D., Rothwell, J. C., Day, B. L., Thompson, P. D., Ferbert, A., … Marsden, C. D. (1993). Corticocortical inhibition in human motor cortex. *Journal of Physiology*, *471*, 501–519.
Laczó, B., Antal, A., Niebergall, R., Treue, S., & Paulus, W. (2012). Transcranial alternating stimulation in a high gamma frequency range applied over V1 improves contrast perception but does not modulate spatial attention. *Brain Stimulation*, *5*(4), 484–91.
Lee, M.-C., Yasuda, R., & Ehlers, M. D. (2010). Metaplasticity at single glutamatergic synapses. *Neuron*, *66*(6), 859–70.
Lemke, C., Hess, A., Clare, S., Bachtiar, V., Stagg, C., Jezzard, P., & Emir, U. (2015). Two-voxel spectroscopy with dynamic B_0 shimming and flip angle adjustment at 7 T in the human motor cortex. *NMR in Biomedicine*, *28*(7), 852–860.
Lepage, J.-F., Saint-Amour, D., & Théoret, H. (2008). EEG and neuronavigated single-pulse TMS in the study of the observation/execution matching system: Are both techniques measuring the same process? *Journal of Neuroscience Methods*, *175*(1), 17–24.
Leung, L. S. (1982). Nonlinear feedback model of neuronal populations in hippocampal CAl region. *Journal of Neurophysiology*, *47*(5), 845–68.
Levy, W. B., & Steward, O. (1983). Temporal contiguity requirements for long-term associative potentiation/depression in the hippocampus. *Neuroscience*, *8*(4), 791–7.
Little, S., & Brown, P. (2014). The functional role of beta oscillations in Parkinson's disease. *Parkinsonism & Related Disorders*, *20 Suppl 1*, S44-8.
Litvak, V., Eusebio, A., Jha, A., Oostenveld, R., Barnes, G., Foltynie, T., … Brown, P. (2012). Movement-related changes in local and long-range synchronization in Parkinson's disease revealed by simultaneous magnetoencephalography and intracranial recordings. *The Journal of Neuroscience*, *32*(31), 10541–53.
López-Alonso, V., Cheeran, B., Río-Rodríguez, D., & Fernández-del-Olmo, M. (2014). Inter-individual Variability in Response to Non-invasive Brain Stimulation Paradigms. *Brain Stimulation*, *7*(3), 372–380.
Maccabee, P. J., Amassian, V. E., Eberle, L. P., & Cracco, R. Q. (1993). Magnetic coil stimulation of straight and bent amphibian and mammalian peripheral nerve in vitro: locus of excitation. *Journal of Physiology*, *460*, 201–19.
MacKay, W. A. (1997). Synchronized neuronal oscillations and their role in motor processes. *Trends in Cognitive Sciences*, *1*(5), 176–183.
MacKay, W. A., & Mendonça, A. J. (1995). Field potential oscillatory bursts in parietal cortex before and during reach. *Brain Research*, *704*(2), 167–74.
Mäki, H., & Ilmoniemi, R. J. (2010). EEG oscillations and magnetically evoked motor potentials reflect motor system excitability in overlapping neuronal populations. *Clinical Neurophysiology*, *121*(4), 492–501.
Malenka, R. C. (1993). Long-term depression: not so depressing after all. *Proceedings of the National Academy of Sciences of the United States of America*, *90*(8), 3121–3.
Mangia, S., Tkáč, I., Gruetter, R., Van de Moortele, P.-F., Maraviglia, B., & Uğurbil, K. (2007). Sustained Neuronal Activation Raises Oxidative Metabolism to a New Steady-State Level: Evidence from ^{1}H NMR Spectroscopy in the Human Visual Cortex. *Journal of Cerebral Blood Flow & Metabolism*, *27*(5), 1055–1063.

Mann, E. O., & Mody, I. (2010). Control of hippocampal gamma oscillation frequency by tonic inhibition and excitation of interneurons. *Nature Neuroscience*, *13*(2), 205–212.

Mann, E. O., & Paulsen, O. (2007). Role of GABAergic inhibition in hippocampal network oscillations. *Trends in Neurosciences*, *30*(7), 343–9.

Manseau, F., Marinelli, S., Méndez, P., Schwaller, B., Prince, D. A., Huguenard, J. R., & Bacci, A. (2010). Desynchronization of Neocortical Networks by Asynchronous Release of GABA at Autaptic and Synaptic Contacts from Fast-Spiking Interneurons. *PLoS Biology*, *8*(9), e1000492.

Maris, E., Fries, P., & van Ede, F. (2016). Diverse Phase Relations among Neuronal Rhythms and Their Potential Function. *Trends in Neurosciences*, *39*(2), 86–99.

Markram, H., Lübke, J., Frotscher, M., & Sakmann, B. (1997). Regulation of synaptic efficacy by coincidence of postsynaptic APs and EPSPs. *Science*, *275*(5297), 213–5.

Márquez-Ruiz, J., Ammann, C., Leal-Campanario, R., Ruffini, G., Gruart, A., & Delgado-García, J. M. (2016). Synthetic tactile perception induced by transcranial alternating-current stimulation can substitute for natural sensory stimulus in behaving rabbits. *Scientific Reports*, *6*, 19753.

Mathiowetz, V., Volland, G., Kashman, N., & Weber, K. (1985). Adult Norms for the Box and Block Test of Manual Dexterity. *American Journal of Occupational Therapy*, *39*(6), 386–391.

Matsumoto, H., & Ugawa, Y. (2017). Adverse events of tDCS and tACS: A review. *Clinical Neurophysiology Practice*, *2*, 19–25.

Matthews, P. M., Johansen-Berg, H., & Reddy, H. (2004). Non-invasive mapping of brain functions and brain recovery: applying lessons from cognitive neuroscience to neurorehabilitation. *Restorative Neurology and Neuroscience*, *22*(3–5), 245–60.

McDonnell, M. N., Orekhov, Y., & Ziemann, U. (2006). The role of GABA(B) receptors in intracortical inhibition in the human motor cortex. *Experimental Brain Research*, *173*(1), 86–93.

Merlet, I., Birot, G., Salvador, R., Molaee-Ardekani, B., Mekonnen, A., Soria-Frish, A., … Wendling, F. (2013). From Oscillatory Transcranial Current Stimulation to Scalp EEG Changes: A Biophysical and Physiological Modeling Study. *PLoS ONE*, *8*(2), e57330.

Mescher, M., Merkle, H., Kirsch, J., Garwood, M., & Gruetter, R. (1998). Simultaneous in vivo spectral editing and water suppression. *NMR in Biomedicine*, *11*(6), 266–72.

Miller, K. J., Hermes, D., Honey, C. J., Hebb, A. O., Ramsey, N. F., Knight, R. T., … Fetz, E. E. (2012). Human Motor Cortical Activity Is Selectively Phase-Entrained on Underlying Rhythms. *PLoS Computational Biology*, *8*(9), e1002655.

Minhas, P., Bikson, M., Woods, A. J., Rosen, A. R., & Kessler, S. K. (2012). Transcranial direct current stimulation in pediatric brain: A computational modeling study. In *2012 Annual International Conference of the IEEE Engineering in Medicine and Biology Society* (Vol. 2012, pp. 859–862). IEEE.

Miranda, P. C., Lomarev, M., & Hallett, M. (2006). Modeling the current distribution during transcranial direct current stimulation. *Clinical Neurophysiology*, *117*(7), 1623–1629.

Mitchell, W. K., Baker, M. R., & Baker, S. N. (2007). Muscle responses to transcranial stimulation in man depend on background oscillatory activity. *The Journal of*

Physiology, *583*(2), 567–579.
Mockett, B., Coussens, C., & Abraham, W. C. (2002). NMDA receptor-mediated metaplasticity during the induction of long-term depression by low-frequency stimulation. *The European Journal of Neuroscience*, *15*(11), 1819–26.
Moisa, M., Polania, R., Grueschow, M., & Ruff, C. C. (2016). Brain Network Mechanisms Underlying Motor Enhancement by Transcranial Entrainment of Gamma Oscillations. *The Journal of Neuroscience*, *36*(47), 12053–12065.
Moliadze, V., Antal, A., & Paulus, W. (2010). Boosting brain excitability by transcranial high frequency stimulation in the ripple range. *The Journal of Physiology*, *588*(Pt 24), 4891–904.
Moliadze, V., Atalay, D., Antal, A., & Paulus, W. (2012). Close to threshold transcranial electrical stimulation preferentially activates inhibitory networks before switching to excitation with higher intensities. *Brain Stimulation*, *5*(4), 505–11.
Müller-Dahlhaus, F., & Ziemann, U. (2015). Metaplasticity in human cortex. *The Neuroscientist : A Review Journal Bringing Neurobiology, Neurology and Psychiatry*, *21*(2), 185–202.
Müller, J. F. M., Orekhov, Y., Liu, Y., & Ziemann, U. (2007). Homeostatic plasticity in human motor cortex demonstrated by two consecutive sessions of paired associative stimulation. *The European Journal of Neuroscience*, *25*(11), 3461–8.
Murakami, S., & Okada, Y. (2006). Contributions of principal neocortical neurons to magnetoencephalography and electroencephalography signals. *The Journal of Physiology*, *575*(3), 925–936.
Murakami, T., Müller-Dahlhaus, F., Lu, M.-K., & Ziemann, U. (2012). Homeostatic metaplasticity of corticospinal excitatory and intracortical inhibitory neural circuits in human motor cortex. *The Journal of Physiology*, *590*(22), 5765–81.
Murase, N., Duque, J., Mazzocchio, R., & Cohen, L. G. (2004). Influence of interhemispheric interactions on motor function in chronic stroke. *Annals of Neurology*, *55*(3), 400–9.
Murthy, V. N., & Fetz, E. E. (1992). Coherent 25- to 35-Hz oscillations in the sensorimotor cortex of awake behaving monkeys. *Proceedings of the National Academy of Sciences*, *89*(12), 5670–5674.
Murthy, V. N., & Fetz, E. E. (1996). Oscillatory activity in sensorimotor cortex of awake monkeys: synchronization of local field potentials and relation to behavior. *The Journal of Neurophysiology*, *76*(6), 3949–67.
Muthukumaraswamy, S. D. (2010). Functional properties of human primary motor cortex gamma oscillations. *The Journal of Neurophysiology*, *104*(5), 2873–2885.
Muthukumaraswamy, S. D. (2011). Temporal dynamics of primary motor cortex gamma oscillation amplitude and piper corticomuscular coherence changes during motor control. *Experimental Brain Research*, *212*(4), 623–633.
Muthukumaraswamy, S. D. (2013). High-frequency brain activity and muscle artifacts in MEG/EEG: a review and recommendations. *Frontiers in Human Neuroscience*, *7*, 138.
Muthukumaraswamy, S. D., Carhart-Harris, R. L., Moran, R. J., Brookes, M. J., Williams, T. M., Errtizoe, D., … Nutt, D. J. (2013). Broadband Cortical Desynchronization Underlies the Human Psychedelic State. *The Journal of Neuroscience*, *33*(38).
Muthukumaraswamy, S. D., Edden, R. A. E., Jones, D. K., Swettenham, J. B., & Singh, K. D. (2009). Resting GABA concentration predicts peak gamma frequency and

fMRI amplitude in response to visual stimulation in humans. *Proceedings of the National Academy of Sciences of the United States of America*, *106*(20), 8356–61.
Muthukumaraswamy, S. D., Myers, J. F. M., Wilson, S. J., Nutt, D. J., Lingford-Hughes, A., Singh, K. D., & Hamandi, K. (2013). The effects of elevated endogenous GABA levels on movement-related network oscillations. *NeuroImage*, *66*, 36–41.
Nakazono, H., Ogata, K., Kuroda, T., Tobimatsu, S., Buzsáki, G., Draguhn, A., … Herrmann, C. (2016). Phase and Frequency-Dependent Effects of Transcranial Alternating Current Stimulation on Motor Cortical Excitability. *PLOS ONE*, *11*(9), e0162521.
Naros, G., & Gharabaghi, A. (2017). Physiological and behavioral effects of β-tACS on brain self-regulation in chronic stroke. *Brain Stimulation*, *10*(2), 251–259.
Neuling, T., Rach, S., & Herrmann, C. S. (2013). Orchestrating neuronal networks: sustained after-effects of transcranial alternating current stimulation depend upon brain states. *Frontiers in Human Neuroscience*, *7*, 161.
Neuling, T., Rach, S., Wagner, S., Wolters, C. H., & Herrmann, C. S. (2012). Good vibrations: oscillatory phase shapes perception. *NeuroImage*, *63*(2), 771–8.
Neuling, T., Ruhnau, P., Fuscà, M., Demarchi, G., Herrmann, C. S., & Weisz, N. (2015). Friends, not foes: magnetoencephalography as a tool to uncover brain dynamics during transcranial alternating current stimulation. *NeuroImage*. *118*, 406-13
Neuling, T., Ruhnau, P., Weisz, N., Herrmann, C. S., & Demarchi, G. (2016). Faith and oscillations recovered: On Analyzing EEG/MEG signals during tACS. *NeuroImage*. *147*, 960-963
Neuling, T., Wagner, S., Wolters, C. H., Zaehle, T., & Herrmann, C. S. (2012). Finite-Element Model Predicts Current Density Distribution for Clinical Applications of tDCS and tACS. *Frontiers in Psychiatry*, *3*, 83.
Ni, J., Lewis, C., Wunderle, T., Jendritza, P., Diester, I., & Fries, P. (2017). Gamma-Band Resonance Of Visual Cortex To Optogenetic Stimulation. *bioRxiv*.
Ni, Z., Gunraj, C., & Chen, R. (2007). Short interval intracortical inhibition and facilitation during the silent period in human. *The Journal of Physiology*, *583*(Pt 3), 971–82.
Nicolás, M. J., López-Azcárate, J., Valencia, M., Alegre, M., Pérez-Alcázar, M., Iriarte, J., & Artieda, J. (2011). Ketamine-Induced Oscillations in the Motor Circuit of the Rat Basal Ganglia. *PLoS ONE*, *6*(7), e21814.
Niedermeyer E, L. da S. F. (2005). *Electroencephalography: Basic Principles, Clinical Applications, And Related Fields* (5th ed.). Wolters Kluwer.
Nitsche, M. A., & Paulus, W. (2000). Excitability changes induced in the human motor cortex by weak transcranial direct current stimulation. *The Journal of Physiology*, *527 Pt 3*, 633–9.
Nitsche, M. A., Roth, A., Kuo, M.-F., Fischer, A. K., Liebetanz, D., Lang, N., … Paulus, W. (2007). Timing-dependent modulation of associative plasticity by general network excitability in the human motor cortex. *The Journal of Neuroscience, 27*(14), 3807–12.
Nitsche, M. A., Seeber, A., Frommann, K., Klein, C. C., Rochford, C., Nitsche, M. S., … Tergau, F. (2005). Modulating parameters of excitability during and after transcranial direct current stimulation of the human motor cortex. *The Journal of Physiology*, *568*(Pt 1), 291–303.
Noury, N., Hipp, J. F., & Siegel, M. (2016). Physiological processes non-linearly affect

electrophysiological recordings during transcranial electric stimulation. *NeuroImage*. *140*, 99-109

Novotny, E. J., Fulbright, R. K., Pearl, P. L., Gibson, K. M., & Rothman, D. L. (2003). Magnetic resonance spectroscopy of neurotransmitters in human brain. *Annals of Neurology*, *54 Suppl 6*, S25-31.

Nowak, M., Hinson, E., van Ede, F., Pogosyan, A., Guerra, A., Quinn, A., … Stagg, C. J. (2017). Driving Human Motor Cortical Oscillations Leads to Behaviorally Relevant Changes in Local GABAA Inhibition: A tACS-TMS Study. *The Journal of Neuroscience*, *37*(17), 4481-4492

O'Shea, J., Boudrias, M.-H., Stagg, C. J., Bachtiar, V., Kischka, U., Blicher, J. U., & Johansen-Berg, H. (2014). Predicting behavioural response to TDCS in chronic motor stroke. *NeuroImage*, *85*(Pt 3), 924–33.

Oostenveld, R., Fries, P., Maris, E., & Schoffelen, J.-M. (2011). FieldTrip: Open source software for advanced analysis of MEG, EEG, and invasive electrophysiological data. *Computational Intelligence and Neuroscience*, *2011*, 156869.

Otte, S., Hasenstaub, A., & Callaway, E. M. (2010). Cell type-specific control of neuronal responsiveness by gamma-band oscillatory inhibition. *The Journal of Neuroscience*, *30*(6), 2150–9.

Owens, D. F., & Kriegstein, A. R. (2002). Is there more to gaba than synaptic inhibition? *Nature Reviews Neuroscience*, *3*(9), 715–727.

Ozen, S., Sirota, A., Belluscio, M. A., Anastassiou, C. A., Stark, E., Koch, C., & Buzsáki, G. (2010). Transcranial electric stimulation entrains cortical neuronal populations in rats. *The Journal of Neuroscience*, *30*(34), 11476–85.

Pahor, A., & Jaušovec, N. (2014). The effects of theta transcranial alternating current stimulation (tACS) on fluid intelligence. *International Journal of Psychophysiology : Official Journal of the International Organization of Psychophysiology*, *93*(3), 322–31.

Pascual-Leone, A., Walsh, V., & Rothwell, J. (2000). Transcranial magnetic stimulation in cognitive neuroscience--virtual lesion, chronometry, and functional connectivity. *Current Opinion in Neurobiology*, *10*(2), 232–7.

Paulus, W. (2011). Transcranial electrical stimulation (tES - tDCS; tRNS, tACS) methods. *Neuropsychological Rehabilitation*, *21*(5), 602–17.

Penfield, Wilder, Rasmussen, T. (1950). *The cerebral cortex of man: a clinical study of localization of function* (New York:). New York.

Penfield, W., & Boldrey, E. (1937). Somatic motor and sensory representation in the cerebral cortex of man as studied by electrical stimulation. *Brain*, *60*(4), 389–443.

Perrenoud, Q., Pennartz, C. M. A., Gentet, L. J., Pennartz, C., Pennartz, C., & Barth, A. (2016). Membrane Potential Dynamics of Spontaneous and Visually Evoked Gamma Activity in V1 of Awake Mice. *PLOS Biology*, *14*(2), e1002383.

Peurala, S. H., Müller-Dahlhaus, J. F. M., Arai, N., & Ziemann, U. (2008). Interference of short-interval intracortical inhibition (SICI) and short-interval intracortical facilitation (SICF). *Clinical Neurophysiology*, *119*(10), 2291–7.

Pfurtscheller, G., & Berghold, A. (1989). Patterns of cortical activation during planning of voluntary movement. *Electroencephalography and Clinical Neurophysiology*, *72*(3), 250–8.

Pfurtscheller, G., Graimann, B., Huggins, J. E., Levine, S. P., & Schuh, L. A. (2003). Spatiotemporal patterns of beta desynchronization and gamma synchronization in corticographic data during self-paced movement. *Clinical Neurophysiology*,

114(7), 1226–36.
Pfurtscheller, G., & Lopes da Silva, F. H. (1999). Event-related EEG/MEG synchronization and desynchronization: basic principles. *Clinical Neurophysiology*, *110*(11), 1842–1857.
Pfurtscheller, G., Stancák, A., & Neuper, C. (1996). Post-movement beta synchronization. A correlate of an idling motor area? *Electroencephalography and Clinical Neurophysiology*, *98*(4), 281–293.
Pike, F. G., Goddard, R. S., Suckling, J. M., Ganter, P., Kasthuri, N., & Paulsen, O. (2000). Distinct frequency preferences of different types of rat hippocampal neurones in response to oscillatory input currents. *The Journal of Physiology*, *529*(Pt 1), 205–13.
Pikovsky, A., Rosenblum, M., and Kurths, J. (2003). *Synchronization: A Universal Concept in Nonlinear Sciences*. New York: Cambridge University Press.
Pogosyan, A., Gaynor, L. D., Eusebio, A., & Brown, P. (2009). Boosting cortical activity at Beta-band frequencies slows movement in humans. *Current Biology*, *19*(19), 1637–41.
Polanía, R., Nitsche, M. A., Korman, C., Batsikadze, G., & Paulus, W. (2012). The importance of timing in segregated theta phase-coupling for cognitive performance. *Current Biology, 22*(14), 1314–8.
Pollok, B., Boysen, A.-C., & Krause, V. (2015). The effect of transcranial alternating current stimulation (tACS) at alpha and beta frequency on motor learning. *Behavioural Brain Research*, *293*, 234–240.
Pollok, B., Krause, V., Martsch, W., Wach, C., Schnitzler, A., & Südmeyer, M. (2012). Motor-cortical oscillations in early stages of Parkinson's disease. *The Journal of Physiology*, *590*(13), 3203–12.
Pollok, B., Latz, D., Krause, V., Butz, M., & Schnitzler, A. (2014). Changes of motor-cortical oscillations associated with motor learning. *Neuroscience*, *275*, 47–53.
Popoli, M., Yan, Z., McEwen, B. S., & Sanacora, G. (2011). The stressed synapse: the impact of stress and glucocorticoids on glutamate transmission. *Nature Reviews. Neuroscience*, *13*(1), 22–37.
Pouwels, P. J., & Frahm, J. (1998). Regional metabolite concentrations in human brain as determined by quantitative localized proton MRS. *Magnetic Resonance in Medicine*, *39*(1), 53–60.
Pozo, K., & Goda, Y. (2010). Unraveling mechanisms of homeostatic synaptic plasticity. *Neuron*, *66*(3), 337–51.
Prokic, E. J., Weston, C., Yamawaki, N., Hall, S. D., Jones, R. S. G., Stanford, I. M., … Woodhall, G. L. (2015). Cortical oscillatory dynamics and benzodiazepine-site modulation of tonic inhibition in fast spiking interneurons. *Neuropharmacology*, *95*, 192–205.
Proudfoot, M., Rohenkohl, G., Quinn, A., Colclough, G. L., Wuu, J., Talbot, K., … Turner, M. R. (2017). Altered cortical beta-band oscillations reflect motor system degeneration in amyotrophic lateral sclerosis. *Human Brain Mapping*, *38*(1), 237–254.
Provencher, S. W. (1993). Estimation of metabolite concentrations from localized in vivo proton NMR spectra. *Magnetic Resonance in Medicine*, *30*(6), 672–9.
Provencher, S. W. (2001). Automatic quantitation of localizedin vivo1H spectra with LCModel. *NMR in Biomedicine*, *14*(4), 260–264.
Purcell, E. M., Torrey, H. C., & Pound, R. V. (1946). Resonance Absorption by Nuclear

Magnetic Moments in a Solid. *Physical Review*, *69*(1–2), 37–38.
Puts, N. A. J., & Edden, R. A. E. (2012). In vivo magnetic resonance spectroscopy of GABA: a methodological review. *Progress in Nuclear Magnetic Resonance Spectroscopy*, *60*, 29–41.
Raco, V., Bauer, R., Olenik, M., Brkic, D., & Gharabaghi, A. (2014). Neurosensory Effects of Transcranial Alternating Current Stimulation. *Brain Stimulation*, *7*(6), 823-31.
Raco, V., Bauer, R., Tharsan, S., & Gharabaghi, A. (2016). Combining TMS and tACS for Closed-Loop Phase-Dependent Modulation of Corticospinal Excitability: A Feasibility Study. *Frontiers in Cellular Neuroscience*, *10*, 143.
Reato, D., Rahman, A., Bikson, M., & Parra, L. C. (2010). Low-intensity electrical stimulation affects network dynamics by modulating population rate and spike timing. *The Journal of Neuroscience*, *30*(45), 15067–79.
Reato, D., Rahman, A., Bikson, M., & Parra, L. C. (2013). Effects of weak transcranial alternating current stimulation on brain activity-a review of known mechanisms from animal studies. *Frontiers in Human Neuroscience*, *7*, 687.
Reynolds, C., & Ashby, P. (1999). Inhibition in the human motor cortex is reduced just before a voluntary contraction. *Neurology*, *53*(4), 730–5.
Riecke, L., Formisano, E., Herrmann, C. S., & Sack, A. T. (2015). 4-Hz transcranial alternating current stimulation phase modulates hearing. *Brain Stimulation*. *8*(4), 777-83.
Robertson, E. M., Press, D. Z., & Pascual-Leone, A. (2005). Off-Line Learning and the Primary Motor Cortex. *Journal of Neuroscience*, *25*(27), 6372–6378.
Romei, V., Bauer, M., Brooks, J. L., Economides, M., Penny, W., Thut, G., … Bestmann, S. (2016). Causal evidence that intrinsic beta-frequency is relevant for enhanced signal propagation in the motor system as shown through rhythmic TMS. *NeuroImage*, *126*, 120–30.
Roopun, A. K., Middleton, S. J., Cunningham, M. O., LeBeau, F. E. N., Bibbig, A., Whittington, M. A., & Traub, R. D. (2006). A beta2-frequency (20-30 Hz) oscillation in nonsynaptic networks of somatosensory cortex. *Proceedings of the National Academy of Sciences*, *103*(42), 15646–15650.
Rossi, S., Hallett, M., Rossini, P. M., & Pascual-Leone, A. (2009). Safety, ethical considerations, and application guidelines for the use of transcranial magnetic stimulation in clinical practice and research. *Clinical Neurophysiology, 120*(12),
Rossini, P. M., Burke, D., Chen, R., Cohen, L. G., Daskalakis, Z., Di Iorio, R., … Ziemann, U. (2015). Non-invasive electrical and magnetic stimulation of the brain, spinal cord, roots and peripheral nerves: basic principles and procedures for routine clinical and research application. An updated report from an I.F.C.N. Committee. *Clinical Neurophysiology*, *126*(6), 1071–1107.
Rossini, P. M., Zarola, F., Stalberg, E., & Caramia, M. (1988). Pre-movement facilitation of motor-evoked potentials in man during transcranial stimulation of the central motor pathways. *Brain Research*, *458*(1), 20–30.
Rossiter, H. E., Boudrias, M.-H., & Ward, N. S. (2014). Do movement-related beta oscillations change after stroke? *Journal of Neurophysiology*, *112*(9), 2053–8.
Rossiter, H. E., Davis, E. M., Clark, E. V, Boudrias, M.-H., & Ward, N. S. (2014). Beta oscillations reflect changes in motor cortex inhibition in healthy ageing. *NeuroImage*, *91*, 360–5.
Rossiter, H. E., Eaves, C., Davis, E., Boudrias, M.-H., Park, C.-H., Farmer, S., …

Ward, N. S. (2012). Changes in the location of cortico-muscular coherence following stroke. *NeuroImage. Clinical*, *2*, 50–5.
Rothkegel, H., Sommer, M., & Paulus, W. (2010). Breaks during 5Hz rTMS are essential for facilitatory after effects. *Clinical Neurophysiology*, *121*(3), 426–30.
Rothman, D. L. (1994). *1H NMR Studies of Human Brain Metabolism and Physiology*. San Diego: Elsevier Science and Technology Books.
Saiote, C., Turi, Z., Paulus, W., & Antal, A. (2013). Combining functional magnetic resonance imaging with transcranial electrical stimulation. *Frontiers in Human Neuroscience*, *7*, 435.
Salmelin, R., & Hari, R. (1994a). Characterization of spontaneous MEG rhythms in healthy adults. *Electroencephalography and Clinical Neurophysiology*, *91*(4), 237–48.
Salmelin, R., & Hari, R. (1994b). Spatiotemporal characteristics of sensorimotor neuromagnetic rhythms related to thumb movement. *Neuroscience*, *60*(2), 537–50.
Sanes, J. N., & Donoghue, J. P. (1993). Oscillations in local field potentials of the primate motor cortex during voluntary movement. *Proceedings of the National Academy of Sciences of the United States of America*, *90*(10), 4470–4.
Sanes, J. N., & Donoghue, J. P. (1997). Dynamic Motor Cortical Organization. *The Neuroscientist*, *3*(3), 158–165.
Sanes, J. N., & Donoghue, J. P. (2000). Plasticity and Primary Motor Cortex. *Annual Review of Neuroscience*, *23*(1), 393–415.
Sanger, T. D., Garg, R. R., & Chen, R. (2001). Interactions between two different inhibitory systems in the human motor cortex. *The Journal of Physiology*, *530*(2), 307–317.
Santarnecchi, E., Biasella, A., Tatti, E., Rossi, A., Prattichizzo, D., & Rossi, S. (2017). High-gamma oscillations in the motor cortex during visuo-motor coordination: A tACS interferential study. *Brain Research Bulletin*, *131*, 47–54.
Santarnecchi, E., Polizzotto, N. R., Godone, M., Giovannelli, F., Feurra, M., Matzen, L., … Rossi, S. (2013). Frequency-dependent enhancement of fluid intelligence induced by transcranial oscillatory potentials. *Current Biology*, *23*(15), 1449–53.
Sauseng, P., Klimesch, W., Gerloff, C., & Hummel, F. C. (2009). Spontaneous locally restricted EEG alpha activity determines cortical excitability in the motor cortex. *Neuropsychologia*, *47*(1), 284–288.
Scheenen, T. W. J., Klomp, D. W. J., Wijnen, J. P., & Heerschap, A. (2008). Short echo time1H-MRSI of the human brain at 3T with minimal chemical shift displacement errors using adiabatic refocusing pulses. *Magnetic Resonance in Medicine*, *59*(1), 1–6.
Schmidt, S. L., Iyengar, A. K., Foulser, A. A., Boyle, M. R., & Fröhlich, F. (2014). Endogenous Cortical Oscillations Constrain Neuromodulation by Weak Electric Fields. *Brain Stimulation*, *7*(6), 878-89
Schulz, H., Ubelacker, T., Keil, J., Muller, N., & Weisz, N. (2014a). Now I am Ready--Now I am not: The Influence of Pre-TMS Oscillations and Corticomuscular Coherence on Motor-Evoked Potentials. *Cerebral Cortex*, *24*(7), 1708–1719.
Schulz, H., Ubelacker, T., Keil, J., Muller, N., & Weisz, N. (2014b). Now I am Ready--Now I am not: The Influence of Pre-TMS Oscillations and Corticomuscular Coherence on Motor-Evoked Potentials. *Cerebral Cortex*, *24*(7), 1708–1719.
Schutter, D. J. L. G., & Hortensius, R. (2010). Retinal origin of phosphenes to

transcranial alternating current stimulation. *Clinical Neurophysiology*, *121*(7), 1080–4.
Schwenkreis, P., Witscher, K., Janssen, F., Addo, A., Dertwinkel, R., Zenz, M., … Tegenthoff, M. (1999). Influence of the N-methyl-D-aspartate antagonist memantine on human motor cortex excitability. *Neuroscience Letters*, *270*(3), 137–40.
Sederberg, P. B., Kahana, M. J., Howard, M. W., Donner, E. J., & Madsen, J. R. (2003). Theta and gamma oscillations during encoding predict subsequent recall. *The Journal of Neuroscience*, *23*(34), 10809–14.
Sederberg, P. B., Schulze-Bonhage, A., Madsen, J. R., Bromfield, E. B., McCarthy, D. C., Brandt, A., … Kahana, M. J. (2006). Hippocampal and Neocortical Gamma Oscillations Predict Memory Formation in Humans. *Cerebral Cortex*, *17*(5), 1190–1196.
Sejnowski, T. J. (1977). Storing covariance with nonlinearly interacting neurons. *Journal of Mathematical Biology*, *4*(4), 303–21.
Sela, T., Kilim, A., & Lavidor, M. (2012). Transcranial alternating current stimulation increases risk-taking behavior in the balloon analog risk task. *Frontiers in Neuroscience*, *6*, 22.
Semyanov, A., Walker, M. C., & Kullmann, D. M. (2003). GABA uptake regulates cortical excitability via cell type–specific tonic inhibition. *Nature Neuroscience*, *6*(5), 484–90.
Semyanov, A., Walker, M. C., Kullmann, D. M., & Silver, R. A. (2004). Tonically active GABAA receptors: modulating gain and maintaining the tone. *Trends in Neurosciences*, *27*(5), 262–269.
Senkowski, D., Schneider, T. R., Foxe, J. J., & Engel, A. K. (2008). Crossmodal binding through neural coherence: implications for multisensory processing. *Trends in Neurosciences*, *31*(8), 401–409.
Siebner, H. R., Dressnandt, J., Auer, C., & Conrad, B. (1998). Continuous intrathecal baclofen infusions induced a marked increase of the transcranially evoked silent period in a patient with generalized dystonia. *Muscle & Nerve*, *21*(9), 1209–12.
Siebner, H. R., Lang, N., Rizzo, V., Nitsche, M. A., Paulus, W., Lemon, R. N., & Rothwell, J. C. (2004). Preconditioning of low-frequency repetitive transcranial magnetic stimulation with transcranial direct current stimulation: evidence for homeostatic plasticity in the human motor cortex. *The Journal of Neuroscience*, *24*(13), 3379–85.
Siegel, M., Donner, T. H., Oostenveld, R., Fries, P., & Engel, A. K. (2007). High-Frequency Activity in Human Visual Cortex Is Modulated by Visual Motion Strength. *Cerebral Cortex*, *17*(3), 732–741.
Siegel, M., Engel, A. K., & Donner, T. H. (2011). Cortical network dynamics of perceptual decision-making in the human brain. *Frontiers in Human Neuroscience*, *5*, 21.
Singer, W. (1993). Synchronization of Cortical Activity and its Putative Role in Information Processing and Learning. *Annual Review of Physiology*, *55*(1), 349–374.
Singh, K. D., Hamdy, S., Aziz, Q., & Thompson, D. G. (1997). Topographic mapping of trans-cranial magnetic stimulation data on surface rendered MR images of the brain. *Electroencephalography and Clinical Neurophysiology*, *105*(5), 345–51.
Soekadar, S. R., Witkowski, M., Cossio, E. G., Birbaumer, N., Robinson, S. E., &

Cohen, L. G. (2013). In vivo assessment of human brain oscillations during application of transcranial electric currents. *Nature Communications*, *4*, 2032.
Sohal, V. S., Zhang, F., Yizhar, O., & Deisseroth, K. (2009). Parvalbumin neurons and gamma rhythms enhance cortical circuit performance. *Nature*, *459*(7247), 698–702.
Song, S., & Abbott, L. F. (2001). Cortical development and remapping through spike timing-dependent plasticity. *Neuron*, *32*(2), 339–50.
Spinks, R. L., Kraskov, A., Brochier, T., Umilta, M. A., & Lemon, R. N. (2008). Selectivity for Grasp in Local Field Potential and Single Neuron Activity Recorded Simultaneously from M1 and F5 in the Awake Macaque Monkey. *The Journal of Neuroscience*, *28*(43), 10961–10971.
Stagg, C., Rothman, D. (2014). *Magnetic Resonance Spectroscopy: Tools for neuroscience research and emerging clinical applications*. Elsevier Inc.
Stagg, C. J., Bachtiar, V., & Johansen-Berg, H. (2011). The role of GABA in human motor learning. *Current Biology*, *21*(6), 480–4.
Stagg, C. J., Bestmann, S., Constantinescu, a O., Moreno, L. M., Allman, C., Mekle, R., … Rothwell, J. C. (2011). Relationship between physiological measures of excitability and levels of glutamate and GABA in the human motor cortex. *The Journal of Physiology*, *589*(Pt 23), 5845–55.
Stancák, A., & Pfurtscheller, G. (1995). Desynchronization and recovery of beta rhythms during brisk and slow self-paced finger movements in man. *Neuroscience Letters*, *196*(1–2), 21–4.
Stent, G. S. (1973). A physiological mechanism for Hebb's postulate of learning. *Proceedings of the National Academy of Sciences of the United States of America*, *70*(4), 997–1001.
Stinear, C. M., & Byblow, W. D. (2004). Impaired Modulation of Intracortical Inhibition in Focal Hand Dystonia. *Cerebral Cortex*, *14*(5), 555–561.
Stonkus, R., Braun, V., Kerlin, J., Volberg, G., & Hanslmayr, S. (2016). Probing the causal role of prestimulus interregional synchrony for perceptual integration via tACS. *Scientific Reports, 6*, 32065
Strüber, D., Rach, S., Trautmann-Lengsfeld, S. a, Engel, A. K., & Herrmann, C. S. (2014). Antiphasic 40 Hz oscillatory current stimulation affects bistable motion perception. *Brain Topography*, *27*(1), 158–71.
Swann, N. C., de Hemptinne, C., Miocinovic, S., Qasim, S., Wang, S. S., Ziman, N., … Starr, P. A. (2016). Gamma Oscillations in the Hyperkinetic State Detected with Chronic Human Brain Recordings in Parkinson's Disease. *The Journal of Neuroscience*, *36*(24), 6445–58.
Swettenham, J. B., Muthukumaraswamy, S. D., & Singh, K. D. (2009). Spectral Properties of Induced and Evoked Gamma Oscillations in Human Early Visual Cortex to Moving and Stationary Stimuli. *Journal of Neurophysiology*, *102*(2), 1241–1253.
Takemi, M., Masakado, Y., Liu, M., & Ushiba, J. (2013). Event-related desynchronization reflects downregulation of intracortical inhibition in human primary motor cortex. *Journal of Neurophysiology*, *110*(5), 1158–1166.
Takemi, M., Masakado, Y., Liu, M., & Ushiba, J. (2015). Sensorimotor event-related desynchronization represents the excitability of human spinal motoneurons. *Neuroscience*, *297*, 58–67.
Takeuchi, N., & Izumi, S.-I. (2013). Rehabilitation with poststroke motor recovery: a

review with a focus on neural plasticity. *Stroke Research and Treatment*, *2013*, 128641.

Tan, H., Wade, C., & Brown, P. (2016). Post-Movement Beta Activity in Sensorimotor Cortex Indexes Confidence in the Estimations from Internal Models. *The Journal of Neuroscience*, *36*(5), 1516-1528.

Taulu, S., & Simola, J. (2006). Spatiotemporal signal space separation method for rejecting nearby interference in MEG measurements. *Physics in Medicine and Biology*, *51*(7), 1759–68.

Tecchio, F., Cancelli, A., Cottone, C., Tomasevic, L., Devigus, B., Zito, G., … Carducci, F. (2013). Regional personalized electrodes to select transcranial current stimulation target. *Frontiers in Human Neuroscience*, *7*, 131.

Thibaut, A., Simis, M., Battistella, L. R., Fanciullacci, C., Bertolucci, F., Huerta-Gutierrez, R., … Fregni, F. (2017). Using Brain Oscillations and Corticospinal Excitability to Understand and Predict Post-Stroke Motor Function. *Frontiers in Neurology*, *8*, 187.

Thut, G., Miniussi, C., & Gross, J. (2012). The functional importance of rhythmic activity in the brain. *Current Biology*, *22*(16), R658-63.

Thut, G., Schyns, P. G., & Gross, J. (2011). Entrainment of perceptually relevant brain oscillations by non-invasive rhythmic stimulation of the human brain. *Frontiers in Psychology*, *2*, 170.

Tiesinga, P., & Sejnowski, T. J. (2009). Cortical enlightenment: are attentional gamma oscillations driven by ING or PING? *Neuron*, *63*(6), 727–32.

Tkáč, Ivan, Öz, Gülin, Gregor, Adriany, Uğurbil, K., & Gruetter, R. (2009). In vivo 1 H NMR spectroscopy of the human brain at high magnetic fields: Metabolite quantification at 4T vs. 7T. *Magnetic Resonance in Medicine*, *62*(4), 868–879.

Tkác, I., Andersen, P., Adriany, G., Merkle, H., Ugurbil, K., & Gruetter, R. (2001). In vivo 1H NMR spectroscopy of the human brain at 7 T. *Magnetic Resonance in Medicine*, *46*(3), 451–6.

Tkáč, I., Rao, R., Georgieff, M. K., & Gruetter, R. (2003). Developmental and regional changes in the neurochemical profile of the rat brain determined by in vivo ^{1} H NMR spectroscopy. *Magnetic Resonance in Medicine*, *50*(1), 24–32.

Tort, A. B. L., Komorowski, R. W., Manns, J. R., Kopell, N. J., & Eichenbaum, H. (2009). Theta-gamma coupling increases during the learning of item-context associations. *Proceedings of the National Academy of Sciences of the United States of America*, *106*(49), 20942–7.

Towers, S. K., Gloveli, T., Traub, R. D., Driver, J. E., Engel, D., Fradley, R., … Whittington, M. A. (2004). Alpha 5 subunit-containing GABAA receptors affect the dynamic range of mouse hippocampal kainate-induced gamma frequency oscillations in vitro. *The Journal of Physiology*, *559*(Pt 3), 721–8.

Traub, R. D., Bibbig, A., LeBeau, F. E. N., Buhl, E. H., & Whittington, M. A. (2004). Cellular mechanisms of neuronal population oscillations in the hippocampus in vitro. *Annual Review of Neuroscience*, *27*(1), 247–278.

Traub, R. D., Cunningham, M. O., Gloveli, T., LeBeau, F. E. N., Bibbig, A., Buhl, E. H., & Whittington, M. A. (2003). GABA-enhanced collective behavior in neuronal axons underlies persistent gamma-frequency oscillations. *Proceedings of the National Academy of Sciences of the United States of America*, *100*(19), 11047–52.

Traub, R. D., Whittington, M. A., Colling, S. B., Buzsáki, G., & Jefferys, J. G. (1996).

Analysis of gamma rhythms in the rat hippocampus in vitro and in vivo. *The Journal of Physiology*, *493 (Pt 2*, 471–84.
Tremblay, R., Lee, S., & Rudy, B. (2016). GABAergic Interneurons in the Neocortex: From Cellular Properties to Circuits. *Neuron*, *91*(2), 260–292.
Tremblay, S., Beaulé, V., Proulx, S., de Beaumont, L., Marjanska, M., Doyon, J., … Théoret, H. (2013). Relationship between transcranial magnetic stimulation measures of intracortical inhibition and spectroscopy measures of GABA and glutamate+glutamine. *Journal of Neurophysiology*, *109*(5), 1343–9.
Trepel, C., & Racine, R. J. (2000). GABAergic modulation of neocortical long-term potentiation in the freely moving rat. *Synapse*, *35*(2), 120–8.
Turi, Z., Ambrus, G. G., Janacsek, K., Emmert, K., Hahn, L., Paulus, W., & Antal, A. (2013). Both the cutaneous sensation and phosphene perception are modulated in a frequency-specific manner during transcranial alternating current stimulation. *Restorative Neurology and Neuroscience*, *31*(3), 275–85.
Turrigiano, G. G., & Nelson, S. B. (2000). Hebb and homeostasis in neuronal plasticity. *Current Opinion in Neurobiology*, *10*(3), 358–64.
Tzagarakis, C., Ince, N. F., Leuthold, A. C., & Pellizzer, G. (2010). Beta-Band Activity during Motor Planning Reflects Response Uncertainty. *The Journal of Neuroscience*, *30*(34).
Tzagarakis, C., West, S., & Pellizzer, G. (2015). Brain oscillatory activity during motor preparation: effect of directional uncertainty on beta, but not alpha, frequency band. *Frontiers in Neuroscience*, *9*, 246.
Ueno, S., Tashiro, T., & Harada, K. (1988). Localized stimulation of neural tissues in the brain by means of a paired configuration of time-varying magnetic fields. *Journal of Applied Physics*, *64*(10), 5862–5864.
Uhlhaas, P. J., & Singer, W. (2010). Abnormal neural oscillations and synchrony in schizophrenia. *Nature Reviews. Neuroscience*, *11*(2), 100–13.
Uhlhaas, P. J., Singer, W., Gielen, S., Nuechterlein, K. H., Green, M. F., Maurer, K., … Greengard, P. (2006). Neural synchrony in brain disorders: relevance for cognitive dysfunctions and pathophysiology. *Neuron*, *52*(1), 155–68.
Valls-Solé, J., Pascual-Leone, A., Wassermann, E. M., & Hallett, M. (1992). Human motor evoked responses to paired transcranial magnetic stimuli. *Electroencephalography and Clinical Neurophysiology/Evoked Potentials Section*, *85*(6), 355–364.
Van Vreeswijk, C., Abbott, L. F., & Ermentrout, G. B. (1994). When inhibition not excitation synchronizes neural firing. *Journal of Computational Neuroscience*, *1*(4), 313–21.
Varlet, M., Wade, A., Novembre, G., & Keller, P. E. (2017). Investigation of the effects of transcranial alternating current stimulation (tACS) on self-paced rhythmic movements. *Neuroscience*, *350*, 75–84.
Veniero, D., Benwell, C. S. Y., Ahrens, M. M., & Thut, G. (2017). Inconsistent Effects of Parietal α-tACS on Pseudoneglect across Two Experiments: A Failed Internal Replication. *Frontiers in Psychology*, *8*, 952.
Veniero, D., Vossen, A., Gross, J., & Thut, G. (2015). Lasting EEG/MEG Aftereffects of Rhythmic Transcranial Brain Stimulation: Level of Control Over Oscillatory Network Activity. *Frontiers in Cellular Neuroscience*, *9*, 477.
Vogt, C., & Vogt, O. (1926). Die vergleichend-architektonische und die vergleichend-reizphysiologische Felderung der Grosshirnrinde unter besonderer

Berucksichtigung der menschlichen. *Die Naturwissenschaften*, *14*(1),190-4.
Vossen, A., Gross, J., & Thut, G. (2015). Alpha Power Increase After Transcranial Alternating Current Stimulation at Alpha Frequency (α-tACS) Reflects Plastic Changes Rather Than Entrainment. *Brain Stimulation*, *8*(3), 499–508.
Vosskuhl, J., Huster, R. J., & Herrmann, C. S. (2015). BOLD signal effects of transcranial Alternating Current Stimulation (tACS) in the alpha range: A concurrent tACS-fMRI study. *NeuroImage*, *140*, 118-25
Wach, C., Krause, V., Moliadze, V., Paulus, W., Schnitzler, A., & Pollok, B. (2013). Effects of 10Hz and 20Hz transcranial alternating current stimulation (tACS) on motor functions and motor cortical excitability. *Behavioural Brain Research*, *241*, 1–6.
Wach, C., Krause, V., Moliadze, V., Paulus, W., Schnitzler, A., & Pollok, B. (2013). The effect of 10 Hz transcranial alternating current stimulation (tACS) on corticomuscular coherence. *Frontiers in Human Neuroscience*, *7*, 511.
Wagner, T., Fregni, F., Fecteau, S., Grodzinsky, A., Zahn, M., & Pascual-Leone, A. (2007). Transcranial direct current stimulation: A computer-based human model study. *NeuroImage*, *35*(3), 1113–1124.
Wang, H., & Wagner, J. J. (1999). Priming-induced shift in synaptic plasticity in the rat hippocampus. *Journal of Neurophysiology*, *82*(4), 2024–8.
Wang, X. J., & Buzsáki, G. (1996). Gamma oscillation by synaptic inhibition in a hippocampal interneuronal network model. *The Journal of Neuroscience*, *16*(20), 6402–13.
Ward, L. M. (2003). Synchronous neural oscillations and cognitive processes. *Trends in Cognitive Sciences*, *7*(12), 553–9.
Wassermann, E. M. (1998). Risk and safety of repetitive transcranial magnetic stimulation: report and suggested guidelines from the International Workshop on the Safety of Repetitive Transcranial Magnetic Stimulation, June 5-7, 1996. *Electroencephalography and Clinical Neurophysiology*, *108*(1), 1–16.
Weinrich, C. A., Brittain, J.-S., Nowak, M., Salimi-Khorshidi, R., Brown, P., & Stagg, C. J. (2017). Modulation of Long-Range Connectivity Patterns via Frequency-Specific Stimulation of Human Cortex. *Current Biology*, *27*(19), 3061-3068.e3.
Werhahn, K. J., Kunesch, E., Noachtar, S., Benecke, R., & Classen, J. (1999). Differential effects on motorcortical inhibition induced by blockade of GABA uptake in humans. *The Journal of Physiology*, *517*(Pt 2), 591–7.
Wespatat, V., Tennigkeit, F., & Singer, W. (2004). Phase Sensitivity of Synaptic Modifications in Oscillating Cells of Rat Visual Cortex. *The Journal of Neuroscience*, *24*(41), 9067–9075.
Whitham, E. M., Lewis, T., Pope, K. J., Fitzgibbon, S. P., Clark, C. R., Loveless, S., … Willoughby, J. O. (2008). Thinking activates EMG in scalp electrical recordings. *Clinical Neurophysiology*, *119*(5), 1166–1175.
Whittington, M. A., Traub, R. D., & Jefferys, J. G. (1995). Synchronized oscillations in interneuron networks driven by metabotropic glutamate receptor activation. *Nature*, *373*(6515), 612–5.
Whittington, M. A., Traub, R. D., Kopell, N., Ermentrout, B., & Buhl, E. H. (2000). Inhibition-based rhythms: experimental and mathematical observations on network dynamics. *International Journal of Psychophysiology*, *38*(3), 315–36.
Wilson, H. R., & Cowan, J. D. (1972). Excitatory and inhibitory interactions in localized populations of model neurons. *Biophysical Journal*, *12*(1), 1–24.

Winfree, A. T. (1980). *The Geometry of Biological Time*. New York: Springer.
Witkowski, M., Cossio, E. G., Chander, B. S., Braun, C., Birbaumer, N., Robinson, S. E., & Soekadar, S. R. (2015). Mapping entrained brain oscillations during transcranial alternating current stimulation (tACS). *NeuroImage*, *140*, 89-98.
Wu, J.-F., Wang, H.-J., Wu, Y., Li, F., Bai, Y.-L., Zhang, P.-Y., & Chan, C. C. H. (2016). Efficacy of transcranial alternating current stimulation over bilateral mastoids (tACSbm) on enhancing recovery of subacute post-stroke patients. *Topics in Stroke Rehabilitation*, 1–10.
Yamawaki, N., Stanford, I. M., Hall, S. D., & Woodhall, G. L. (2008). Pharmacologically induced and stimulus evoked rhythmic neuronal oscillatory activity in the primary motor cortex in vitro. *Neuroscience*, *151*(2), 386–95.
Yousry, T. (1997). Localization of the motor hand area to a knob on the precentral gyrus. A new landmark. *Brain*, *120*(1), 141–157.
Yuval-Greenberg, S., Tomer, O., Keren, A. S., Nelken, I., & Deouell, L. Y. (2008). Transient Induced Gamma-Band Response in EEG as a Manifestation of Miniature Saccades. *Neuron*, *58*(3), 429–441.
Z'Graggen, W. J., Conforto, A. B., Wiest, R., Remonda, L., Hess, C. W., & Kaelin-Lang, A. (2009). Mapping of direction and muscle representation in the human primary motor cortex controlling thumb movements. *The Journal of Physiology*, *587*(Pt 9), 1977–87.
Zaaroor, M., Pratt, H., & Starr, A. (2003). Time course of motor excitability before and after a task-related movement. *Clinical Neurophysiology*, *33*(3), 130–137.
Zaehle, T., Rach, S., & Herrmann, C. S. (2010). Transcranial alternating current stimulation enhances individual alpha activity in human EEG. *PloS One*, *5*(11), e13766.
Zaghi, S., Acar, M., Hultgren, B., Boggio, P. S., & Fregni, F. (2010). Noninvasive brain stimulation with low-intensity electrical currents: putative mechanisms of action for direct and alternating current stimulation. *The Neuroscientist, 16*(3), 285–307.
Zaghi, S., de Freitas Rezende, L., de Oliveira, L. M., El-Nazer, R., Menning, S., Tadini, L., & Fregni, F. (2010). Inhibition of motor cortex excitability with 15Hz transcranial alternating current stimulation (tACS). *Neuroscience Letters*, *479*(3), 211–4.
Zarkowski, P., Shin, C. J., Dang, T., Russo, J., & Avery, D. (2006). EEG and the Variance of Motor Evoked Potential Amplitude. *Clinical EEG and Neuroscience*, *37*(3), 247–251.
Zhu, H., & Barker, P. B. (2011). MR spectroscopy and spectroscopic imaging of the brain. *Methods in Molecular Biology*, *711*, 203–26.
Ziemann, U. (2004). TMS and drugs. *Clinical Neurophysiology, 115*(8), 1717–29.
Ziemann, U., Chen, R., Cohen, L. G., & Hallett, M. (1998). Dextromethorphan decreases the excitability of the human motor cortex. *Neurology*, *51*(5), 1320–4.
Ziemann, U., Hallett, M., & Cohen, L. G. (1998). Mechanisms of deafferentation-induced plasticity in human motor cortex. *The Journal of Neuroscience*, *18*(17), 7000–7.
Ziemann, U., Lönnecker, S., & Paulus, W. (1995). Inhibition of human motor cortex by ethanol. A transcranial magnetic stimulation study. *Brain : A Journal of Neurology*, *118*(Pt 6), 1437–46.
Ziemann, U., Lönnecker, S., Steinhoff, B. J., & Paulus, W. (1996a). Effects of antiepileptic drugs on motor cortex excitability in humans: a transcranial magnetic stimulation study. *Annals of Neurology*, *40*(3), 367–78.

Ziemann, U., Lönnecker, S., Steinhoff, B. J., & Paulus, W. (1996b). The effect of lorazepam on the motor cortical excitability in man. *Experimental Brain Research*, *109*(1), 127–35.

Ziemann, U., Rothwell, J. C., & Ridding, M. C. (1996). Interaction between intracortical inhibition and facilitation in human motor cortex. *The Journal of Physiology*, *496*(Pt 3), 873–81.